

Removal of Perfluorinated Compounds from Ultrapure and Surface Waters by Adsorption and Ion Exchange

by

Mohammad Feisal Rahman

A thesis
presented to the University of Waterloo
in fulfillment of the
thesis requirement for the degree of
Doctor of Philosophy
in
Civil Engineering

Waterloo, Ontario, Canada, 2014

©Mohammad Feisal Rahman 2014

AUTHOR'S DECLARATION

I hereby declare that I am the sole author of this thesis. This is a true copy of the thesis, including any required final revisions, as accepted by my examiners.

I understand that my thesis may be made electronically available to the public.

Disclaimer

The views and ideas expressed in this paper are those of the author and do not necessarily reflect the views and policies of the agencies that funded this research: the Ontario Research Fund ‘Center for Control of Emerging Contaminants’, the Natural Sciences and Engineering Research Council of Canada (NSERC), and our NSERC Industrial Research Chair partners: Associated Engineering Group Ltd., the cities of Barrie, Brantford, Guelph, Hamilton and Ottawa, Conestoga-Rovers & Associates Limited, EPCOR Water Services, GE Water & Process Technologies Canada, Lake Huron and Elgin Area Water Supply Systems, the Ontario Clean Water Agency (OCWA), the Regions of Durham, Halton, Niagara and Waterloo, RAL Engineering Ltd., Toronto Water, and the Walkerton Clean Water Centre.

The mention of trade names or commercial products does not constitute endorsement of or recommendation for their use.

Adsorbate samples were donated by Calgon Carbon, Mead WestVaco (MWV Specialty Chemicals), Cabot Norit Activated Carbon, Purolite, Apelsa Carbon, Evoqua Water Technologies (formerly Siemens Water Technologies), and Char Technologies.

Abstract

Perfluorinated compounds (PFCs) have been detected globally in drinking water at trace concentrations. This is attributable to the chemical properties that characterize these compounds: strong saturated carbon-fluorine bonds which make them resistant to chemical, physical, and biological degradation. Manufacturing wastes, sewage treatment plants, and leaching from consumer products are the primary pathways by which PFCs enter the environment. Drinking water occurrence studies indicate that PFCs, if present in source water, can pass through drinking water treatment processes and be present in finished drinking water. While they are currently not regulated, several PFCs have been included in the USEPA's 3rd unregulated contaminant monitoring list. As yet there is no clear understanding of the fate of PFCs during drinking water treatment. Full-scale surveys and bench-scale studies indicate that activated carbon adsorption and ion exchange treatment may be effective. Elucidation of the fate of selected PFCs at environmentally relevant concentrations during granular activated carbon (GAC) and ion exchange treatment was the primary objective of this research.

A gas chromatography/mass spectrometry (GC/MS)-based analytical method employing electron impact ionization was developed to analyze perfluorinated carboxylic acids (PFCAs), the selected target class of PFCs. Solid phase extraction was used to concentrate samples, and the PFCAs were derivatized using butanol in the presence of sulfuric acid and heat. The method detection limits for PFCAs with six to nine carbons were 16 ng/L-30 ng/L in ultrapure water and 16 ng/L-49 ng/L in Grand River water (GRW). Three PFCAs were selected as targets for adsorption studies: perfluoroheptanoic acid (PFHpA), perfluorooctanoic acid (PFOA) and perfluorononanoic acid (PFNA).

Adsorption behaviour of the target PFCAs in ultrapure water was assessed using four GACs, two anion exchange resins, and two alternative adsorbents. Single solute isotherms show that macroporous polystyrenic A-500P[®] (A-500P) ion exchange resin has a higher equilibrium capacity compared to the coal-based Filtrasorb[®] (F-400) GAC or the macroporous polyacrylic A-860[®] (A-860) ion exchange resin. During time dependent PFCA removal experiments at a target initial PFCA concentration of 3 µg/L, A-500P resin achieved the highest removal of the target PFCAs at equilibrium (> 95%) followed by the F-400 GAC (92% at equilibrium). This was

followed by coconut shell-based AquaCarb CX 1230[®] (CX) GAC and the two wood-based GACs – Norit C-Gran[®] (C-Gran) and NuChar WV B-30[®] (B-30). The A-860 resin achieved 66%-80% removal of the target PFCAs. BET surface area was not a good indicator of comparative PFCA removal performance, although pore size distribution, surface charge and particle size appeared to play a role. The alternative sorbents – cattle bone-based Fija Fluor[®] and a dairy manure-based Biochar – could not substantially remove the target PFCAs, potentially attributable to low micropore content and a predominantly mesoporous structure. Kinetics with the anion exchange resins were substantially faster compared to the GACs and the alternative sorbents, with A-500P as the fastest resin. Direct competition among the PFCAs for sorption sites was observed only on the A-860 resin. Further, chain length-dependent removal trends were not observed with the F-400 or CX GACs or the A-500P resin.

Based on kinetics data in ultrapure water the GACs CX and F-400, the ion exchange resins-A500P and A860, and the alternative adsorbent Biochar were selected for further evaluation in surface water using GRW. As with ultrapure water, the A-500P resin achieved the fastest and highest removal of the target PFCAs in GRW (~ 95%); however, the A-860 resin failed to achieve any substantial removal. Among the carbonaceous adsorbents, F-400 better removed the target PFCAs than CX and the Biochar. The presence of natural organic material (NOM) and inorganic anions in GRW lowered the equilibrium PFCA sorption amounts by 90 to 99% compared to those in ultrapure water. The humic fraction of NOM was the dominant competitor for the GACs and Biochar; however, both NOM and inorganic anions, especially sulfate, exerted competition on the anion exchange resins. Low removal of NOM with Biochar indicate that Biochar may not be used as an NOM pretreatment while high removal of NOM with ion exchange resins indicated that the tested resins may be effective as a pretreatment for GAC adsorbers.

Overall, this research demonstrates that GAC adsorption and strong base ion exchange can be promising PFCA removal techniques for drinking water. However, such premises should not be generalized as surface water matrix, adsorbent properties and PFCA characteristics may affect their removal.

Acknowledgements

This thesis would not have been possible without the contribution and support of a great number of people. I am deeply pleased to express my gratitude to all of them (and to the ones that I failed to remember here). I pray and thank the Almighty Allah for giving me the strength, energy and patience to continue this work.

I would like to express my sincere gratitude and thanks to my supervisors Dr. Sigrid Peldszus, Dr. William Anderson and Dr. Peter M. Huck for their unwavering and continuous support and, timely and relevant guidance throughout the program. During some of most challenging times of this project they remained calm and gave me encouragements and hope. Indeed working with them has been such a tremendous learning experience for me which will guide throughout the rest of my career.

I also fully recognize the exceptional support from the NSERC Chair in Water Treatment team and its partners. Thanks to Dana Herriman for her kind and selfless support. I cannot possibly say enough thanks to Monica Tudorancea for her very generous assistance with the LC-OCD instrument and her help in the lab. Thanks to Xiaohui Jin for his guidance during the initial phase of my research. Thanks to Dr. Michele Van Dyke for her thoughts on laboratory procedures. Thanks to the Co-Op students especially Hilary Cameron, Rachel Trower and Cloud Zhang for making my life in the lab a lot easier. I express my sincere gratitude to Victoria Chennette for her activated carbon surface charge determination work and sharing the results with me.

This research has been funded by the Ontario Research Fund ‘Center for Control of Emerging Contaminants’, the Natural Sciences and Engineering Research Council of Canada (NSERC), and partners of the NSERC Chair in Water Treatment at the University of Waterloo.

I greatly acknowledge the tremendous support from Mark Merlau and Mark Sobon who were always there to help. Thanks to Leslie Bragg from the Department of Biology at the University of Waterloo her help and suggestions with the GC/MS maintenance work. Also thanks to Brian Johnston at Agilent Technologies for his guidance on the GC/MS instrument and also for servicing the instrument. Thanks to the custodians at the University of Waterloo who would often come by the lab when it was late at night to check if everything was alright or would just

drop by to have a chat and give me encouragement. Also thanks to the Civil and Environmental Engineering staff at UW for their assistance throughout my program.

I am grateful to Mr. Don Downey at Purolite Canada for his assistance in acquiring the ion exchange resins and the resin beads. Also thanks to Calgon Carbon, Mead WestVaco (MWV Specialty Chemicals), Cabot Norit Activated Carbon, Apelsa Carbon, Evoqua Water Technologies (formerly Siemens Water Technologies), and Char Technologies for their donation of adsorbent samples.

I thank all the members of my thesis defense committee: Dr. Wayne Parker, Dr. Xianshe Feng and Dr. William Anderson and acknowledge their valuable feedback and guidance. Thanks to Dr. Luuk Rietveld for kindly agreeing to be the external examiner for my thesis.

Thanks to my fellow graduate students and friends Ahmed-El-Hadidy, Fei Chan, Mark Spanjers, Silvia Vlad, Leila Munla, Ishita Rahman, Shoeleh Shams, Avid Banihashemi, Lizanne Pharand, Brad Wilson, Yulang Wang (Micheal), Mohamed Hamouda, Daniel Scott (to name a few) with whom I have shared my time here at Waterloo. Thanks to all my colleagues at the University of Waterloo library who were extremely supportive these last few years.

My special thanks to Shahed vai, Pallab, Keya, Rudaba Apu, Rahi, Tariq Opu, Razon, Rubel vai, Moon Moon, Mrinmoy, Leonore Schaller (Léo), Bipasha, Farooq Chowdhury, Bilkis Auntie, and Uncle, Omar vai, Sukanta da and Sudeshna di, Anju Vabi and Mahboob Bhai for their kind support, help and for taking care of me. Thanks to my friends Fahad, Fahim, Rupam, Al-Mamun, Muhit, Sami, Nazrul, Reza, Sakeb, Sazu, Shahed, Rayhan, Touhid, Mehedi, Mazruk, Borhan, Choton, Leon, Ariful, Rashedul, Ahsan, Karim, Mahmud, Moshiur, Shams, Nazmush Shams, Adil, Mainul, Sohel, Shohan vai, Sufian vai, Papia Apu, Nekvi, Ridun vai, Saikat, Saidur vai, Rashed, Opu, Rana, Bappi, Asif, Russel, Sabreena, Moushumi, Palash, Naima, Amy (to name a few). Also my sincere thanks to the family members of all my friends. I am thankful to the members of the Bangladeshi community in Kitchener-Waterloo and in London, ON. Thanks to all my teachers and supervisors who have shared their knowledge with me and have enlightened me.

I am grateful to my parents, Dola, Shakil, my brothers and brother-in-laws, sisters and sister-in-laws, cousins, nephews and nieces, uncles, aunts and all my other family members for their kind prayers, love, encouragement and patience which helped me accomplish this endeavor. Finally, I express gratitude from the core of my heart to the hard working people of Bangladesh and Canada for providing me the necessary support throughout my academic career which helped me to achieve this feat.

Dedication

As threats on the planet's water resource continue to rise, we increasingly are being made aware of them and communities are working harder than ever to protect our water. The stories of initiatives to overcome existing and emerging challenges on our water inspire me and give me hope that one day my big hairy audacious dream of clean and safe water for everyone on this planet will come true. I hope and pray that my journey on the road towards making that dream a reality will continue to amaze me.

This work is a significant milestone in my journey. I am humbled and dedicate this work to previous, on-going and future pursuit of mankind to ensure clean and safe water.

Table of Contents

Author's Declaration	ii
Disclaimer	iii
Abstract	iv
Acknowledgements	vi
Dedication	ix
List of Figures	xiv
List of Tables	xxi
List of Acronyms	xxii
Chapter 1	1
Introduction	1
1.1 Problem statement	1
1.2 Research objectives and scope	5
1.3 Research Approach and Thesis Organization	6
Chapter 2	9
Behaviour and Fate of Perfluoroalkyl and Polyfluoroalkyl Substances (PFASs) in Drinking Water Treatment: A Review	9
Summary	9
2.1 Introduction	10
2.1.1 Occurrence in the aquatic environment	16
2.1.2 Occurrence in humans	17
2.1.3 Toxicity and regulatory framework	18
2.2 PFAS Properties	21
2.3 PFASs in Drinking Water	22
2.4 PFAS Removal during Drinking Water Treatment	26
2.4.1 Conventional coagulation, flocculation, sedimentation, and filtration	38
2.4.2 Oxidation processes	39
2.4.3 Granular activated carbon adsorption	41
2.4.4 Powdered activated carbon adsorption	47
2.4.5 Biodegradation	48

2.4.6 High pressure membranes	49
2.4.7 Resin Treatment	52
2.5 Knowledge Gaps and Research Needs	54
2.6 Conclusions	56
Chapter 3	58
Quantitative Analysis of Linear and Branched Perfluoroalkyl Carboxylic Acids in Water by Gas Chromatography/Mass Spectrometry (GC/MS)	58
Summary	58
3.1 Introduction	59
3.2 Experimental Section	62
3.2.1 Materials and Chemicals	62
3.2.2 Sample Preparation, Preservation and Background Contamination Prevention...	63
3.2.3 Solid Phase Extraction (Optimized Process)	64
3.2.4 Derivatization (Optimized Procedure)	66
3.2.5 Instrumentation and Quantification	66
3.2.6 Optimization of Reaction Conditions using Experimental Design	69
3.2.7 Calibration Curves, MDL, LOQ, Recoveries and Instrument Precision	72
3.3 Results and Discussion	73
3.3.1 Extraction Efficiency	73
3.3.2 Optimization of Derivatization Method	77
3.3.3 Identification and Quantification PFCAs with $C \geq 5$	82
3.3.4 Sample Preservation	85
3.3.5 PFBA Analysis	87
3.3.6 PFOA Isomer Analysis	88
3.4 Conclusions	89
Chapter 4	92
Treatment of Selected Perfluorinated Carboxylic Acids (PFCAs) using GAC, Ion Exchange Resins and Alternative Adsorbents in Ultrapure Water	92
Summary	92
4.1 Introduction	93
4.2 Materials and Methods	96

4.2.1 Target compounds and water	96
4.2.2 Adsorbents	96
4.2.3 Kinetic and isotherm tests.....	98
4.2.4 Analyses	99
4.3 Results and discussion.....	100
4.3.1 Adsorbent properties	100
4.3.2 Adsorption Kinetics	102
4.3.3 Adsorption isotherms	125
4.3.4 Comparison of PFCA adsorption with other trace organic contaminants	134
4.3.5 Effect of inorganic anions on PFOA removal by anion exchange resins	137
4.3.6 Effect of Resin Matrix and PFCA uptake mechanism by Anion Exchange Resins	141
4.3.7 Data Reproducibility.....	143
4.4 Conclusions	146
Chapter 5	149
PFCA Removal during Drinking Water Treatment by GAC and Ion Exchange from Surface Water: Effect of NOM and Inorganic Anions.....	149
Summary	149
5.1 Introduction	150
5.2 Materials and methods.....	154
5.2.1 Target compounds.....	154
5.2.2 Waters	154
5.2.3 Adsorbents	155
5.2.4 Kinetic tests.....	156
5.2.5 Analysis.....	157
5.3 Results and discussion.....	158
5.3.1 Adsorbent properties.....	158
5.3.2 PFCA Adsorption Kinetics	159
5.3.3 Effect of Surface water Matrix on PFCA Adsorption	167
5.3.4 Effect of PFCA Chain Length on PFCA adsorption.....	173
5.3.5 Effect of Solute Mixture on PFCA Removal.....	176

5.3.6 NOM Removal in GRW during Adsorption	178
5.3.7 Data Reproducibility	184
5.4 Conclusions	190
Chapter 6	193
Conclusions and Recommendations	193
6.1 Conclusions	193
6.1.1 Development of a GC/MS Analytical Method and Target Compound Selection	194
6.1.2 PFCA Adsorption Performance of the Selected Adsorbents	195
6.1.3 Effect of Adsorbent Properties on PFCA Adsorption.....	197
6.1.4 Effect of PFCA Carbon Chain Length.....	197
6.1.5 PFCA Mixtures vs. Adsorption of Individual PFCAs	198
6.1.6 Effect of Surface Water Matrix on PFCA Adsorption.....	198
6.1.7 NOM pretreatment potential of the selected adsorbents.....	199
6.2 Recommendations	200
References	202
APPENDIX-A	221
Quantification of Physico-Chemical Properties of PFCs Using Molecular Descriptors and Selection of Treatment Processes	221
APPENDIX-B	240
Blood Serum Half- life of Selected PFCs and Reported Drinking Water Occurrence of PFOA and PFOS	240
APPENDIX- C	248
Properties of the Selected Adsorbents.....	248
APPENDIX-D	282
Time Dependent PFCA Removal in Single Solute Adsorption Kinetic Experiments	282
APPENDIX-E	284
Additional Data on Kinetics and Isotherm Model Derived Adsorption Parameters	284

List of Figures

Figure 1.1: Thesis structure and relevance of the thesis chapters.....	8
Figure 2.1: Reported global concentration of PFOS/PFOA in drinking water by longitude (locations are approximate and were obtained using Google Earth®). Detailed data and study references can be found in Table B2 in Appendix B.....	24
Figure 2.2: Reported finished and raw drinking water concentration of selected PFASs at various full scale plants. A value of 0.1 ng/L was assigned when PFAS concentrations were either below the limit of detection (<LOD) or limit of reporting (<LOR) or not detected (ND). Boxed data points denote data from plants that use NF/RO membranes indicating high PFAS removals at those plants.....	29
Figure 2.3: PFOA-concentration in drinking water in Arnsberg, Germany between May 2006 and April 2008 indicating frequent need for GAC filter reactivation for PFOA removal (Hölzer et al. 2009; reprinted with permission from the publisher). Please note, PFOA concentration is reported in this figure in µg/L. Calgon F-100® was used as the GAC at the treatment plant. GAC info collected via personal communication with the corresponding author.	44
Figure 2.4: PFOA-concentration in raw and finished drinking water at Little Hocking, West Virginia, USA. Calgon F-600® GAC used at the treatment plant. Data collected from (Little Hocking Water Association 2010) and by personal communication with Mr. Bob Griffin, General Manager, Little Hocking Water Association.....	45
Figure 3.1: Overview of the derivatization reaction optimization procedure (adapted from Yu et. al. 2007)	72
Figure 3.2: A. 0.1% NH ₄ OH in methanol elution volume profile for C4-C9 (duplicates) extracted with WAX cartridges and B. Methanol elution volume profile for C5-C9 (duplicates) extracted with HLB cartridges, PFBA could not be analyzed using HLB cartridges.	75

Figure 3.3: Effect of drying eluates from A. WAX cartridges and B. HLB cartridges with nitrogen; butanol to n-hexane ratio 1:19 for WAX and 1:4 for HLB (n-hexane is used to extract derivatized butyl esters of PFCAs. Hence, the GC/MS response for WAX cartridges is represented as the adjusted mean by multiplying the mean area count by a factor 4.75); PFBA (C4) could not be analyzed using HLB cartridges; RSD: relative standard deviation of 3 replicates of each sample. 77

Figure 3.4: Contour plots for total desirability. 79

Figure 3.5: Summary of the derivatization process 81

Figure 3.6: Characteristic μ SIS (m/z: 131) chromatogram for: A) blank; B) 0.05 μ g/L; C) 3.0 μ g/L, D) characteristics full scale GC-EI-MS spectra of PFNA. 83

Figure 3.7: Analysis results in ultrapure (A) and river water (B) when water samples were stored at 4°C for 4 and 7 days and then extracted and analyzed; Error bars indicate standard deviation of 3 replicates of each sample 85

Figure 3.8: Analysis results in A) ultrapure water and B) river water when HLB cartridges were stored for up to 7 days in the freezer following sample extraction. After storage analytes were eluted from the cartridges and processed further; Error bars indicate standard deviation of 3 replicates of each sample 86

Figure 3.9: Full-scan chromatograms (A, B, C) showing PFCA peaks and effect of butanol to n-hexane ratio on PFBA detection; D) GC-EI-MS spectra of PFBA; E) μ SIS chromatogram (m/z: 131 + 169) showing C4-C9 PFCAs. 88

Figure 3.10: GC-EI-MS chromatograms showing several PFOA isomers, PFHpA, and PFHxA present in a PFOA technical mixture. 89

Figure 4.1: PFCA removal (%) as a function of time (d) for the tested sorbents in ultrapure water; plots A-C show presents data for mixed solute experiments (all three target PFCAs were spiked simultaneously); plot D shows data for single solute PFOA experiments (spiked individually);

target nominal spiked PFCA concentration was 3 µg/L; adsorbent dose was 10 mg/L; no pH adjustments were done. 106

Figure 4.2: Application of the pseudo-second-order model to the adsorption data of A) PFHpA, B) PFOA, C) PFNA onto selected carbonaceous adsorbents. Plots A1 and B1 show close-up view of plots A and B, respectively. The lines show linear fitting of the PFCA removals presented in Figure 4.1. 112

Figure 4.3: Application of the pseudo-second-order model to the adsorption of A) PFHpA, B) PFOA, C) PFNA onto the selected anion exchange resins. The lines show linear fitting of the PFCA removals presented in Figure 4.1 113

Figure 4.4: Graphical representation of the pseudo-second-order kinetic model parameters- A) equilibrium adsorption amount (q_e), and B) initial adsorption rate (θ). Model R^2 values for all sorbents except for CX indicate good fit to the data. The model was fitted to mixed solute data for all the sorbents except for the WV B-30 and C-Gran carbons using PFCA removal data presented in Figure 4.1. 115

Figure 4.5: Comparison of mixed solute addition vs individual solute addition in PFCA removal as a function of time in ultrapure water; A) PFHpA, B) PFOA, C) PFNA (open symbols indicate all three PFCAs were spiked simultaneously, colored symbols indicate only single solute spiked); nominal spiked PFCA concentration was 3 µg/L; adsorbent dose was 10 mg/L; no pH adjustments were done; plots A1, B1 and C1 present a close-up of the data points up to 5 days. 117

Figure 4.6: Graphical presentation of parameters for pseudo-second-order adsorption kinetics model fitted to time dependent PFCA removal data for mixed solute addition and single solute addition in ultrapure water; m- for mixed solute addition and s- for single solute addition. 118

Figure 4.7: Effect of PFCA chain length on PFCA removal as a function of time by different adsorbents in ultrapure water: A) A-500P ion exchange resin, B) A-860 ion exchange resin, C) F-400 GAC, D) Biochar. 120

Figure 4.8: Kinetics of PFCA adsorption on different adsorbents fitted by the intraparticle diffusion model. The model was fitted to mixed solute data presented in Figure 4.1 123

Figure 4.9: Single solute adsorption isotherms in ultrapure water on three adsorbents for the three target PFCAs: A. PFHpA, B. PFOA, C. PFNA. Data points; kin= kinetics data points (see Figure 4.1). 129

Figure 4.10: Single solute adsorption isotherms of the target PFCAs onto A) A-500P, B) A-860 and C) F-400 in ultrapure water. 133

Figure 4.11: Comparison of adsorbabilities of the three target PFCAs with other micropollutants on F-400 carbon in ultrapure water (ATZ- atrazine, CBZ-carbamazepine, NAP- naproxen, NP-Nonylphenol). Plotted lines were drawn based on fitted Freundlich isotherm parameters; isotherm data for PFCAs were used from the current study while those of other micropollutants were obtained from Yu et al. (2008) (for naproxen, carbamazepine and nonylphenol), Scheideman et al. (2006) (for atrazine) and Pirbazari et al. (1993) (for geosmin and MIB). 136

Figure 4.12: Effect of sulfate anion at different concentrations on PFOA removal kinetics in ultrapure water; Resin dose- 10 mg/L; plot A1 provides a closer look at the initial data points shown in plot A. 138

Figure 4.13: Graphical representation of the estimated pseudo-second-order model parameters for PFOA adsorption onto- A) A-500P and B) A-860 at different background sulfate concentration 139

Figure 4.14: Sulfate removal kinetics for A-500P and A-860 resins; ultrapure water (control) was spiked at two different concentrations: A) Control A- 1 mg/L sulfate and B) Control B- 30 mg/L sulfate; Resin dose- 10 mg/L. 140

Figure 4.15: Removal kinetics of PFOA in ultrapure water by anion exchange resins and uncharged resin beads; Open symbols are anion exchange resins and colored symbols indicate uncharged resin beads; adsorbent dose- 10 mg/L. 143

Figure 4.16: Removal of PFOA by anion exchange illustrating the reproducibility of removal trends by A) A-500P, B) A-860..... 145

Figure 4.17: Graphical representation of the pseudo-second-order model parameters for PFOA adsorption onto (A) A-500P and (B) A-860 during three different sets of experiments; data used for the model fitting is presented in Figure 4.16..... 146

Figure 5.1: PFCA removal over time for the selected adsorbents in Grand River water (GRW); plots A- C show results of mixed solute adsorption experiments (all three target PFCAs were spiked into single flasks of ultrapure water); plot D shows results of single solute experiments (only PFOA was spiked); no pH adjustments were done; PFCA initial concentrations for mixed solute experiments: PFHpA- 4.05 $\mu\text{g/L}$, PFOA- 3.58 $\mu\text{g/L}$; and PFNA- 3.56 $\mu\text{g/L}$; PFOA concentrations for single solute only experiments: 3.41-3.81 $\mu\text{g/L}$; adsorbent dose was 100 mg/L. 161

Figure 5.2: Application of the pseudo-second-order model to the PFCA adsorption in GRW onto the selected adsorbents; Plots: A) PFHpA, B) PFOA and C) PFNA; Plots A1, B1 and C1 provide close look at the plots A, B and C, respectively. The lines show linear fitting of the PFCA removals presented in Figure 5.1. 164

Figure 5.3: Graphical representation of pseudo-second-order kinetics parameters; the model was fitted to time dependent PFCA removal data presented in Figure 5.1. Plot A: Estimated equilibrium sorption amount (q_e); Plot B: Initial sorption rate (ϑ). 166

Figure 5.4: Comparison of pseudo-second-order kinetics model parameters (q_e -equilibrium adsorption amount, ϑ - initial adsorption rate) for the target PFCAs in ultrapure water (UPW) and GRW (mixed solute) illustrating the impact of GRW matrix on PFCA sorption kinetics; PFCA removal data presented in Figure 4.1 and Figure 5.1..... 169

Figure 5.5: Removal of selected anions present in GRW over time (Set 1). 171

Figure 5.6: Effect of carbon chain length on adsorption of target PFCAs in GRW for selected adsorbents. Plots show results of time dependent PFCA removal for mixed solute experiments

for different adsorbents; no pH adjustments were done; PFCA initial concentrations for mixed solute experiments: PFHpA- 4.05 $\mu\text{g/L}$, PFOA- 3.58 $\mu\text{g/L}$; and PFNA- 3.56 $\mu\text{g/L}$; adsorbent dose:100 mg/L. 175

Figure 5.7: Comparison of mixed solute addition vs. individual solute addition on PFCA removal in untreated Grand River water (GRW); adsorbent dose: 100 mg/L; initial target nominal PFOA spiking concentration - 3 $\mu\text{g/L}$; Plot A: Open symbols are for single solute spiking (PFOA only) and solid symbols indicate all 3 PFCAs were spiked simultaneously; data for the A-500P and A-860 resins are average to two replicates. Plot B: pseudo-second order model parameters fitted to data presented in plot A. CX and F-400 single solute experiments were conducted along with Set 1 mixed solute experiments. A-500P and A-860 single solute experiments were conducted along Set 2 mixed solute experiments. 177

Figure 5.8: Removal of DOC and different DOC fractions in GRW water over time; A) DOC, B) SUVA, C) biopolymers (BP), D) humics, E) building blocks (BB), F) UV_{254} ; Data presented here is for Set 1 experiments; initial DOC- 5.0 mg C/L, humics- 3.6 mg C/L, BP- 0.25 mg C/L, BB- 0.65 mg C/L; adsorbent dose- 100 mg/L. 180

Figure 5.9: Graphical representation of pseudo-second-order model parameters for removal data presented in Figure 5.8. Plot A: Estimated parameters for DOC Plot B: Estimated parameters for humics. 181

Figure 5.10: Removal of PFCAs by anion exchange resin in GRW illustrating the reproducibility of removal trends. Set 1 experiments were conducted on GRW collected in February 2012 and Set 2 experiments were conducted in GRW collected in May 2012. Error bars in Set-2 experiments indicate the maximum and minimum removals of two replicates..... 187

Figure 5.11: Graphical representation of pseudo-second-order model parameters for kinetics data presented in Figure 5.10. Plot A: Estimated equilibrium sorption amount (q_e); Plot B: Initial sorption rate (θ)..... 188

Figure 5.12: Removal of DOC and various DOC fractions by anion exchange resins in GRW illustrating the reproducibility of NOM removal trends. Set 1 experiments were conducted on

GRW collected in February 2012 and Set 2 experiments were conducted in GRW collected in
May 2012. DOC: 5.0 mg/L for Set 1 and DOC: 4.7 mg/L for Set 2. 189

List of Tables

Table 2.1: Structure and physico-chemical properties of selected perfluoroalkyl and polyfluoroalkyl substances (PFASs).....	13
Table 2.2. Drinking water advisory levels/goals/guideline values for PFOA and PFOS	20
Table 2.3: Reported full-scale drinking water treatment plant PFASs removal data.....	30
Table 3.1: Analysis parameters and method performance parameters	68
Table 3.2: Full matrix for the factorial design	70
Table 3.3 Statistical analysis of main effects and two factor interactions	80
Table 4.1: Properties of the GACs and the alternative adsorbents	101
Table 4.2: Properties of the anion exchange resins and the uncharged resin beads	102
Table 4.3: Fitted pseudo-second-order model parameters for adsorption kinetics data	114
Table 4.4: Intraparticle diffusion parameters	124
Table 4.5: Freundlich isotherm parameters for selected adsorbents in ultrapure water	128
Table 5.1: Properties of Grand River Water (GRW)	155
Table 5.2: Pseudo-Second-Order Kinetics Model Parameters in GRW for the target PFCAs for Set 1 Experiments.....	165
Table 5.3: PFCA concentrations at different time intervals showing PFCA removals by the anion exchange resins from spiked Grand River water for Set 1 and Set 2 experiments	186

List of Acronyms

AOP	Advanced oxidation process
BB	Building block
BET	Brunauer-Emmett-Teller
BP	Bipolymer
CAS	Chemical abstract
CBZ	Carbamazepine
CCL3	3 rd contaminant candidate list
CI	Chemical ionization
C4	Perfluorobutanoic acid
C5	Perfluoropentanoic acid
C6	Perfluorohexanoic acid
C7	Perfluoroheptanoic acid
C8	Perfluorooctanoic acid
C9	Perfluorononanoic acid
DFT	Density functional theory
DI	De-ionized
DOC	Dissolved organic carbon
EI	Electron impact
EfOM	Effluent organic matter
FASAs	Perfluoroalkane sulfonamides
FOSA	Perfluorooctane sulfonamide
FASEs	Perfluoroalkane sulfonamidoethanols
GAC	Granular activated carbon
GC/MS	Gas chromatography/mass spectrometry

GRW	Grand River Water
HLB	Hydrophilic lipophilic balance
H ₂ SO ₄	Sulfuric acid
IP	Instrument precision
IX	Ion exchange
kDa	Kilodalton
LC/MS	Liquid chromatography/mass spectrometry
LHWA	Little Hocking Water Association
LOQ	Limit of quantification
MDL	Method detection limit
MIEX [®]	Magnetic ion exchange resin
MRL	Method reporting limit
MS	Mass spectrometry
MW	Molecular weight
MWCO	Molecular weight cut-off
NAP	Naproxen
N-EtFOSE	N-ethyl perfluorooctane-sulfonamido ethanol
N-MeFOSE	N-methyl perfluorooctane-sulfonamido ethanol
NF	Nanofiltration
NCI	Negative chemical ionization
NOM	Natural organic matter
NP	Nonylphenol
NTU	Nephelometric turbidity unit
O ₃	Ozone
·OH	Hydroxyl radical

PAC	Powdered activated carbon
PFAAs	Perfluoroalkyl acids
PFASs	Perfluoroalkyl and polyfluoroalkyl substances
PFBA	Perfluorobutanoic acid
PFBS	Perfluorobutane sulfonic acid
PFCs	Perfluorinated compounds
PFCAs	Perfluoroalkyl carboxylic acids
PFDA	Perfluorodecanoic acid
PFDoDA	Perfluorododecanoic acid
PFHpA	Perfluoroheptanoic acid
PFHxA	Perfluorohexanoic acid
PFHxS	Perfluorohexane sulfonic acid
PFNA	Perfluorononanoic acid
PFOA	Perfluorooctanoic acid
PFOS	Perfluorooctane sulfonic acid
PFPeA	Perfluoropentanoic acid
PFSA _s	Perfluoroalkane sulfonic acids
PFUnDA	Perfluoroundecanoic acid
pg	Pico gram
pH _{pzc}	Point of zero charge
PP	Polypropylene
RO	Reverse osmosis
RSD	Relative standard deviation
4:2 FTOH	4:2 Fluorotelomer alcohol
6:2 FTOH	6:2 Fluorotelomer alcohol

8:2 FTOH	8:2 Fluorotelomer alcohol
10:2 FTOH	10:2 Fluorotelomer alcohol
SPE	Solid phase extraction
SPME	Solid phase microextraction
SUVA	Specific UV absorbance
UCMR3	3 rd unregulated contaminant monitoring rule
UF	Ultrafiltration
USEPA	United States Environmental Protection Agency
UV	Ultraviolet
UPW	Ultrapure water
WAX	Weak anion exchange
WTP	Wastewater treatment plant

Chapter 1

Introduction

1.1 Problem statement

Perfluorinated compounds (PFCs) are an emerging class of anthropogenic environmental contaminants that have been ubiquitously detected in various environmental matrices around the globe. These compounds are a diverse class of chemicals that have in common, a carbon backbone usually 4-14 carbons in length, in which all hydrogen atoms have been replaced by fluorine, hence, they are termed as perfluorinated (Lau et al. 2007). Different groups of PFCs are characterized by their functional groups. PFCs exhibit high thermal and chemical stability owing to the carbon-fluorine bond, and as such have found applications in numerous industrial and consumer products. In about the year 2000 the scientific community became aware of the widespread occurrence of PFCs at low concentrations in the environment, wildlife, and humans (Betts 2007), and since then there has been a heightened interest in properties, occurrence, fate, and toxicological significance of these compounds.

Perfluorinated alkyl acids (PFAAs) contain a hydrophobic alkyl chain and a hydrophilic charged functional group which typically includes carboxylate, sulfonate, or phosphonate. Surfactants are generally categorized into four classes: anionic, cationic, nonionic and amphoteric, with PFAAs being in the anionic class (Kissa 2001). Perfluorooctane sulfonate (PFOS) and perfluorooctanoic acid (PFOA) are the two anionic PFCs which have received most attention to date. They have been produced in large volumes since the inception of commercial production in the late 40's. The 3M Company started commercial manufacturing of fluorinated alkyl substances using Joseph Simons' electrochemical fluorination process in 1949 (Schultz et al. 2003; Paul et al. 2009). Later in the 1970's the DuPont Company developed the telomerization fluorination

process (Schultz et al. 2003; Vestergren and Cousins 2009). Typically, electrochemical fluorination products contain many branched isomers while telomerization predominantly produces linear isomers (Martin et al. 2004).

The toxicological effects of PFCs on humans are yet to be fully quantified. However, adverse health impacts including cancer and birth defects have been reported in laboratory animals and wildlife (Lau et al. 2007; USEPA 2009a). Studies have linked PFCs to thyroid disease, fecundity, obesity, increased impulsivity, and delayed puberty (Fei et al. 2009; Fei et al. 2007; Gump et al. 2011; Melzer et al. 2010; Holtcamp 2012).

PFCs have been detected in wastewater, surface water, groundwater, drinking water, and even in rainwater at trace concentration levels ($\mu\text{g/L}$ - ng/L) (Ullah et al. 2011; Rahman et al. 2014; Ahrens 2011; Ahrens et al. 2011; Moeller et al. 2010; Boulanger et al. 2005). Considering their occurrence in drinking water, the USEPA included PFOA and PFOS in its third drinking water contaminant candidate list (CCL3) (USEPA 2011a). In addition, the USEPA also included six PFCs in the final list of the 3rd unregulated contaminant monitoring list (UCMR3) (USEPA 2011b). PFOS was listed as a persistent organic pollutant at the 2009 United Nations Stockholm convention on persistent organic pollutants (Wang et al. 2009). The manufacture, use, or sale of PFOS related products are 'prohibited' in Canada (except for fume suppressants, semiconductors or similar components, and available stock of PFOS based aqueous film forming foams) under the Canadian Environmental Protection Act (Government of Canada 2008). Considering potential environmental impacts, 3M, the largest manufacturer of PFOS, voluntarily phased out PFOS production in 2001. However, since PFCs were produced in large volumes since the 1970's, large amounts of these products have been released in the environment or are still on the market. Ironically, while production in developed countries becomes regulated, production of

PFCs such as PFOS has been increasing sharply in other countries that lack appropriate regulations (USEPA 2009a). Thus, environmental threats remain a valid concern as PFC containing products continue to be imported.

PFCs are released in the environment following their industrial production and widespread application in consumer products. They can also occur from the degradation of precursor compounds. Since most sewage treatment processes cannot remove them efficiently, PFCs find their way into surface water and as they are resistant to environmental degradation and most conventional drinking water treatment processes, they may be detected in drinking water at low ng/L concentrations (Mak et al. 2009; Quinones and Snyder 2009; Takagi et al. 2011; Takagi et al. 2008). From a precautionary principle, drinking water should contain the least possible number and concentration of synthetic organic compounds (McDowell et al. 2005; Huber et al. 2003). As the demand for clean water increases, occurrence of contaminants such as PFCs in raw and finished water has added another challenge to the burgeoning number of challenges the drinking water industry is facing.

Few full-scale and bench-scale studies focusing on PFCs removal during drinking water treatment are available. PFC surveys of raw and finished drinking water indicate that conventional coagulation, flocculation, and sedimentation processes are unable to remove these compounds. Oxidation processes are also not expected to be effective (Takagi et al. 2008; Appleman et al. 2014; Thompson et al. 2011b). From the limited database, membrane filtration, activated carbon adsorption, and ion exchange look promising. Steinle-Darling and Reinhard (2008) indicated that NF and RO membranes can achieve high removal. There are studies available that indicate that adsorption and ion exchange treatment may also be promising techniques (Yu et al. 2009a; Lampert et al. 2007; Hansen et al. 2002; Appleman et al. 2013).

Activated carbon (AC), both in powdered (PAC) or granular (GAC) form, is widely employed for controlling regulated synthetic organic chemicals, taste and odor compounds, and natural organic matter (NOM) in drinking water. GAC has been suggested as the ‘best available technology’ for controlling synthetic organic compounds by USEPA (USEPA 2009b). Ion exchange treatment has been found to be effective in controlling inorganic anions such nitrate in drinking water and has been approved by the USEPA as a ‘best available technology’ for removal of nitrate (USEPA 2009b). Thus, ion exchange treatment although not frequently employed at full-scale fresh water drinking water treatment utilities, may as well be effective in removing anionic PFCs. The effects of GAC base material type, pore size distribution, and surface charge on PFCA adsorption are not well documented. The effect of ion exchange resin matrix on PFCA adsorption is not clear and studies have reported varying PFCA adsorption trends. In addition, there is a lack of knowledge regarding the mechanisms that are involved during ion exchange treatment of PFCAs. Overall, there is a lack of understanding regarding the fate of PFCs during GAC adsorption and ion exchange treatment in drinking water.

PFCs are diverse in chemical structure with varying carbon chain length and functional groups leading to numerous congeners. Thus, selecting suitable target compounds for a treatment study from a large a pool of PFCs that may be relevant for drinking water industry is challenging. Physico-chemical properties can greatly influence the behaviour and fate of contaminants during water treatment processes. Experimental values of various physico-chemical properties of PFCs are often not known or are the subject of debate. Researchers have previously calculated properties of various PFCs using computer models (Goss 2008; Rayne and Forest 2009; Wang et al. 2011a,b; Bhattacharai and Gramatica 2011). Due to their presence in the aquatic environment at only trace levels their detection in aquatic matrices poses an analytical challenge. Liquid

chromatography/mass spectroscopy (LC/MS) methods have been typically used by researchers to analyze PFCs in environmental samples. At present, only a few methods have been published using gas chromatography/mass spectrometry (GC/MS) which in part can be attributed to the low volatility of these compounds (Moody and Field 1999; Langlois et al. 2007; Scott et al. 2006; Dufková et al. 2012). In addition, there are complexities involving the derivatization and pre-concentration steps. However, GC/MS can generate reliable results if an analytical method can be successfully implemented or developed. Therefore, developing or adopting an effective analytical method utilizing GC/MS was integral to the conduct of the proposed research.

1.2 Research objectives and scope

The primary objective of this research was to investigate the behaviour and fate of selected perfluorinated compounds (PFCs) during adsorption and ion exchange treatment of drinking water. The specific objectives were to:

- Select target PFCs that are relevant to the drinking water industry and are also amenable to a GC/MS analytical method
- Develop a GC/MS analytical method for simultaneously analyzing selected PFCs at trace concentrations (ng/L- µg/L) in water
- Assess removal efficiency of selected PFCs using a suite of commercially available GACs, ion exchange resins, and alternative adsorbents in ultrapure water, to understand adsorption capacity and adsorption behaviour of the target PFCs onto the selected adsorbents and to narrow down the number of adsorbents for further performance evaluation in surface water

- Investigate the effect of physico-chemical properties of the selected adsorbents on adsorption of the target PFCs in ultrapure water and surface water
- Study the effect of PFC chain length and direct competition among the selected PFCs on their adsorption in ultrapure and surface water
- Evaluate the impact of surface water characteristics such as NOM, various NOM constituents, and inorganic anions on adsorption of the target PFCs onto the selected adsorbents
- Evaluate the NOM removal potential of the selected adsorbents from surface water to assess the potential of anion exchange resins and the alternative adsorbent, Biochar, as possible NOM pretreatment for GAC adsorbents targeting PFCs

1.3 Research Approach and Thesis Organization

This thesis is organized in six chapters. Chapters 2, 3, 4 and 5 were prepared in journal article format with one (Chapter 2) having been published at the time of publication of this dissertation. Chapter 2 provides a literature review of PFC removal during drinking water treatment with particular focus being on full-scale plant survey data. Discussions on treatment processes other than GAC adsorption and ion exchange treatment, although not part of the current investigation were included for completeness. Chapter 3 discusses the GC/MS method development work for several PFCs belonging to the class of perfluorinated carboxylic acids (PFCAs). Following the development of the GC/MS analytical method, three PFCAs- perfluoroheptanoic acid (PFHpA), perfluorooctanoic acid (PFOA), and perfluorononanoic acid (PFNA) were selected for subsequent treatment studies. Chapter 4 describes the study to elucidate adsorption behaviour of the PFCAs on selected adsorbents in ultrapure water. Results included in Chapter 4 assisted with

narrowing down the number of adsorbents for subsequent evaluation of PFCA removal performance in surface water. Details of the study conducted on PFCA removal and adsorption behaviour onto selected adsorbents in surface water is provided in Chapter 5. Finally, Chapter 6 provides a summary of the research project findings. In addition, several relevant recommendations for future studies investigating PFC removal during drinking water treatment are suggested. Figure 1.1 presents the thesis structure and relevance of each chapter.

To facilitate accomplishment of the research objectives some preliminary work was conducted. Initially, a suite of candidate PFCs were selected as potential target compounds for the project. Following that, physico-chemical properties of the selected target PFC candidates, along with a number of other micropollutants that have been widely studied or belong to a similar category of chemicals, were assessed and compared with the PFCs. Molecular descriptors values were either acquired from a database or in absence of a database values were calculated using established computer models to determine or predict physico-chemical properties. In the absence of experimental values, evaluation using computer models assisted with the prediction of the behaviour and fate of PFCs during drinking water treatment. The evaluation and review of the published literature assisted in selecting the PFCs used in this project. In addition, this preliminary work allowed narrowing down the drinking water treatment processes that could be used to remove the target PFCs. Details of the preliminary work are provided in Appendix-A. Appendix B-E provides information regarding the analysis of the adsorbent properties and also includes supporting information pertaining to Chapters 2, 4 and 5.

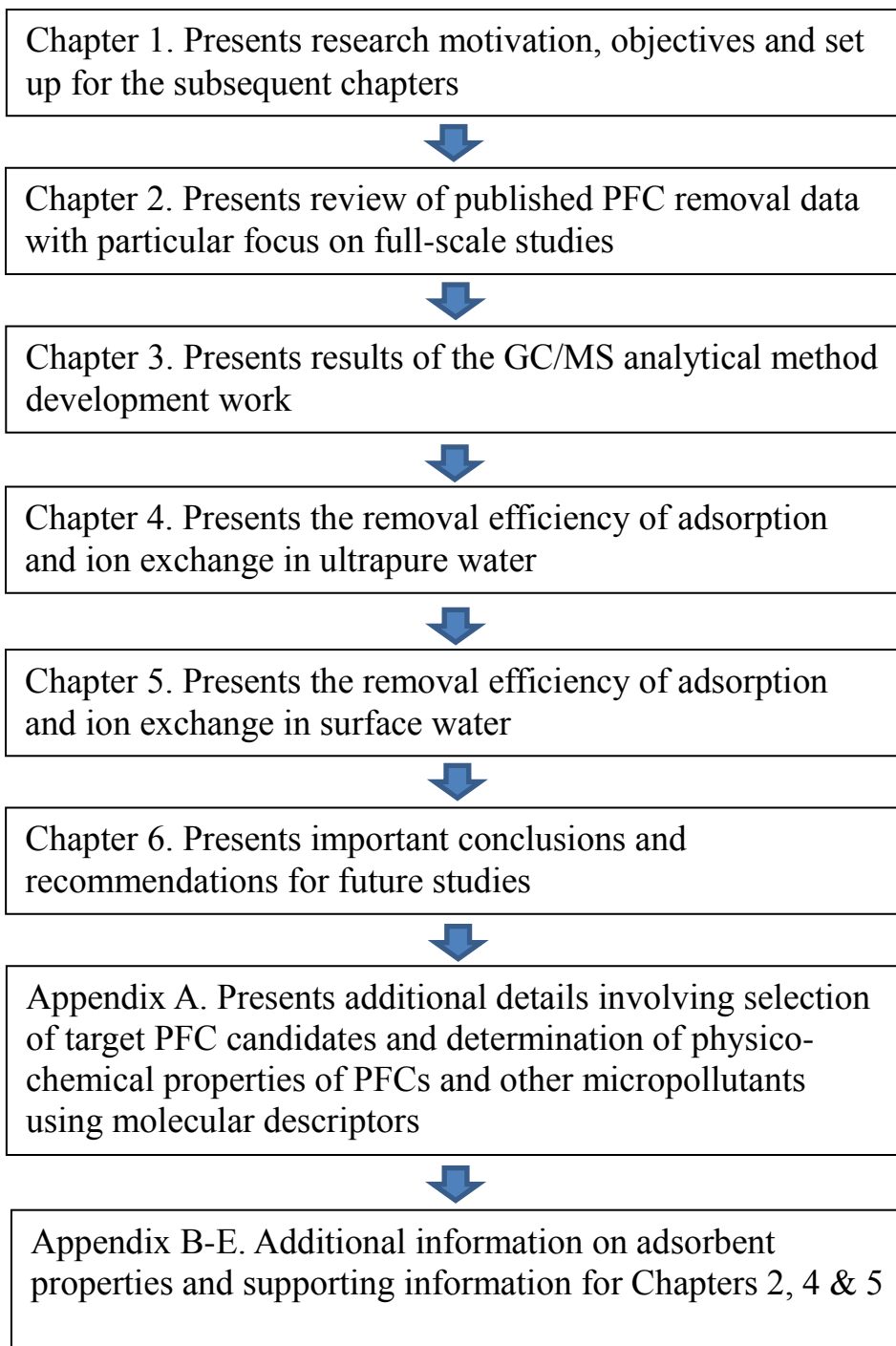


Figure 1.1: Thesis structure and relevance of the thesis chapters

Chapter 2

Behaviour and Fate of Perfluoroalkyl and Polyfluoroalkyl Substances (PFASs) in Drinking Water Treatment: A Review

This chapter forms the basis of a published article with the same title in the Journal Water Research (March 2014) volume 50 issue 7 pages 318-340. Cited references are in the consolidated list of references at the end of the thesis.

The article reviewed the behavior of PFASs during drinking water treatment. It focused on the available full-scale plant data (as reported in the peer-reviewed literature), with some brief discussion of bench-scale studies. In addition, the article identifies research gaps which will need to be addressed should regulation of these compounds come to pass. To introduce readers to the issue, the article set the stage with a brief discussion of PFAS toxicity, regulatory considerations, and properties of this unique and widely used class of chemicals. The article was intended to contribute to the ongoing discussion on behaviour, fate and treatment of PFASs in drinking water.

Summary

This article reviews perfluoroalkyl and polyfluoroalkyl substance (PFAS) characteristics, their occurrence in surface water, and their fate in drinking water treatment processes. PFASs have been detected globally in the aquatic environment including drinking water at trace concentrations and due, in part, to their persistence in human tissue some are being investigated for regulation. They are aliphatic compounds containing saturated carbon-fluorine bonds and are resistant to chemical, physical, and biological degradation. Functional groups, carbon chain

length, and hydrophilicity/hydrophobicity are some of the important structural properties of PFASs that affect their fate during drinking water treatment. Full-scale drinking water treatment plant occurrence data indicate that PFASs, if present in raw water, are not substantially removed by most drinking water treatment processes including coagulation, flocculation, sedimentation, filtration, biofiltration, oxidation (chlorination, ozonation, AOPs), UV irradiation, and low pressure membranes. Early observations suggest that activated carbon adsorption, ion exchange, and high pressure membrane filtration may be effective in controlling these contaminants. However, branched isomers and the increasingly used shorter chain PFAS replacement products may be problematic as it pertains to the accurate assessment of PFAS behaviour through drinking water treatment processes since only limited information is available for these PFASs.

2.1 Introduction

Perfluoroalkyl and polyfluoroalkyl substances (PFASs) are a diverse class of chemicals that have in common an aliphatic carbon backbone in which hydrogen atoms have been completely (prefix: per-) or partially (prefix: poly-) replaced by fluorine. These substances, owing to their highly polar and strong carbon-fluorine bonds, have some unique chemical attributes including extremely high thermal and chemical stability. They are primarily used as surfactants in numerous industrial and consumer products such as firefighting foams, alkaline cleaners, paints, non-stick cookware, carpets, upholstery, shampoos, floor polishes, fume suppressants, semiconductors, photographic films, pesticide formulations, food packaging, masking tape, denture cleaners, etc. (e.g. Kissa 2001; Brooke et al. 2004).

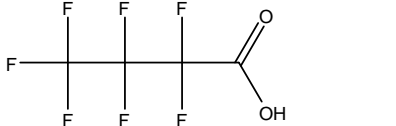
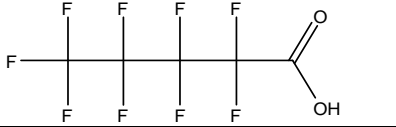
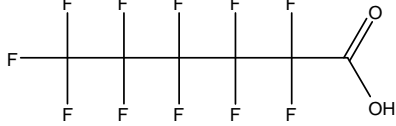
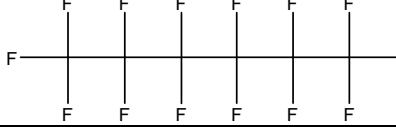
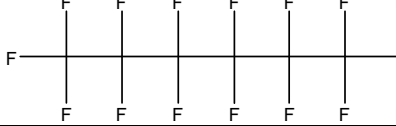
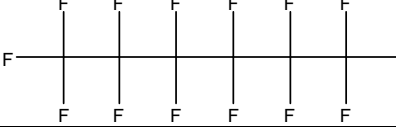
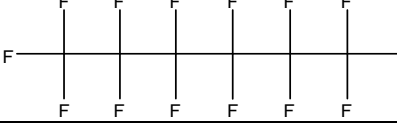
This review follows the terminology recommended by Buck et al. (2011) and uses PFAS instead of the more commonly used acronym PFC (perfluorinated compound). PFASs are characterized

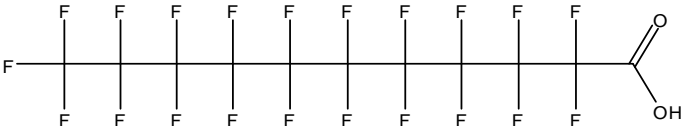
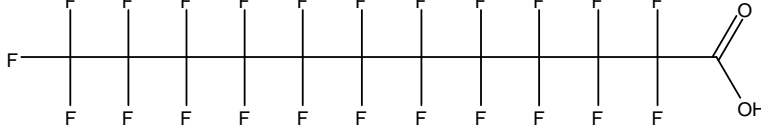
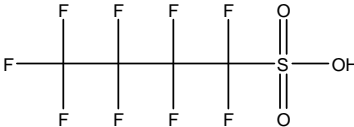
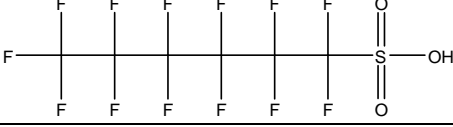
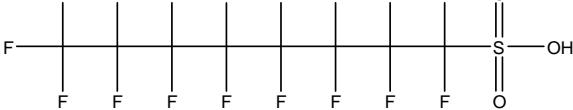
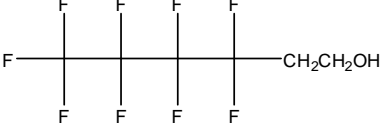
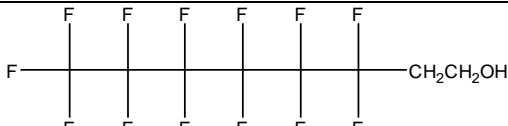
by their functional groups. Table 2.1 presents the structures and some important environmental properties of selected, most prominently studied PFASs. There are numerous other PFAS compounds in use, for example phosphorus containing PFASs which have only very recently been detected in surface, drinking, and waste waters (D'Eon et al. 2009; Ding et al. 2012). Further details regarding structure and nomenclature of PFASs are provided in Buck et al. (2011). Those that to-date have received most attention are the perfluoroalkyl acids (PFAAs), perfluoroalkyl sulfonamides (FASAs), and telomer alcohols (FTOHs). Two important classes of PFAAs are the perfluoroalkyl carboxylic acids (PFCAs) and the perfluoroalkyl sulfonic acids (PFSAs). A wide range of perfluoroalkyl chain lengths and branching patterns exists. Since PFASs are usually applied in technical mixtures both linear and branched isomers occur in the environment. However, the current lack of knowledge about the detailed composition of these technical mixtures and the inaccessibility of suitable analytical standards for branched isomers make it challenging to quantify many PFAS isomers accurately in environmental matrices. This constrains the understanding of the fate and toxicity of individual PFAS isomers in the environment, and also limits our understanding of their behaviour in water treatment processes.

Most PFASs are extremely resistant to degradation (e.g. Kissa 2001) and have therefore been detected ubiquitously in the aquatic environment. Some have even been detected at low concentrations in drinking water (pg/L to $\mu\text{g/L}$) making it a potential PFAS exposure route for humans. Post et al. (2012) reviewed available information on PFOA, its sources and occurrence in drinking water, toxicokinetics, and health effects. Information covered in their review “suggests that the continued human exposure to even low concentrations of PFOA in drinking water results in elevated body burdens that may increase the risk of health effects.”

Earlier reviews (Rayne and Forest 2009; Vecitis et al. 2009; Lutze et al. 2011, Eschauzier et al. 2011) on removal of PFASs from drinking water and wastewater focused primarily on bench scale studies and have discussed various conventional and promising, though less commonly employed treatment options (e.g. photolysis, sonolysis, thermolysis etc.). However, there is a growing body of literature on PFAS in full-scale water treatment plants. Thus, the objective of this article is to critically review and summarize published PFAS drinking water treatment data reported in full-scale plants and to explain, where possible, the underlying mechanisms for the observed behaviour of PFASs by integrating the findings of select bench-scale studies. To provide further context this review also includes brief summaries of the occurrence of PFASs in source water, their toxicological significance and regulatory status, occurrence of PFASs in drinking water globally, and PFAS properties relevant to drinking water treatment.

Table 2.1: Structure and physico-chemical properties of selected perfluoroalkyl and polyfluoroalkyl substances (PFASs)

Compound Name & CAS Registry #	Structure	^a MW	log K _{OC} (L/kg)	Solubility (mg/L)	Vapor Pressure (Pa)
Perfluoroalkyl acids (PFAAs)					
<i>Perfluoroalkyl carboxylic acids (PFCAs)</i>					
Perfluorobutanoic acid (PFBA) [375-22-4]		214.1			851 ^b (25°C)
Perfluoropentanoic acid (PFPeA) [2706-90-3]		264.1			
Perfluorohexanoic acid (PFHxA) [307-24-4]		314.1			
Perfluoroheptanoic acid (PFHpA) [375-85-9]		364.1		118,000 ^c (21.6°C)	20.89 ^b (25°C)
Perfluorooctanoic acid (PFOA) [335-67-1]		414.1	1.47 ^d	4340 ^c (24.1°C)	4.17 ^b (25°C)
Perfluorononanoic acid (PFNA) [375-95-1]		464.1	2.06 ^d		1.29 ^b (25°C)
Perfluorodecanoic acid (PFDA) [335-76-2]		514.1	2.37 ^d	260 ^c (22.4°C)	0.23 ^b (25°C)

Compound Name & CAS Registry #	Structure	^a MW	log K _{OC} (L/kg)	Solubility (mg/L)	Vapor Pressure (Pa)
Perfluoroundecanoic acid (PFUnDA) [2058-94-8]		564.1	2.32 ^d	92.3 ^c (22.9°C)	0.10 ^b (25°C)
Perfluorododecanoic acid (PFDoA) [307-55-1]		614.1			0.008 ^b (25°C)
Perfluoroalkane sulfonic acids (PFSAs)					
Perfluorobutane sulfonic acid (PFBS) [375-73-5]		300.1		510 ^e	
Perfluorohexane sulfonic acid (PFHxS) [355-46-4]		400.1	0.97 ^d		
Perfluorooctane sulfonic acid (PFOS) [1763-23-1]		500.1	2.10 ^d	570 ^f	3.31×10 ⁻⁴ (25°C) ^f
Precursor compounds— Fluorotelomer alcohols, perfluoroalkane sulfonamides and perfluoroalkane sulfonamidoethanols					
Fluorotelomer alcohols (FTOHs)					
4:2 Fluorotelomer alcohol (4:2 FTOH) [2043-47-2]		264.1	0.93 ^g	974 ^g (22.5°C)	992 ^h (25°C)
6:2 Fluorotelomer alcohol (6:2 FTOH) [647-42-7]		364.1	2.43 ^g	18.8 ^g (22.5°C)	713 ^h (25°C)

Compound Name & CAS Registry #	Structure	^a MW	log K _{OC} (L/kg)	Solubility (mg/L)	Vapor Pressure (Pa)
8:2 Fluorotelomer alcohol (8:2 FTOH) [678-39-7]		464.1	3.84 ⁱ	0.194 ⁱ (22.3°C)	254 ^h (25°C)
10:2 Fluorotelomer alcohol (10:2 FTOH) [865-86-1]		564.1	6.20 ^g	0.011 ^g	144 ^h (25°C)
Perfluoroalkane sulfonamides (FASAs)					
Perfluorooctane sulfonamide (FOSA) [754-91-6]		499.14	2.56 ^d		
N-Alkyl Perfluoroalkane sulfonamidoethanols (FASEs)					
N-methyl perfluorooctane sulfonamidoethanol (N-MeFOSE) [24448-09-7]		557.22		0.81 ^b (25°C)	0.70 ⁱ (25°C)
N-ethyl perfluorooctane sulfonamidoethanol (N-EtFOSE) [1691-99-2]		571.25		0.89 ^b (25°C)	0.35 ^j (25°C)

- a) United States National Library of Medicine (2011); b) Bhatarai and Gramatica (2011); c) Kaiser et al. (2006); d) Awad et al. (2011); e) Jensen et al. (2008); f) Stock et al. (2009); g) Liu and Lee (2007); h) Stock et al. (2004); i) Liu and Lee (2005); j) Lei et al. (2004)
- Data presented in this table are mostly experimental data; detailed model predicted data can be found at Bhatarai and Gramatica (2011)

2.1.1 Occurrence in the aquatic environment

Giesy and Kannan (2001) were among the first to report the widespread distribution of PFASs, which are released in the environment during their industrial production and application, and also as a result of leaching from, and degradation of, consumer products. Eventually, PFASs enter wastewater treatment plants (WWTPs) and as such WWTPs have been suggested as one of the major point sources of PFASs to surface waters (Boulanger et al., 2005; Sinclair and Kannan, 2006; Moeller et al. 2010; Xiao et al. 2012a) and the atmosphere (Ahrens et al. 2011). In addition, discharge of PFASs contained in industrial waste or biosolids has been reported to contaminate surface and groundwater (Paustenbach et al. 2007; Hölzer et al. 2008; Minnesota Department of Health 2008). Degradation of compounds such as FTOHs and FASAs lead to the formation of PFAAs (Ellis et al. 2003; Dinglasan et al. 2004; Wallington et al. 2006; Stock et al. 2007) and hence, these are often termed PFAA precursors.

High water solubility, simultaneous hydrophobic/hydrophilic properties, and low volatility of most PFAA contribute to their presence in all aquatic environments and even rain water. Although about 40 different PFASs have been detected in water (Ahrens 2011), most studies have targeted PFOS and PFOA since, in many cases where several PFASs were monitored in water, PFOS and PFOA were detected more frequently and at the highest concentrations (Yamashita et al. 2005; Hoehn et al. 2007; Quinones and Snyder 2009; Thompson et al. 2011a). Other frequently detected compounds include PFBA, PFH_xA, PFHpA, PFNA, PFDA, PFBA, PFH_xS, and FOSA (Table 2.1). PFBS and PFBA, two possible short chain replacement compounds for PFOS and PFOA (Renner 2006; USEPA 2012) were found to be the dominant PFASs in recent studies (Minnesota Department of Health 2008; Moeller et al. 2010; Ahrens et al. 2010). As the regulations around PFOA and PFOS become more stringent it is probable that

the use of other fluorinated organics will increase. In addition, many other PFASs not covered in this review are currently in use. An example are phosphorus containing fluorinated organics such as polyfluoroalkyl phosphates (PAPs), perfluorinated phosphonic acids (PFPA), and perfluorinated phosphinic acids (PFPIA) which have been detected in surface water, wastewater, effluents and in drinking water (D'Eon et al. 2009; Ding et al. 2012). Hence, compounds other than PFOA and PFOS should also be considered for monitoring studies.

Typical PFAS concentrations in water range from pg/L to ng/L. However, higher concentrations ($\mu\text{g/L}$ to even mg/L) have been detected in surface and groundwater following firefighting activities or explosions (Moody and Field 1999; Moody et al. 2002; Moody et al. 2003; Rumsby et al. 2009), and in some waters adjacent to fluorochemical manufacturing facilities (Hansen et al. 2002; Minnesota Department of Health 2008; Hoffman et al. 2011). A critical review of the occurrence of PFASs in the aquatic environment has been published by Ahrens (2011). The occurrence of PFASs in drinking water is discussed in detail in Section 2.3.

2.1.2 Occurrence in humans

Low-level (typically ng/mL concentrations) of PFASs, notably PFOA and PFOS, have been detected in human tissue and blood serum worldwide (Kannan et al. 2004; Karrman et al. 2007; Monroy et al. 2008; Pan et al. 2010, Llorca et al. 2010; Ingelido et al. 2010; Liu et al. 2011a). PFOA was detected in blood serum at a mean concentrations of 122 ± 81 and 424 ± 333 ng/mL in two communities in Ohio that were exposed to PFOA-contaminated drinking water (Bartell et al. 2010). Emmett et al. (2006) have previously shown that drinking water contaminated with PFOA (released from the nearby DuPont Washington Water Works) was the major exposure route and the “residential water source was the primary determinant of serum PFOA.”

2.1.3 Toxicity and regulatory framework

Although there is a growing body of literature on PFAS toxicity in animal models, data on the toxicological effects of PFASs on humans are limited (e.g. Steenland et al. 2010). Even for PFOA, “to-date data are insufficient to draw firm conclusions regarding the role of PFOA for any of the diseases of concern” (Steenland et al. 2010). However, a recently published study conducted on a large cohort of mid-Ohio valley residents that were exposed to contaminated drinking water or had worked at the local DuPont Washington Works chemical plant found PFOA to be associated with kidney and testicular cancer in that community (Barry et al. 2013). Other epidemiological studies have suggested a link between blood serum levels of certain PFASs and low birth weight (Fei et al. 2007), infertility-measured as longer waiting time to pregnancy (Fei et al. 2009), onset of early menopause in women (Knox et al. 2011), increased impulsivity and delayed puberty in children (Gump et al. 2011; Lopez-Espinosa et al. 2011), low semen quality in young men (Joensen et al. 2009), and thyroid disease in the US general adult population (Melzer et al. 2010). PFOA has recently been included on a list of ‘obesogens’, chemicals that may contribute to obesity (Janesick and Blumberg 2011; Holtcamp 2012). Longer chain carbon PFASs (> C8) have been reported to bioaccumulate in wildlife and humans (Hekster et al. 2003; Martin et al. 2003; Houde et al. 2008; Conder et al. 2008). Once PFASs enter the body they are poorly eliminated. The reported serum half-life of perfluorohexane sulfonate (PFHxS), PFOS, and PFOA in humans is 8.5 years, 5.4 years, and 2.9-8.5 years, respectively (USEPA 2009a; Seals et al. 2011) (Table B1 in Appendix-B). The slow elimination rates of PFASs suggest that “continued exposure could increase body burdens to levels that would result in adverse outcomes” (USEPA 2009a).

The USEPA has recently included PFOA and PFOS in its pared-down third drinking water contaminant candidate list (CCL3) of 32 compounds for further regulatory studies (USEPA 2011a). The agency also included six PFASs (PFBS, PFHxS, PFOS, PFHpA, PFOA and PFNA) in its final list of 32 contaminants for the unregulated contaminants monitoring rule 3 (UCMR3) (USEPA 2011b) thereby collecting occurrence data to assist with the development of future regulations should they be required. Drinking water advisory levels/goals/guideline values for PFOS and PFOA in various jurisdictions are listed in Table 2.2. It is evident that wide variations in drinking water guidelines among jurisdictions exist. This is likely due to differences in interpreting toxicity data or the safety factors taken into consideration to calculate those guideline values.

PFOS was recently listed as a persistent organic pollutant by the Persistent Organic Pollutants Review Committee (POPRC) of the United Nations Stockholm Convention on Persistent Organic Pollutants (POPRC 2009; Wang et al. 2009) and efforts are underway in various jurisdictions in the developed world to limit or ban PFAS use (EU Directive 2006; Government of Canada 2008). A review of existing regulatory guidelines surrounding PFASs can be found in Zushi et al. (2012). However, concern for potential environmental release remains, in part due to emissions from the existing inventories. Also, while production in the US, Europe, and other developed countries becomes increasingly regulated, production of PFASs such as PFOS has been increasing sharply in other regions (USEPA 2009a) thereby merely shifting production from one region to another (Lindstrom et al. 2011). Hence, strong concerted global regulatory initiatives are highly desirable to address PFAS emissions on a global scale (Lindstrom et al. 2011).

Table 2.2. Drinking water advisory levels/goals/guideline values for PFOA and PFOS

Regulatory body (Jurisdiction)		PFOS (ng/L)	PFOA (ng/L)	References
USEPA (US) <i>Provisional health advisory value</i>		200	400	USEPA (2011c)
Minnesota Department of Health (MDH) (Minnesota, US) ^a <i>Health risk limit</i>		300	300	Minnesota Department of Health (2011)
New Jersey Department of Environmental Protection (New Jersey, US) <i>Health-based drinking water concentration for PFOA</i>			40	Post et al. (2009)
German Drinking Water Commission (Germany) <i>Health-based precautionary values</i>		Immediate precautionary action value (combined PFOA and PFOS) Infants and pregnant women: 500 Adult: 5000		Trinkwasserkommission (2006)
		Chronic precautionary action value (combined PFOA and PFOS): >100-600 ng/L; combined PFOA and PFOS value for maximum of 10 years >600-1500 ng/L for a maximum of 3 years		
Drinking water inspectorate (DWI) (UK) <i>Guidance values</i>	Tier 2	>300	>300	DWI (2009)
		Action: Monitor levels and consult with health professionals		
	Tier 3	>1,000	>5,000	
		Action: In addition to Tier 2 actions take measures to reduce concentration to < 1,000 ng/L and <10,000 ng/L for PFOS and PFOA, respectively as soon as is practicable.		
Tier 4	>9,000	>45,000		
	Action: In addition to Tier 3 actions take measures to reduce exposure from drinking water within 7 days; ensure consultation with health professionals takes place as soon as possible.			

^a MDH has also set health guideline values for PFBS and PFBA at 7000 ng/L

2.2 PFAS Properties

In fluorinated surfactants (including PFASs), the hydrophobic part of the molecule is either partially or completely fluorinated and can be straight chained or branched. The C—F bond is one of the strongest known and the bond is stronger with increasing replacement of hydrogen by fluorine at each carbon (O'Hagan 2008). As such the more substituted the PFASs are, the less reactive (i.e. more chemically inert) they become. PFASs in general can withstand heat, acids, bases, reducing agents, oxidants, as well as photolytic, microbial, and metabolic degradation processes (Kissa 2001; Schultz et al. 2003). Limited experimental data on hydrophobicity, acidity constants (pKa), and partitioning constants are available (Rayne and Forest 2009) and what is available is often limited to linear forms of PFASs. The available experimental data and calculated pKa values indicate that both PFCAs and PFASs are strong acids which will predominantly be in their dissociated, negatively-charged form at environmentally relevant pH values (Kaiser et al. 2006; Rayne and Forest 2009; Buck et al. 2011). Precursor compounds (i.e. FTOHs and FASAs) are generally neutral and will remain undissociated at pH values typically encountered in water.

PFCAs and PFSAs have low vapor pressures which decrease with increasing carbon chain length. This suggests low potential for volatilization (Prevedouros et al. 2006) and hence, they are unlikely to be removed from drinking water by air stripping. FTOHs, FASAs and perfluoroalkane sulfonamidoethanols (FASEs) such as 8:2 FTOHs are much more volatile (indicated by relatively higher vapor pressure) than PFAAs (Table 2.1).

Water solubility of PFASs increases as carbon chain length decreases (Bhatarai and Gramatica 2011). PFCAs and PFSAAs which carry a charged functional group have high water solubilities, whereas FTOH, FOSA, and N-EtFOSE have much lower water-solubilities (Ahrens 2011) since their hydrophilic functional heads are uncharged (Table 2.1). As surfactants, PFAAs are likely to aggregate at the interface between octanol and water, and log K_{OW} values which are an indicator of compound hydrophobicity, are therefore difficult to determine experimentally (Tolls et al. 1994; Tolls and Sijm 1995). When interpreting log K_{OW} values obtained through modelling this surfactant behaviour should be kept in mind. Sorption studies of long chain PFASs in sediment revealed that log K_{OC} values increased with increasing fluorocarbon chain length (Higgins and Luthy 2006; Ahrens et al. 2010).

2.3 PFASs in Drinking Water

In comparison to occurrence surveys in surface and groundwater, fewer finished drinking water occurrence studies are available in the Table B2 in the Appendix B which lists studies that have reported occurrence of PFOS and PFOA in treated drinking/tap water worldwide. A summary of global PFOA/PFOS occurrence data is presented in Figure 2.1. Although instances of $\mu\text{g/L}$ concentrations of PFASs in drinking water have been reported (e.g. Emmett et al. 2006; Skutlarek et al. 2006; Minnesota Department of Health 2008), detected concentrations are typically in the lower ng/L range provided that there is no obvious PFAS point source close to a drinking water treatment plant intake. Drinking water occurrence studies have typically targeted PFOS and PFOA, and as a result these two are the most commonly detected compounds. Hence, this discussion focuses primarily on PFOS and PFOA. However, other compounds including PFBA, PFPA, PFHxA, PFHpA, PFNA, PFUnDA, PFHxS, and FOSA have also been detected in drinking water (e.g. Wilhelm et al. 2010; Ahrens 2011; Ullah et al. 2011). For instance, PFBA

was detected at a mean concentration of ~2000 ng/L in treated water entering the City of Oakdale, Minnesota, distribution system which is adjacent to the 3M Cottage Grove PFAS manufacturing facility (Minnesota Department of Health 2008). Some recent European studies have detected the shorter chain replacement PFASs such as PFBA, PFBS, and PFHxA in drinking water at concentrations even higher than PFOA and/or PFOS at some locations (Ullah et al. 2011; Eschauzier et al. 2012) indicating the change in production and usage patterns. PFBA and PFBS detected at average concentrations of 30 ng/L and 20 ng/L, respectively, were the highest detected PFASs in finished water collected from a treatment plant in Amsterdam (Eschauzier et al. 2012). Branched isomers of PFOS and PFOA have also been detected in drinking water (Eschauzier et al. 2012).

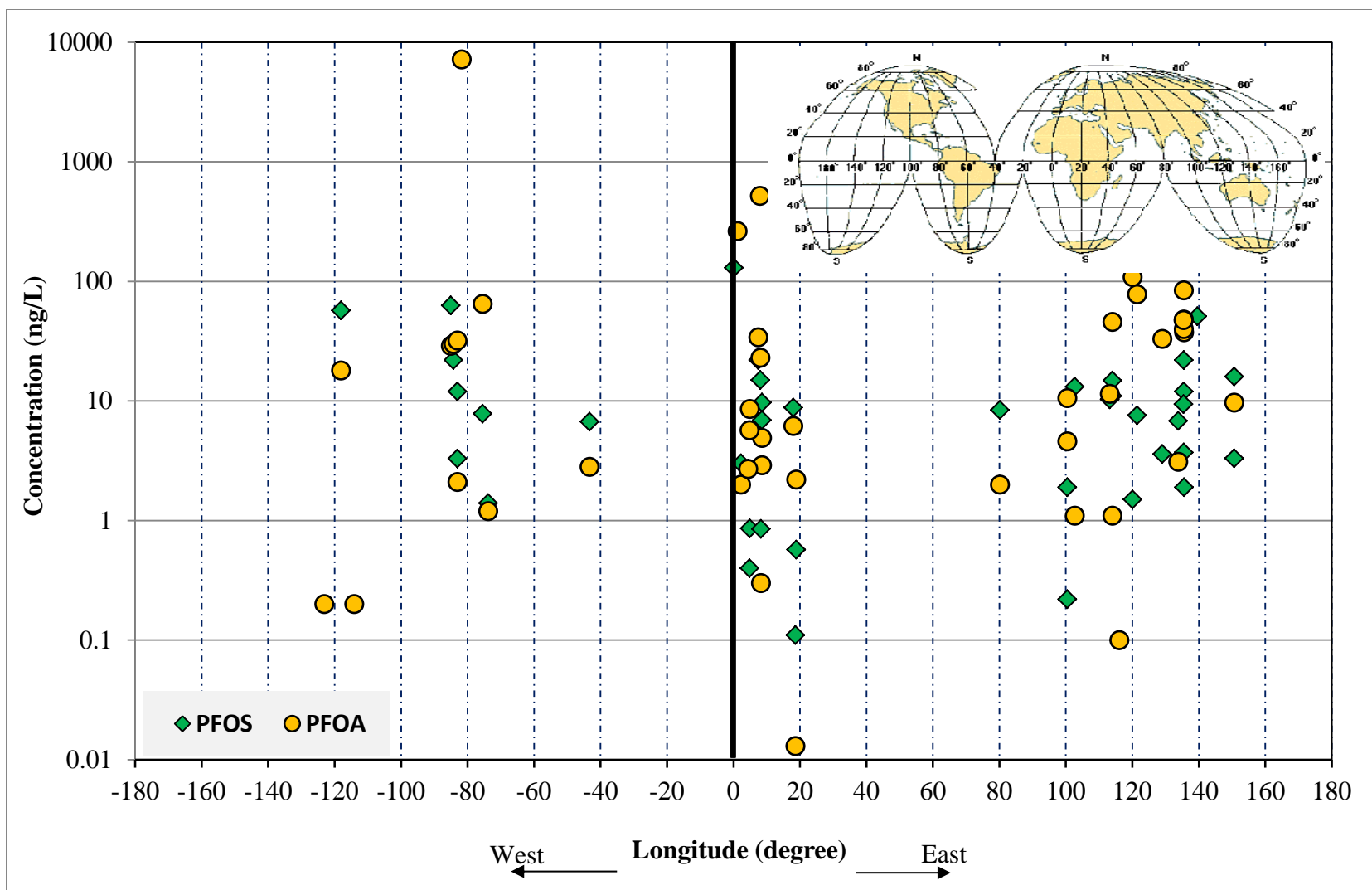


Figure 2.1: Reported global concentration of PFOS/PFOA in drinking water by longitude (locations are approximate and were obtained using Google Earth[®]). Detailed data and study references can be found in Table B2 in Appendix B.

High concentrations of PFOA have been detected in the Little Hocking community adjacent to the DuPont fluoropolymer manufacturing facility in Washington, West Virginia (Figure 2.1, near -80°). PFOA was detected in the distribution system at an average concentration of 4,800 ng/L (range 487 to 10,100 ng/L) (Paustenbach et al. 2007) and in private drinking water wells in surrounding communities at a mean concentration of 200 ng/L (Hoffman et al. 2011). Data from the Little Hocking Water Association indicate that PFOA was present at µg/L levels in raw water prior to GAC treatment and varied from 2400 ng/L to 8500 ng/L in the period from October, 2007 to April, 2010 (Little Hocking Water Association 2010). High concentrations of PFOA in drinking water (500-640 ng/L) were also reported in the Arnsberg-Neheim, Sauerland area, Germany in 2006 (Skutlarek et al. 2006). Subsequent investigation identified an agricultural area, where organic soil conditioners mixed with industrial waste were applied, as the contamination point source. A study by Quinones and Snyder (2009) monitoring seven US drinking water utilities demonstrated that the occurrence and concentration of PFASs are more likely to be higher in the finished waters of treatment plants whose raw water sources are impacted by wastewater treatment plants than those that are pristine or less impacted by wastewater discharge. PFASs in finished water have also been detected in the UK, China, Canada, India, Japan, Poland, and Sweden. Typical concentrations in drinking water in different countries are quite comparable (<50 ng/L PFOS; <100 ng/L PFOA) (Figure 2.1), except for the point source contamination scenarios in Germany, the United States, and the United Kingdom. PFASs have also been detected in bottled water (Rostkowski et al. 2008; Kunacheva et al. 2010) and in tap water-based beverages including coffee and cola (Eschauzier et al. 2013).

While dietary intake is likely one of the important exposure routes to PFOA and PFOS (Haug et al. 2011), in the previously described cases in Little Hocking, US, and Arnsberg, Germany, drinking water was found to be the major exposure route (Emmett et al. 2006; Hölzer et al. 2008). Concentrations of PFOA in blood plasma of inhabitants of Arnsberg, Germany were 4.5 to 8.3 times higher compared to a nearby reference population where PFASs were not detected in drinking water. The higher blood plasma PFOA level in Arnsberg residents was found to be clearly associated with consumption of tap water and PFOA concentrations were higher in residents who consumed more tap water at home (Hölzer et al. 2008). The concentration of PFOA in Little Hocking water was about 7-fold higher compared to Arnsberg and the mean serum level PFOA concentration of the population from Little Hocking was 16 to 18 fold higher compared to that of Arnsberg residents. In an effort to reduce the concentration of PFOA in drinking water, granular activated carbon (GAC) filters were installed in both cases. Follow-up studies noted that GAC adsorption decreased the levels of PFOA in treated water to below their limits of detection (Hölzer et al. 2009; Bartell et al. 2010), however, GAC needed frequent replacement or regeneration to maintain this level of PFOA removal (see section 2.4.3). In both cases blood serum level PFAS concentrations decreased by as much as 28% over the year following the installation of the GAC filters.

2.4 PFAS Removal during Drinking Water Treatment

Treatment efficiency is expected to vary widely across classes of perfluorinated compounds due to differences in their physical-chemical properties. Only a few studies focusing on PFAS removal during full-scale drinking water treatment were located which is not surprising considering the relatively recent emergence of this issue and the fact that they are disbursed

throughout the scientific literature. These are, however, sufficient in number to be able to make some preliminary observations.

PFAS plant surveys quickly demonstrated that conventional treatment processes were unable to substantially remove PFASs. For example, Tabe et al. (2010) reported that PFOA and PFOS were detected in more than 90% of treated water samples collected from drinking water treatment plants in the Detroit River watershed (highest occurrence frequency among 51 micro-contaminants monitored). To further illustrate this observation, a list of selected PFAAs (PFOA, PFOS, PFHxA, and PFHxS) reported in both raw and finished water at full-scale plants has been compiled (Table 2.3). This table lists only studies that provided some details on the treatment schemes employed. Raw water or influent concentrations ranged from 0.4 to 182 ng/L and are similar to what is typically observed in surface water surveys in general. Observed influent and effluent concentrations at the majority of the listed plants are similar indicating minimal removal of PFASs through treatment. Figure 2.2 clearly illustrates, that with the exception of nanofiltration (NF) and reverse osmosis (RO), water treatment technologies used at the treatment plants, including ozonation and advanced oxidation, failed to achieve appreciable PFAS removals. In fact, in several instances, detected concentrations of PFOA and PFOS in finished water were higher than in raw water prior to treatment (Figure 2.2 and Table 2.3). While analytical error at these extremely low analyte concentrations may be partially responsible, breakdown of certain precursor compounds to PFOS and PFOA during treatment may also be possible (Takagi et al. 2008; Shivakoti et al. 2010). Other potential sources for higher finished water concentrations include leaching from Teflon[®]-coated treatment equipment components (Tabé et al. 2010) and desorption from GAC filters that had been in service for long periods without reactivation (Takagi et al. 2011). Shorter chain PFASs concentrations, in particular, may

be higher after treatment as a result of desorption from GAC due to competition for active sorption sites with longer chain PFASs (Eschauzier et al. 2012) or natural organic matter (NOM) constituents.

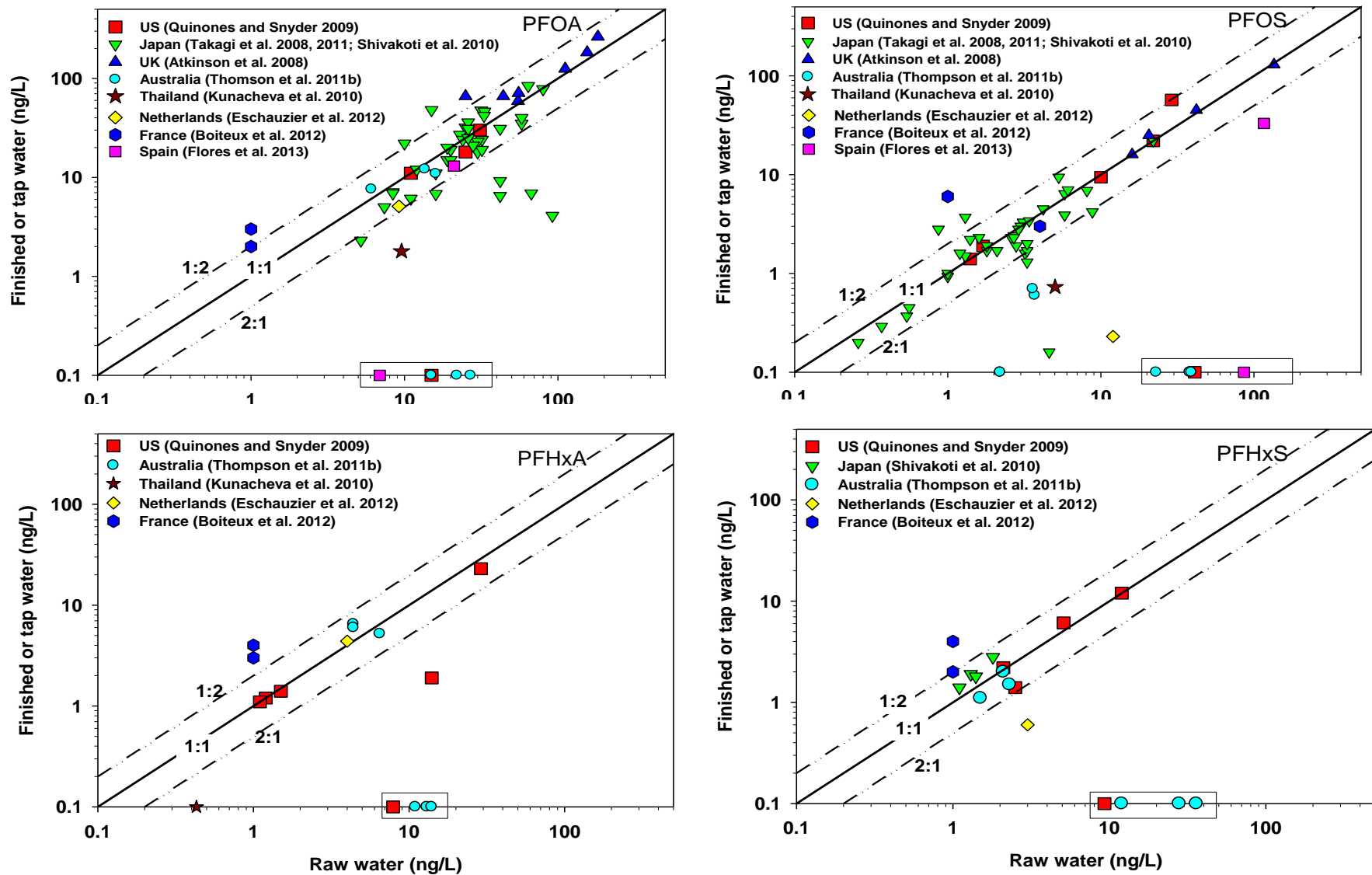


Figure 2.2: Reported finished and raw drinking water concentration of selected PFASs at various full scale plants. A value of 0.1 ng/L was assigned when PFAS concentrations were either below the limit of detection (<LOD) or limit of reporting (<LOR) or not detected (ND). Boxed data points denote data from plants that use NF/RO membranes indicating high PFAS removals at those plants.

Table 2.3: Reported full-scale drinking water treatment plant PFASs removal data

Water source	Treatment	Raw / influent [ng/L] (frequency/season/month)	Finished/ tap water [ng/L] (frequency/season/month)	Percent removal* (%)	Reference
PFOS					
Groundwater	DBF,UV, Cl ₂	10.0 (100%)	9.4 (100%)	6	Quinones and Snyder (2009)
Surface water	O ₃ , COA/FLOC, DBF, Cl ₂	1.4 (67%)	1.4 (64%)	0	
Surface water	PAC, CHLM, DBF	1.7 (50%)	1.9 (43%)	-12	
Surface water	Cl ₂ , COA/FLOC, DBF,UV	22 (100%)	22 (100%)	0	
Planned potable indirect reuse facility	MF/RO, UV/ H ₂ O ₂ , SAT	41 (100%)	ND	100	
Planned potable indirect reuse facility	Cl ₂ , DL, SAT	29 (100%)	57 (100%)	-97	
River water	RSF, O ₃ , GAC, Cl ₂	1.0 (Summer)	0.93 (Summer)	7	Takagi et al. (2008)
River water	RSF, O ₃ , GAC, Cl ₂	0.87 (Summer) 3.2 (Winter)	2.8 (Summer) 1.6 (Winter)	-222 50	
Lake water	RSF, GAC, Cl ₂	4.6 (Summer) 4.5 (Winter)	0.16 (Summer) <0.1 (Winter)	97 > 98	
River, lake, subsoil and ground water (data from seven plants)	RSF, Cl ₂	0.56—22 (Sum) 0.54—4.2 (Win)	0.45—22 (Sum) 0.37—4.5 (Win)	20—0 31—(-7)	
River water	Membranes (no further information), Cl ₂	0.37 (Summer) 0.26 (Winter)	0.29 (Summer) 0.20 (Winter)	22 23	
Lake water	SSF, Cl ₂	2.7 (Summer) 1.8 (Winter)	2.3 (Summer) 1.9 (Winter)	15 -6	
River water	COA/FLOC/SED, SF, O ₃ , GAC, Cl ₂	1.3 (Summer) 3.3 (Winter)	3.7 (Summer) 1.3 (Winter)	-185 60	Takagi et al. (2011)
River water	COA/FLOC/SED, SF, O ₃ , GAC, Cl ₂	1.6 (Summer) 3.3 (Winter)	2.3 (Summer) 1.7 (Winter)	44 48	
River water	COA/FLOC/SED, SF, O ₃ , GAC, Cl ₂	1.2 (Summer) 2.8 (Winter)	1.6 (Summer) 1.9 (Winter)	-33 32	
River water	SED, O ₃ , GAC, Cl ₂ , SF	1.4 (Summer) 3.3 (Winter)	2.2 (Summer) 2.0 (Winter)	-57 39	
Lake water	COA/FLOC/SED, SF, GAC (reactivated), Cl ₂	4.4 (Summer) 4.1 (Winter)	<0.5 (Summer) <0.5 (Winter)	>89 >88	

Water source	Treatment	Raw / influent [ng/L] (frequency/season/month)	Finished/ tap water [ng/L] (frequency/season/month)	Percent removal* (%)	Reference	
Groundwater	UF, Cl ₂	16	16	0	Atkinson et al. (2008)	
Groundwater	GAC (not in operation), super chlorination and dechlorination	135	130	3		
Groundwater	GAC (2 parallel GAC trains each having 6 beds; contactors are mature and act as biological contactors; not been regenerated for some years), Cl ₂	59 ^a	45 (post GAC 42 ng/L)	-7		
		29 ^a				42 ^b
		38 ^a				
Ground and surface water (60:40)	SSF, O ₃ , GAC (6 beds- no regeneration for several years), Cl ₂ using NaOCl	21 ^a	25	-21		
		28 ^a			20.6 ^c	
		20 ^a				
River water	COA/FLOC/SED,O ₃ , GAC, RSF	5.3 (Aug) 5.8 (Oct)	9.4 (Aug) 6.4 (Oct)	-77 (Aug) -10 (Oct)	Shivakoti et al. (2010)	
River water	COA/FLOC/SED,O ₃ , GAC, RSF	5.8 (Aug) 8.8 (Oct)	3.9 (Aug) 4.2 (Oct)	33 (Aug) 53 (Oct)		
Treated wastewater	De-nitrification, pre O ₃ , COA/FLOC/SED, DAFF, O ₃ , GAC(acts as biological contactors), O ₃ ,	2.2 (Oct) 3.7 (Nov) 3.6 (Nov)	<LOR (0.3ng./L) (Oct) 0.6(Nov) 0.7 (Nov)	100 (Oct) 84 (Nov) 81 (Nov)	Thompson et al. (2011b)	
River water	COA/FLOC/SED, RSF, Cl ₂	5.02	0.73	85	Kunacheva et al. (2010)	
Treated wastewater	Clarifier /lamellar settler (FeCl ₃ & (NH ₄) ₂ S0 ₄ , NaOCl addition), UF, RO, UV+H ₂ O ₂ , Stabilization/disinfection (addition of lime, CO ₂ , NaOCl)	38	<LOR (0.5ng/L)	100	Thompson et al. (2011b)	
		39	ND	100		
		23	<LOR (0.2ng/L)	100		

Water source	Treatment	Raw / influent [ng/L] (frequency/ season/month)	Finished/ tap water [ng/L] (frequency/ season/month)	Percent removal* (%)	Reference
River water	COA/FLOC, RSF, O ₃ , GAC, SSF	8.2	<0.23	<97	Eschauzier et al. (2012)
River water	Cl ₂ , COA/FLOC, RSF, O ₃ , GAC	116	33	69**	Flores et al. (2013)
River water	Cl ₂ , COA/FLOC, RSF, O ₃ , GAC, UF, RO	86	13	86**	
PFOA					
Groundwater	DBF,UV, Cl ₂	11 (100%)	11 (100%)	0	Quinones and Snyder (2009)
Surface water	O ₃ , COA/FLOC, DBF, Cl ₂	5.6 (3%)	<MRL (5 ng/L)	~ 0***	
Surface water	PAC, CHLM, DBF	9 (17%)	<MRL (5 ng/L)	~ 0***	
Surface water	Cl ₂ , COA/FLOC, DBF,UV	31 (100%)	30 (100%)	3	
Planned potable indirect reuse facility	MF/RO, UV/ H ₂ O ₂ , SAT	15 (100%)	ND	100	
Planned potable indirect reuse facility	Cl ₂ , DL, SAT	25 (100%)	18 (100%)	28	
River water	COA/FLOC/SED, SF, O ₃ , GAC, Cl ₂	15 (Summer) 24 (Winter)	48 (Summer) 24 (Winter)	-220 0.0	Takagi et al. (2011)
River water	COA/FLOC/SED, SF, O ₃ , GAC, Cl ₂	33 (Summer) 26 (Winter)	42(Summer) 25 (Winter)	-27 4	
River water	COA/FLOC/SED, SF, O ₃ , GAC, Cl ₂	10 (Summer) 19 (Winter)	22 (Summer) 20 (Winter)	-120 -5	
River water	SED, O ₃ , GAC, Cl ₂ , SF	26 (Summer) 26 (Winter)	36 (Summer) 31 (Winter)	-38 -19	
Lake water	COA/FLOC/SED, SF, GAC (reactivated), Cl ₂	42 (Summer) 42 (Winter)	6.5 (Summer) 9.2 (Winter)	85 78	

Water source	Treatment	Raw / influent [ng/L] (frequency/ season/month)	Finished/ tap water [ng/L] (frequency/ season/month)	Percent removal* (%)	Reference
River water	COA/FLOC/SED,O ₃ , GAC, RSF	32.0 (Aug) 31.6 (Oct)	24.0 (Aug) 47.5 (Oct)	25 (Aug) 50 (Oct)	Shivakoti et al. (2010)
River water	COA/FLOC/SED,O ₃ , GAC, RSF	12.0 (Aug) 33.2 (Oct)	12.0 (Aug) 46.3 (Oct)	0 (Aug) -39 (Oct)	
River water	RSF, O ₃ , GAC, Cl ₂	25 (Summer)	32 (Summer)	-28	Takagi et al. (2008)
River water	RSF, O ₃ , GAC, Cl ₂	64 (Winter)	84 (Winter)	-31	
River water	RSF, O ₃ , GAC, Cl ₂	19 (Summer) 58 (Winter)	15 (Summer) 35 (Winter)	21 40	
Lake water	RSF, GAC, Cl ₂	67 (Summer) 92 (Winter)	6.9 (Summer) 4.1 (Winter)	90 92	
River, lake, subsoil and ground water (data from seven plants)	RSF, Cl ₂	8.4—58 (Sum) 8.4—42 (Win)	6.9—40 (Sum) 7.1—31 (Win)	18—31 15—26	
River water	Membranes (no further information), Cl ₂	5.2 (Summer) 7.4 (Winter)	2.3 (Summer) 5.0 (Winter)	56 32	
Lake water	SSF, Cl ₂	28 (Summer) 32 (Winter)	21 (Summer) 19 (Winter)	25 41	
Treated wastewater	De-nitrification, pre O ₃ , COA/FLOC/SED, DAFF, O ₃ , GAC(acts as biological contactors), O ₃ ,	6.1 (Oct) 16 (Nov) 13.6 (Nov)	7.6 (Oct) 10.9 (Nov) 12.1 (Nov)	-24 (Oct) 32 (Nov) 11 (Nov)	
Treated wastewater	Clarifier /lamellar settler (FeCl ₃ & (NH ₄) ₂ S ₀ ₄ , NaOCl addition), UF, RO, UV+H ₂ O ₂ , Stabilization/disinfection (addition of lime, CO ₂ , NaOCl)	22 27 15	<LOR (0.7ng/L) <LOR (0.7ng/L) <LOR (0.9ng/L)	100 100 100	

Water source	Treatment	Raw / influent [ng/L] (frequency/ season/month)	Finished/ tap water [ng/L] (frequency/ season/month)	Percent removal* (%)	Reference	
River water	Cl ₂ , COA/FLOC, RSF, O ₃ , GAC	21	13	52**	Flores et al. (2013)	
River water	Cl ₂ , COA/FLOC, RSF, O ₃ , GAC, UF, RO	6.9	3.0	89**		
Ground water	UF, Cl ₂	25	66	-164	Atkinson et al. (2008)	
Ground water	Cl ₂	155	183	-18		
Ground water	IX, nitrate removal, Cl ₂ , phosphate dosing	55	59	-7		
Groundwater	air stripping, Cl ₂	182	263	-45		
Groundwater	GAC (2 parallel GAC trains each having 6 beds ; contactors are mature and act as biological contactors; not been regenerated for some years), Cl ₂	46 ^a	44 ^b	66		-50
		45 ^a				
		41 ^a				
Ground and surface water (60:40)	SSF, O ₃ , GAC (6 beds- no regeneration for several years), Cl ₂ using NaOCl	48 ^a	55.4 ^c	71		-28
		66 ^a				
		31 ^a				
Groundwater	Cl ₂ using NaOCl	105 ^a	111.5 ^b	125	-12	
		118 ^a				
River water	Cl ₂ , COA/FLOC, RSF, O ₃ , GAC	21	13	52**	Flores et al. (2013)	
River water	Cl ₂ , COA/FLOC, RSF, O ₃ , GAC, UF, RO	6.9	3.0	89**		
River water	COA/FLOC/SED, RSF, Cl ₂	9.57	1.79	81	Kunacheva et al. (2010)	

Water source	Treatment	Raw / influent [ng/L] (frequency/ season/month)	Finished/ tap water [ng/L] (frequency/ season/month)	Percent removal* (%)	Reference
River water	COA/FOC, RSF, O ₃ , GAC, SSF	4.4	5.1	-16	Eschauzier et al. (2012)
PFHxA					
Groundwater	DBF,UV, Cl ₂	1.5 (67%)	1.4 (83%)	7	Quinones and Snyder (2009)
Surface water	O ₃ , COA/FLOC, DBF, Cl ₂	1.2 (30%)	1.2 (39%)	0	
Surface water	PAC, CAM, DBF	1.1 (33%)	1.1 (14%)	0	
Surface water	Cl ₂ , COA/FLOC, DBF,UV	29 (100%)	23 (100%)	21	
Planned potable indirect reuse facility	Cl ₂ , DL, SAT	14 (100%)	1.9 (100%)	86	
Planned potable indirect reuse facility	MF/RO, UV/ H ₂ O ₂ , SAT	7.9 (100%)	ND	100	
Treated wastewater	De-nitrification, pre O ₃ , COA/FLOC/SED, DAFF, O ₃ , GAC(acts as biological contactors), O ₃ ,	6.5 (Oct) 4.4 (Nov) 4.4 (Nov)	5.2 (Oct) 6.0 (Nov) 6.5 (Nov)	20 (Oct) -36 (Nov) -48 (Nov)	Thompson et al. (2011b)
Treated wastewater	Clarifier /lamellar settler (FeCl ₃ & (NH ₄) ₂ S ₀ ₄ , NaOCl addition), UF, RO, UV+H ₂ O ₂ , Stabilization/disinfection (addition of lime, CO ₂ , NaOCl)	13 14 11	ND ND ND	100 100 100	

Water source	Treatment	Raw / influent [ng/L] (frequency/ season/month)	Finished/ tap water [ng/L] (frequency/ season/month)	Percent removal* (%)	Reference
PFHxS					
Groundwater	DBF,UV, Cl ₂	2.1 (83%)	2.2 (100%)	-5	Quinones and Snyder (2009)
Surface water	PAC, CAM, DBF	2.5 (33%)	1.4 (43%)	44	
Surface water	Cl ₂ , COA/FLOC, DBF,UV	12 (100%)	12 (100%)	0	
Planned potable indirect reuse facility	Cl ₂ , DL, SAT	5.1 (100%)	6.1 (100%)	-20	
Planned potable indirect reuse facility	MF/RO, UV/ H ₂ O ₂ , SAT	9.3 (100%)	ND	100	
Treated wastewater	De-nitrification, pre O ₃ , COA/FLOC/SED, DAFF, O ₃ , GAC (acts as biological contactors), O ₃ ,	1.5 (Oct) 2.3 (Nov) 2.1 (Nov)	1.1 (Oct) 1.5 (Nov) 2.0 (Nov)	27 (Oct) 35 (Nov) 5 (Nov)	Thompson et al. (2011b)
Treated wastewater	Clarifier /lamellar settler (FeCl ₃ & (NH ₄) ₂ S ₀ ₄ , NaOCl addition), UF, RO, UV+H ₂ O ₂ , Stabilization/disinfection (addition of lime, CO ₂ , NaOCl)	36 28 12	<LOR (0.4ng/L) <LOR (0.1ng/L) <LOR (0.3ng/L)	100 100 100	
River water	COA/FOC, RSF, O ₃ , GAC, SSF	2.0	0.6	70	
PFBA					
River water	COA/FOC, RSF, O ₃ , GAC, SSF	33	30	9.1	Eschauzier et al. (2012)

Water source	Treatment	Raw / influent [ng/L] (frequency/season/month)	Finished/ tap water [ng/L] (frequency/season/month)	Percent removal* (%)	Reference
PFBS					
Treated wastewater	De-nitrification, pre O ₃ , COA/FLOC/SED, DAFF, O ₃ , GAC(acts as biological contactors), O ₃ ,	ND (Oct) ND (Nov) ND (Nov)	1.7 (Oct) 0.8 (Nov) 1.3 (Nov)	- - -	Thompson et al. (2011b)
Treated wastewater	Clarifier /lamellar settler (FeCl ₃ & (NH ₄) ₂ S ₀ ₄ , NaOCl addition), UF, RO, UV+H ₂ O ₂ , Stabilization/disinfection (addition of lime, CO ₂ , NaOCl)	6.4 4.8 2.4	<LOR (0.1ng/L) ND ND	100 100 100	
River water	COA/FOC, RSF, O ₃ , GAC, SSF	35	20	43	

AC- activated carbon, CHLM- chloramination, Cl₂- Chlorination, COA/FLOC/SED-coagulation/flocculation/sedimentation, DAFF- dissolved air flotation and sand filtration, DBF-deep bed filtration, DL- dilution, UV- medium pressure ultraviolet, GAC- granular activated carbon, MF/RO- microfiltration/reverse osmosis, NaOCl- sodium hypochlorite, O₃- ozonation, PAC-powder activated carbon, RSF- rapid sand filtration, SSF- slow sand filtration, SAT- soil aquifer treatment.

ND- not detected; LOR- limit of reporting.

^a- concentration of compound in intake from ground water borehole (session 1)

^b- calculation: average concentration of groundwater borehole intakes

^c- calculation: 0.4×surface water concentration + 0.6× average concentration of 3 groundwater boreholes

* % removal estimated using the formula $(1-C/C_0) \times 100\%$ and rounded; where C₀ is the raw/influent water concentration and C is the effluent/tap water concentration (when ND or <LOR, a value of zero was assigned)

** Overall % removal reported by Flores et al. (2013)

** *PFOA was detected at concentrations below the method reporting limit (MRL) in both influent and effluent samples but could not be quantified. For each utility only one influent sample contained PFOA in concentrations slightly above the MRL. Hence, it is likely that no significant removal took place.

2.4.1 Conventional coagulation, flocculation, sedimentation, and filtration

The extremely low concentrations of PFASs, together with their high hydrophilicity, make them unlikely candidates for removal by conventional coagulation/flocculation/sedimentation processes. In fact, no differences in PFAS concentrations were found between plant influent and sedimentation unit effluent samples collected from two drinking water treatment plants in Kansai, Japan (Shivakoti et al. 2010). Similarly, PFAS concentrations in samples collected from five full-scale plants in Osaka, Japan following coagulation and sedimentation, and sand filtration preceded by sedimentation, indicated that essentially no removal took place through either combination of unit processes (Takagi et al. 2011). Similarly, no removals by conventional coagulation treatment were reported by Thompson et al. (2011b) and Eschauzier et al. (2012). This is also consistent with a bench-scale coagulation study investigating PFOA and PFOS removal, which found removals of less than 35% under a variety of conditions tested (Xiao et al. 2012b).

Eschauzier et al. (2010) based on their study on infiltrated rain water and river water commented that both rapid- and slow-sand filtration are unlikely to be effective for PFAS removal. This is supported with observations made by Takagi et al. (2008 and 2011), Shivakoti et al. (2010), Eschauzier et al. (2012), and Flores et al. (2013). Only Kunacheva et al. (2010) observed that rapid sand filters achieved high removals of PFOA (85%) and PFOS (86%) which, at least for the time being, is inconsistent with the other reports.

2.4.2 Oxidation processes

Fluorine is the most electronegative element and as such resists oxidation to retain its electrons. Being the most powerful inorganic oxidant (redox potential $E^\circ = 3.06 \text{ V}$) (Beltrán 2004), it is thermodynamically unfavorable to oxidize fluorine. The presence of functional groups with high electron density such as double bonds, activated aromatic systems, and amino groups generally increase the reactivity of a compound with ozone (O_3) ($E^\circ = 2.07 \text{ V}$), while the presence of electron withdrawing groups (e.g. $-\text{Cl}$, $-\text{NO}_2$, $-\text{COOH}$) lowers their reactivity (von Gunten 2003). PFAAs do not contain aromatic bonds or phenolic structures (Table 2.1). Thus, the presence of the strong C-F bond together with the electron withdrawing functional groups $-\text{COOH}$ and $-\text{SO}_3\text{H}$ in the structures of PFCAs and PFSAs, respectively, indicates that these compounds will likely be resistant to oxidation, even by molecular ozone and hydroxyl radicals. Hydroxyl radicals ($\cdot\text{OH}$) ($E^\circ = 2.8 \text{ V}$), the primary oxidant in advanced oxidation processes (AOPs), generally withdraw H-atoms from saturated organics to form water thus PFAAs due to perfluorination (i.e. replacement of all hydrogen by fluorine) are also unlikely candidates for oxidation by AOPs (Vecitis et al. 2009). Szajdzinska-Pietek and Gebicki (2000) found that PFOA was practically nonreactive with $\cdot\text{OH}$, and estimated the upper limit of the second order reaction rate constants for $\cdot\text{OH}$ with PFOA to be $3 \times 10^7 \text{ M}^{-1}\text{S}^{-1}$, which is quite low for reactions with $\cdot\text{OH}$. For example, the estimated upper limit of the reaction rate is at least two orders of magnitude lower than the average reaction rate between $\cdot\text{OH}$ and sodium octanoate ($5.6 \times 10^9 \text{ M}^{-1}\text{S}^{-1}$), the corresponding unfluorinated hydrocarbon of PFOA (Szajdzinska-Pietek and Gebicki 2000), and thus PFAAs are likely to be recalcitrant to AOPs. Based on the low reactivity of PFAAs with ozone and in AOPs it is expected that chlorine-based oxidation processes, due to their lower redox potentials ($E^\circ = 1.36\text{-}1.50 \text{ V}$), will also very likely not oxidize PFASs under typical drinking water treatment conditions.

Limited full-scale treatment plant surveys conducted to-date confirm these theoretical considerations in that chlorine and ozone-based oxidation processes, at typical water treatment plant doses and contact times, were not effective for the removal of PFASs (Atkinson et al. 2008; Quinones and Snyder 2009; Takagi et al. 2011). PFASs have been shown to be resistant to chlorination or chloramination even when combined with other unit processes such as coagulation/flocculation/sedimentation, powdered activated carbon (PAC), deep bed filtration, and UV irradiation (Quinones and Snyder 2009). Inefficacy of chlorine-based oxidants for PFAS removal during drinking water treatment has also been reported by Atkinson et al. (2008) and Takagi et al. (2011). Ozone-based oxidation processes have been reported to fail to transform PFAAs (Takagi et al. 2008; Tabe et al. 2010; Shivakoti et al. 2010; Takagi et al. 2011; Thompson et al. 2011b; Eschauzier et al. 2012; Flores et al. 2013). At a full-scale water reclamation plant in Australia, even multiple stages of ozonation with doses as high as 5 mg/L with 15 minutes contact time failed to achieve PFAS removal (Thompson et al. 2011b). Ozone doses and contact times as high as 0.87 mg/L and 120 min, respectively, were not effective for PFOA and PFOS removal (Takagi et al. 2011) [ozone residuals not available for either study above]. PFOS and PFOA can be formed from the degradation of precursor compounds such FASAs, FASEs and FTOHs. These precursors are mostly polyfluorinated compounds thereby containing C-H bonds which may be oxidizable. Thus, if ozone or advanced oxidation processes (AOPs) were able to oxidize polyfluorinated precursors present in the raw water, the concentration of terminal compounds such as PFOS or PFOA may actually increase in finished water. Takagi et al. (2011), however, did not observe any degradation of precursor compounds such as N-EtFOSE and 8:2 FTOH to PFOS and PFOA by ozonation. Further studies are needed to resolve this.

2.4.3 Granular activated carbon adsorption

GAC is widely used in drinking water treatment plants for reducing the concentrations of synthetic organic contaminants, taste and odour compounds, and sometimes natural organic matter (NOM). GAC has been used to treat PFASs in a few full-scale installations (Atkinson et al. 2008; Minnesota Department of Health 2008; Hölzer et al. 2009; Little Hocking Water Association 2010; Takagi et al. 2011; Eschauzier et al. 2012; Flores et al. 2013). GAC filters when new, or in use for less than nine months, were found to achieve 69% to 100% removal of ng/L level PFOS and PFOA at five treatment plants in Osaka, Japan (Takagi et al. 2011).

Sorption capacity of virgin activated carbon used in one of the plants studied by Takagi et al. (2011) was estimated to be about 520 ng/g considering flow, GAC volume, and concentration of PFASs in GAC influent (empty bed contact time, hydraulic loading, and GAC type were not specified). Although under very different conditions, Hansen et al. (2010) estimated a maximum PFOA sorption capacity in a similar range with 1100 ng/g for GAC in contaminated groundwater.

Eschauzier et al. (2012) observed that only the GAC filters (Norit ROW 0.8 Supra[®]), and not the preceding coagulation, rapid sand filtration, and ozonation steps, were effective in removing PFASs in a treatment plant in Amsterdam, Netherlands. While GAC alone effectively removed PFNA, PFOS and PFHxS, it only partially removed PFOA (~ 50%) and failed to remove shorter chain PFASs such as PFBA, PFBS, PFPA, PFHxA and PFHpA (Eschauzier et al. 2012). Flores et al. (2013) reported partial removal of both PFOA (41%) and PFOS (63%) by GAC adsorbers (containing Filtrasorb 400[®], Norit ROW 0.8[®] and Norit 1240 EN[®]) when these compounds were present at low ng/L levels in the raw water at a Spanish drinking water treatment plant. When looking into isomer-specific behaviour of PFOA and PFOS during GAC treatment it was found

that branched isomers were less sorbable to GAC compared to linear isomers (Eschauzier et al. 2012).

GAC filters (containing Calgon Carbon Filtrasorb 100[®]) were installed in a water treatment plant in Arnsberg, Germany to treat PFAS-contaminated water in July 2006 (Hölzer et al. 2009). PFOA was not detected in water samples collected during the next two months (Figure 2.3). In late August, 2006, however, re-appearance of PFOA was observed and its level eventually exceeded the precautionary value of 100 ng/L in early December, 2006 at which point the GAC was reactivated (Hölzer et al. 2009). The Little Hocking Water Association, Ohio, US also reported frequent replacement (~ 3 months) of GAC (Calgon Carbon Filtrasorb 600[®]) to achieve PFOA removal from drinking water at albeit elevated influent concentrations (1900-8500 ng/L) (Figure 2.4) (Little Hocking Water Association 2010). Takagi et al. (2011) also observed that GAC when not reactivated for longer periods (>1 year), was unable to effectively remove PFOA and PFOS. They further observed that once activated, GAC lasted for about 130 days until the re-appearance of PFOA in the GAC filtered water. A reduction in the service life of GAC filters used for PFAS removal due to NOM preloading was also noticed by Eschauzier et al. (2012). The City of Oakdale, Minnesota started using GAC filters in October 2006 at a newly constructed pilot plant to remove PFASs from groundwater using two GAC filters in series, each filter containing 20,000 pounds of GAC (Minnesota Department of Health 2008). PFBA was the first compound to be detected between the first and second set of GAC filters at the plant after only six weeks of operation while breakthrough of PFOA and PFOS were observed after 286 days and 550 days, respectively (Minnesota Department of Health 2008; Kolstad 2010). Kolstad (2010) reported that the Oakdale plant, by replacing GAC based on PFOA breakthrough, was able to treat 1.9 billion gallons of water over a period of 23 months which amounted to a GAC

replacement cost of about \$0.12 per 1000 gallons of water. Early breakthrough of PFBA is also consistent with Eschauzier et al. (2012) who did not observe removal of PFBA. Decreased log K_{oc} values of PFASs with decreasing carbon chain length (Higgins and Luthy 2006; Ahrens et al. 2010) indicate lower sorption potential of shorter chain PFASs compared to their longer chain counterparts. This may explain the observed earlier breakthrough of PFBA.

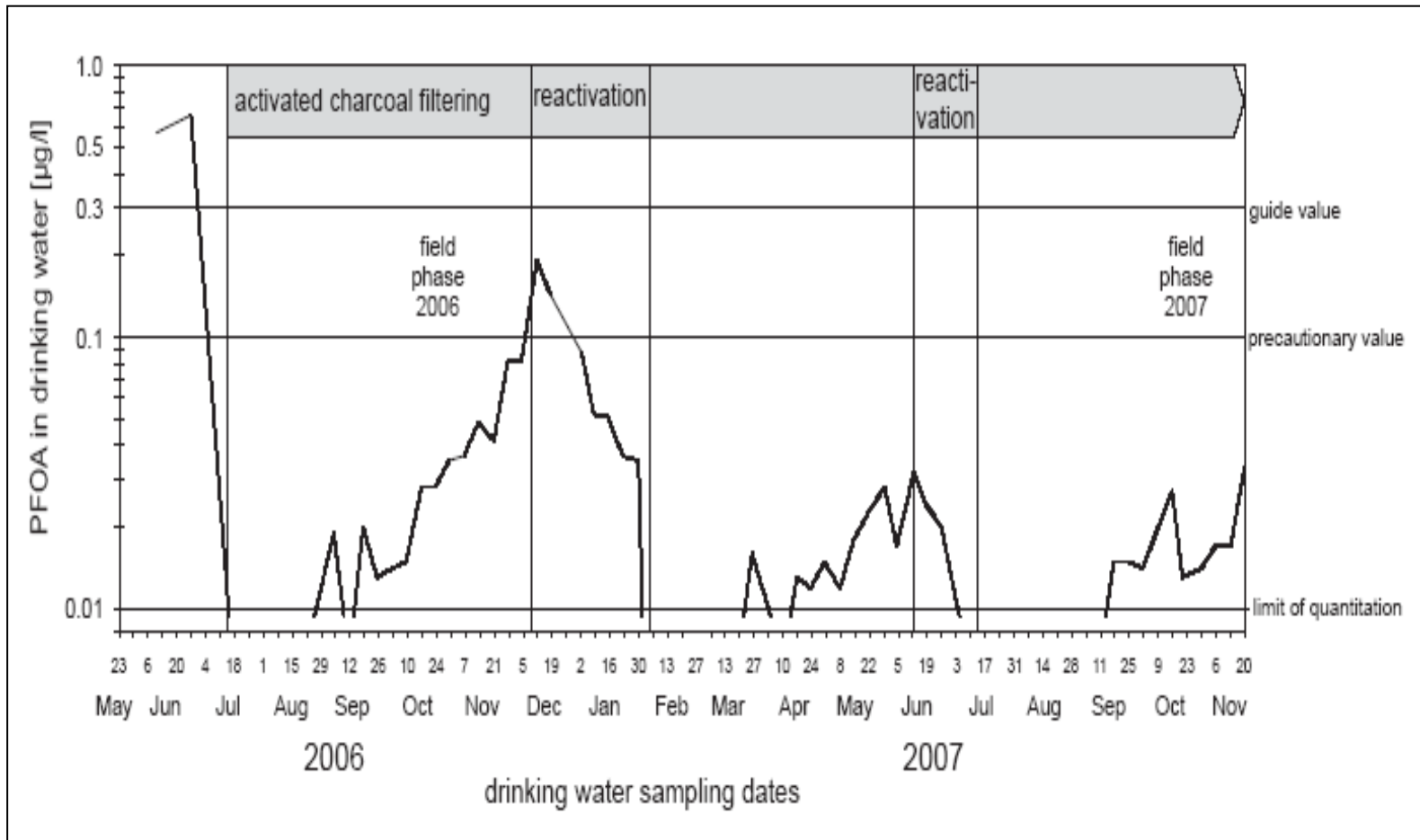


Figure 2.3: PFOA-concentration in drinking water in Arnsberg, Germany between May 2006 and April 2008 indicating frequent need for GAC filter reactivation for PFOA removal (Hölzer et al. 2009; reprinted with permission from the publisher). Please note, PFOA concentration is reported in this figure in µg/L. Calgon F-100® was used as the GAC at the treatment plant. GAC info collected via personal communication with the corresponding author.

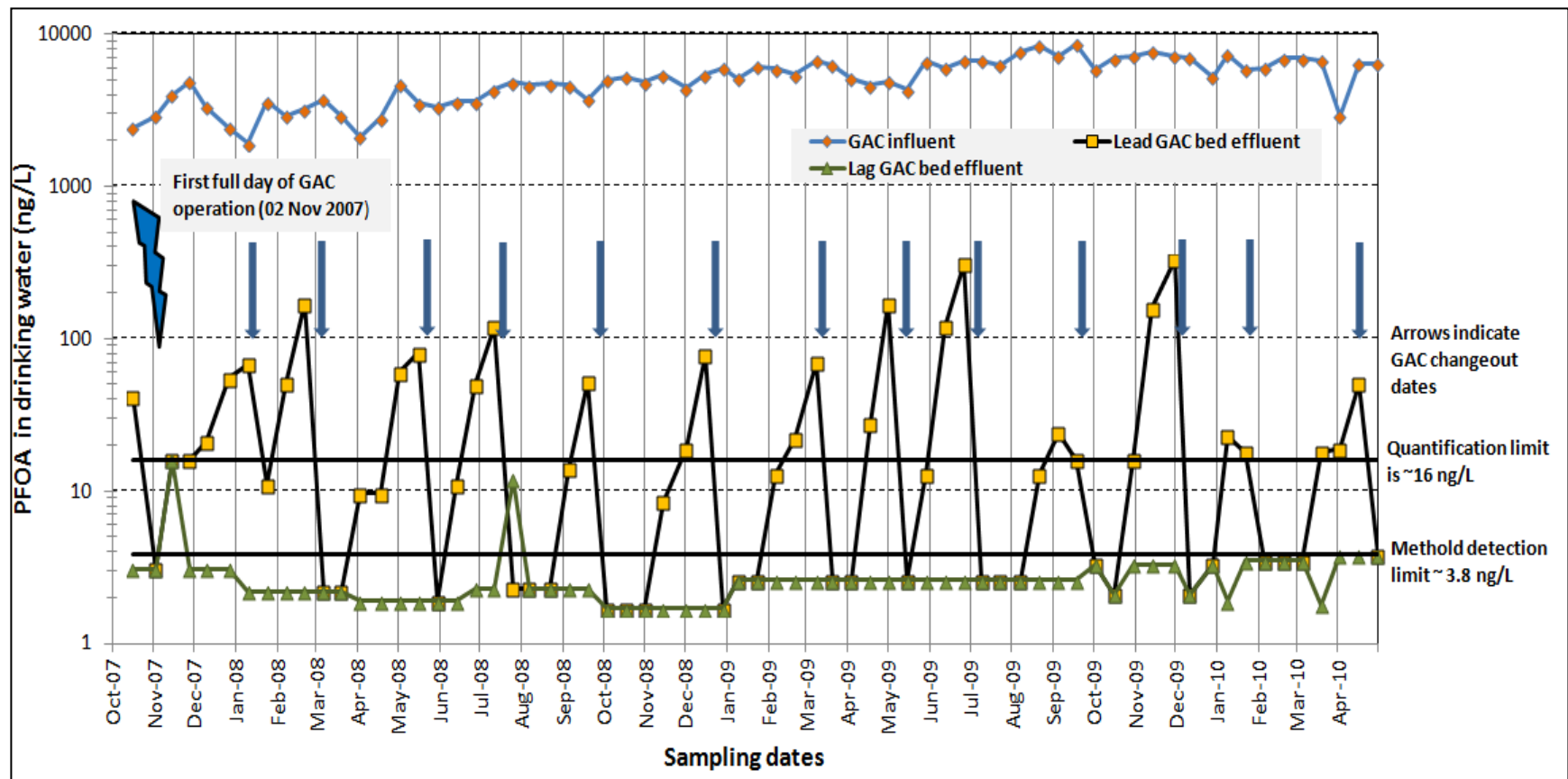


Figure 2.4: PFOA-concentration in raw and finished drinking water at Little Hocking, West Virginia, USA. Calgon F-600® GAC used at the treatment plant. Data collected from (Little Hocking Water Association 2010) and by personal communication with Mr. Bob Griffin, General Manager, Little Hocking Water Association.

Two important adsorption phenomena that arise during treatment of natural water due to the presence of dissolved organic carbon (DOC) are competitive adsorption and preloading or fouling of GAC. It is likely that both direct competition and in particular preloading phenomena are responsible for the observed early breakthrough of PFASs during GAC filtration at full-scale treatment plants. Slow sorption kinetics of PFASs onto GAC may also contribute to early breakthrough (Yu et al. 2009a). Failure to reactivate or replace GAC likely explains why Atkinson et al. (2008) did not see any removal of PFASs at water treatment sites where GAC filters were in place but had not been regenerated for years. Reactivating carbon 2 to 3 times per year has been suggested to achieve and maintain good removal of PFASs (Takagi et al. 2011) but this strategy has considerable implications in terms of cost and operations. Taking into account the low health-based guideline values being suggested for PFOA and PFOS (Table 2.2), GAC applications specifically targeting PFASs need to be carefully designed and optimized to reduce the frequency of activated carbon regeneration. Once in place it may require enhanced monitoring to assess performance and to determine timing of the regeneration.

PFAS isotherms and kinetic parameters in ultrapure water at environmentally relevant concentrations may provide an initial basis for evaluating the suitability of a particular type of carbon for PFAS treatment. Studies in natural water will be useful to assess pre-loading and direct competition effects. Previously, Yu et al. (2009b) observed that GAC preloaded for 16 weeks had about 2-10% of its capacity remaining for the hydrophilic and ionic compound naproxen. PFAAs are similarly hydrophilic and ionic and their adsorption when present at trace concentrations may as well be severely impacted by NOM preloading. Yu et al. (2009b) using other non PFAS trace contaminants also demonstrated that isotherms generated at high concentrations, if used to extrapolate capacity at very low target contaminant concentrations,

may result in overestimation of GAC removal capacity. Thus for isotherm studies it is important to employ concentrations which are similar to those encountered in natural water.

Reported data from full-scale treatment applications demonstrate that PFAS breakthrough may occur relatively early in GAC adsorbers, but the actual breakthrough time is compound- and water-specific. Therefore, pilot-scale studies are likely needed to optimally design filters or contactors thereby providing the basis for balancing capital investment in terms of filter design, carbon cost, and frequency of regeneration. Pilot-scale studies in natural water at environmentally relevant PFAS concentrations may assist in obtaining more accurate assessments of GAC adsorption capacity that may be encountered under real water treatment scenarios.

2.4.4 Powdered activated carbon adsorption

Powdered activated carbon (PAC) has also been studied for PFAS removal (Qu et al. 2009; Yu et al. 2009a; Hansen et al. 2010; Dudley 2012) but only at bench-scale. Dudley (2012) found that thermally activated wood-based PAC was more efficient in removing PFASs when compared to coconut, lignite, and bituminous PAC. In buffered ultrapure water (pH 7.0), at an initial PFAS concentration of 500 ng/L, thermally activated wood-based PAC at a dose of 15 mg/L achieved >70% removal of eight target PFAS within 15 minutes of contact time. However, less than 40% removal of PFPeA was observed, with no removal for the shorter chain PFBA, confirming the negative effect of decreasing hydrophobicity with decreased carbon chain length on adsorption. Similar to GAC, PFAS adsorption on PAC is also negatively affected by the presence of NOM. The same thermally activated wood-based PAC at the same dose in North Carolina reservoir water in the presence of 4.5 mg/L of TOC achieved a maximum of only 55% removal for PFDA (C10) and PFOS. The study concluded that significant removal of PFBA, PFPeA, PFHxA,

PFHpA, and PFBS from drinking water may not be achieved at practical PAC dosages (Dudley 2012).

Experiments with PFOA and PFOS not surprisingly indicate that PFAS adsorption kinetics are much faster for PAC compared to GAC. About 168 h and 4 h were required to reach equilibrium for GAC and PAC, respectively, for both compounds (Yu et al. 2009a). Higher PFAS removal using PAC (60-90%) as opposed to GAC (20-40%) in short duration adsorption tests (10 min) were observed by Hansen et al. (2010) at trace concentration levels and in the presence of NOM. Thus, PAC likely adsorbs PFASs faster than GAC due to its smaller particle size resulting in higher surface area for the same volume of carbon, shorter internal diffusion distances, and additional available surface functional groups (Yu et al. 2009a; Hansen et al. 2010). Also, the poorer performance of GAC relative to PAC may be attributable to the rigidity of the CF₂ backbone which may not energetically favor sorption into the inner pores of GAC (Hansen et al. 2010). PFASs have been detected in water throughout the year and hence, GAC adsorbers may be a better long term solution if PFAS is the contaminant of concern. PAC may be a more appropriate choice for removing PFASs in situations that require a prompt short-term response (e.g. spills).

2.4.5 Biodegradation

PFAAs will likely not be biodegraded under typical drinking water treatment conditions. Although reductive defluorination appears to be thermodynamically favorable and releases enough energy for microbes to thrive, the compounds do not seem to be commonly used as a carbon source (Parsons et al. 2008). Meesters and Schroder (2004) reported complete removal of both PFOS and PFOA from wastewater samples under anaerobic conditions in a lab-scale closed-loop bioreactor, however, biodegradation was not observed under aerobic conditions. In-

plant biological drinking water treatment processes operate almost exclusively under aerobic conditions thereby not creating conditions favorable for reductive defluorination. Microbial metabolization of FTOHs and the FTOH-based products, FASAs, FASEs as well as other PFAA precursor compounds has been reported to occur during wastewater treatment (under aerobic conditions) and in the environment (Wang et al. 2005a; Wang et al. 2005b; Rhoads et al. 2008; Martin et al. 2010) and may eventually lead to formation of PFAAs (e.g. PFOS, PFOA). Degradation of precursors to PFAAs during drinking water treatment remains to be systematically investigated. Two full-scale drinking water occurrence and treatment studies have suggested that the presence and subsequent degradation of such precursors may be possible and may even lead to increased concentrations of PFOA and PFOS in finished water (Takagi et al. 2008; Takagi et al. 2011).

2.4.6 High pressure membranes

Wastewater reclamation and reuse programs, desalination, and the demand for high quality drinking water are some of the driving forces behind the increasingly growing application of high pressure nanofiltration (NF) and reverse osmosis (RO) membrane processes. The viability of high pressure membrane applications is improving with advances in energy efficiency, operating efficiency, lowered costs, and the ability of membranes to tackle a wide range of water contaminants. In general, high pressure membrane processes are not widely used for the treatment of drinking water other than in the case of localized specific contaminants, softening, and desalination. PFASs, due to their presence at considerably higher concentrations in wastewater compared to surface water, are of concern for drinking water utilities that are employing or are planning to adopt water reclamation or reuse programs.

Low pressure membranes such as microfiltration membranes (MF) alone will not be able to retain PFASs as the effective diameter of these molecules are smaller (~ 1 nm) compared to MF pore sizes which are in the range of ~ 100 nm (Tsai et al. 2010). Available bench-scale studies involving high pressure membranes indicate that membrane pore size/molecular weight cut-off (MWCO) probably plays the most important role with respect to rejection of PFASs by NF/RO (Tang et al. 2006; Tang et al. 2007; Steinle-Darling and Reinhard 2008; Lipp et al. 2010; Appleman et al. 2013). High removals of charged PFASs with a size of 300 Da or greater can be expected. For charge neutral PFASs such as FOSA, rejection may vary and can be substantially lower (Steinle-Darling and Reinhard 2008, Steinle-Darling et al. 2010). While size is probably the dominant factor, solute-membrane interactions which will depend on factors such as charge, hydrophobicity, and dipole moment are also expected to be significant if the solute molecular weight is close to or smaller than the MWCO of the membrane. Adsorption onto membrane surfaces (Kwon et al. 2012) and back diffusion can also play important roles in the rejection of PFASs. Membrane fouling layers may hinder back diffusion of the retained PFAS molecules which eventually facilitates transport of the retained solutes across the membrane thereby decreasing net rejection (Steinle-Darling and Reinhard 2008). However, contrasting results showing better performance of fouled membranes in rejecting PFAAs were reported by Appleman et al. (2013). This is not surprising as others have observed an increase in rejection for pharmaceuticals for fouled membranes filtering water from different sources (Comerton et al. 2009). Under certain conditions Comerton et al. (2009) also reported a decrease in rejection.

It was observed in a study involving two Australian water reclamation plants that the one with an RO unit preceded by an UF unit and followed by an advanced oxidation process (AOP) (UV+H₂O₂) unit achieved almost complete removal (not detected or below detection limit) of PFASs (Thompson et al. 2011b). A slight decrease in the concentration of some PFASs following the UF unit was attributed to the removal of suspended and colloidal particles with which PFASs may have been associated. Much higher concentration of PFASs in the RO concentrate compared to feed water corroborates that PFASs were primarily removed by the RO unit (Thompson et al. 2011b). In contrast, no decrease in PFOA and other shorter PFAS concentrations was observed in the finished water of the other plant that had three ozonation stages located at different points in the treatment train and a biological activated carbon filtration stage (in addition to conventional coagulation). Quinones and Snyder (2009) in their survey of seven US drinking water utilities observed that PFASs were only removed at a utility whose treatment included an RO unit. Complete removal ($\geq 99\%$) of PFOA and PFOS following RO membrane treatment has also been reported by Flores et al. (2013). Data collected from these studies strongly suggest that high pressure membranes are capable of substantial PFAS removal (Table 2.3 and Figure 2.2). This is consistent with bench-scale studies conducted with ng to $\mu\text{g/L}$ concentrations of PFASs found in surface water (Loi-Brügger et al. 2008; Stein-Darling and Reinhard 2008; Lipp et al. 2010; Appleman et al. 2013).

Bench-scale studies have for the most part been conducted in water matrices lacking DOC. Rejection mechanisms can be affected by the presence of DOC in water and hence, future studies are needed to elucidate PFAS behaviour during membrane filtration in the presence of DOC. An

issue inherent to contaminant removal by membrane processes is the disposal of the PFAS-enriched concentrate which will have to be carefully considered.

2.4.7 Resin Treatment

PFAAs, being anionic at ambient water pH values, would be expected to be amenable to removal by anion exchange. Hence, this discussion focuses predominantly on strong base anion exchange resins. Electrostatic interactions as well as adsorption via hydrophobic interactions are the two primary mechanisms proposed for removal with ion exchange resins. Transport to binding sites may also play a role. The pH of typical drinking waters (6 to 9) is not expected to have any significant effect on removal by ion exchange due to the ionization of PFOA and PFOS. Important resin characteristics that may affect removal include functional groups, polymer matrix, and porosity (Deng et al. 2010). It is unclear from existing studies which mechanism prevails and if it varies among PFAAs. Thus, the term ‘uptake’ when used in this section indicates binding to the resins by both electrostatic and hydrophobic interactions.

Only one study reported full-scale demonstration of PFAS removal by ion exchange from raw water used for drinking water production. Purolite FerrIX A33[®], a strong base, porous anion exchange resin impregnated with iron oxide was used at a New Jersey DWTP for arsenic removal. It was observed that at low level (ng/L) PFAS influent concentrations appreciable removal of longer chain PFCAs (54% for PFHpA and 76% for PFOA) and high removal of PFSAAs (83%, >97% and >90% for PFBS, PFHxS and PFOS, respectively) (Dickenson et al. 2012) was achieved. However, the resin failed to remove shorter chain PFCAs (PFBA, PFPeA and PFHxA). Magnetic ion exchange (MIEX[®]) which is predominantly used for DOC removal, was also reported to be ineffective (<10%) for the removal of PFASs at a plant in Alabama (Dickenson et al. 2012).

In addition to binding by electrostatic and hydrophobic interactions, transport to binding sites may also play a role in the uptake of PFASs. Acrylic resins are more hydrophilic than styrenic resins. Hence, acrylic resins may achieve better removal of hydrophilic PFASs as they facilitate transport to the acrylic resin pores. This hypothesis is supported by the results of Deng et al. (2010), who, when studying PFOS removal during wastewater treatment with ion exchange resins, observed that polyacrylic resins, regardless of resin porosity and functional groups, had faster uptake rates and higher equilibrium capacities than did polystyrene resins. Similar trends have also been observed by Lampert et al. 2007 and Dudley (2012). Dudley (2012) reported that although macroporous polyacrylic strong base anion resin had faster uptake kinetics, the resin exhibited lower uptake capacity compared to both the gel and macroporous types of polystyrenic strong base anion resins used in their study.

Study results of Deng et al. (2010) further indicate that macroporous resins are expected to exhibit better uptake compared to gel resins due to easier accessibility to resin exchange sites. Hydrophilicity and the open structure of macroporous resins probably facilitate uptake of PFAAs by inducing faster diffusion into the anion exchange sites. Dudley (2012), however, observed that uptake kinetics for macroporous polystyrenic and gel type polystyrenic resins were similar.

Compared to activated carbon, a significantly improved removal of shorter chain PFASs has been reported with strong base anion resins. Polystyrenic strong base anion resin achieved > 90% removal of PFBA and PFPeA at 'doses' of 5 and 10 mL/L in natural water. The author hypothesized (but could not confirm) that NOM potentially alters the resins in a way that facilitates PFAS uptake (Dudley 2012).

Non-ion exchange resins have also been tested at bench-scale for removal of PFASs (Senevirathna et al. 2011; Xiao et al. 2012c; Chularueangaksorn et al. 2013). Findings of Xiao et al. (2012c) show that moderately polar non-ionic Amberlite XAD-7HP performed better than the non-polar Amberlite XAD-2 resin. The authors also indicated regeneration did not significantly affect performance of the XAD-7HP resin. Chularueangaksorn et al. (2013) however, observed that anionic resins had higher sorption capacity for PFOA compared to non-ionic resins.

Regardless of some of the contrasting trends observed during the studies conducted to-date, it is evident that resin treatment has the potential to be a promising technology for the removal of PFASs from water. However, resin studies to-date were mostly conducted in the absence of DOC and results may be different in its presence. Thus, further investigations are warranted before recommending ion exchange for PFAS. It is also important to note that when selecting an ion exchange resin, regeneration issues can be as important as the removal capacities of the resin. The presence of other competing anions (e.g. SO_4^{2-} , NO_3^-) should also be considered as they may also affect uptake capacity of resins. Another consideration is the potential for breakthrough and a subsequent contaminant spike (dumping) into the treated water as the resin approaches exhaustion. Moreover, it may be challenging to elucidate uptake mechanisms and trends as typically the exact structure and nature of ion exchange sites for various commercially available resins are proprietary in nature.

2.5 Knowledge Gaps and Research Needs

The current knowledge gap with regard to an adequate physico-chemical property database of PFASs creates a challenge for the assessment of the fate of PFASs. Limited information is available about isomeric profiles for PFCAs and PFSAAs. Since isomers are also likely to be present in the aquatic environment (Houde et al. 2008), and considering the recent observation

that linear isomers are preferentially sorbed onto GAC compared to their branched counterparts (Eschauzier et al. 2012), the behavior and fate of isomers of various PFASs during drinking water treatment needs to be investigated.

The presence of precursor compounds may play a role as they may convert to terminal products such as PFOA and PFOS during drinking water treatment (Takagi et al. 2011) and may therefore lead to increased concentrations in finished water. As such, removal and degradation studies of PFAS precursors are also warranted.

Most studies to-date have focused on PFOA and PFOS, however, as new PFASs, for example shorter chain PFASs are introduced (Renner 2006) it is likely that those compounds will eventually become significant contributors to total PFAS levels in drinking water. Data on PFAS occurrence in finished drinking water are still limited and even sparse for some of the more recently detected PFASs. Thus human exposure to these compounds via water is still poorly understood. Future studies and regulatory considerations need to consider that PFASs found in the aquatic environment may eventually be detected in drinking water. Limited but available data suggest that those shorter chain PFASs are also more challenging to treat.

Although efforts are underway to regulate the production of some PFASs (USEPA 2009a), they will remain on the market, at least in the near future, and continue to be detected in the environment. Thus, it is becoming increasingly evident that both understanding of the fate of PFASs during drinking water treatment as well as optimization of existing treatment schemes will be necessary if there are societal or regulatory pressures to remove these compounds.

Finally, better coordination among regulatory bodies in different jurisdictions in terms of understanding, characterizing, and minimizing the risk of exposure to PFASs via drinking water is desirable. Such initiatives would minimize the wide variations in prevailing emergency regulatory guidelines and will help utilities set realistic treatment goals if this becomes necessary.

2.6 Conclusions

This article identifies the limitations of present day drinking water treatment technologies and potential advantages of currently less-exploited technologies (ion exchange and high pressure membrane filtration). This compilation of available full-scale drinking water removal surveys/studies of perfluoroalkyl and polyfluoroalkyl substances (PFASs), along with select bench-scale studies suggests that:

- Conventional coagulation, flocculation, and sedimentation cannot achieve substantial removal (< 20%) of PFASs nor can rapid granular media filtration.
- Free chlorine at residuals commonly employed for disinfection or distribution system residual maintenance is ineffective for PFAS removal.
- Oxidation and advanced oxidation processes, under typical drinking water treatment plant conditions, will not oxidize most PFASs. Some oxidation of FTOHs and FASAs may be possible; however, they may simply be oxidized to other PFASs.
- UV irradiation at commonly utilized disinfection doses and at the higher doses used for contaminant removal is also ineffective.
- GAC may be useful for removing PFASs from drinking water. Longer chain PFASs will sorb better onto sorbents compared to the shorter chain compounds. However, short chain PFASs such as PFBA and PFBS may pass through or reach breakthrough very quickly.

The efficiency of GAC is compromised in the presence of NOM and frequent carbon reactivation may be necessary. Future studies should consider the elucidation of the effects of preloading and direct competition in natural water on the PFAS removal efficiency by activated carbon adsorption.

- Biodegradation of most PFASs in aerobic GAC contractors or in other forms of biofiltration used under current drinking water treatment conditions is unlikely.
- Ion exchange/non-ion exchange resins, while not commonplace in drinking water treatment facilities, may be useful for removing PFASs. Additional data is needed to understand the effect of resin type and water matrix (competing anions and NOM). Resin regeneration and disposal of brine needs to be taken into consideration.
- NF/RO membranes will achieve high rejection of most PFASs. However, lower molecular weight PFASs (such as PFBA, PFPeA), and the neutral FOSA may be less well rejected by some loose NF membranes. Data on rejection following long term operation of membranes and in the presence of NOM are not available. Disposal of concentrate, which will contain elevated concentrations of PFASs, will need to be addressed.

Chapter 3

Quantitative Analysis of Linear and Branched Perfluoroalkyl Carboxylic Acids in Water by Gas Chromatography/Mass Spectrometry (GC/MS)

Summary

A gas chromatography-mass spectrometry (GC/MS) analytical method employing electron impact ionization has been developed to simultaneously determine selected perfluorinated carboxylic acids (PFCAs) (C4-C9) concentrations in ultrapure and surface water samples. The target PFCAs were derivatized using butanol in the presence of sulfuric acid and heat. By employing central composite factorial design, the optimum derivatization reaction conditions were established. Prior to derivatization, samples were concentrated using solid phase extraction pretreatment. Two different cartridges - Oasis HLB[®] and Oasis WAX[®] cartridges were evaluated for extraction efficiency of PFCAs with different carbon chain lengths. All target PFCAs could be analyzed with both cartridges, except for PFBA which could only be analyzed using WAX[®] cartridges. Using the developed method, several isomers of PFOA present in technical mixtures were also successfully analyzed. The method detection limits for PFCAs with six or more carbons were less than 31 ng/L in ultrapure water and less than 50 ng/L in surface water. Method recoveries for the target PFCAs were greater than 92% in both ultrapure water and surface water. Satisfactory levels (1.9%-5.1%) of instrument precisions (calculated by the relative standard deviation of eight injections of the same sample) were also achieved. The developed method was employed for analyzing selected target PFCAs for the subsequent bench-scale drinking water treatment study.

3.1 Introduction

Perfluorinated compounds (PFCs) have been detected globally in wildlife, humans, and in various environmental compartments at trace concentrations (pg/L- μ g/L) (Kannan et al. 2004; Rahman et al. 2014; Ahrens 2011). They are typically aliphatic compounds containing strong saturated carbon-fluorine bonds and hence are resistant to chemical, physical, and biological degradation (Kissa 2001; Buck et al. 2011). High water solubility, simultaneous hydrophobic/lipophobic properties, and low volatility of most PFC anions (Kissa 2001; Bhatarai and Gramatica 2011; Larsen and Kaiser 2007) are reflected in the significance of aqueous environmental compartments as their source and sink in the environment. There are several classes of PFCs that have been detected in the aquatic environment including drinking water. And hence, drinking water has been recognized as a source of human exposure to PFCs. Perfluorinated carboxylic acids (PFCAs) is a class of PFCs that have received attention due to their frequent detection in drinking water. Considering their widespread occurrence in drinking water and potential toxicity, the USEPA has included three PFCAs- perfluoroheptanoic acid (PFHpA), perfluorooctanoic acid (PFOA), and perfluorononanoic acid (PFNA) in its final list of the 3rd unregulated contaminant monitoring rule (UCMR3) (USEPA 2011b). Indeed, PFOA has also been listed in USEPA's final list of third contaminant candidate list (CCL3) (USEPA 2011a) and is also being considered for regulatory directives by several other jurisdictions around the world (Zushi et al. 2012; Rahman et al. 2014). Perfluorinated sulfonic acids are another class of PFCs that have been widely reported in drinking water. Reports on drinking water occurrence of other classes such as perfluorinated sulfonamides and telomer alcohols are sparse.

PFC analysis is predominantly carried out using LC/MS/MS. Only a limited number of GC/MS methods have been reported for analysis of select PFCs in aqueous and other matrices. However,

many labs do not have access to LC/MS/MS instrumentation and therefore, favor the more commonly available GC techniques. In addition, GC analysis has a higher separation efficiency compared to LC analysis and is much less prone to matrix effects which are specific to the transfer of the analytes from the LC column into the MS detector. Following some preliminary works, the current study, selected PFCAs as the target PFC class for the GC/MS analytical method development work. The new method was subsequently used to investigate the removal of PFCAs during drinking water treatment.

PFCAs, having an acid moiety in their structure are not directly amenable to GC analysis. Their high polarity may cause tailing effects resulting in high detection limits (Monteleone et al. 2012). Derivatization can assist in alleviating those problems by increasing the volatility of PFCAs and improving their chromatographic behaviour. Subsequent GC/MS analysis can be performed in either electron impact ionization (EI) or chemical ionization (CI) mode. While EI can take advantage of mass spectral libraries, CI typically provides higher sensitivity showing the pseudo-molecular ion $[M+H]^+$ or $[M-H]^-$ in the positive or negative ion mode, respectively (Martin et al. 2004; Jahnke and Berger 2009).

Published methods for GC/MS analysis of PFCAs in various matrices have used esterification processes with end products being methyl esters (Moody and Field 1999), propyl esters (Langlois et al. 2007), butyl esters (Alzaga and Bayona 2004; Dufková et al. 2009; Liu et al. 2011b; Dufková et al. 2012), and benzyl esters (Fujii et al. 2012). Another process involving derivatization with 2,4-difluoroaniline in presence of *N,N*-dicyclohexylcarbodiimide to generate 2,4 difluoroanilide derivatives of PFCAs has also been published (Scott et al. 2006; De Silva and Mabury 2004). Methyl esters of PFCAs have been found to be highly volatile and methylated shorter carbon chain length ($C < 6$) PFCAs could not be separated with GC column films as thick

as 4 μm (Moody and Field 1999). Langlois et al. (2007) used isopropanol in the presence of concentrated H_2SO_4 to derivatize PFOA and other longer chain PFCAs and measured these with a thin film column (0.25 μm). Alzaga and Bayona (2004) used ion-pair solid phase micro extraction (SPME) coupled with in-port derivatization with tetra-butyl ammonium (TBA) as the ion-pair and derivatizing reagent. A derivatization method using isobutanol and isobutyl chloroformate in presence of pyridine has been described by Dufková et al. (2009). Formed PFCA-butyl esters were then extracted in hexane to be analyzed by GC/MS. Dufková et al. (2012) successfully reported using this method for trace level analysis of C5-C12 PFCAs in river water using a solid phase extraction (SPE) for sample preconcentration and extraction. The GC-NCI-MS method published by Dufková et al. (2012) is the first method to achieve low detection limits (pg/L-ng/L) of PFCAs in surface water. However, if samples processed by this method were measured using GC-EI-MS conditions, detection limits would certainly be higher (Dufková et al. 2009). In addition, this methods also seems rather time consuming. All other derivatization methods discussed previously have limitations when aiming to analyse a wide range of PFCAs including shorter chain ones at low concentrations in surface water for water treatment studies. A number of these methods have been developed for matrices other than water (Liu et al. 2011b; Fujii et al. 2012; De Silva and Mabury 2004; Alzaga et al. 2005). Some methods developed for aqueous samples used chemical or negative chemical ionization for PFCA analysis (Monteleone et al. 2012; Alzaga and Bayona 2004; Dufková et al. 2012). Indeed only a few GC-EI-MS methods have been used for trace level analysis of aqueous samples (Moody and Field 1999; Dufková et al. 2009; Scott et al. 2006). Of these methods both the Moody and Field (1999) and Dufková et al. (2009) methods have high detection limits which limit their application only to highly contaminated samples. Also neither of the two methods could detect short Chain PFBA.

The method developed by Scott et al. (2006) has low detection limits and can analyze both short and long chain PFCAs. However, the method is very time consuming and not suitable for treatment studies since the water samples were concentrated by evaporating water thereby reducing sample volume from 1 L down to 50 mL. This was followed by derivatization and GC/MS measurement.

The objective of this study was to develop a simple derivatization method and combine it with solid phase extraction pretreatment method for GC-EI-MS analysis of short and long chain PFCAs in water at environmentally relevant concentrations. PFCAs were derivatized to form butylesters and a systematic approach was undertaken by using a multi-factorial experimental design and statistical analyses to identify and optimize the significant experimental factors for the derivatization reaction. In addition tests were conducted to simplify sample processing. Finally, the method was applied to spiked river water samples thereby demonstrating the suitability of the method for analyzing drinking water treatment study samples. The method has also been slightly modified to analyze short chain PFBA in water. In addition, the method can be applied to identify branched PFOA isomers in technical mixtures of PFOA. The developed derivatization method is economically and ecologically friendly since it uses only microliters of solvents and other chemicals.

3.2 Experimental Section

3.2.1 Materials and Chemicals

Solvents methanol (HPLC grade), n-hexane (GC grade), anhydrous n-butanol and PFCAs standards perfluorobutanoic acid (PFBA), perfluoropentanoic acid (PFPeA), perfluorohexanoic acid (PFHxA), perfluoroheptanoic acid (PFHpA), perfluorooctanoic acid (PFOA), and perfluorononanoic acid (PFNA) were obtained from Sigma-Aldrich (St. Louis, MO). The purity

of all standards and solvents was $\geq 97\%$. Mass labeled $^{13}\text{C}_8$ -PFOA (49 $\mu\text{g/mL}$) and a technical mixture of PFOA (T-PFOA) (50 $\mu\text{g/mL}$), both dissolved in methanol were obtained from Wellington Laboratories (Guelph, ON). $^{13}\text{C}_8$ -PFOA was used as an internal standard. Anhydrous sodium carbonate was purchased from VWR (West Chester, PA). Sulfuric acid and ammonium hydroxide (reagent grade) were obtained from Fisher Scientific, Canada. Oasis[®] HLB (6 cc, 150 mg, 60 μm ; hereafter referred to as HLB for hydrophilic–lipophilic balance) and Oasis[®] WAX (6cc, 150 mg, 60 μm ; hereafter referred to as WAX for weak anion exchange) SPE cartridges were purchased from Waters (Milford, MA). Milli-Q[®] water used during the study was produced from a Millipore[®] system (Milli-Q UV Plus[®], Mississauga, ON). Surface water was collected from the nearby Grand River. The collected surface water was refrigerated at 4°C overnight prior to use. The concentration of dissolved organic carbon (DOC) in the surface water sample was 5.1 mg C/L and turbidity was about 3.0 nephelometric turbidity units (NTU). No filtration was done to remove particulate matter from the collected water prior to SPE.

Except for the mass labelled internal standard, all PFCA standards were obtained as solids, and stock solutions of individual PFCAs were prepared at a concentration of 1,000 mg/L in methanol and stored at 4°C. Working standards of PFCA mixtures or individual PFCAs were prepared by diluting stock solutions appropriately to either 10 mg/L or 1 mg/L and also kept refrigerated at 4°C. Prepared solutions (both stock solutions and working standards) were stored for no longer than 9 months in the refrigerator. Table 2.1 in Chapter 2 includes the PFCAs (C4-C9) that were analyzed using this newly developed method.

3.2.2 Sample Preparation, Preservation and Background Contamination Prevention

Milli-Q[®] water and surface water were spiked with target PFCAs to establish calibration curves, method detection levels (MDLs), and levels of quantification (LOQ). Glass containers have been

reported to irreversibly adsorb PFCAs (Martin et al. 2004) and hence, polypropylene (PP) containers and lab-ware were used whenever possible. Teflon[®]-based labware was also avoided to minimize potential background contamination. Surface water collected from the nearby Grand River was stored in a PP container at 4°C in darkness. Derivatization reactions were performed in 15 mL conical PP vials (VWR, West Chester, PA). All sample containers were washed thoroughly with ultrapure water, methanol, and ultrapure water three times each in sequence to avoid contamination. Sample containers were air dried prior to use. Water samples were passed through extraction cartridges in polypropylene transfer lines. Solvents and reagents were stored in vials covered by aluminum foil under their caps to minimize contamination from PTFE containing caps.

Tests were conducted to understand the effect of preservation time. PFCAs (C6-C9) were spiked at a target PFCA concentration of 3 µg/L in water together with an internal standard (¹³C₈-PFOA) at a concentration of 0.588 µg/L. Spiked ultrapure water and river water samples were stored in polypropylene containers for 4 days, 7 days in the lab at 4°C in darkness and then extracted, eluted and analyzed. Experiments were also conducted to simplify processing of samples during the extraction process. Spiked ultrapure and river water samples were passed through HLB cartridges and a sub set was eluted and analyzed immediately. The remainders of the extracted cartridges were stored at 4°C in darkness, and were dried, eluted and subsequently analyzed after 4 days and 7 days.

3.2.3 Solid Phase Extraction (Optimized Process)

A previously published SPE method by Taniyasu et al. (2005) was used as basis for the current study. Taniyasu et al. (2005) analyzed the samples using HPLC-MS/MS. The SPE method was adapted during the current study to accommodate GC/MS instrumentation. Both HLB and WAX

cartridges were examined. Sample preconditioning, sample introduction, and elution steps were followed as described by Taniyasu et al. (2005). However, for the current GC/MS method 500 mL of sample instead of 100 mL was introduced to increase method sensitivity. Also, $^{13}\text{C}_8$ -PFOA instead of 1,2 ^{13}C -PFOA was used as the internal standard. In addition, eluted samples were blown down to dryness to facilitate the subsequent derivatization process by eliminating moisture and by swapping eluting solvent. Briefly: prior to sample introduction HLB Cartridges were preconditioned using 5 mL methanol and then 5 mL of Milli-Q[®] water and WAX cartridges with 5 mL of 0.1% NH_4OH in methanol followed by 5 mL methanol and then 5 mL of Milli-Q[®] water at about 2-3 drops/sec. Prior to extraction all samples were spiked with 150 μL of 1.96 mg/L internal standard solution prepared in methanol (corresponding to a final concentration of 0.588 $\mu\text{g/L}$ in the sample). Spiked water samples (500 mL) were then passed through the conditioned cartridges at a rate of 1-2 drops/second. Effort was made to ensure that cartridges did not get dry at any time during preconditioning and sample introduction. Cartridges were then washed. For HLB cartridges, 5 mL of 5% methanol in Milli-Q[®] water and for WAX 4 mL of 25mM acetate buffer (pH 4) were used as wash solution at 2-3 drops/sec. The cartridges were then dried thoroughly under vacuum to remove any excess water. Once dried, HLB cartridges were eluted with 10 mL methanol. WAX cartridges were eluted first with 4 mL of methanol, which was discarded, and then with 4 mL 0.1% NH_4OH in methanol. Elution solvent volume required to elute all target PFCAs was examined to optimize the elution volume. The eluates were collected in 15 mL polypropylene vials and were then blown to dryness under a gentle stream of nitrogen at room temperature. The effect of blowing under nitrogen to dryness and to near dryness was examined.

3.2.4 Derivatization (Optimized Procedure)

The residue resulting from the drying step was then reconstituted in 100 μL of anhydrous n-butanol which acted as the derivatizing reagent. The reconstituted extract solution was then stirred in a vortex mixer for 10-30 seconds. The derivatization reaction (Eq. 3.1) took place under heat and acidic conditions. To provide acidic conditions, 10 μL of concentrated sulfuric acid (H_2SO_4) was added, stirred and capped. Vials were then heated at 50°C for three hours to form butyl esters of the PFCAs. The mixture was then allowed to cool down for approximately 20 min to room temperature and 100 μL of saturated Na_2CO_3 was added to neutralize the acid added previously. The mixture was then stirred in a vortex mixer for 10-30 seconds and allowed to settle for 3-5 minutes. Following the acid neutralization step, n-hexane was added to extract the PFCA butyl esters using liquid-liquid extraction. One of two different volumes of n-hexane, 400 μL or 1900 μL , was added making the final volume of the mixture 610 μL or 2110 μL , respectively. The mixture was stirred again in a vortex mixer for 10-30 seconds and was allowed to settle for 3-5 minutes. The upper hexane layer was collected for subsequent analysis by GC/MS. The derivatized sample extract can be stored in refrigerator at 4°C up to 30 days.



$\text{R} = \text{C}_n \text{F}_{2n+1}$; Heat and H_2SO_4 were used as catalyst for the reaction

3.2.5 Instrumentation and Quantification

A Varian 3800[®] GC equipped with an 8210 Auto-sampler was used for all analyses. Helium was used as the carrier gas (constant flow at 1.0 mL/min). A DB-1701 fused silica column (30 m x 0.25 mm, 1.0 μm) coupled to a length of deactivated guard column was used for separation of the analytes. Injection of a 1 μL sample was performed with a split/splitless injector at temperature of 250°C and held splitless for 1 min. Derivatized samples were kept at room

temperature in the auto-sampler tray prior to analysis. The initial temperature of the column oven was 40°C, at which it was held for 5 min; the temperature was then programmed to increase to 50°C at a rate of 2°C /min and then to 120°C at a rate of 5°C/min. Then the column was heated to 240°C at a rate of 30°C/min and the final temperature was maintained for 5 min. Mass spectrometry was performed using a Varian 4000[®] MS set in EI mode. Transfer line and ionization source temperatures were 250°C and 150°C, respectively. The solvent delay time was set to 12.5 min. The emission current was at 10 μ amps. Mass spectra of the butylated derivatives were obtained in full scan mode in preliminary experiments, and later selected ion storage (μ SIS) was used for identification and quantification. The analytical conditions for PFCA analysis by GC–EI-MS are shown in Table 3.1.

Table 3.1: Analysis and method performance parameters

Name	MW of butyl ester	Qualification and quantitation ion (m/z)	Ultrapure water				River water			
			MDL (ng/L)	LOQ (ng/L)	IP	Recovery (± RSD) (%)	MDL (ng/L)	LOQ (ng/L)	IP	Recovery (± RSD) (%)
PFBA	270	100, 119, <i>169</i>	N/A							
PFPeA	320	100, <i>131</i> , 169	N/A							
PFHxA	370		30	95	5.1%	92.4 (5.2)	35	113	2.3%	107 (5.0)
PFHpA	420		23	74	4.6%	92.7 (4.0)	16	52	3.6%	108.1 (2.3)
PFOA	470		11	35	2.2%	115.2 (1.5)	20	65	3.4%	106.8 (2.8)
PFNA	520		16	51	1.9%	104.7 (2.4)	49	157	3.6%	95.7 (7.4)

IP- Instrument precision; MW-molecular weight; MDL- method detection level; LOQ- level of quantification; RSD - relative standard deviation; m/z in bold and italic are quantitation ions; N/A- data not available; n= 7 for MDL and LOQ calculations; n =8 for IP calculations

3.2.6 Optimization of Reaction Conditions using Experimental Design

To optimize the derivatization reaction conditions, a statistical experimental design approach involving central composite design (Engineering Statistics 2014) was used. Three derivatization reaction factors- reaction time, reaction temperature, and volume of H₂SO₄ were selected and their effect was systematically investigated. The experimental domain or the range of each factor was selected based on preliminary experiments. Experiments consisting of a 2³ factorial design with six star points were performed. To ensure rotability of the circumscribed design, a value of 1.682 was chosen for the axial distance α (Engineering Statistics 2014). In total, the experimental design matrix required 18 runs including four center point replicates.

All experiments were conducted using a stock solution of 10 mg/L of PFCA in n-butanol and the experimental order was fully randomized. A fixed volume of 100 μ L of n-butanol was used. The following experimental domains were used: temperature: 30°C – 80°C; time: 10 min – 180 min; volume of H₂SO₄: 10 μ L – 20 μ L. Optimization derivatization reactions were conducted in glass reaction vessels since PP was only compatible for temperatures up to and including 50°C. Once the optimized reaction temperature was established, subsequent experiments were conducted in 15 mL polypropylene (PP) vials that were used to collect eluted solvent during SPE process. Table 3.2 presents the full matrix used for the experimental design. All experiments were conducted on the same date and were injected in the same GC/MS run.

Table 3.2: Full matrix for the factorial design

Run#	Point type	Temperature (°C)	Time (min)	Volume (µL)	Remarks
1	Center	55	95	15	Block 1
2	Center	55	95	15	
3	Center	55	95	15	
4	Center	55	95	15	
5	Time Star	55	237.8	15	
6	Time Star	55	1.0	15	
7	Vol. Star	55	95	23.4	
8	Vol. Star	55	95	6.6	
9	Temp. Star	97	95	15	Block 4
10	Temp. Star	13	95	15	
11	Corner	30	10	10	Block 2
12	Corner	30	180	10	
13	Corner	30	10	20	
14	Corner	30	180	20	
15	Corner	80	10	10	Block 3
16	Corner	80	180	10	
17	Corner	80	10	20	
18	Corner	80	180	20	

The GC/MS conditions were set as described earlier. Full scan mode was used to detect the PFCAs (C4, C6-C9). For C4, m/z 169 was used and for the rest of the PFCAs, m/z 131 was used to quantify response area under each peak. The response data for each peak were then transformed into a dimensionless single desirability scale (d_i) ranging from 0 to 1 where the maximum response of the 18 runs for each compound was a value of 1 (Yu et al. 2007). Consequently the lowest response for each compound was assigned a value of zero. It was assumed that each target compound has resulted in a single derivative and thus for a given target compound, the single desirability, d_i for a single experimental run was calculated as follows (Eq. 3.2) (Yu 2007):

$$d_i = \frac{x_i - x_{low}}{x_{high} - x_{low}} \dots \dots (3.2)$$

X_i = the i^{th} (1~n) response for a specific compound in 18 runs; n
= total number of runs

X_{low} = the lowest response for a specific compound in 18 runs;

X_{high} = the highest response for a specific compound in 18 runs

Overall quality of response for each run is measured by using the total desirability function as shown below and the function was used to seek the optimal derivatization conditions. The total desirability (D_i) (Eq. 3.3) is calculated by the geometric mean of the single desirabilities of all 18 runs.

$$\text{Total Desirability } D_i = \sqrt[m]{d_1, d_2, \dots, \dots, d_m} \dots \dots (3.3)$$

m = total number of single desirabilities i.e. total target compounds

Stepwise regression analyses of the single desirabilities for individual compounds were then performed to determine the factors (reaction time, reaction temperature, and H₂SO₄ volume) and factor interactions significant at the 5% significance level. The main effect, two-effect interactions, and the quadratic main effects were considered for the stepwise regression process using a commercial software (SYSTAT[®]). The regression analyses of total desirabilities were performed using response surface methodology by a commercial statistical software package JMP pro[®]. The optimal reaction conditions were also established subsequently using this software package. In addition, contour plots of the total desirability were used to examine the optimized reaction conditions. An overview of the optimization process used in this study can be found in Figure 3.1.

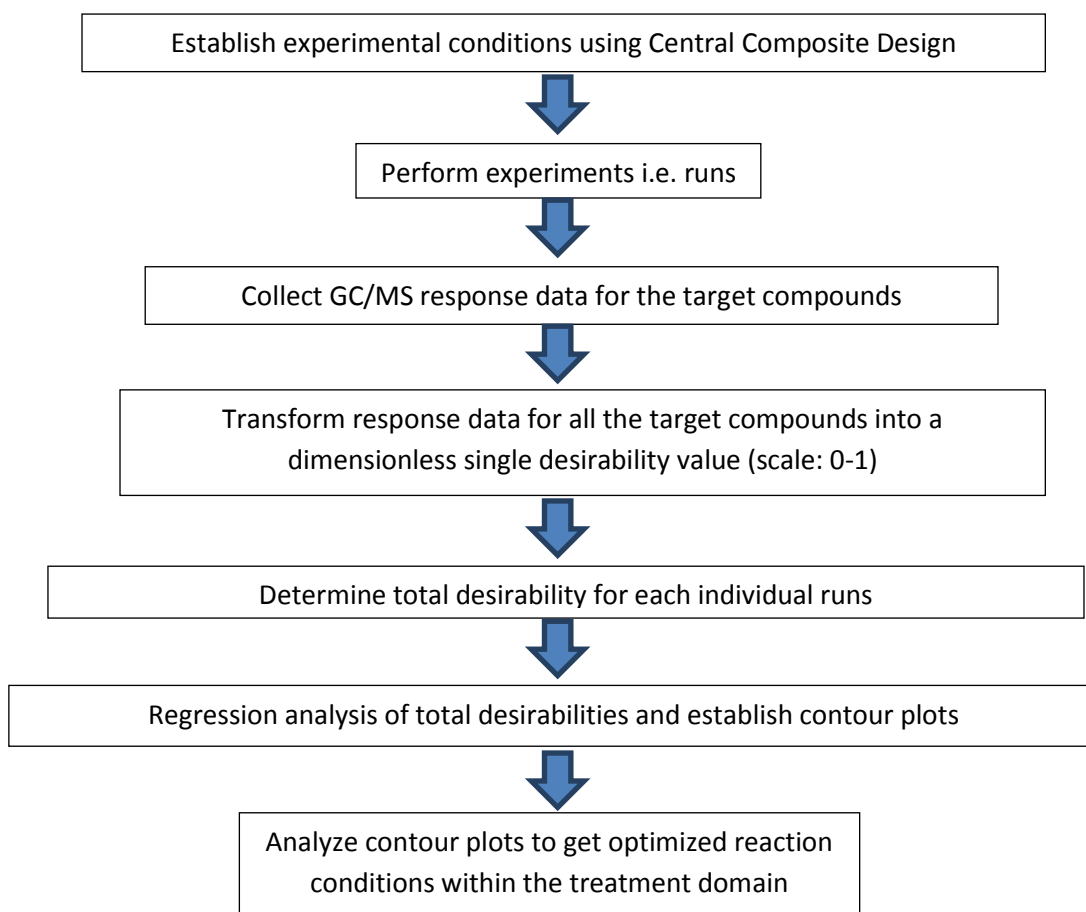


Figure 3.1: Overview of the derivatization reaction optimization procedure (adapted from Yu 2007)

3.2.7 Calibration Curves, MDL, LOQ, Recoveries and Instrument Precision

Calibration curves were built by plotting the ratio of analyte peak area to the internal standard ($^{13}\text{C}_8\text{-PFOA}$) peak area against the analyte concentration to the internal standard concentration. Eight point calibration curves with concentration levels ranging from 0.05 $\mu\text{g/L}$ to 4.0 $\mu\text{g/L}$ in ultrapure water and river water were established. The MDL of individual compounds in Milli-Q[®] water and surface water was determined by calculating the standard deviation of seven replicates (spiked at a concentration of 0.2 $\mu\text{g/L}$) at the 99% confidence level (APHA 2005). The LOQs was established by multiplying the standard deviation by 10 (APHA 2005). Instrument precision (IP) was calculated by determining the relative standard deviation (% RSD) of eight consecutive

injections of one of the replicate extracts used for MDL determination. Method recoveries were determined by the following formula (Harris 2007):

$$\% \text{ recovery} = \frac{C_{\text{Spiked sample}} - C_{\text{unSpiked sample}}}{C_{\text{added}}} \dots \dots (3.4)$$

$C_{\text{spiked sample}}$ = concentration determined in a spiked samples

$C_{\text{unspiked sample}}$ = concentration determined in a unspiked samples

C_{added} = target spiked concentration added to a unspiked sample

Sample replicates used for MDL calculation spiked at target concentration of 0.2 µg/L (C_{added}) were used to calculate method recoveries.

3.3 Results and Discussion

Results are presented following the typical sample processing scheme. Once the extraction and derivatization protocols were established, the method was used to determine the effect of preservation and was also used to analyze samples from a drinking water treatment study conducted using both Milli-Q[®] and surface water.

3.3.1 Extraction Efficiency

Extraction efficiencies of two types of cartridges namely Oasis HLB and WAX were studied. Following Taniyasu et al. (2005) methanol was used as the extraction eluent. Profiling of the eluate was also conducted to optimize the eluent volume. PFBA could not be detected with the HLB cartridges using the current method due to the low extraction yield with the HLB cartridges as has been reported previously (Taniyasu et al. 2005). For WAX cartridges, only PFOA and PFNA were eluted to more than 50% within the first 2 mL of eluate, however, a total of 4 mL eluted all the extracted PFCAs (Figure 3.2A). There were no PFCAs detected in the 4-6 mL

eluate fraction. Thus, 4 mL of 0.1% NH₄OH in methanol solution was sufficient to elute the extracted PFCAs from WAX cartridges. For HLB cartridges, more than 65% of all the extracted PFCAs were eluted within the first 2 mL of eluate and more than 99% were eluted within the first 6 mL (Figure 3.2B). However, very small amounts of PFCAs could still be detected in the 6-8 mL and 8-10 mL eluates. Hence, for HLB cartridges a methanol volume of 10 mL was used to elute the extracted PFCAs. Also, it can be observed from Figure 3.2 that for WAX cartridge for the first 2 mL the % elution of the extracted PFCAs increased as the chain length increased (e.g. nearly 29% of PFPeA, as opposed to 63% for PFNA, was eluted within the first 2 mL eluate). For the HLB cartridge, however, the opposing trend was observed within the first 2 mL— as the chain length increased the % elution of the extracted PFCAs decreased (e.g. nearly 82% of PFPeA was eluted as opposed to about 67% for PFNA).

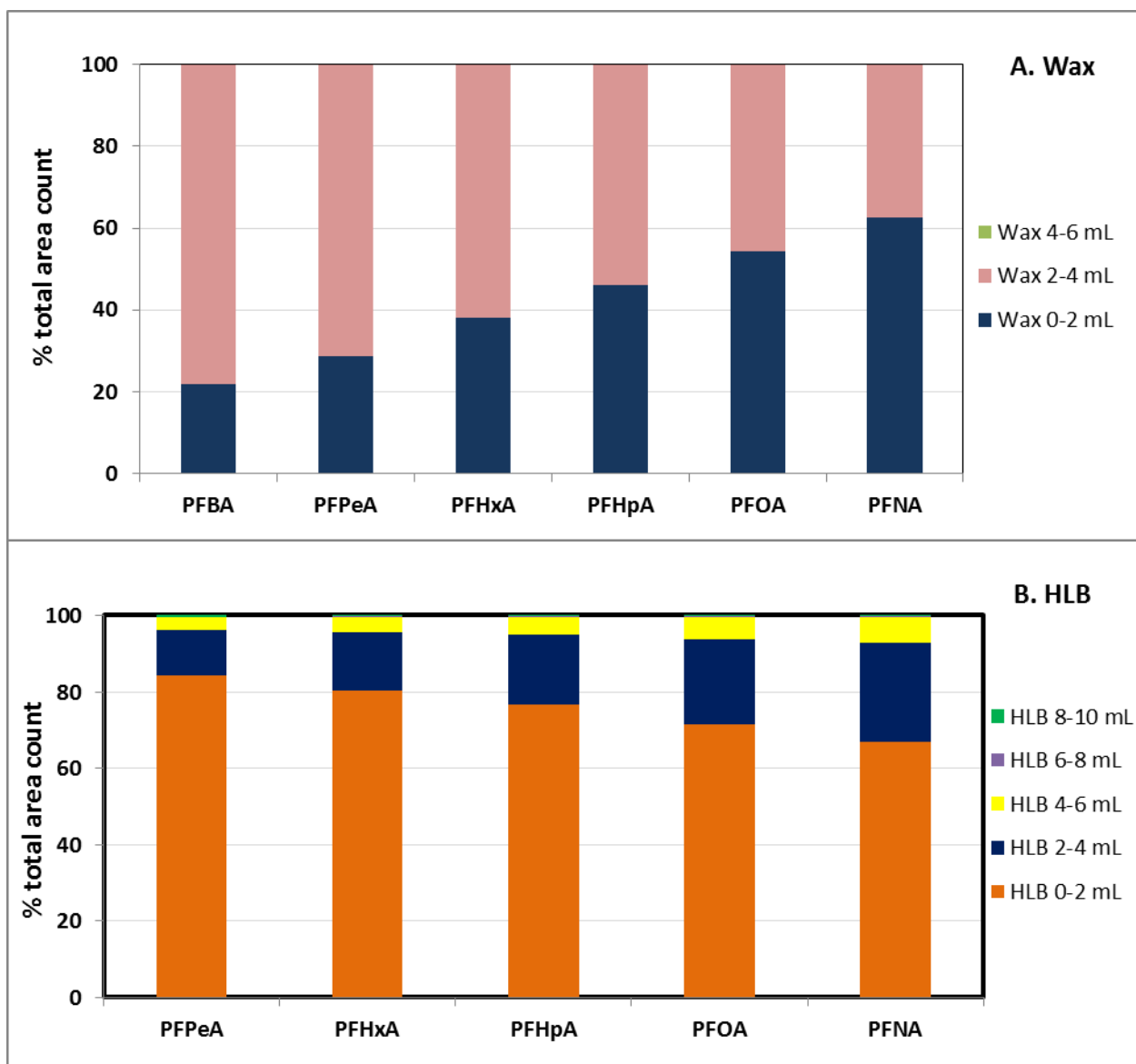


Figure 3.2: A) 0.1% NH₄OH in methanol elution volume profile for C4-C9 (duplicates) extracted with WAX cartridges and B) Methanol elution volume profile for C5-C9 (duplicates) extracted with HLB cartridges, PFBA could not be analyzed using HLB cartridges.

Responses of target PFCAs were higher for the WAX cartridges compared to the HLB cartridges, especially for the shorter chain PFCAs (Figure 3.3). For example, when blown off to dryness, the adjusted average response of PFPeA with WAX cartridges was nearly 4.2 times that obtained with the HLB cartridges, and for higher chain C6-C9 compounds the responses were

still 1.2-1.5 times higher with WAX cartridges vs. those for the HLB cartridges. Taniyasu et al. (2005) also observed higher recoveries of PFCAs with WAX cartridges.

Since the goal of the derivatization process was to form butyl esters of PFCAs via esterification with butanol under sulfuric acid catalysis, methanol used to elute the analytes needed to be swapped with microliter volumes of anhydrous n-butanol. Hence, methanol was blown down to dryness under a gentle stream of nitrogen. Short chain PFCAs such as PFBA and PFPeA having high volatility compared to longer chain PFCAs may suffer more losses during blowing down to dryness. Therefore the effect of blowing off to dryness and near dryness was investigated for both HLB and WAX cartridges extracts. Target contaminant responses for both types of cartridges were nearly double when the methanol eluates were blown down to dryness compared to near dryness (approximately 10 μ L) (Figure 3.3). A possible explanation is that during derivatization with butanol analytes may have also been transformed into methyl esters with the remaining methanol, and thus responses for the butyl esters were decreased. Hence, care needed to be taken to ensure complete evaporation of methanol to avoid potential formation of methyl esters. Also evident from Figure 3.3 is that blowing off to dryness has a similar low range of standard deviations for both types of cartridges. Although adjusted responses were higher when WAX cartridges used, HLB cartridges were employed to assess performance of the method primarily because HLB cartridges are more economical compared to WAX cartridges. In addition, blowing off to dryness was facilitated much faster with the methanol eluates from the HLB cartridges compared to the 0.1% NH_4OH in methanol eluates from the WAX cartridges.

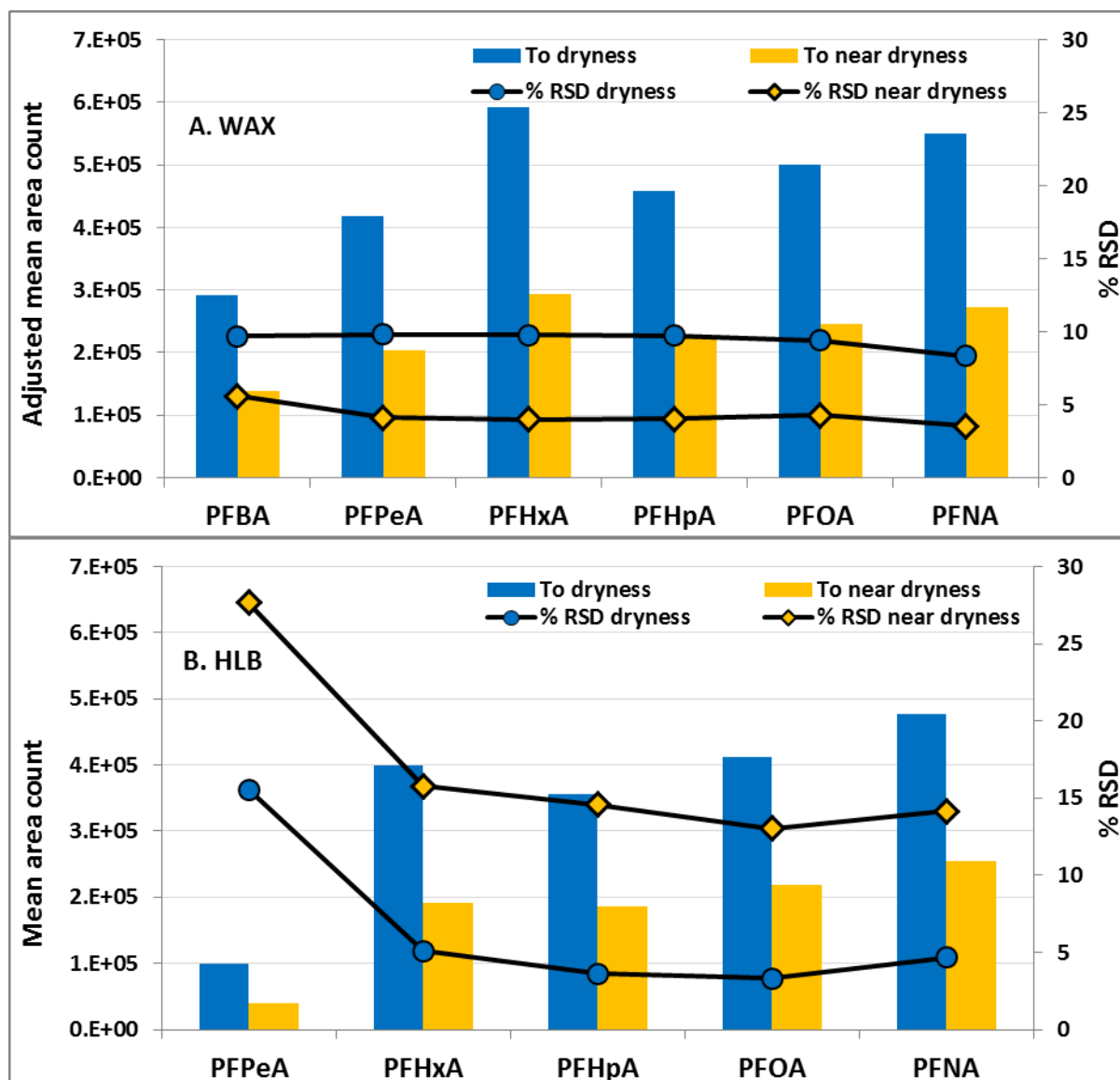


Figure 3.3: Effect of drying eluates from A. WAX cartridges and B. HLB cartridges with nitrogen; butanol to n-hexane ratio 1:19 for WAX and 1:4 for HLB (n-hexane is used to extract derivatized butyl esters of PFCAs). Hence, the GC/MS response for WAX cartridges is represented as the adjusted mean by multiplying the mean area count by a factor 4.75); PFBA (C4) could not be analyzed using HLB cartridges; RSD: relative standard deviation of 3 replicates of each sample.

3.3.2 Optimization of Derivatization Method

Preliminary experiments in the lab indicated that the developed derivatization reaction seemed to be influenced by the several factors – namely reaction temperature (A), reaction time (B), and

volume of H_2SO_4 (C). By understanding the effects of these three factors and by optimizing these reaction conditions analyte response can be improved. As described in section 3.2.6, a central composite design was employed to determine the significant factors and factor interactions. Experiments were run and single desirabilities of individual compounds for 18 central composite design runs were obtained. Table 3.3 shows that in terms of main effects, reaction time was significant for all the target compounds while temperature was only significant for PFOA, and the volume of H_2SO_4 was only significant for PFOA and PFNA. Among the two factor interactions, the factor involving temperature and time (AB), and quadratic effects of temperature (A^2) and time (B^2) were significant for all target PFCAs while the factor involving time and volume of H_2SO_4 (BC) was significant for PFOA and PFNA only. Two factor interactions involving temperature and volume of H_2SO_4 (AC), and also the quadratic effect of volume of H_2SO_4 (C^2) were not significant.

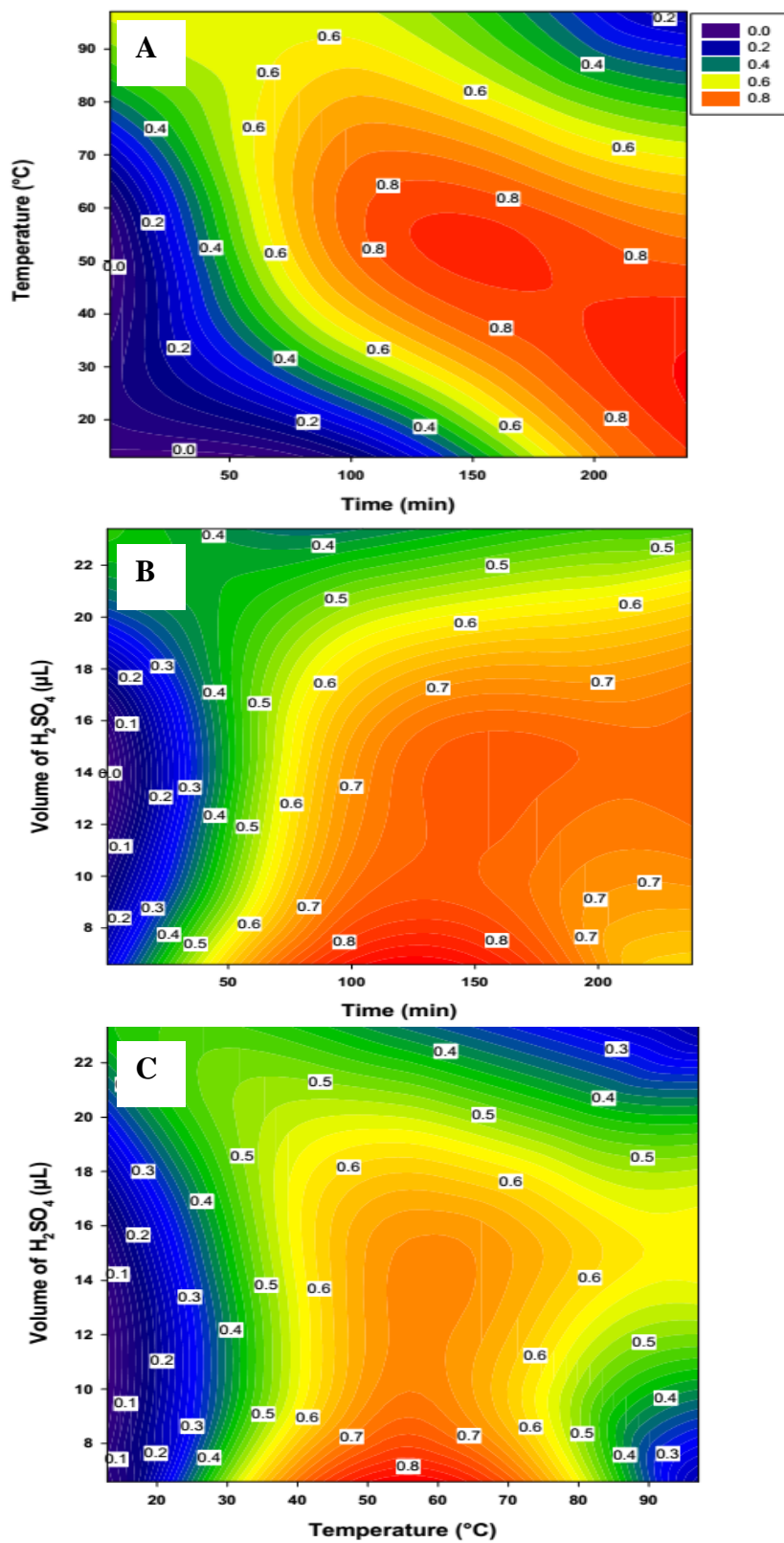


Figure 3.4: Contour plots for total desirability.

Table 3.3 Statistical analysis of main effects and two factor interactions

Compound	Main effects			Two factor interactions					
	A Temp	B Time	C Volume	AB	BC	CA	A ²	B ²	C ²
PFBA	-	+	-	+	-	-	+	+	-
PFHxA	-	+	-	+	-	-	+	+	-
PFHpA	-	+	-	+	-	-	+	+	-
PFOA	+	+	+	+	+	-	+	+	-
PFNA	-	+	+	+	+	-	+	+	-

A = temperature; B = time; C = volume of H₂SO₄; (+) significant; (-) non-significant

Contour plots of the total desirability were generated and examined to establish the optimized reaction conditions (Figure 3.4). As can be seen from Figure 3.4A, which presents the effect of temperature and reaction time, the total desirability contour has a value greater than 0.8 in two regions: i) temperature 45°C to 60°C and time 125 min to 180 min, ii) temperature 15°C to 40°C and time 200 min to 238 min. The total desirability contour plotted as a function of volume of H₂SO₄ and reaction time (Figure 3.4 B) exhibited a value higher 0.8 in the region: volume of H₂SO₄-6.6 µL to 7 µL and time- 95 min to 160 min. When plotted as a function of the volume of H₂SO₄ and the reaction temperature (Figure 3.4C) the total desirability contour showed a value greater than 0.8 in the region: volume of H₂SO₄- 6.6 µL to 7.0 µL and reaction temperature 47°C to 64°C. Using the response surface prediction profiler option of the commercial software package *JMP-pro*, the maximum desirability was determined to be 0.96 and the optimum reaction conditions were found to be as following- temperature: 50°C, reaction time: 180 min and volume of H₂SO₄: 10 µL. This results in the ratio of the volume of derivatization reagent n-

butanol and the volume of H_2SO_4 to be added being 10:1. Liu et al. (2011b) also used a similar derivatization reaction for analyzing PFCAs in sediments followed by a supercritical fluid extraction using in-situ headspace SPME coupled to a GC/MS unit. The authors reported the same n-butanol to H_2SO_4 ratio as the current study for optimum esterification efficiency. However, Liu et al (2011b) reported a higher optimum temperature (70°C) for extraction and esterification efficiency which may be due to the use of supercritical fluid extraction. A flow diagram of the optimized derivatization process of the current method is shown in Figure 3.5.

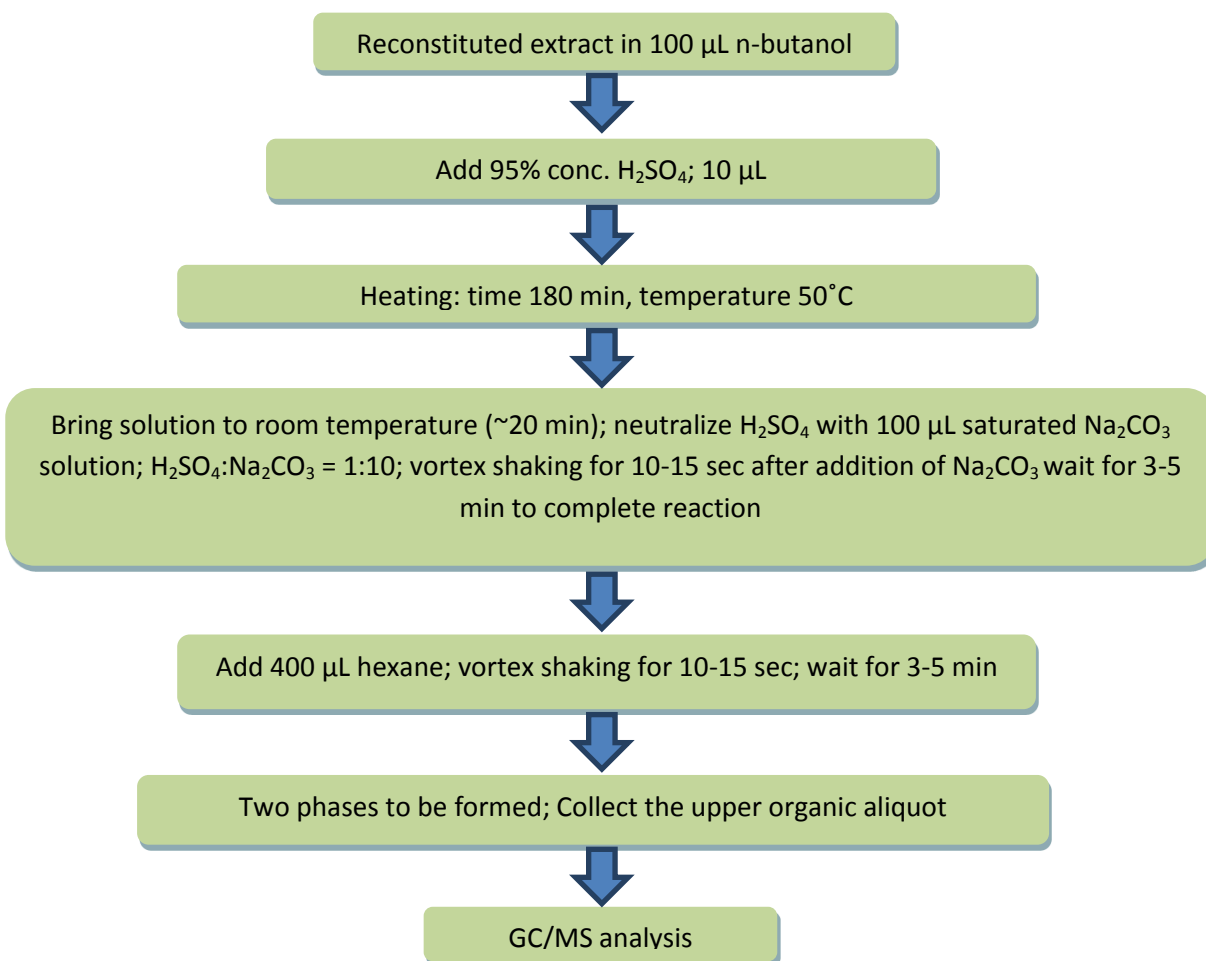


Figure 3.5: Summary of the derivatization process

3.3.3 Identification and Quantification PFCAs with C ≥ 5

Following derivatization with n-butanol and neutralization of the H₂SO₄, n-hexane was added to provide a non-polar phase and extract the formed PFCa butyl esters. n-hexane having a lower boiling point (69°C) compared to n-butanol (117.4°C) will elute earlier in the GC column. Hence, any remaining n-butanol in the hexane extract may affect the separation of the more volatile, earlier eluting shorter chain PFCAs such as PFBA and PFPeA by overlapping with the n-butanol peak. It was observed that an n-hexane to butanol ratio of 4:1 could successfully be used to extract the derivatized butyl esters and separate PFCAs with five or more carbons. An n-hexane to n-butanol ratio lower than that affected the separation of the shorter chain PFPeA and made the peak broader. Details of quantification of the target PFCAs are listed in Table 3.1.

Figure 3.6 presents GC/MS chromatograms for PFCAs with five or more carbons extracted with HLB cartridges at two different concentrations from ultrapure water samples. Good response was achieved for all PFCAs at 3 µg/L (Fig 3.6b) and even at 0.5 µg/L good response is evident for PFCAs with carbon chain length of C₆ and higher. The differences in retention time between each set of two consecutive PFCa peaks are equidistant which is indicative of a homologous series.

The major EI fragmentation ions for PFCAs belong to two typical fragmentation series and differ by 50 amu corresponding to the mass of CF₂. One of the fragmentation series includes ions 69 [CF₃]⁺, 119 [C₂F₅]⁺, 169 [C₃F₇]⁺, 219 [C₄F₉]⁺ and the other series includes: 131 [C₃F₅]⁺, 181 [C₄F₇]⁺, 281 [C₅F₉]⁺ (Alzaga and Bayona 2004; Moody and Field 1999; Dufková et al. 2009). In addition, other fragments (93[C₃F₃]⁺ and 100 [C₂F₄]⁺) have also been reported (Langlois et al. 2007). The GC-EI-MS spectra of PFNA (Figure 3.6d) shows the presence of the characteristic fragmentation ions listed earlier. Three ions- m/z= 100, 131, and 169 were used as qualification

ions while $m/z = 131$ was used as the quantification ion for PFCAs with $C \geq 5$. Previously Taniyasu et al. (2005) indicated that mass labeled 1,2 ^{13}C -PFOA can be used a suitable internal standard for PFCAs with chain lengths between C6 and C10. Based on the conclusion drawn by Taniyasu et al. (2005) it was presumed that the recoveries of the mass labeled ^{13}C -PFOA (the internal standard for the current study) may also only be valid for chain length between C6 and C10 as the recoveries of the short chain PFCAs such as PFPeA and PFBA may differ from the longer chain PFCAs. Since PFPeA and PFBA were not used as target contaminants for the subsequent water treatment study, no quantitative work was performed on these PFCAs during this method development study.

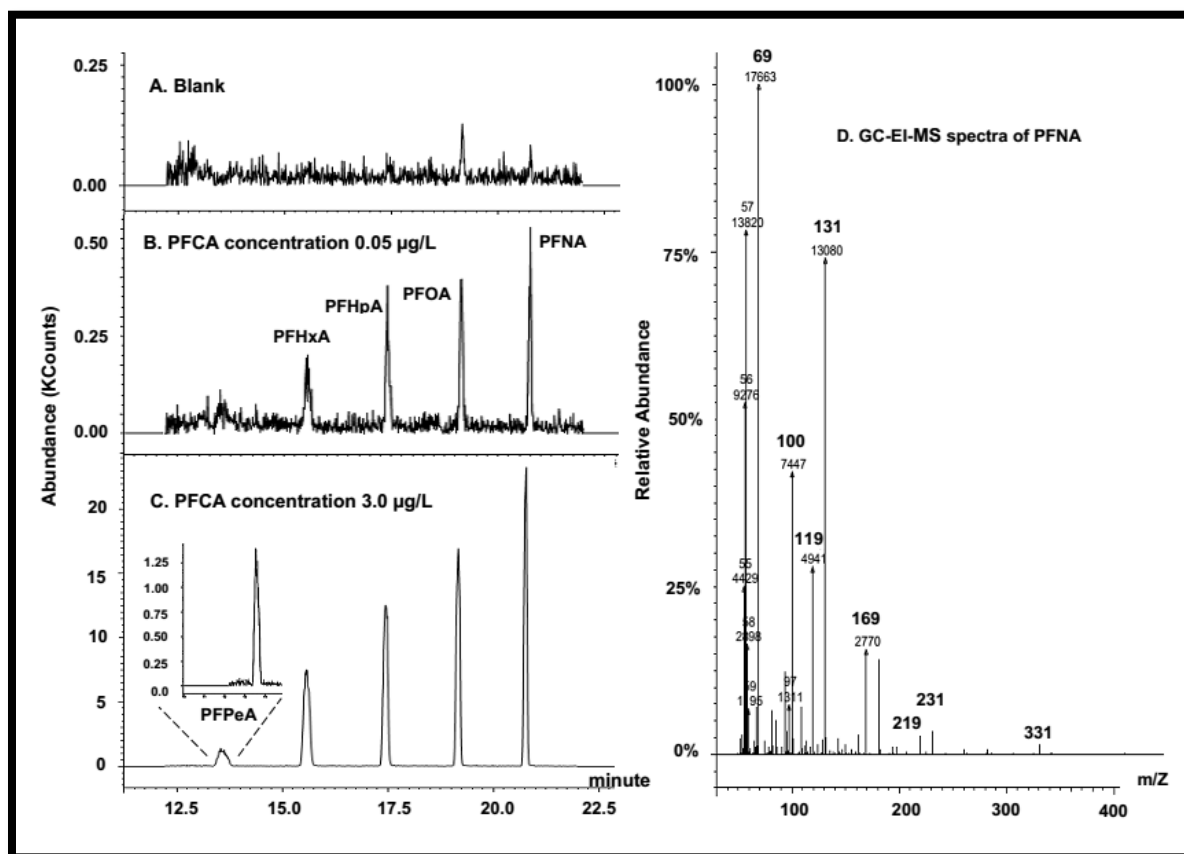


Figure 3.6: Characteristic μSIS (m/z : 131) chromatogram for: A) blank; B) 0.05 $\mu\text{g/L}$; C) 3.0 $\mu\text{g/L}$, D) characteristics full scale GC-EI-MS spectra of PFNA.

The developed GC/MS method was successfully applied to analyze PFCAs spiked in ultrapure and surface water. None of the target PFCAs were detected in unspiked ultrapure and surface water. Therefore, in Eq. 3.4, the concentration in unspiked samples ($C_{\text{unspiked samples}}$) was assigned a value of zero. Method recovery for the target PFCAs in ultrapure water ranged from 92% for PFHxA to 115% for PFOA and in surface water they ranged from 96% for PFNA to 108% for PFHpA. MDLs and LOQs were calculated for all target PFCAs except for PFBA and PFPeA. The MDLs and LOQs determined in both ultrapure water and surface water are listed in Table 3.1. The established MDLs for the target PFCAs range from 11 ng/L to 30 ng/L. The concentrations of the target PFCAs in the surface water were below MDLs. Although similar, the MDLs of the PFCAs in surface water were somewhat higher compared to ultrapure water. It can be seen that MDLs and LOQs increased as the carbon chain length of PFCAs decreased which can be attributed to the decreased extraction yield of HLB cartridges as the carbon chain length decreased. Thus it can be presumed that the MDL and LOQ for PFPeA when extracted with HLB will be higher than that of PFHxA. Considering that this method applied EI ionization, the MDLs achieved using the method are satisfactory for conducting drinking water treatment studies for PFCA removal at trace concentrations. However, future studies can take advantage of negative chemical ionization to increase the sensitivity of the newly developed method.

The instrument precision limits were also determined for PFHxA, PFHpA, PFOA and PFNA (Table 3.1). The determined instrument precision limits for the GC/MS in both ultrapure water (1.9%-5.1%) and surface water (2.3%-3.6%) samples are very satisfactory.

3.3.4 Sample Preservation

PFCAs are non-biodegradable and thus degradation of the PFCAs during sample storage was not expected. Figure 3.7 presents the results of sample preservation experiments. It can be seen that PFCA concentrations in both ultrapure (Figure 3.7A) and surface water (Figure 3.7B) samples on Day 1 are comparable to PFCA concentrations on Day 4 and Day 7. Thus samples can be stored at 4°C for 7 days after collection without any substantial degradation of PFCAs.

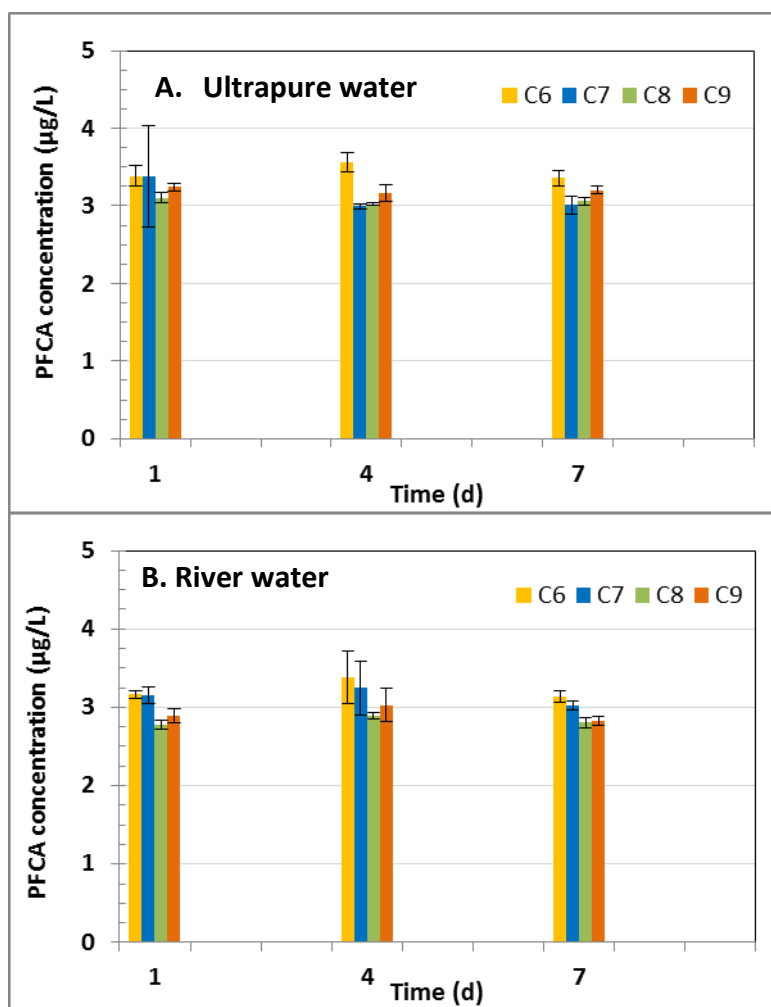


Figure 3.7: Analysis results in ultrapure (A) and river water (B) when water samples were stored at 4°C for 4 and 7 days and then extracted and analyzed; Error bars indicate standard deviation of 3 replicates of each sample

Results of experiments to investigate the impact of pausing sample processing after extraction and storing cartridges in the refrigerator until further processing are presented in Figure 3.8. For both ultrapure water (Figure 3.8A) and surface water (Figure 3.8B) no substantial variations between samples processed on Day 1 as opposed to those samples which were processed on Day 4 and Day 7 were observed. This suggests that, if needed, sample processing can be halted once samples have been extracted and cartridges can be stored up to 7 days.

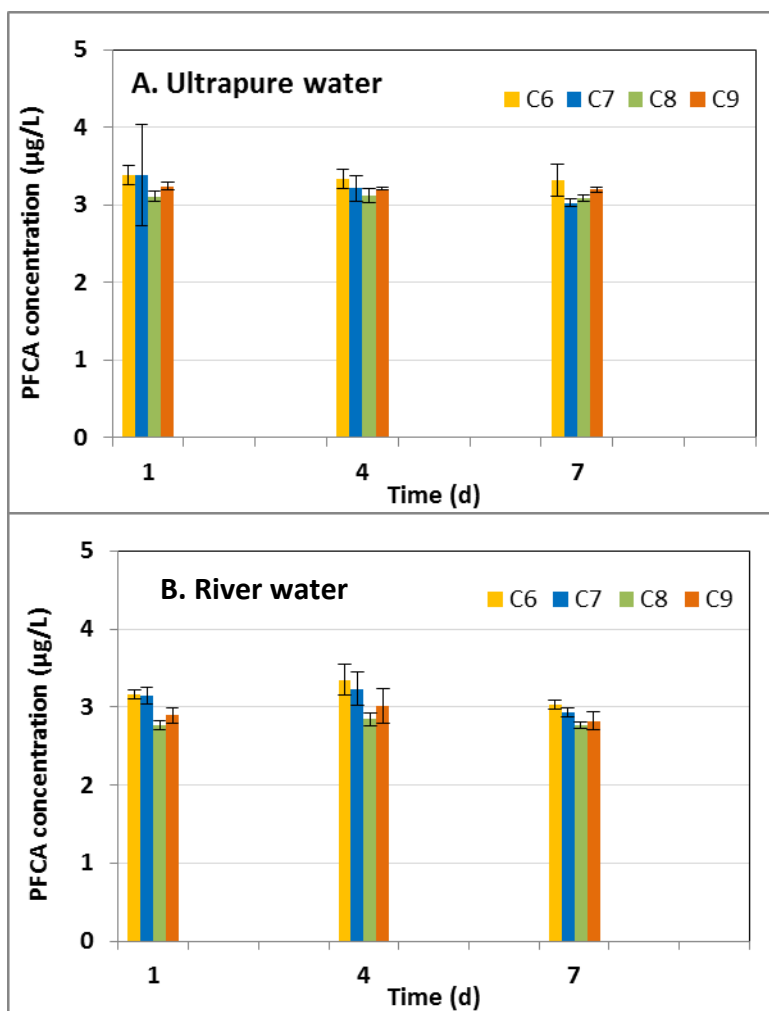


Figure 3.8: Analysis results in A) ultrapure water and B) river water when HLB cartridges were stored for up to 7 days in the freezer following sample extraction. After storage analytes were eluted from the cartridges and processed further; Error bars indicate standard deviation of 3 replicates of each sample

3.3.5 PFBA Analysis

As discussed in Section 3.3.3, the n-hexane to n-butanol ratio can affect the separation of shorter chain PFCAs such as PFBA and PFPeA. Figure 3.9 shows the effect of n-hexane to butanol ratio on the separation of PFBA in the GC column. It is evident from Figure 3.9A and Figure 3.9B that at low n-hexane to butanol ratios (e.g. 4:1, 8:1, 10:1) the solvent peak becomes broad and masks the PFBA peak which elutes very early from the GC column due to the high volatility of this short chain butylester. As the ratio is increased (e.g. 1:14, 1:19) the solvent peak gets narrower (Figure 3.9C) enabling the PFBA peak to be separated. Figure 3.9D shows the GC-EI-MS spectra of PFBA. All the characteristic fragmentation ions (69, 93, 100, 119, 131, and 169) are present. However, unlike the other PFCAs examined during the current study, the abundance of $m/z = 131$ is significantly lower. Several n-hexane to butanol ratios were tested during the study and finally a ratio of 19:1 was found adequate for subsequent GC/MS analysis of PFBA (Figure 3.9E). Due to the relatively high volume of n-hexane required for the extraction (19:1) the resulting PFBA extract was more dilute compared to the other PFCAs which required a lower (4:1) n-hexane to butanol ratio for extraction. Hence, the MDL of PFBA is expected to be considerably higher than for these other PFCAs. As discussed in Section 3.3.3 no further quantitative work was done on short chain PFBA during the current study.

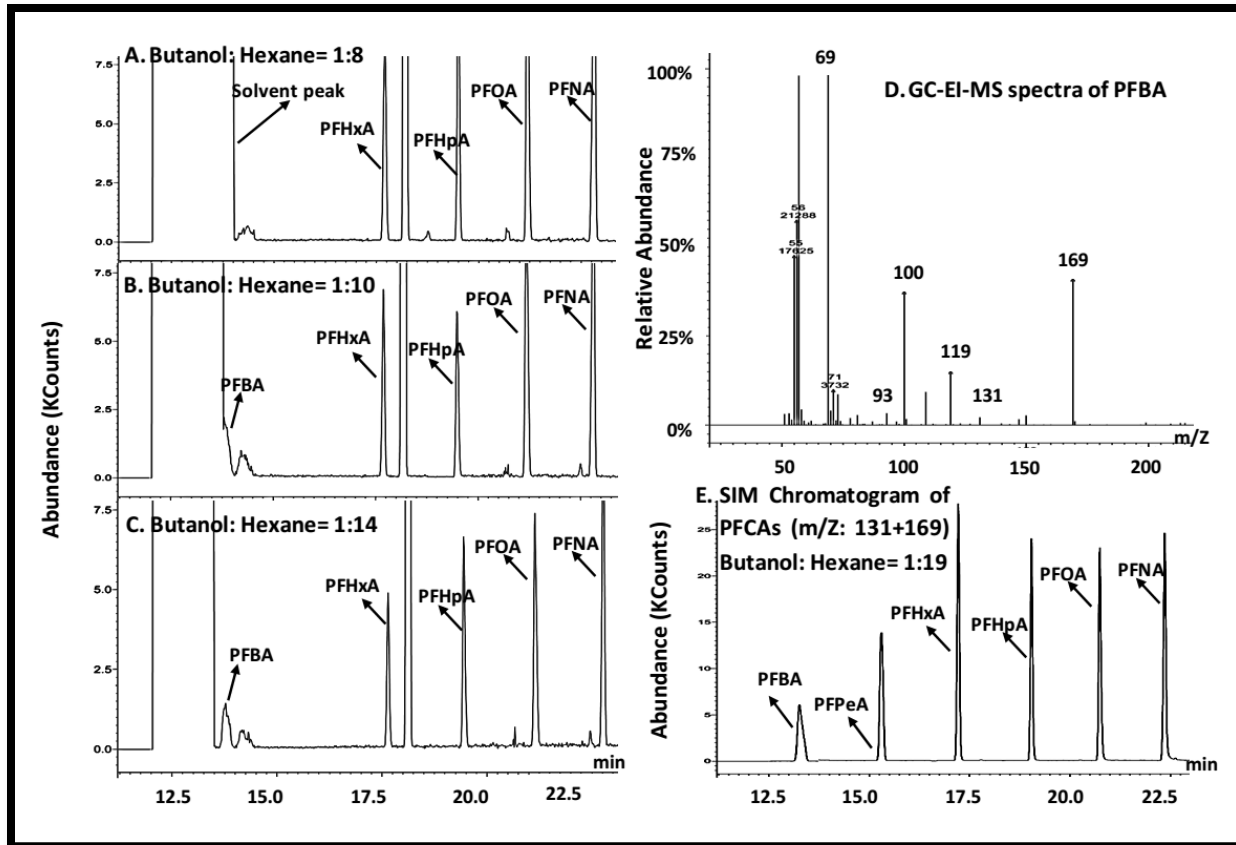


Figure 3.9: Full-scan chromatograms (A, B, C) showing PFCA peaks and effect of butanol to n-hexane ratio on PFBA detection; D) GC-EI-MS spectra of PFBA; E) μ SIS chromatogram (m/z: 131 + 169) showing C4-C9 PFCAs.

3.3.6 PFOA Isomer Analysis

The developed method was applied successfully to a PFOA technical mixture isolating five PFOA isomers (Figure 3.10). The linear isomer, being the major component in the technical mixture, had the highest abundance. Using a combination of ^{19}F NMR and LC/MS analyses the manufacturer Wellington Laboratories indicated the presence of seven structural isomers of PFOA with two isomers having percent composition no greater than 0.5%. It seems that the current method was not able to detect these latter two isomers but the method has not been optimized for isomer detection. Due to a lack of appropriate standards, it is challenging to perform quantitative work on PFCA isomers. However, Benskin et al. (2010) noted “during the

GC/MS analysis the quantitative isomer composition of a sample may be possible by comparison of relative peak areas of the molecular ion.” Thus the current method can be used to perform semi-quantitative analysis of PFOA isomers using this approach.

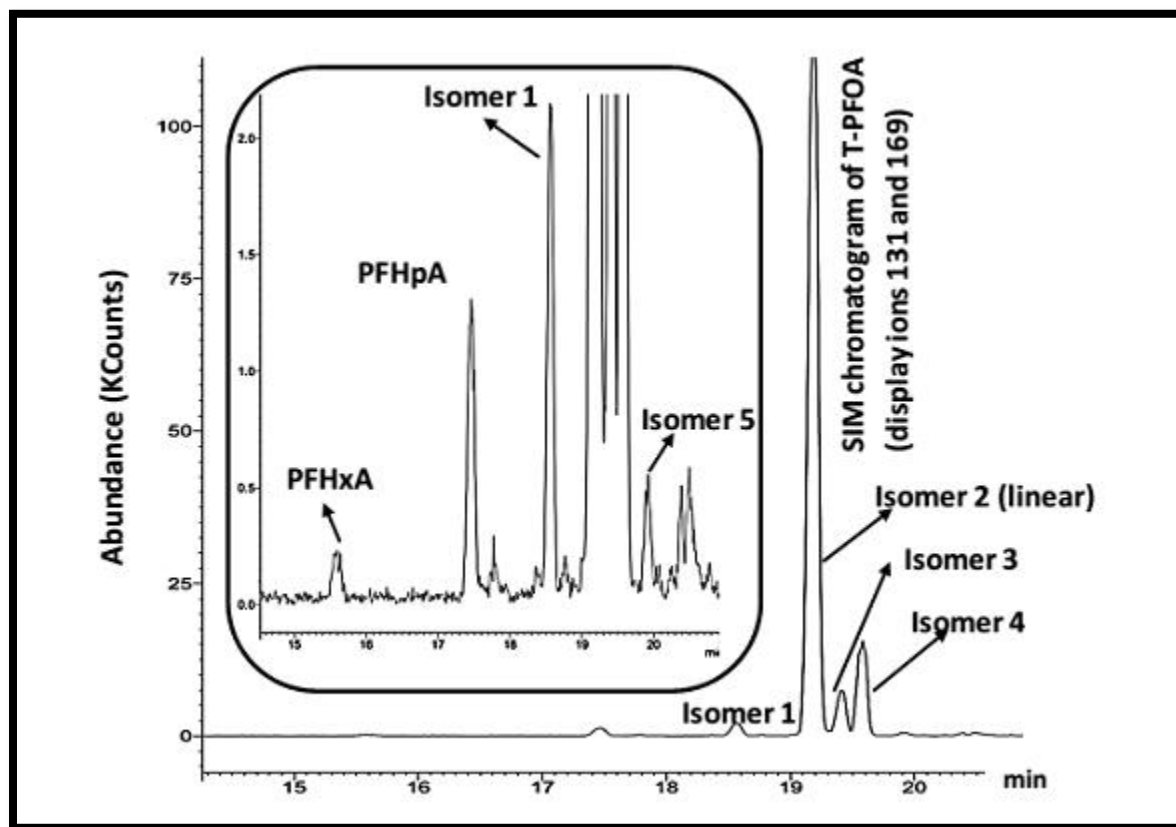


Figure 3.10: GC-EI-MS chromatograms showing several PFOA isomers, PFHxA, and PFHxA present in a PFOA technical mixture.

3.4 Conclusions

A GC-EI-MS method using SPE and a subsequent derivatization has been successfully developed to measure short and long chain PFCAs (C4-C9) in ultrapure and surface water at trace concentrations. Key findings are summarized below:

- The target PFCAs can be quantified in ultrapure and surface water using the developed GC/MS method at trace concentrations (ng/L- μ g/L).

- Target PFCAs were derivatized using butanol as a derivatization reagent in presence of H_2SO_4 and heat. The optimal derivatization reaction conditions (10 μL H_2SO_4 , 180 min, and 50°C) were systematically established by using a central composite design.
- Two types of cartridges, the Oasis HLB and Oasis WAX were examined. Shorter chain PFCAs had lower extraction yields compared to longer chain PFCAs. Indeed PFBA could only be detected with WAX cartridges. The developed method has adequate MDLs for longer chain PFCAs ($C \geq 6$). For example: the MDLs for PFOA in ultrapure water and surface water when HLB cartridges were used were found to be 11 ng/L and 20 ng/L, respectively. However, shorter chain PFCAs such as PFPeA and PFBA will likely have significantly higher MDLs due to lower extraction yields.
- The ratio of n-hexane to butanol during liquid-liquid extraction of derivatized butyl esters affected the analysis of short chain PFCAs. A lower ratio (4:1) of n-hexane to butanol was used to analyze PFCAs with five or more carbons ($C \geq 5$) while a higher ratio (1:19) was used to separate PFBA. The lower n-hexane to butanol ratio resulted in a wider solvent peak thereby affecting the subsequent separation of shorter chain PFCAs such PFBA and PFPeA.
- The developed method has also been successfully applied to separate isomers in a technical PFOA mixture. However, due to lack of availability of commercial isomer standards only qualitative work can be done using the method at the present time. As appropriate standards become more readily available, the developed GC/MS-based method can be applied to detect isomers in the environment.

The method is currently being applied to study the removal of PFCAs during drinking water treatment using adsorption processes.

Chapter 4

Treatment of Selected Perfluorinated Carboxylic Acids (PFCAs) using GAC, Ion Exchange Resins and Alternative Adsorbents in Ultrapure Water

Summary

The removal potentials of three perfluorinated carboxylic acids (PFCAs) - PFHpA, PFOA, and PFNA from ultrapure water were evaluated using four conventional granular activated carbons (GACs), two anion exchange resins, and two alternative adsorbents. Bottle point mixed solutes kinetic experiments indicate that A-500P resin and coal-based F-400 GAC exhibited removal capacities higher than the other adsorbents. The capacity of the coconut shell-based CX GAC was similar to F-400 and A-500P but the removal kinetics were slower. The wood-based GACs exhibited lower PFCA adsorption capacities compared to the other GACs and the anion exchange resins. The alternative adsorbents did not substantially remove any of the target PFCAs. Single solute isotherm experiments show that the A-500P ion exchange resin had a higher uptake capacity vs. the F-400 GAC and the A-860 ion exchange resin. F-400 had a higher removal capacity for PFHpA and PFOA than the A-860 resin. However, for PFNA the removal capacities of F-400 and A-860 were similar. With regard to the GACs, pore size distribution and surface charge played important roles in the removal of PFCAs. Kinetic experiments revealed that removal kinetics were substantially faster with anion exchange resins compared to GACs and the alternative adsorbents. Both resins displayed similar PFCA removal kinetics.

Uncharged acrylic and styrenic beads (i.e. base materials) of the two anion exchange resins were not able to remove PFOA. This indicates that the target PFCA anions were primarily removed by

charge interactions. The PFOA removal capacity of both anion exchange resins decreased in the presence of the inorganic anion, sulfate. The adverse impact of sulfate on PFOA removal capacity was more pronounced for A-860. Solute mixture effects (mixture of PFCAs as opposed to an individual PFCA) on PFCA removal kinetics were not apparent for the A-500P resin or the F-400 GAC. However, for A-860 higher removals of individual PFCAs were observed when present in mixtures with other target PFCAs. For the compounds investigated, PFCA chain length was found to be irrelevant in the case of the F-400 and CX GACs and the A-500P resin. However, the A-860 resin and Biochar removals increased as PFCA chain length increased.

4.1 Introduction

Perfluorinated carboxylic acids (PFCAs) are an emerging class of drinking water contaminants that have been detected globally at trace concentrations in drinking water (Post et al. 2013; Ullah et al. 2011; Mak et al. 2009; Rahman et al. 2014). Due to their widespread occurrence, long half-life in human tissue, and potential human health impacts (USEPA 2009a; Holtcamp 2012; Melzer et al. 2010) several PFCAs are currently being considered for regulation in various jurisdictions (USEPA 2011a,b,c; Zushi et al. 2012). In fact, three PFCAs-perfluoroheptanoic acid (PFHpA), perfluorooctanoic acid (PFOA), and perfluorononanoic acid (PFNA)- have been included in the final list of the USEPA's 3rd unregulated contaminant monitoring rule (UCMR3) (USEPA 2011b).

PFCAs, owing to the presence of strong carbon-fluorine bonds, are extremely resistant to environmental and physico-chemical degradation. In addition, their high water solubility, low volatility, and presence at trace concentrations make them challenging to treat by a variety of drinking water treatment processes. Studies have reported that PFCAs are typically not amenable

to conventional coagulation-flocculation, biofiltration, ozonation, and even advanced oxidation processes (Appleman et al. 2014; Thompson et al. 2011b; Quinones and Snyder 2009).

Activated carbon adsorption processes have been reported to be effective in removing PFCAs, especially in the case of the longer chain PFCAs (Hansen et al. 2010; Eschauzier et al. 2012). Several bench-scale studies have assessed the effectiveness of granular activated carbon (GAC) adsorption (Carter and Farrell 2010; Senevirathna et al. 2011; Yu et al. 2009a; Ochoa-Herrera and Sierra-Alvarez 2008). These studies have primarily focused on PFOA and perfluorooctane sulfonate (PFOS). Limited information is available on adsorption behaviour of PFHpA and PFNA. Some of the studies (Carter and Farrell 2010; Yu et al. 2009a; Ochoa-Herrera and Sierra-Alvarez 2008) were conducted at initial concentrations several orders of magnitude higher than environmentally-relevant concentrations which may not accurately represent treatment efficiencies at the lower environmental concentrations. Most bench-scale studies have been conducted using coal-based GACs with the exception of that of Appleman et al. (2013) who, in addition to coal-based GACs, investigated coconut shell-based AquaCarb[®] 1240 C. Thus there is a gap in understanding the effect of different types of GAC base material on PFCA adsorption in ultrapure water.

In terms of alternative adsorbents, recent studies by Cao and Harris (2010) and Cao et al. (2011) reported promising removal of atrazine using dairy manure-based Biochar and indicated that dairy manure-based Biochar can be an effective alternative adsorbent for organic contaminant removal. Another alternative adsorbent - cattle bone-derived bone char has been reported to remove inorganic fluoride Medellin-Castillo et al. (2007). To date no information is available on adsorption potential of PFCAs onto dairy manure based Biochar and bone char.

PFCAs, due to their low pKa values (Ahrens et al. 2012; Wang et al. 2011b), usually exist in anionic form at typical drinking water pH levels. Therefore, anion exchange resin treatment offers a potential drinking water removal technique for PFCAs. Available bench-scale studies also corroborate the promise of anion exchange resins for the removal of PFCAs from ultrapure and surface water (Yu et al. 2009a; Dudley 2012; Arevalo Perez 2014). Dudley (2012) reported that macroporous polyacrylic strong base anion exchange resin had faster PFCA uptake kinetics but the resin exhibited lower uptake capacity compared to both the gel and macroporous types of polystyrenic strong base anion resins used in their study. Deng et al. (2010), however, observed higher removal of PFOS with polyacrylic resins compared to polystyrenic resins. Thus, investigation is needed to understand the effect of resin matrix on PFCA removal. Ion exchange resins remove organic contaminants via several mechanisms. However, the effect of electrostatic interaction vs. hydrophobic interaction during PFCA adsorption using ion exchange resins is not clearly understood. Also molecular structures of the anion exchange sites that are the cationic functional groups may also play role in removing organic contaminants. However, information about the exact structure of the anion exchange functional groups is typically proprietary and hence not readily available. Limited information regarding the effect of inorganic anions typically present in surface water on PFCA removal capacity of ion exchange resins is available.

The primary objectives of the current study were to evaluate the effectiveness of two anion exchange resins, four GACs, and two alternative adsorbents for the removal of three PFCAs - PFHpA, PFOA and PFNA - from ultrapure water at environmentally relevant concentrations using bottle point kinetics and isotherm experiments. In addition the study investigated the effect of adsorbent properties such as surface area, pore size distribution, and surface charge on adsorption of PFCAs. Furthermore, the study looked into underlying mechanisms for PFCA

removal by ion exchange resins i.e. elucidate the role of electrostatic vs hydrophobic interactions when removing PFCAs. Finally, the study investigated the effect of direct competition among PFCAs on their removal (i.e. comparing the removal of individual PFCAs present in solution as opposed to when they are present in mixtures with other target PFCAs).

4.2 Materials and Methods

4.2.1 Target compounds and water

PFHpA (99%), PFOA (96%), and PFNA (97%) were purchased from Sigma-Aldrich (St. Louis, MO, USA). Molecular structures and the physicochemical properties for each of the selected target compounds are provided in Chapter 2 Table 2.1. Ultrapure water (18.2 Ω) generated from a Millipore Milli-Q UV Plus[®] system (Mississauga, ON) was used throughout the study. DOC levels in the ultrapure water were always below 0.3 mg C/L and pH values ranged between 4.9—6.1. No pH adjustments were done during this study. The target PFCAs are strongly acidic (estimated $pK_a < 1$) and are expected to be in anionic form in the pH ranges of ultrapure and surface water (Ahrens et al. 2012; Wang et al. 2011b). Stock solutions of the target PFCAs were prepared in ultrapure water at a concentration of 10 mg/L without any organic solvent and stored for a maximum of 9 months at 4°C. Throughout this phase of study, ultrapure water was spiked as required using the stock prepared in ultrapure water. The individual, nominal compound target spike concentration was 3.0 $\mu\text{g/L}$ in all tests. The actual spiked concentrations were measured at the beginning of each experiment.

4.2.2 Adsorbents

Four types of traditional GACs used in drinking water treatment—coal-based Filtrasorb 400[®] (F400) (Calgon Carbon, Pittsburgh, PA, USA), coconut shell-based AquaCarb CX 1230[®] (CX 1230) (Evoqua Water Technologies, Warrendale, PA, USA), and wood-based C-Gran[®] (C-Gran)

(Cabot Norit Activated Carbon, Marshall, TX, USA) and WV B30[®] (B30) (Mead Westvaco, North Charleston, SC, USA) were selected for evaluation. In addition, two alternative adsorbents - a digested dairy manure-based Biochar (Char Technologies, Toronto, ON, Canada) and cattle bone-based Fija Fluor (Apelsa Carbon, Jalisco, Mexico) were assessed. All the carbonaceous adsorbents were donated by their respective manufacturer. The GACs and the alternative adsorbents were sieved through a 12 × 30 US standard mesh, washed in ultrapure water (18.2 Ω) to remove fine particles and dissolved contaminants, and dried at 110°C for at least 24 h to remove any moisture. The tested GACs and the alternative adsorbents were not crushed. Following drying, the adsorbents were sealed with aluminum foil and stored in a desiccator until further use.

Two organic scavenging strong-base anion exchange resins from Purolite- macroporous polystyrenic A-500P[®] and macroporous acrylic A-860[®] (Purolite, Bala Cynwyd, PA) were selected for study. Both ion exchange resins were used as received without further treatment. Base materials of the two resins, the uncharged resin beads (polyacrylic and polystyrenic resin beads), were donated by Purolite Canada. The uncharged beads were washed with 200 bed volumes of ultrapure water (18.2 Ω) to remove fines and organics in which they were stored or produced.

All the adsorbents used during the study were sent to a commercial lab for surface area and pore size distribution analysis (Quantachrome, Boynton Beach, FL). The specific surface area was calculated using the Brunauer-Emmett-Teller (BET) equation, and pore volume and pore size distribution were calculated using the density functional theory (DFT).

The point of zero charge (pH_{pzc}) of the GACs and alternative adsorbents was determined according to Summers (1986). Briefly, the pH of 20 mL of 0.1 M NaCl solution in a sealed Erlenmeyer flask was adjusted to several values between 2 and 12 using 0.1 M HCl or 0.1 M NaOH solutions. The adsorbents (100 mg) were then placed in the flasks on orbital shakers at 120 rpm at room temperature. The final pH was measured after 24 hours. The pH_{pzc} is the point where the curve pH_{final} vs. $\text{pH}_{\text{initial}}$ crosses the line $\text{pH}_{\text{initial}} = \text{pH}_{\text{final}}$ (Summers 1986).

4.2.3 Kinetic and isotherm tests

Batch adsorption kinetics and isotherm experiments were conducted in 1 L polypropylene (PP) opaque bottles (VWR, West Chester, PA) at 150 rpm on an orbital shaker without any pH modification. All experiments were conducted at room temperature ($\sim 20^\circ\text{C}$) to minimize the effect of temperature variation during adsorption. .

Prior to spiking PFCAs, a large batch of ultrapure water was collected and left overnight for pH equilibration. Individual or mixtures of target PFCAs were spiked as needed in a large polypropylene container to achieve PFCA target concentration of 3 $\mu\text{g}/\text{L}$ using PFCA solutions in ultrapure water which were prepared without the use of solvents. The spiked solution was then stirred with a stainless steel bar to facilitate mixing of the PFCAs and then left overnight. PFCA concentrations in the spiked solution were measured subsequently to determine the exact starting concentrations. For each set of experiments, all samples were prepared from the same batch of spiked ultrapure water to ensure uniform starting pH and PFCA concentrations across all bottles. For kinetics experiments, 10 mg (dry weight) of adsorbent material was added to 1 L of spiked ultrapure water solution containing PFCAs. Sample bottles were then taken of the shaker and processed at different time intervals to monitor the time dependent removal of the spiked contaminants. Ultrapure water blanks, spiked ultrapure water blanks (positive controls), and

ultrapure water blanks containing adsorbents only (negative controls) were also added and taken of the shaker at preset time intervals for processing together with the bottles for the kinetics or isotherm tests. Spiked blanks were used as controls and were added to the sample queue to monitor if sample degradation was taking place. Kinetics experiments were used to determine the time to reach adsorption equilibrium. In addition, the effect of target contaminant mixtures on adsorption of individual PFCAs was investigated by spiking ultrapure water samples with a mixture of PFCAs (termed here as mixed solute, concentrations of the individual PFCAs were additive) and comparing to those spiked with target PFCAs individually (termed single solute).

For isotherm experiments (to determine the adsorption capacity of each adsorbent), different amounts (dry weights ranging from 0.5 mg to 12 mg) of adsorbent material were added to 1 L of ultrapure water solution. All isotherm experiments were conducted with single solutes at a target nominal concentration of 3 $\mu\text{g/L}$. Samples were then shaken for the time to adsorption equilibrium as was determined during the kinetic experiments (10 days for resins and 18-21 days for GAC and alternative adsorbents).

4.2.4 Analyses

Analyses of the target compounds in water samples were performed using gas chromatography with mass spectrometry (GC/MS) preceded by solid phase extraction (SPE) and derivatization. Details of the analytical method can be found in Chapter 3. The method detection limits (MDLs) were 11-30 ng/L in ultrapure water and 16-49 ng/L in surface water depending on the target compounds.

The DOC content of the ultrapure water was measured using a wet oxidation TOC analyzer OI Analytical Model 1010 TIC-TOC analyzer (College Station, TX). The oxidizing agent was 100

g/L $\text{Na}_2\text{S}_2\text{O}_8$. The samples were initially preserved by lowering the pH to 2-3 using 1N H_3PO_4 . The instrument was calibrated using standard solutions of potassium biphthalate ($\text{C}_8\text{H}_5\text{KO}_4$) at appropriate concentrations to measure low DOC levels in ultrapure water. The injection volume was 5 mL and 3 replicates of each sample were processed.

Sample pH was measured using an ORION 720A pH meter (Boston, MA) and conductivity was measured with a Mandel conductivity meter (Weilheim, Germany). Inorganic anions were analyzed with a Dionex AS-DV ion chromatography system (Thermo Scientific) using standard ASTM test methods for anions in water (ASTM Designation D4327-11).

4.3 Results and discussion

4.3.1 Adsorbent properties

Properties of the selected adsorbents and the results of the surface area and pore size distribution analyses are presented in Tables 4.1 and 4.2. Among the tested GACs, the wood-based C-Gran has the highest BET surface area ($1813 \text{ m}^2/\text{g}$) and pore volume ($1.44 \text{ cm}^3/\text{g}$) while the coal-based F-400 has the lowest BET surface area ($963 \text{ m}^2/\text{g}$) and pore volume ($0.503 \text{ cm}^3/\text{g}$). Wood-based WV B-30 and coconut-based CX carbon have similar BET surface areas but the latter has less pore volume. The alternative adsorbents Fija Fluor bone char and Biochar have much lower BET surface areas and pore volumes compared to the conventional GACs. BET surface area and pore volume of the tested anion exchange resins and the resin beads are very low with values below $10 \text{ m}^2/\text{g}$ and $0.05 \text{ cm}^3/\text{g}$, respectively. Pore size distribution of the tested adsorbents indicates that the two wood-based GACs, Fija Fluor and Biochar, are mesoporous since the major fraction of their pore volume is distributed in the size range between 2 and 34.5 nm. On the other hand, the F-400 and CX carbons are microporous (Table 4.1, and Figures C1 and Figure C2 in Appendix C) since F-400 and CX carbon have majority of their respective pore volume distributed at less

than 2 nm range. This suggests that the coal- and coconut-based carbons will be better adsorbents. However, CX carbon has a higher percentage of primary and secondary micropores.

Except for the resin matrix, both anion exchange resins have similar properties (Table 4.2). Typically styrenic resins and styrenic beads are more hydrophobic while acrylic resins and acrylic beads are more hydrophilic in nature. The resin beads are uncharged while both ion exchange resins have quaternary ammonium groups as their anion exchange functional groups. The exact compositions of these functional groups are proprietary.

Table 4.1: Properties of the GACs and the alternative adsorbents

Product	Base material	EPMD (mm)	pH_{pzc}	S_{BET} (m^2/g)	DFT pore volume (cm^3/g)	DFT pore size distribution		
						< 0.8 nm (cm^3/g)	< 2 nm (cm^3/g)	2- < 34.5 nm (cm^3/g)
CX	Coconut shell	1.21	9.7	1568	0.67	0.33	0.63	0.08
F-400	Coal	1.16	9.6	963	0.50	0.21	0.37	0.15
C-Gran	Wood based	1.03	4.6	1813	1.44	0.12	0.40	0.93
WV B-30		1.40	6.25	1565	1.13	0.056	0.33	0.75
Biochar	Digested dairy manure	N/A		222	0.21	0.04	0.07	0.14
Bone char	Cattle bone	N/A		161	0.34	0.013	0.013	0.32

S_{BET} - BET surface area; EPMD- effective particle mean diameter; pH_{pzc} - point of zero charge; pore size ranges: primary micropore <0.8 nm, secondary micropore < 2 nm and mesopore 2-50 nm; DFT- density functional theory.

Table 4.2: Properties of the anion exchange resins and the uncharged resin beads

Resin/ bead	Matrix	Capacity (Cl ⁻ form)* (eq/L)	Functional group*	Moisture content (%)**	Particle size range (mm)*	pH _{pzc}	S _{BET} (m ² /g)	DFT pore volume (cm ³ /g)
A-860	Macroporous polyacrylic	0.8	Quaternary ammonium	67.7	0.3—1.2	5.5	< 1	could not be measured
A-500P	Macroporous polystyrenic	0.8	Quaternary ammonium	68.0	0.425— 1.2	6.8	4.06	0.021
Styrenic beads	Macroporous polystyrenic	N/A	uncharged	36.7	N/A	7.0	< 1	could not be measured
Acrylic beads	Macroporous polyacrylic	N/A	uncharged	48.3	N/A	7.4	9	0.044

* Data from manufacturer; N/A- not available (the particles visibly appear to be similar); ** determined by drying resin beads in oven at 105°C for 24 h; moisture content of the beads were determined on bead samples that were washed with 200 bed volumes of ultrapure water

4.3.2 Adsorption Kinetics

The subsequent sections discuss the results obtained during bottle point adsorption experiments designed to determine adsorption kinetics by measuring PFCA removal as a function of time. The time and labour intensive nature of the analytical method for PFCA detection used for the current study restricted the inclusion of replicates. However, to ensure quality of the obtained data and also to confirm reproducibility of the PFCA removal trends, selected kinetic experiments were repeated with sample replicate. Reproducibility of the PFCA removal data is discussed in greater detail in Section 4.3.7.

4.3.2.1 Effect of adsorbent materials

The adsorbents used in this study can be grouped in three categories: anion exchange resins (A-500P, A-860), conventional GAC (F-400, WV B30, C-Gran, CX), and alternative adsorbents (Fija Fluor bone char and Biochar). Results of single solute and mixed solute kinetics experiments showing the effectiveness of different adsorbents in adsorbing target PFCAs are

presented in Figure 4.1. It can be seen that pseudo-equilibrium was achieved near the end of the test. Among the tested adsorbents, the anion exchange resin A-500P achieved the highest removal of the target PFCAs and exhibited faster PFCA adsorption. At the PFCA concentrations spiked (3.0 µg/L), the overall removal of the target PFCAs achieved with A-500P was greater than 97% and more than 90% removal was achieved within five days. Although the polystyrenic A-500P and the polyacrylic A-860 (both macroporous) had similar ion exchange capacities (Table 4.2), overall PFCA removals achieved with A-500P (depending on the PFCA chain length) were about 7% to 28% higher. Dudley (2012) also observed greater removal of PFCAs with polystyrenic strong base anion exchange resins. PFCA removal over time observed during the current study as presented in Figure 4.1 indicate that the removal kinetics for PFCAs were initially (6 h and 1 d data points) similar between the two resins (e.g. PFNA removal was 54% with A-500P after 1 d as opposed to 50% with A-860) and thereafter, faster for the polystyrenic A-500P. Dudley (2012) observed faster kinetics with polyacrylic resins and attributed that to the hydrophilic nature of the polyacrylic resins which helped in making the resin pores accessible to PFCAs. Their kinetics experiments were conducted for a period of up to 120 min as opposed to up to 23 days in the current study. While the PFCA removal kinetics with both resins during the current study were similar up to the initial 1 d, faster kinetics was observed with A-500P thereafter.

Of the GACs tested in single solute kinetic experiments (Figure 4.1 D), the coal-based F-400 outperformed the wood-based C-Gran and WV B30. For both single solute and mixed solute kinetic experiments after 23 days F-400 achieved greater than 85% removal of the target PFCAs. Of the two types of wood-based carbons, after 21 days C-Gran achieved higher removal of the target PFCAs (49%-80%) compared to WV B-30 (31%-55%) (Appendix- D). As can be seen in

Figure 4.1 A-C, the coconut-based CX in mixed solute experiments achieved similar removals as F-400 after 15 days for the target PFCAs. However, the removal with CX was initially slower compared to F-400. Adsorption of PFCAs onto GACs was slower compared to ion exchange resin A-500P. The adsorption kinetics for the GACs F-400 and CX, although initially slower, became equal or faster compared to the ion exchange resin A-860.

Previously, Karanfil and Dastgheib (2004) using TCE adsorption data on various GACs noted that both adsorbate and adsorbent properties affect the adsorption of micropollutants from water and wastewaters. In addition to BET surface area pore volume distribution may play an important role. It was noted that high surface area of activated carbons are results primarily due to the micropores (<2 nm) and most of the adsorption also occur in those pores (Menéndez-Díaza and Martín-Gullón 2006). In addition, micropores also exhibited higher adsorption energies (Karanfil 2006). However, size and geometry of the target micropollutants determine the relevant micropore size range for adsorption. The calculated molecular diameters of PFHpA, PFOA, and PFNA are 0.8 nm, 0.9 nm, and 1.0 nm respectively (Wang et al. 2011a). Thus, the primary micropores (<0.8 nm) in the carbonaceous adsorbents may not be accessible to the target PFCAs. Mesopores and macropores are also important in the sense that they facilitate the passage of the adsorbate molecules to the target micropore region. Data presented in Table 4.1 indicate that the CX carbon is more microporous than the F-400 carbon which has a better distribution of micropores and mesopores. Therefore, it is possible that the higher microporous nature of the CX may have hindered access of the PFCAs molecules to the target micropore regions and resulted in slower removal of PFCAs regardless of its higher BET surface area than the F-400. Wood-based GACs, on the other hand are more mesoporous compared to the F-400. However, the secondary micropore volumes of the two wood-based carbons and the F-400 are similar.

Therefore, the poor performance of the wood-based carbons compared to the F-400, in addition to their mesoporosity, may also be associated with their surface charge. Wood-based GACs are typically chemically activated using a phosphoric acid process which is why they have lower pH_{pzc} than F-400 and CX. For example: C-Gran has a pH_{pzc} of 4.6 as opposed to 9.6 for F-400. Thus, under the pH conditions (4.9-6.1) of the current study surface of the C-Gran was negatively charged while F400 was positively charged. Hence, adsorption of the negatively charged target PFCAs ($\text{pK}_a \ll$ experimental pH range) on the C-Gran carbon may have been impeded due to electrostatic repulsion. Hence, the negative surface charge and mesoporous nature of the wood-based GACs may have been responsible for the observed poor PFCA removal performance. Previously Dudley (2012), in ultrapure water experiments, observed similar removals of PFHpA, PFOA, and PFOA by thermally activated coal- (pH_{pzc} 6.1), coconut- (pH_{pzc} 9.6) and wood-based PACs (pH_{pzc} 10.7) which were however, higher compared to removal by a chemically activated PAC (pH_{pzc} 4.9). Furthermore, similar to Dudley (2012) findings, the current study also observed that BET surface area was not a good indicator of PFCA adsorption capacity of the tested GACs. Similar conclusion was noted by Huck and Sozański (2011).

The alternative adsorbents were not capable of substantial removals of the target PFCAs. Cattle bone-based Fija Fluor in single solute experiments did not remove any PFOA even with 17 days of contact time. After 23 days, the Biochar in mixed solute kinetic experiments removed less than 15% of the PFHpA, and less than 25% and 50% for PFOA and PFNA, respectively. Fewer secondary micropores, as well as a general lack of internal surface area of the two alternative adsorbents (Table 4.1), likely explain their poor adsorption performance.

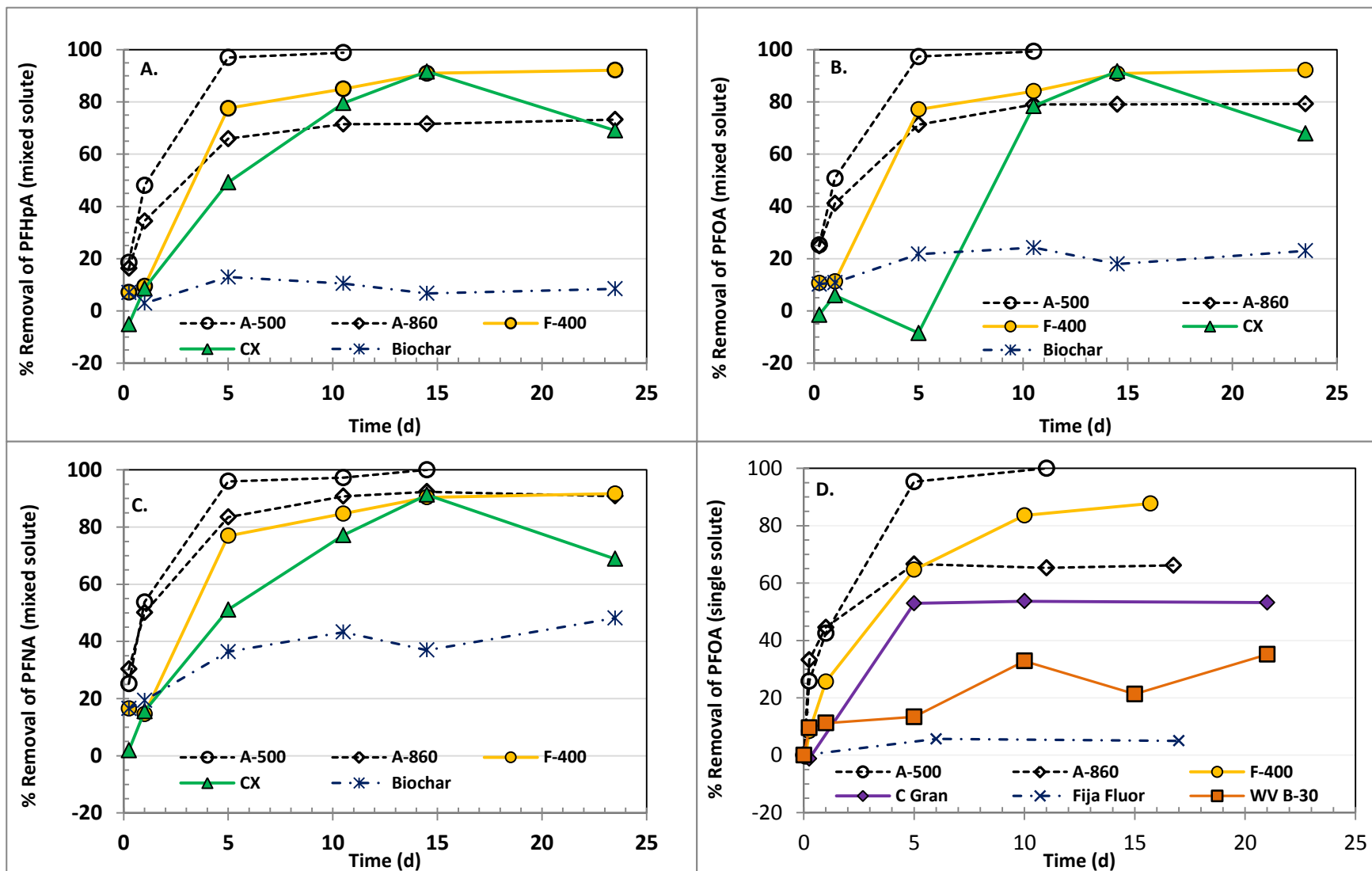


Figure 4.1: PFCA removal (%) as a function of time (d) for the tested sorbents in ultrapure water; plots A-C show presents data for mixed solute experiments (all three target PFCAs were spiked simultaneously); plot D shows data for single solute PFOA experiments (spiked individually); target nominal spiked PFCA concentration was 3 $\mu\text{g/L}$; adsorbent dose was 10 mg/L; no pH adjustments were done.

4.3.2.2 Application of Adsorption Kinetics Modeling

A pseudo-second order model developed by Ho (1995) has been widely used to describe adsorption kinetics (Yu et al. 2009a; Ho and McKay 1998; Ho and McKay 1999; Hameed et al. 2009; Wu et al. 2009). Indeed the review by Ho and McKay (1999) was able to describe 12 adsorptive systems from the literature using the pseudo-second-order model and the review has been cited more than 3000 times (Web of Science®) which demonstrates the potential usefulness of the model describing adsorption systems. The rate law for the pseudo-second-order model can be described as follows (Equation 4.1):

$$\frac{dq_t}{dt} = k_2 (q_e - q_t)^2 \dots\dots\dots (4.1)$$

where k_2 ($\text{mg} \cdot \text{ng}^{-1} \cdot \text{d}^{-1}$) is the rate constant for adsorption and q_e ($\text{ng} \cdot \text{mg}^{-1}$) is the total amount adsorbed at equilibrium and q_t ($\text{ng} \cdot \text{mg}^{-1}$) is the amount adsorbed at time t (d). Integrating Eq. (4.1) for the boundary conditions $t=0$ to $t=t$ and $q_t=0$ to $q_t=q_t$ provides the expression for sorption kinetics as follows (Eq. 4.2):

$$q_t = \frac{q_e^2 k_2 t}{(1 + q_e k_2 t)} \dots\dots\dots (4.2)$$

Eq. (4.2) can be rearranged to obtain

$$q_t = \frac{t}{(1/k_2 q_e^2 + t/q_e)} \dots\dots\dots (4.3)$$

Eventually the pseudo-second-order model can be expressed in a linearized form (Eq. 4.4):

$$\frac{t}{q_t} = \frac{1}{k_2 q_e^2} + \left(\frac{1}{q_e}\right) t \dots\dots\dots (4.4)$$

A linear plot of t/q_t vs t with a good correlation will indicate if the model can be used to describe kinetic data. The initial adsorption rate ϑ (ng/mg/day) may reflect the kinetic performance and is expressed as (Equation 4.5):

$$\vartheta = k_2 q_e^2 \dots\dots\dots (4.5)$$

The experimental equilibrium adsorption amount (experimental q_e) was calculated using the following formula:

$$\text{Experimental } q_e = \frac{(C_{\text{initial}} - C_{\text{final}}) \times \text{volume of sample}}{\text{mass of adsorbent added}} \dots\dots (4.6)$$

where C_{initial} is the initial concentration in ultrapure water ($\mu\text{g/L}$), C_{final} is the concentration in the last sample following treatment, and the sample volume is 1 L.

Figures 4.2 and 4.3 present the pseudo-second-order model plots fitted to the PFCA removal kinetics data presented in Figure 4.1. The model parameters, including the corresponding correlation coefficients along with the experimentally derived equilibrium adsorption amounts, are presented in Table 4.3. The 5 d PFOA removal data with CX and the 21 d removal data with WV B-30 (Figure 4.2) were not included in the model due to potential contamination during sample analysis. In addition, for some early GAC treatment samples (< 24 h), slightly negative removals were recorded. This is likely attributable to the relative standard deviation of the analytical method. For those points (CX and C-Gran carbon samples at $t = 0.25$ d for PFHpA and PFOA, and WV B30 carbon sample at $t = 1$ d for PFOA) a value of zero was assigned to t/q_t and was included in the fitted model accordingly.

In general, high correlation coefficients ($R^2 = 0.81-0.99$) were observed for all adsorbents except for the CX carbon ($R^2 = 0.52-0.79$) (Table 4.3). High correlation coefficients indicate that the

pseudo-second-order model can describe the experimental data. From Table 4.3 it can be seen that there is good agreement between the experimental q_e and the model-derived q_e . The model derived q_e and initial adsorption rate ϑ are graphically presented in Figure 4.4 and numerical values are presented in Table 4.3. Since the q_e and k_2 values are calculated from the slope ($1/q_e$) and the intercept ($1/k_2q_e^2$) of the linear fitting, respectively, complexities may arise when determining confidence intervals for the q_e and k_2 values. Thus, uncertainties involved with the linear fitting of the model to the adsorption data sets were expressed by 95% confidence intervals of the slope ($1/q_e$) and intercept ($1/k_2q_e^2$) of the linear fitting which are listed in Table E1 in Appendix E. The model derived q_e values for PFHpA and PFOA were similar for A-500P and F-400, and those for A-860 and CX were similar. On the other hand, the model derived q_e values for PFNA were similar for A-500P resin, C-Gran, CX and F-400 carbons. The experimental q_e values listed in Table 4.3 for all the tested adsorbents for the target PFCAs are similar to those derived using the model (except for C-Gran for PFNA). In this case, the model derived q_e value is higher (399 ng/mg) compared to the experimentally derived q_e (282 ng/mg). The initial adsorption rate ϑ for the anion exchange resins, however, are greater compared to the GACs indicating slower adsorption kinetics for the GACs compared to the anion exchange resins. Biochar has a lower equilibrium PFCA uptake however, equilibrium was reached quickly.

Adsorption data can be evaluated by both the linearized (Eq. 4.4) and non-linearized form (Eq. 4.2) of the pseudo-second-order adsorption kinetics model. Ho (2006) comparing the linear and non-linear methods concluded that the non-linear method is a more suitable method of calculating adsorption kinetic parameters. The linear form distorts variance structure of the data, and in addition, the model becomes invalid at time $t=0$. Despite these limitations the linear form of the model remains more widely used as opposed to the non-linear form due to the complexity

involved with the calculation of the non-linear least squares regression. For the remaining sections of this thesis, the linear form of the pseudo-second-order model was used to describe adsorption kinetics. Nonetheless, non-linear least squares regression analysis was employed to calculate adsorption kinetic parameters which are listed in Appendix- E (Table E2).

Another model for describing adsorption kinetics is the pseudo-first-order model where the rate order is expressed as per Eq. 4.7:

$$\frac{dq_t}{dt} = k_1 (q_e - q_t) \dots\dots\dots (4.7)$$

where k_1 (d^{-1}) is the rate constant for adsorption, q_e ($ng.mg^{-1}$) is the total amount adsorbed at equilibrium and q_t ($ng.mg^{-1}$) is the amount adsorbed at time t (d). Eq. (4.5) upon integration for the boundary conditions $t=0$ to $t=t$ and $q_t=0$ to $q_t=q_t$ can be rewritten as:

$$\ln(q_e - q_t) = \ln q_e - k_1 t \dots\dots\dots (4.8)$$

Thus, a linear plot of $\ln (q_e - q_t)$ vs t with a good correlation will indicate if the model can be used to describe kinetic data. However, if q_t becomes equal to q_e the term $\ln (q_e - q_t)$ becomes infinite. This may particularly affect the model fitting when there are small number of data points as the q_t value used to calculate experimental q_e cannot be included in the model fitting. For example: for the current study, A-500P has four sample data points (0.25 d, 1 d, 5 d and 10.5 d). Since, the experimental q_e is calculated using the q_t values at 10.5 d, the total number of data points available for model fitting is three as opposed to four data points for the pseudo-second-order model. The number of data points that could be used for fitting becomes even smaller when sample data points have to be excluded because of negative removals. Hence, due to limited data availability the pseudo-second-order model could be applied to more data sets compared to the

pseudo-first-order model. Furthermore, following a theoretical analysis of the two kinetic models, Azizian (2004) noted that when the initial concentration of a solute is not too high the sorption process obeys the pseudo-second-order model. The initial nominal concentration in the current study was 3 µg/L and hence, according to the findings of Azizian (2004) the pseudo-second-order model is more suitable for the current study.

To confirm this, the pseudo-first-order model was used to fit the time dependent PFCA adsorption data for F-400, A-500P and A-860 (Table E3 in Appendix E). Estimated q_e values (Table 4.3 and Table E3) indicate that q_e values for the selected adsorbents derived using the two models are comparable. For example: the pseudo-second-order model derived q_e values for PFOA adsorption onto F-400, A-500P and A-860 are 357, 397 and 303 ng/mg, respectively, as opposed to 330, 346 and 204 ng/mg in the same order. Comparison of R^2 values among the two models indicate that the pseudo-second-order model describes the data better or similarly compared to the pseudo-first-order model for all the data set except for PFHpA adsorption with F-400. Hence, only the pseudo-second-order model was used for analysis of adsorption kinetics data in the remaining sections of the current thesis.

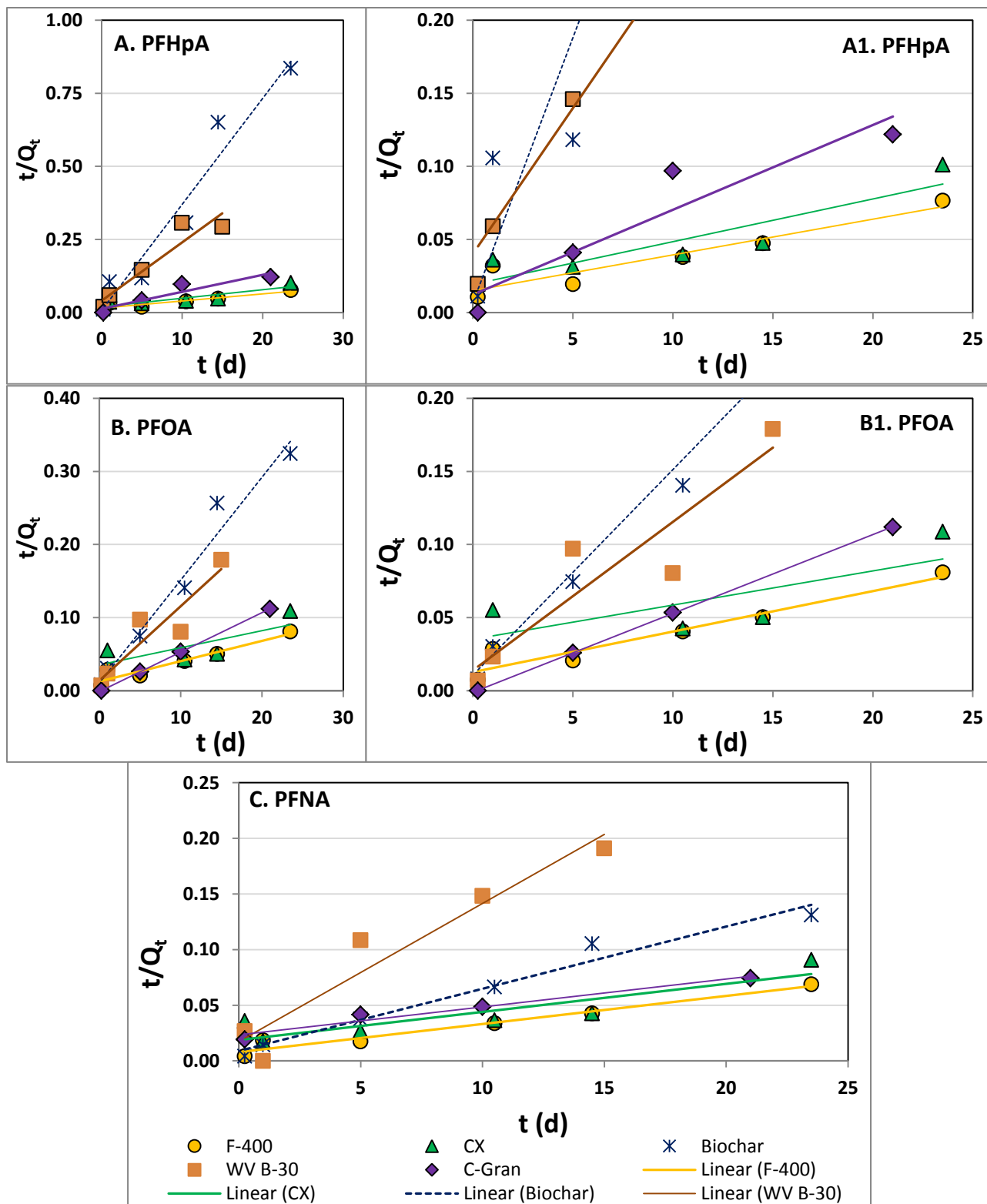


Figure 4.2: Application of the pseudo-second-order model to the adsorption data of A) PFHpA, B) PFOA, C) PFNA onto selected carbonaceous adsorbents. Plots A1 and B1 show close-up view of plots A and B, respectively. The lines show linear fitting of the PFCA removals presented in Figure 4.1.

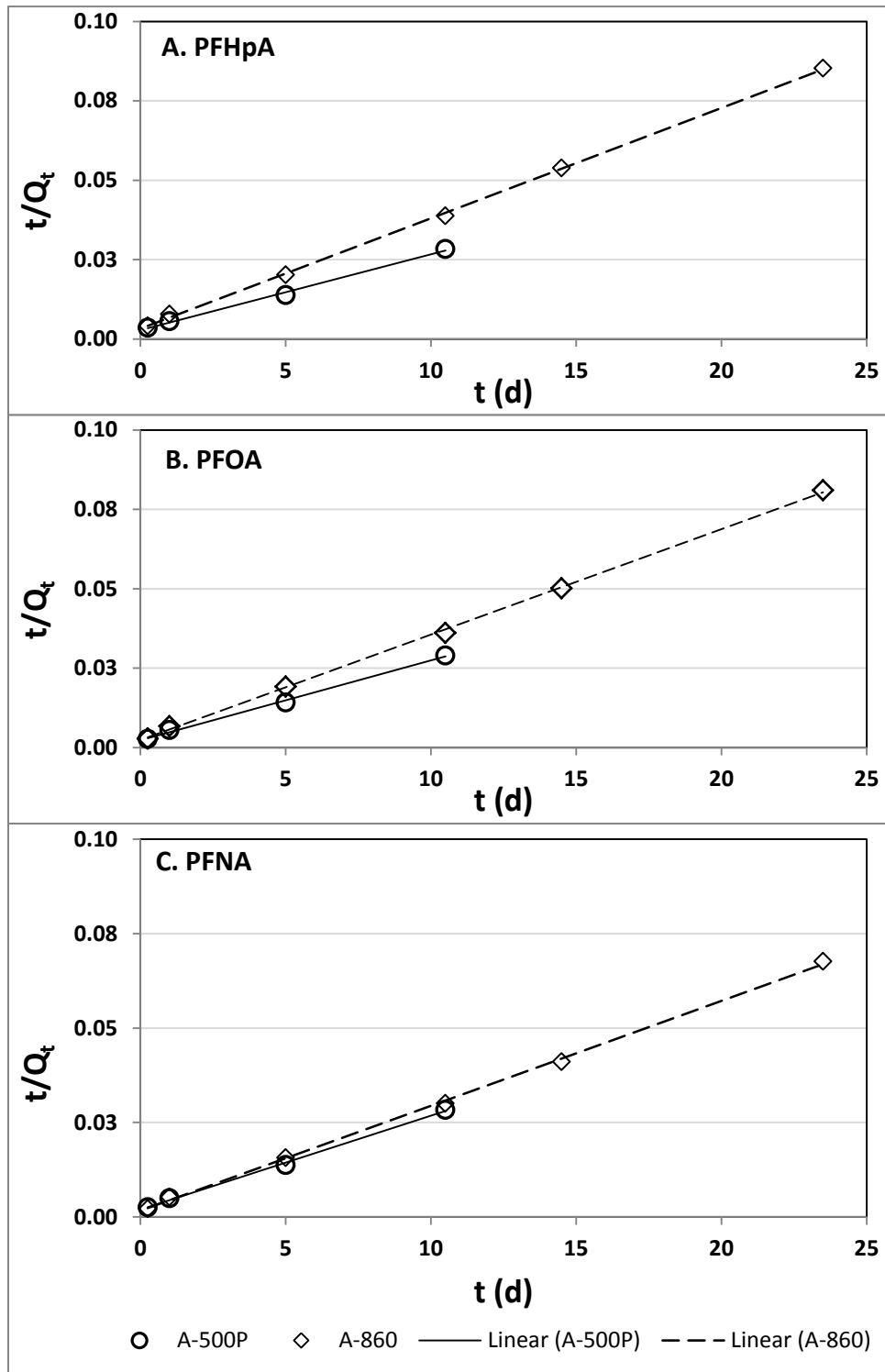


Figure 4.3: Application of the pseudo-second-order model to the adsorption of A) PFHpA, B) PFOA, C) PFNA onto the selected anion exchange resins. The lines show linear fitting of the PFCA removals presented in Figure 4.1

Table 4.3: Fitted pseudo-second-order kinetic model parameters for PFCA removal as function of time (calculated using linear least squares regression)

Adsorbent	q _e (ng/mg)	Exp. q _e (ng/mg)	q _e (ng/mg)	Exp. q _e (ng/mg)	q _e (ng/mg)	Exp. q _e (ng/mg)	k ₂ (mg.ng ⁻¹ .d ⁻¹)			ϑ (ng.mg ⁻¹ .d ⁻¹)			R ²		
	PFHpA		PFOA		PFNA		PFHpA	PFOA	PFNA	PFHpA	PFOA	PFNA	PFHpA	PFOA	PFNA
Biochar	28	28	71	72	179	179	0.1910	0.0186	0.0036	145	93	114	0.94	0.97	0.97
WV B-30	50	53	98	81	81	79	0.0098	0.0075	0.0088	25	72	57	0.89	0.81	0.92
C-Gran	172	172	185	188	400	282	0.0027	*	0.0003	81	*	43	0.88	0.96	0.96
CX	345	305	435	289	400	340	0.0004	0.0001	0.0003	52	28	54	0.79	0.52	0.78
F-400	417	307	357	290	400	341	0.0004	0.0006	0.0008	66	79	127	0.88	0.92	0.96
A-500P	418	371	397	362	403	371	0.0020	0.0028	0.0031	357	435	500	0.99	0.99	0.99
A-860	288	276	303	290	357	347	0.0037	0.0047	0.0046	303	435	588	0.99	0.99	0.99

* negative intercept of the fitted model resulted in negative value indicating that the model cannot be applied to the specific data set

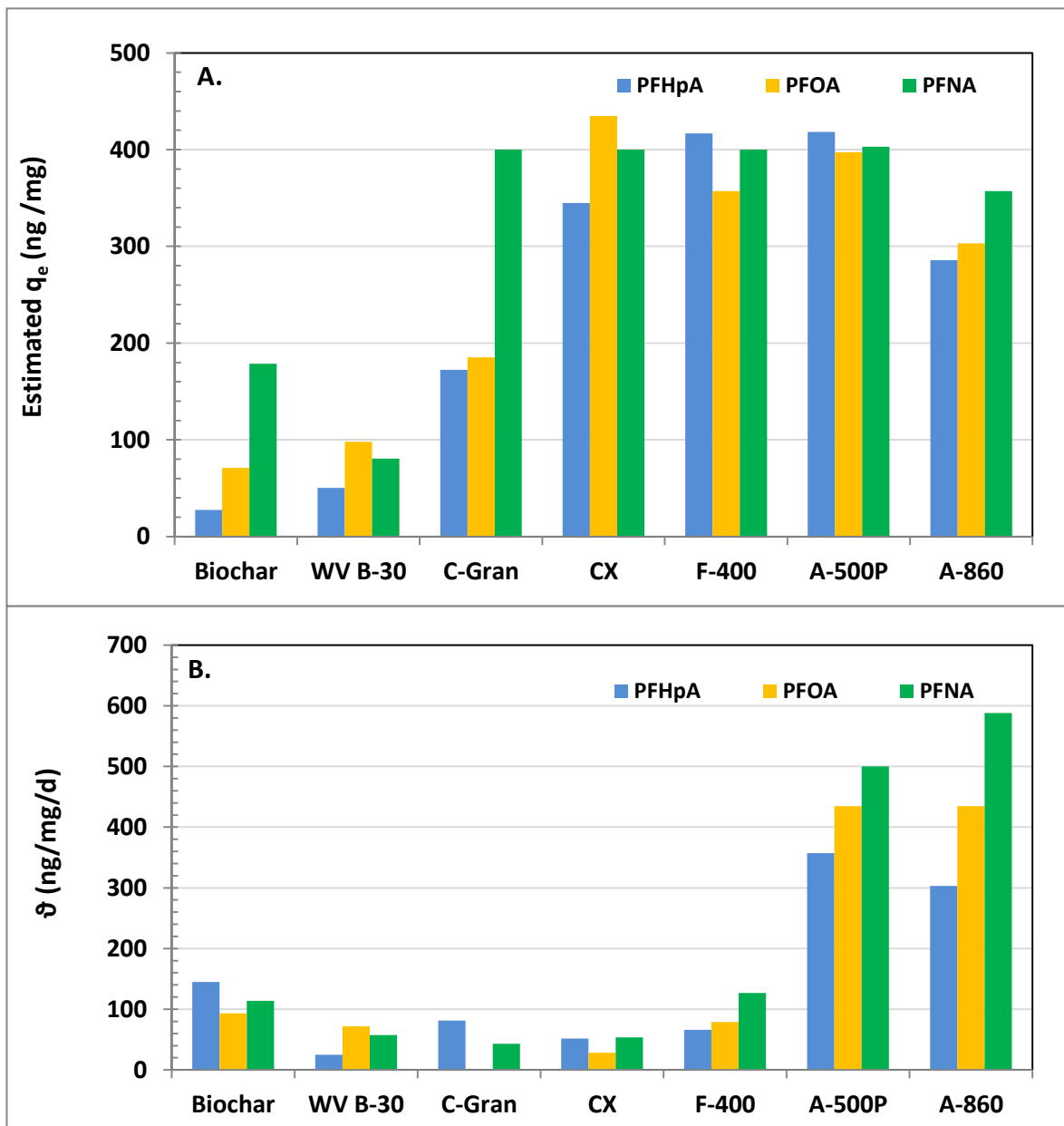


Figure 4.4: Graphical representation of the pseudo-second-order kinetic model parameters- A) equilibrium adsorption amount (q_e), and B) initial adsorption rate (ϑ). Model R^2 values for all sorbents except for CX indicate good fit to the data. The model was fitted to mixed solute data for all the sorbents except for the WV B-30 and C-Gran carbons using PFCA removal data presented in Figure 4.1.

4.3.2.3 Comparison of Single and Mixed Solute Kinetics

Figure 4.5 presents the comparative PFCA removal kinetics in ultrapure water by three adsorbents: A-500P, A-860, and F-400 when PFCAs were spiked as a mixture and when spiked individually. It appears that PFCAs, whether present in mixtures or individually, did not substantially affect the PFCA adsorption amount of A-500P and F-400. This indicates that the effect of direct competition for sorption sites among the target PFCAs is minimal. For A-860 on the other hand, uptakes of PFOA and PFNA were less in single solute solutions as opposed to in mixed solute. Data presented in Figure 4.1 were fitted to the pseudo-second-order adsorption kinetics model for a more quantitative representation of the trends observed. Good correlation was observed for all the adsorbents ($R^2 = 0.83 - > 0.99$) for both single and ultrapure. Figure 4.6 graphically represents the estimated model parameters which show that estimated equilibrium PFCA adsorption quantity and initial sorption rate for the mixed solute and single solute kinetics experiments were comparable for the A-500P resin and the F-400 GAC. For example, the equilibrium PFOA adsorption quantity and the initial PFOA sorption rate for A-500P were 400 mg/g and 435 ng/mg/d, respectively, for mixed solute experiments as opposed to 370 mg/g and 333 ng/mg/d in the same order for single solute experiments. For A-860 resin, single solute experiments resulted in faster initial adsorption rates for all the PFCAs. Nonetheless, the equilibrium adsorption quantities were comparable for both mixed solute and single solute kinetics experiments. Overall, these results indicate that the effect of direct competition for adsorption sites among the target PFCAs is minimal.

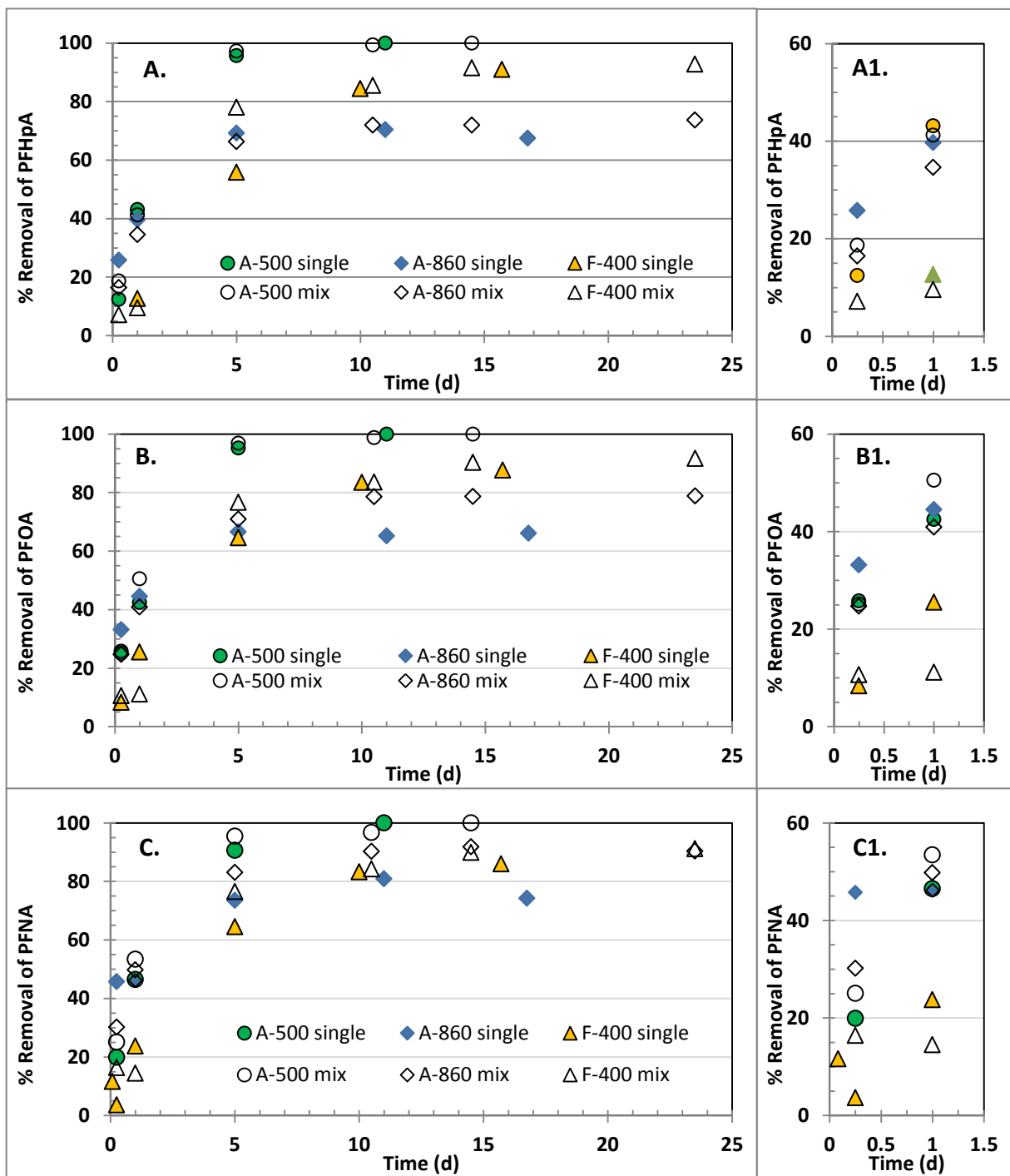


Figure 4.5: Comparison of mixed solute addition vs individual solute addition in PFCA removal as a function of time in ultrapure water; A) PFHpa, B) PFOA, C) PFNA (open symbols indicate all three PFCAs were spiked simultaneously, colored symbols indicate only single solute spiked); nominal spiked PFCA concentration was 3 $\mu\text{g/L}$; adsorbent dose was 10 mg/L; no pH adjustments were done; plots A1, B1 and C1 present a close-up of the data points up to 5 days.

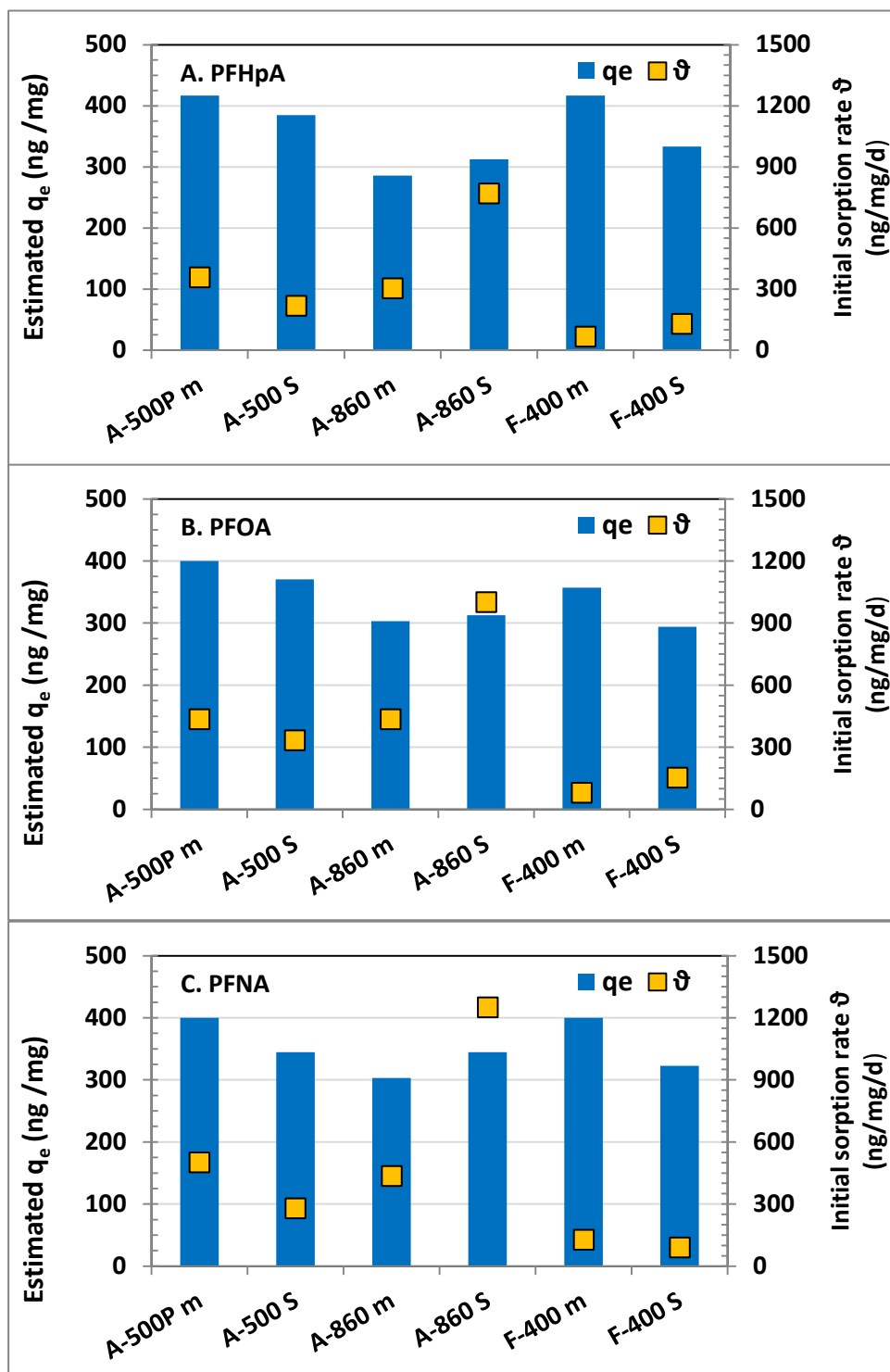


Figure 4.6: Graphical presentation of parameters for pseudo-second-order adsorption kinetics model fitted to time dependent PFCA removal data for mixed solute addition and single solute addition in ultrapure water; m- for mixed solute addition and s- for single solute addition.

4.3.2.4 Effect of PFCA Chain Length on PFCA adsorption

The effect of PFCA chain length on different adsorbents is illustrated in Figure 4.7. In addition equilibrium adsorption amounts (calculated using pseudo-second-order adsorption model) of different PFCAs are graphically represented in Figure 4.4. It is evident from Figures 4.7A and 4.7C, and Figure 4.4A that for mixed solute kinetics experiments conducted in ultrapure water. PFCA chain length does not have any effect on adsorption of the target PFCAs by A-500P ion exchange resin and the GACs- F-400, CX and WV B-30. For example, estimated q_e values for PFHpA, PFOA, and PFNA for A-500P resin are 418 ng/mg, 397 ng/mg and 402 ng/mg, respectively. However, chain length dependant removal of the target PFCAs was observed with ion exchange resin A-860, Biochar and C-Gran carbon (Figures 4.7B and 4.7D, Figure 4.4A and Table 4.3). For example, calculated q_e values for PFHpA, PFOA and PFNA for A-860 resin are 285, 303 and 357 ng/mg, respectively. Previously, Senevirathna et al. (2011) using F-400 carbon in ultrapure water (although conducted at different experimental conditions than the current study) also did not observe chain length dependent removal of PFCAs. However, other studies (Dudley 2012; Arevalo Perez 2014) conducted at different experimental conditions with different adsorbents than those used in the current study observed chain length dependent removal of PFCAs. Appleman et al. (2013) recording breakthrough times of different PFCAs in their rapid small scale GAC column tests, noted that “in general, a chain length dependent pattern was observed, but not for all of the PFCAs.”

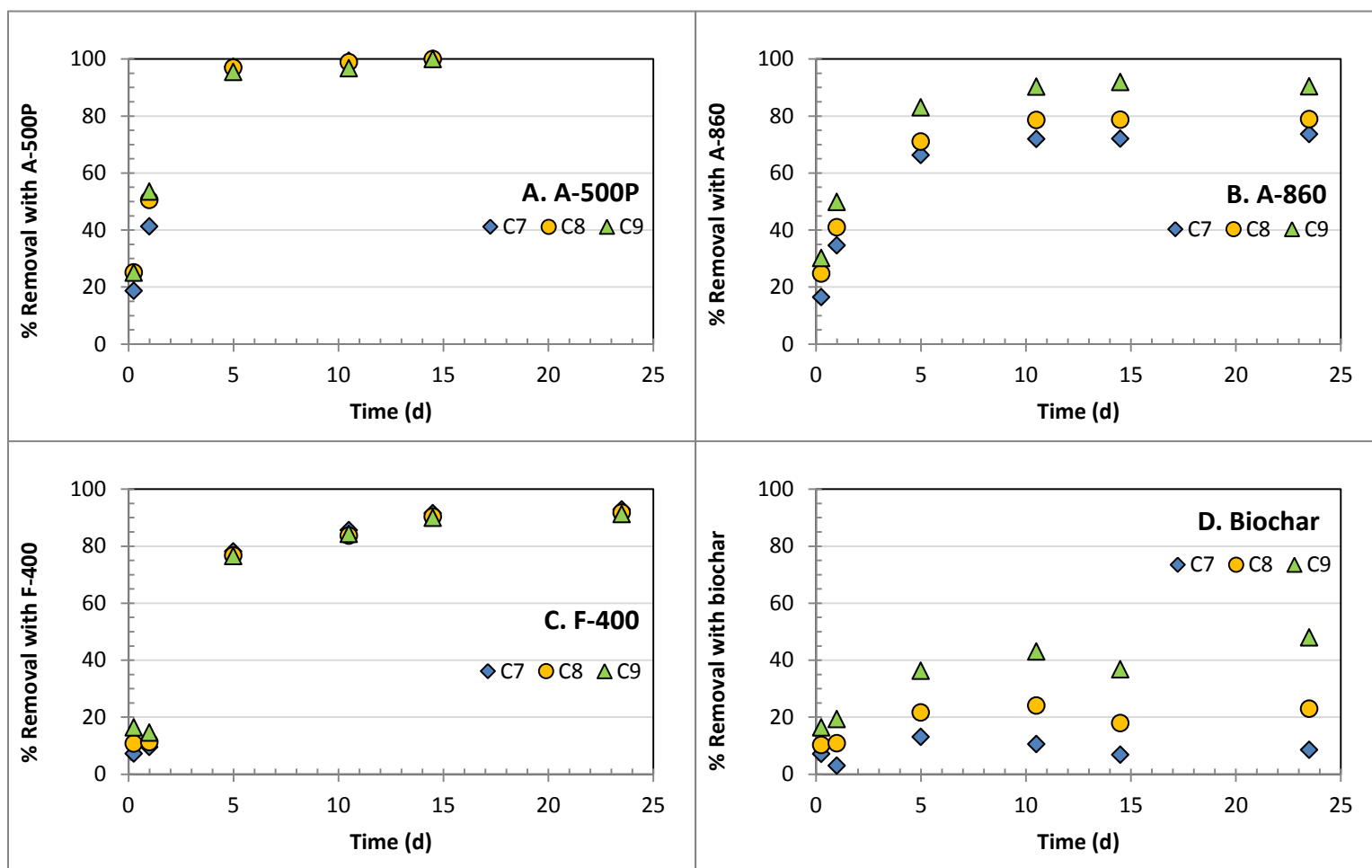


Figure 4.7: Effect of PFCA chain length on PFCA removal as a function of time by different adsorbents in ultrapure water: A) A-500P ion exchange resin, B) A-860 ion exchange resin, C) F-400 GAC, D) Biochar.

4.3.2.5 Adsorption mechanism

Among the various stages of adsorption, mass transfer is typically controlled by either film diffusion (surface processes) or pore diffusion (intraparticle diffusion) and whichever of the processes offers more resistance is assumed to be the rate limiting mechanism (Weber and Morris 1963; McKay 1983). Weber and Morris (1963) introduced the intraparticle diffusion model which can be expressed as following:

$$q_t = k_{id}t^{1/2} + C \dots\dots\dots (4.4)$$

Where k_{id} (ng/mg/d^{0.5}) is the intraparticle diffusion rate constant, q_t is solid phase concentration at time t , and C (ng/mg) is the intercept that provides information regarding the boundary layer effect. According to the model, if intraparticle diffusion is involved in the adsorption process, then the plot of q_t vs $t^{1/2}$ will be linear and if the linear regression passes through the origin, then intraparticle diffusion is the single rate-limiting mechanism. If the linear regression does not pass through the origin, it is indicative of the influence of the boundary layer and that intraparticle diffusion is not the single rate controlling step and other processes may be involved in controlling the rate of adsorption (Crini et al. 2007).

The adsorption kinetics data originally presented in Figure 4.1, when fitted to the intraparticle diffusion model, exhibit a multi-linear trend and as can be seen from Figure 4.8 two adsorption phases exist. Similar to the application of the pseudo-second-order model, the 5-d PFOA removal value for CX was not included in the model. Also the CX carbon samples collected at $t=0.25$ d for PFHpA and PFOA, a value of zero was assigned to q_t and was included in the fitted model accordingly.

As presented in Figure 4.8, the intraparticle diffusion model was applied to the initial phase which lasted up to 5 days for the anion exchange resins, the F-400 GAC, and the Biochar. For CX carbon the initial phase was considered up to 15 d. The intraparticle diffusion model parameters for the adsorption of the target PFCAs are presented in Table 4.4. In general, high correlation coefficients ($R^2 = 0.91-0.99$) were obtained for all the adsorbents except for Biochar for PFHpA ($R^2 = 0.59$) (which may be due to the poor adsorption of PFHpA with Biochar). None of the linear regressions, except for the PFHpA adsorption with A-500P, passes through the origin indicating that adsorption of the target PFCAs onto the tested adsorbents may not be controlled solely by intraparticle diffusion suggesting other processes are involved. The low intercept value and good linear fitting for the PFHpA adsorption data with A-500P indicates that adsorption of the compound onto A-500P may be intraparticle diffusion controlled. Positive values of C, although mathematically possible, are not valid since that would indicate adsorption taking place at $t=0$. Thus, regardless of the high R^2 values high positive C values indicate that the intraparticle diffusion model is not applicable to the adsorption data sets for A-500P, A-860 and Biochar. Due to the time consuming sample analysis, data sets in this current study were small and the conclusions that were derived from the above analysis of the adsorption data, should therefore be interpreted with caution.

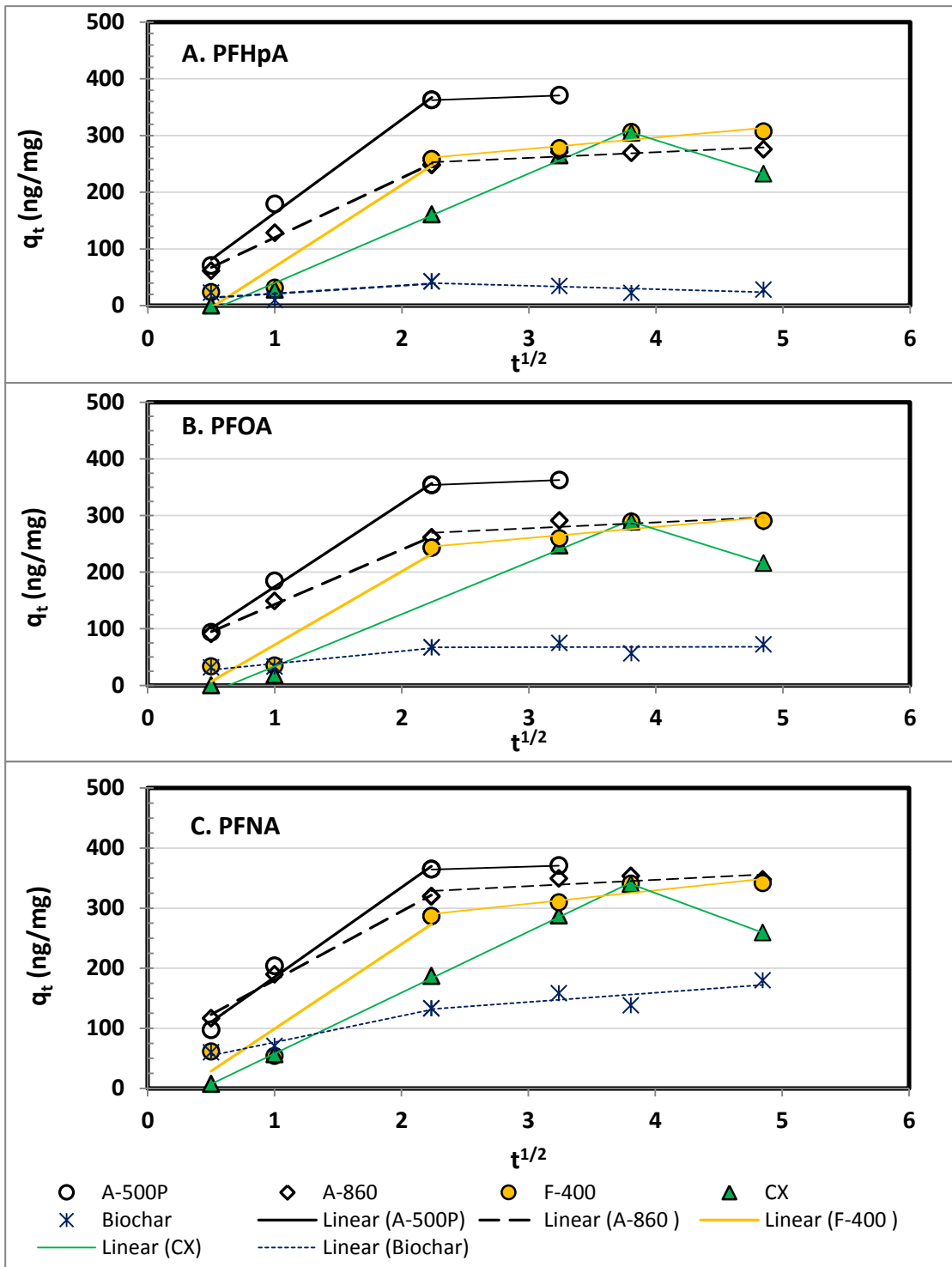


Figure 4.8: Kinetics of PFCA adsorption on different adsorbents fitted by the intraparticle diffusion model. The model was fitted to mixed solute data presented in Figure 4.1

Table 4.4 Intraparticle diffusion parameters*

Adsorbent	k_{id} [ng/(mg.d ^{0.5})]			C (ng/mg)**			R ²		
	PFHpA	PFOA	PFNA	PFHpA	PFOA	PFNA	PFHpA	PFOA	PFNA
Biochar	14	22	44	7	17	33	0.59	0.94	0.98
CX	97	92	102	-57	-58	-43	0.99	0.99	0.99
F-400	144	130	141	-75	-58	-42	0.94	0.93	0.91
A-500P	165	148	149	0.8	26	36	0.99	0.99	0.99
A-860	105	97	115	14	47	65	0.99	0.99	0.99

*The model was fitted to mixed solute data presented in Figure 4.1

**Positive values of C, although mathematically possible, are not valid since that would indicate adsorption taking place at t=0; Thus regardless of the high R² values, a high positive C value indicates that the intraparticle diffusion model is not applicable to the specific data set.

4.3.3 Adsorption isotherms

Adsorption capacity of an adsorbent for a specific contaminant can be illustrated by an isotherm. Single solute adsorption isotherms for F-400, A-860, and A-500P in ultrapure water for the three target PFCAs were determined. The A-500P resin was chosen since it performed best among the tested adsorbents during the kinetics study, while F-400 carbon was picked since it is widely used in water industry and also exhibited better PFCA removal performance among the carbon-based adsorbents. The polyacrylic A-860 resin was selected since the resin during kinetics experiments achieved lower PFCA removals compared to its polystyrenic counterpart regardless of having similar ion exchange capacity and thus could provide insight on the effect of resin matrix on PFCA uptake.

There are various models that can be used to describe isotherms. However, the Freundlich isotherm model is most frequently used in water treatment practice (Huck and Sozański 2011).

The Freundlich model is expressed as below (Equation 4.5):

$$q_e = K_F C_e^{1/n} \dots\dots\dots (4.5)$$

Where q_e is the equilibrium solid phase concentration (ng/mg), C_e is the equilibrium liquid phase concentration, and K_F and $1/n$ are Freundlich parameters.

The adsorption data obtained during the current study were fitted to the Freundlich model. Figure 4.9 illustrates the single solute isotherms of the three target PFCAs onto the adsorbents and the corresponding isotherm parameters are summarized in Table 4.5. While the isotherms in Figure 4.9 are plotted in log-log scale, the isotherm parameters were calculated by the non-linear least squares regression method. Any transformation of data distorts the variance structure of the data and hence, application of linear regression to the log transformed adsorption data may results in

less accurate estimation of the model parameters. Nonlinear least squares regression analysis using the MATLAB[®] curve fitting toolbox was performed to determine the Freundlich isotherm parameters and their corresponding 95% confidence intervals. The isotherm parameters were also calculated by linear regression method using Microsoft Excel's regression analysis on the log equilibrium solution (ng/L) and log adsorbent concentration (ng/mg) data. These results are included in Appendix E (Table E4). Comparison of the Freundlich parameters values derived using the non-linear least squares and linear regression methods indicate that the parameter values calculated by the two different methods are similar. In general, good correlations ($R^2=0.83-0.99$) were observed for all the isotherms except for those of PFNA for the A-860 resin ($R^2=0.74$) (Table 4.5). Among the three adsorbents K_F values of A-500P resin for the selected PFCAs are higher than those for the other two adsorbents and those of A-860 resin were the lowest. For example: K_F values of A-500P, F-400 and A-860 for PFHpA were 229, 60 and 0.60 [(ng/mg)(L/ng)^{1/n}], respectively. As can be observed in Figure 4.9A-C, the A-500P resin had a higher adsorption capacity for all three target PFCAs compared to F-400 and A-860. This is consistent with the adsorption kinetics results presented earlier in Figure 4.1 which also indicated that the A-500P resin achieved the highest percent removal of the target PFCAs among the tested adsorbents. F-400 exhibited greater adsorption capacity for PFOA and PFHpA compared to A-860. However, although the observed K_F value of PFNA was higher for the F-400 carbon than that for the A-860 resin, the adsorption isotherms of the two adsorbents were fairly similar within an equilibrium liquid phase concentration of 100-1000 ng/L. The isotherm trends observed with the F-400 carbon and the A-860 resin are also consistent with the kinetics study results which also indicated that while F-400 achieved higher removals of PFHpA and PFOA compared to A-860 resin, the latter achieved higher removal of PFNA.

The calculated lower boundary of the 95% confidence interval for some of the K_f values were negative (Table 4.5). While it is possible to arrive at negative K_f mathematically, those negative K_f values are not physically possible. As can be seen from Table 4.5 some of the isotherm parameters have overlapping confidence intervals and hence, differences among those values cannot be statistically confirmed.

Table 4.5 Freundlich isotherm parameters for selected adsorbents in ultrapure water (calculated using non linear least squares)

Compound	Freundlich intensity factor 1/n (dimensionless)			Freundlich capacity factor K_f [(ng/mg)(L/ng) ^{1/n}]			R^2		
	A-860 resin	F-400 GAC	A-500P resin	A-860 resin	F-400 GAC	A-500P Resin	A-860 Resin	F-400 GAC	A-500P resin
PFHpA	0.83 (0.57-1.10)	0.36 (0.23-0.49)	0.25 (0.07-0.44)	0.60 (-0.59-1.79)	60 (7-112)	229 (-50-507)	0.91 (0.90)	0.90 (0.89)	0.81 (0.76)
PFOA	1.96 (1.69-2.23)	0.30 (0.16-0.45)	0.33 (0.22-0.44)	<0.01 (-0.0002- <0.001)	60 (0.35-120)	108 (37-179)	0.99 (0.99)	0.84 (0.81)	0.92 (0.91)
PFNA	0.97 (0.35-1.6)	0.43 (0.25-0.62)	0.51 (0.35-0.68)	1 (-3-5)	24 (-7-54)	41 (-5.3-88)	0.74 (0.70)	0.83 (0.81)	0.93 (0.92)

For the 1/n and K_f columns values in parenthesis are 95% confidence intervals; For the R^2 column the values in parenthesis are adjusted R^2 .

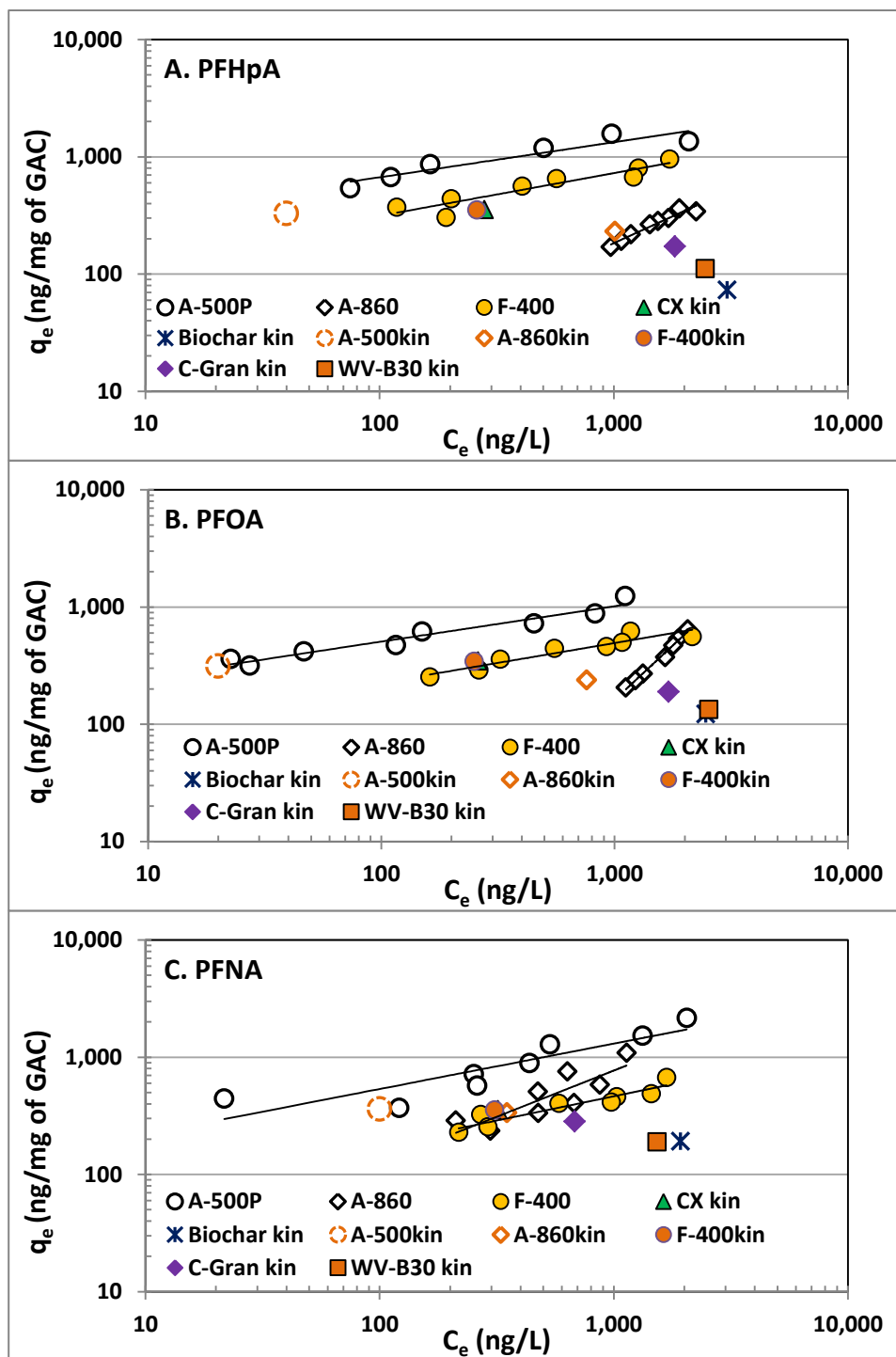


Figure 4.9: Single solute adsorption isotherms in ultrapure water on three adsorbents for the three target PFCAs: A) PFHpA, B) PFOA, C) PFNA. Data points; kin= kinetics data points (see Figure 4.1).

To further examine how the isotherm data of the three adsorbents compare to their respective kinetics removal data as well as those of the other adsorbents, PFCAs adsorbed at equilibrium during the kinetics experiments were also plotted against the liquid phase PFCA concentration at equilibrium in Figures 4.9A-C (single solute kinetics data for WV B-30 and C-Gran and mixed solute kinetics data for the rest of the adsorbents). It is evident that for A-500P, A-860, and F-400 adsorption data at equilibrium during kinetics experiments are similar to the obtained isotherms (except for the PFOA data for A-860) indicating that adsorption trends at equilibrium obtained from both types of experiments are similar. The plotting of the removal data at equilibrium is also indicative of the capacity of the adsorbents that were not used for isotherm experiments. From the position of these data points in Figures 4.9 A-C it follows that the target PFCA adsorption capacity for CX was similar to F-400 while capacities of C-Gran, B-30, and Biochar were lower than those for CX and F-400. These trends are also in line with the equilibrium adsorption amounts (q_e) estimated using the pseudo-second-order model for adsorption kinetics (Figure 4.4A and Table 4.3). The deviation of the PFOA data for A-860 (Figure 4.9B) may have been due to the high $1/n$ value and the narrow equilibrium liquid phase concentration range observed with the specific isotherm.

In the existing literature no previous studies involving treatment of PFCAs in water by A-500P and A-860 resins could be found. However, studies by Ochoa-Herrera and Sierra-Alvarez (2008), and Senevirathna et al. (2011) involving the F-400 carbon provided an opportunity to discuss and compare results of the current study. Despite the fact that the current study was conducted at $\mu\text{g/L}$ PFCA concentrations as opposed to mg/L used by Ochoa-Herrera and Sierra-Alvarez (2008) the obtained isotherm parameter values are comparable. The Freundlich $1/n$ on F-400 for PFOA reported by Ochoa-Herrera and Sierra-Alvarez (2008) was 0.44 compared to 0.30

obtained during the present study (Table 4.5). However, Senevirathna et al. (2011) obtained a much higher value of $1/n$ (1.68). The capacity factor (K_F) value of F-400 carbon for PFOA reported by Ochoa-Herra and Sierra-Alvazez (2008) is 26 $[(\text{ng}/\text{mg})(\text{L}/\text{ng})^{1/n}]$ (converted to the same units as the current study) is comparable to that of the current study (60 $[(\text{ng}/\text{mg})(\text{L}/\text{ng})^{1/n}]$). However, the observed K_F value of F-400 carbon for PFOA determined by Senevirathna et al. (2011) was considerably lower (0.006 $[(\text{ng}/\text{mg})(\text{L}/\text{ng})^{1/n}]$). Using the isotherm obtained during the current study, an equilibrium liquid phase concentration of 100 ng/L of PFOA would result in a solid phase concentration of 239 ng/mg which is comparable to 205 ng/mg at the same liquid phase concentration using the K_F and $1/n$ values reported by Ochoa-Herrera and Sierra-Alvarez (2008). The corresponding equilibrium solid phase concentration reported by Senevirathna et al. (2011) is 13 ng/mg, which is substantially lower. In addition to the high $1/n$ values reported during their study, Senevirathna et al. (2011) conducted their isotherm studies for 96-100 h with crushed GAC as opposed to 21 d with uncrushed GAC during the current study. Also the single solute isotherm experiments were conducted over a wide initial concentration range (10 $\mu\text{g}/\text{L}$ to 5000 $\mu\text{g}/\text{L}$) and did not mention the amount of adsorbent used for the isotherm study and neither did they mention whether equilibrium was achieved during the experimental time range. Therefore, it is not possible to comment on the variation between the studies in PFCA adsorption capacities of F-400.

The effect of PFCA carbon chain length on adsorption capacity of the three adsorbents for the three target PFCAs is explored in Figure 4.10. The adsorption isotherms for the three target PFCAs indicate similar adsorption capacities for A-500P and F-400 which is in line with the trends observed in adsorption kinetics data presented in Figures 4.4A and 4.6. The reported K_F values of the three adsorbents for the target PFCAs (Table 4.5) also did not suggest a chain

length dependant pattern for adsorbability. The fitted isotherms for A-860 resin (Figure 4.10B) show that the adsorbability of PFNA is higher compared to PFOA and PFHpA. However, the R^2 value for isotherm fitting for PFNA adsorption onto A-860 ($R^2 = 0.74$) is low. Higher removals of longer chain PFCAs with A-860 were also observed during the kinetics experiments in the current study. However, the high $1/n$ value (1.96) and low $K_F (<0.01 [(ng/mg) (L/ng)^{1/n}]$ value of the isotherm fitting (with high R^2 value) for PFOA adsorption onto A-860 cannot be explained. The narrow equilibrium liquid concentration range of PFOA and PFHpA isotherms for A-860 resin (Figure 4.10B) which was not observed for any other isotherms could also not be explained. Due to time limitations however, the isotherm experiments could not be repeated during the current study.

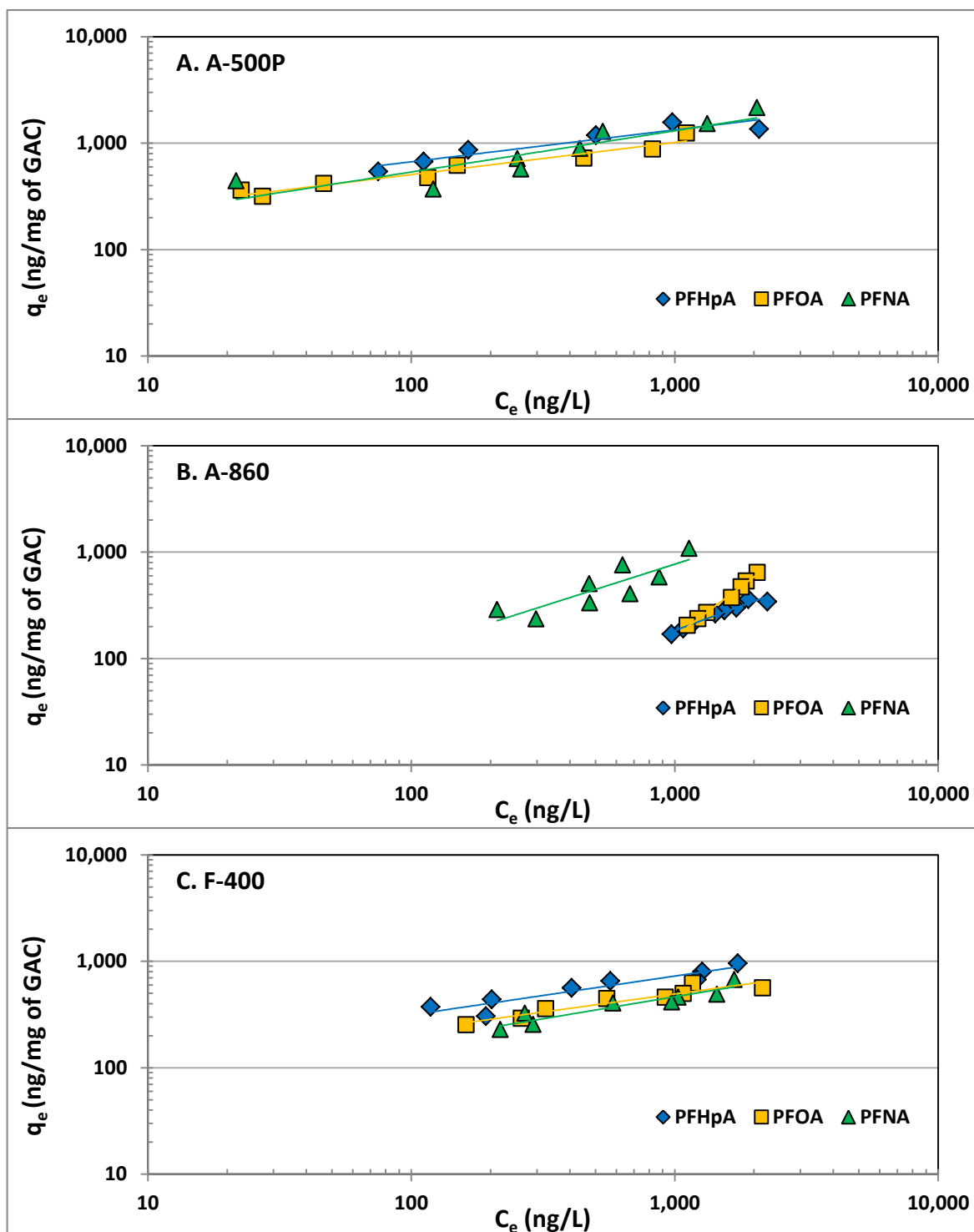


Figure 4.10: Single solute adsorption isotherms of the target PFCAs onto A) A-500P, B) A-860 and C) F-400 in ultrapure water.

4.3.4 Comparison of PFCA adsorption with other trace organic contaminants

F-400 was selected as a treatment adsorbent for this comparison due to its wide application in water treatment. Yu et al. (2008) reported the adsorbabilities of two pharmaceuticals- naproxen (NAP) and carbamazepine (CBZ), and an endocrine disrupting compound- nonylphenol (NP) in ultrapure water at trace concentrations (ng/L) using F-400 carbon. Previous studies have also used to study F-400 carbon for removal of more widely known organic contaminants such as atrazine (ATZ) (Schideman et al. 2006), geosmin and MIB (Pirbazari et al. 1993) at trace concentrations. Figure 4.11 compares the isotherms of the three target PFCA with the micropollutants discussed above based on the reported F-400 isotherms data in low organic content water. When comparing isotherms it is ideal to have the isotherm experiments conducted in similar concentration ranges. Yu (2007) studied adsorption of nonylphenol on F-400 carbon at an initial concentration of about 0.5-1.0 $\mu\text{g/L}$ and observed that the adsorption capacity for nonylphenol was about 100 times lower when compared to capacities calculated by extrapolation of isotherms reported by other studies that were conducted at higher initial nonylphenol concentration (1000-10000 $\mu\text{g/L}$) (Choi et al. 2007; Tanghe and Verstraete 2001). Yu (2007) also noted that such extrapolation of isotherms over a large concentration range overlooks the curvature that may arise. Previous studies (Yu 2007; Pirbazari et al. 1993; Pelekani and Snoeyink 2000) have also reported a decreasing trend of the Freundlich isotherm $1/n$ factor with increasing equilibrium liquid phase concentration and such decreases may be linked to the fact that the exponential factor of the Freundlich model may reach unity in very dilute solutions (Sontheimer et al. (1988)). Thus, data should be carefully interpreted when isotherms conducted at higher initial concentration ranges are extrapolated over a large concentration range. All the micropollutants isotherms compared in Figure 4.11 included liquid phase concentrations lower than 1000 ng/L. As can be observed, the three target PFCA are expected to display similar

adsorptions as naproxen and carbamazepine in the concentration range of 10-1000 ng/L. The target PFCA isotherms at liquid phase concentrations higher than 100 ng/L cross the nonylphenol isotherms and thus will likely be better adsorbed compared to nonylphenol at concentrations lower than 100 ng/L. It can also be presumed that the target PFCAs will likely be adsorbed by F-400 very similarly to the taste and odor compounds, geosmin and MIB, at concentrations below 30 ng/L. Since PFCAs occur in environmental waters at concentrations similar to geosmin and MIB, powdered activated carbon (PAC) dosages required to achieve treatment goals for taste and odor compounds may also achieve comparable removals of the target PFCAs. Atrazine was substantially more adsorbed than the PFCAs. Thus, it cannot be used as a reference compound for the removal of PFCAs at low concentration levels.

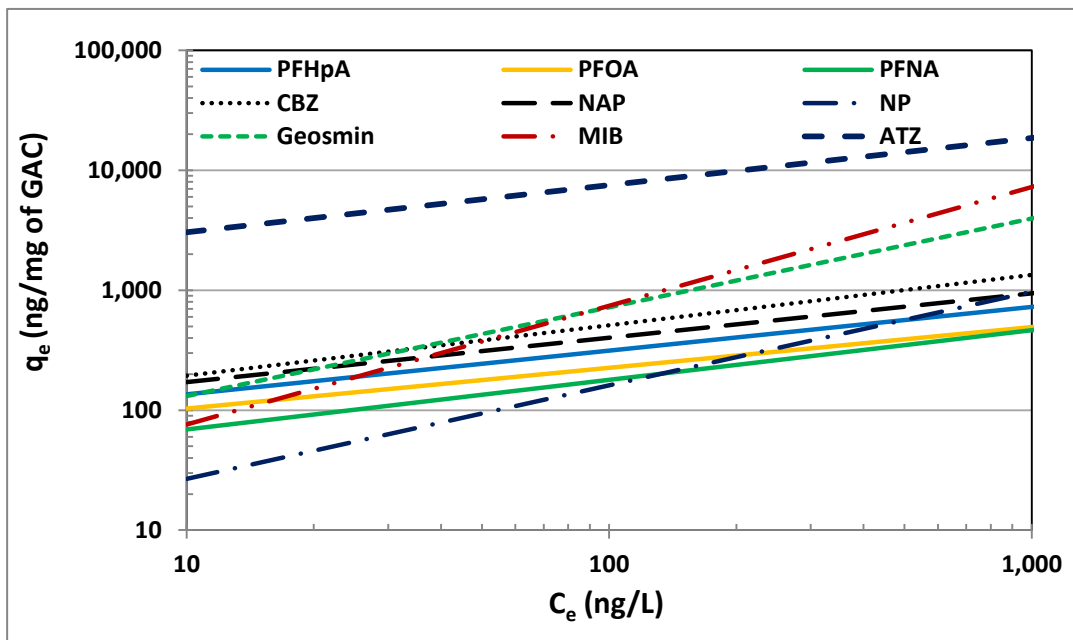


Figure 4.11: Comparison of adsorbabilities of the three target PFCAs with other micropollutants on F-400 carbon in ultrapure water (ATZ- atrazine, CBZ-carbamazepine, NAP- naproxen, NP- Nonylphenol). Plotted lines were drawn based on fitted Freundlich isotherm parameters; isotherm data for PFCAs were used from the current study while those of other micropollutants were obtained from Yu et al. (2008) (for naproxen, carbamazepine and nonylphenol), Scheideman et al. (2006) (for atrazine) and Pirbazari et al. (1993) (for geosmin and MIB).

4.3.5 Effect of inorganic anions on PFOA removal by anion exchange resins

Inorganic anions can impair PFCA adsorption by anion exchange resins by competing for adsorption sites. The current study investigated the effect of SO_4^{2-} on PFOA adsorption by ion exchange and similar trends were expected for the structurally similar PFHpA and PFNA. The effects of SO_4^{2-} concentrations on PFOA removal in ultrapure water by A-500P and A-860 are presented in Figure 4.12. As can clearly be seen, the PFOA uptake capacity of the two tested resins decreased with increasing SO_4^{2-} concentration. For example, the equilibrium uptake of PFOA with A-860 resin decreased by nearly 38% when the background SO_4^{2-} concentration was 1.0 mg/L and by 60% when the concentration was 30 mg/L. This observation is similar to that of Arevalo Perez (2014) who also found reductions in PFCA uptake with increasing anion (bicarbonate, chloride, sulfate, and nitrate) concentrations during their study involving a polyacrylic magnetic anion exchange resin. Deng et al. (2010) also reported reduction in the PFOS adsorption capacity of anion exchange resins in the presence of sulfate (SO_4^{2-}) in non-potable water. During the current study it was observed that the impact of presence of sulfate was more pronounced on A-860 compared to A-500P (which indicates that the former might be more sulfate selective than the latter). For example, at the higher background sulfate concentration examined (30 mg/L), the % removal of PFOA by A-500P decreased by 18% as opposed to 60% for A-860. Also, at a background sulfate concentration of 1 mg/L PFOA uptake capacity of A-500P was not impacted. Similar trends are expected for PFHpA and PFNA.

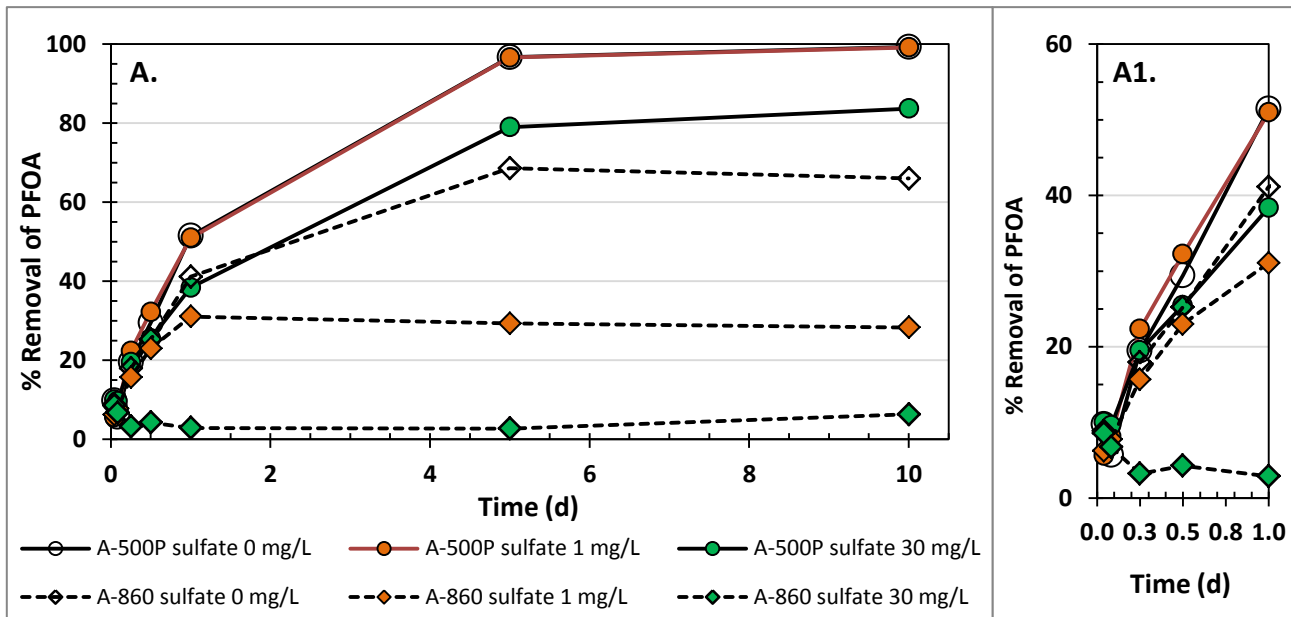


Figure 4.12: Effect of sulfate anion at different concentrations on PFOA removal kinetics in ultrapure water; Resin dose- 10 mg/L; plot A1 provides a closer look at the initial data points shown in plot A.

Data presented in Figure 4.12 were fitted to the pseudo-second-order adsorption kinetics model and the model estimated parameters are presented in Figure 4.13. As can be seen the impact of increasing sulfate concentration is greater on A-860 resin compared to A-500P resin. PFOA adsorption quantity was similar in no sulfate and 1 mg/L of sulfate solution, and was about 22% lower in 30 mg/L sulfate solution compared to when no sulfate was present in solution (Figure 4.13A). On the other hand, the estimated equilibrium the estimated equilibrium PFOA adsorption amount for A-860 at 1 mg/L of sulfate and 30 mg/L of sulfate were, respectively, 60% and 93% lower compared to when no sulfate was present in the solution (Figure 4.13B). The initial adsorption rate for A-500P did not change due to sulfate addition. However, for A-860 resin although the initial adsorption rate was higher when 1 mg/L of sulfate was added to the solution, the initial adsorption rate decreased considerably when 30 mg/L of sulfate was added. Overall,

these results confirm competition from sulfate impacted A-500P only slightly while severe competition was observed for PFOA removal on A-860.

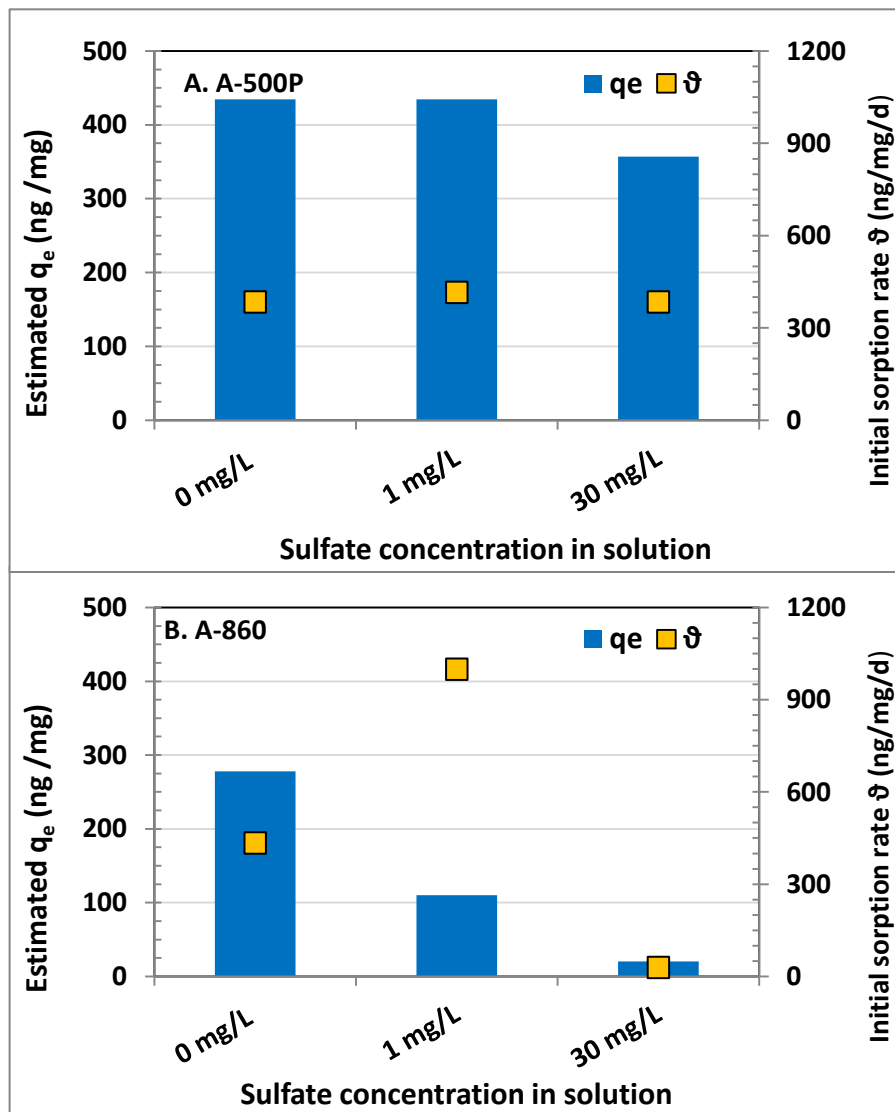


Figure 4.13: Graphical representation of the estimated pseudo-second-order model parameters for PFOA adsorption onto- A) A-500P and B) A-860 at different background sulfate concentration

Figure 4.14 illustrates the sulfate uptake kinetics of the two tested resins. Sulfate uptake kinetics for both resins is substantially slower at the 1 mg/L sulfate concentration (equilibrium reached at 5 d) compared to the 30 mg/L sulfate concentration (12 h). Higher uptake of sulfate by A-860 at the higher sulfate concentration as shown in Figure 4.14 (B) confirms the sulfate selectivity of A-860.

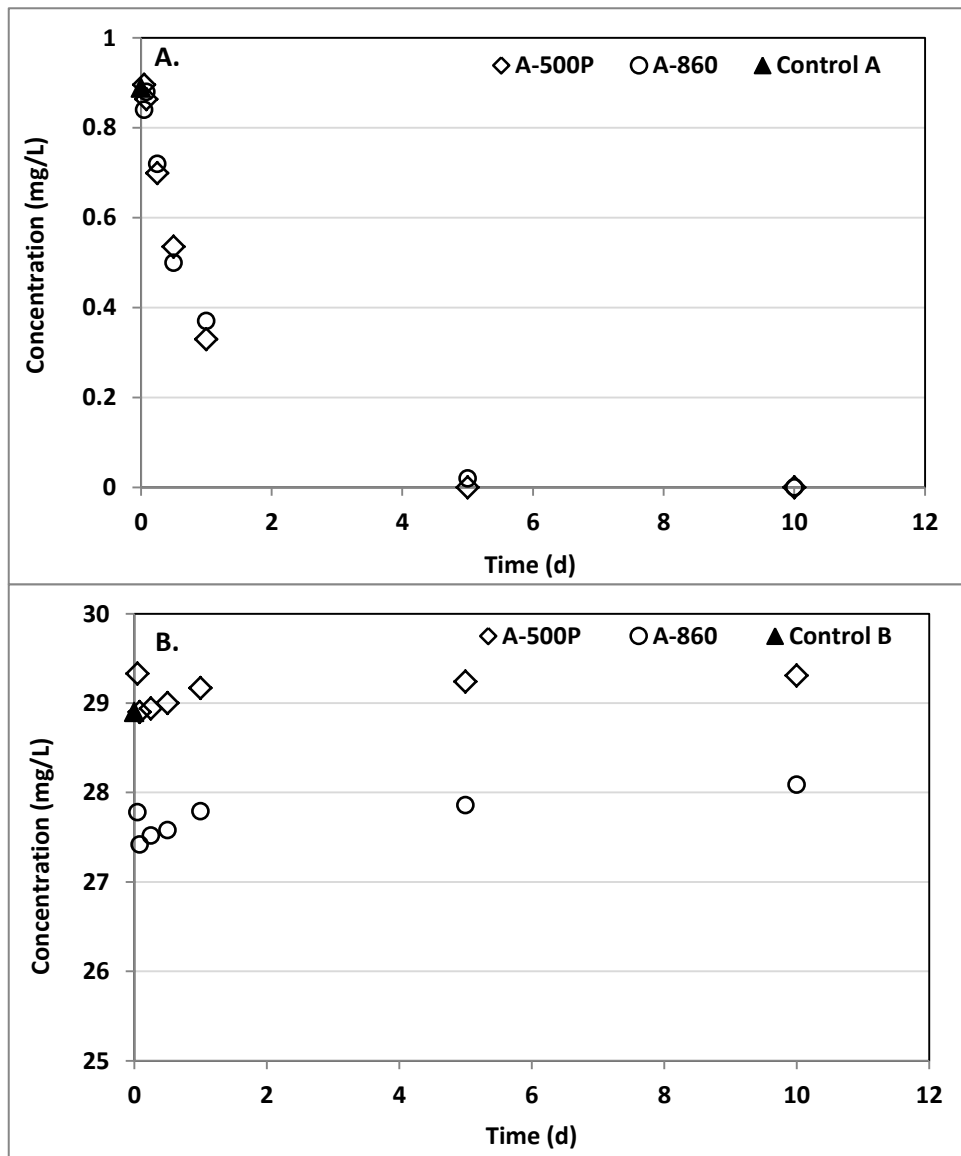


Figure 4.14: Sulfate removal kinetics for A-500P and A-860 resins; ultrapure water (control) was spiked at two different concentrations: A) Control A- 1 mg/L sulfate and B) Control B- 30 mg/L sulfate; Resin dose- 10 mg/L.

4.3.6 Effect of Resin Matrix and PFCA uptake mechanism by Anion Exchange Resins

As mentioned earlier, higher removal of PFCAs were observed with the polystyrenic macroporous A-500P resin compared to the polyacrylic macroporous A-860 resin. Both resins were selected for this study since their physico-chemical properties according to manufacturer's specifications were similar except for the resin matrices (Table 4.2). It is also worth noting that due to proprietary issues, composition of the functional ion exchange groups of the selected resins could not be ascertained which may contribute to differences in surface properties of the two resins. PFCA uptake trends (Figure 4.1) observed during this study suggests that polystyrenic resins (e.g. A-500P) may be more favourable than polyacrylic resins (A-860) for PFCA adsorption. However, in absence of accurate information on surface coating or surface functional groups such premise cannot be generalized.

Two possible mechanisms- ion exchange (electrostatic interaction between the anionic functional group of the PFCAs and the cationic functional group on the anion exchange resin) and adsorption (hydrophobic interactions between the polymer backbone and the hydrophobic PFCA chain) have been suggested previously as two possible adsorbate-adsorbent interactions that may play roles in uptake of PFCAs during treatment with ion exchange resins (Yu et al. 2009a). Considering hydrophobic interaction as a potential uptake mechanism the current study wanted to ascertain the contribution of each type of uptake mechanism during ion exchange treatment. Thus, in addition to the ion exchange resins, PFOA removal kinetics were also evaluated using the two types of base resin beads which were acquired from the manufacturer. It was assumed that since these were uncharged any removal of PFOA by the resin beads should result from the hydrophobic interaction of PFOA molecules and the resin beads. This would then indicate the contribution of hydrophobic/hydrophilic interaction towards the overall uptake of PFOA. The

resin beads acquired (both polyacrylic and polystyrenic), however, were unable to remove the PFOA (Figure 4.15) and thus indicated lack of hydrophobic interaction of PFOA and the styrenic and acrylic resin beads. Similar trends are also expected for PFHpA and PFNA. Indeed, the very low BET surface area ($< 10 \text{ m}^2/\text{g}$) and pore volume ($< 0.044 \text{ cm}^3/\text{g}$) of the uncharged resin beads also support the observation of negligible adsorption potential of PFCAs via hydrophobic interactions. Hence, it can be concluded that the primary mechanism for the anion exchange resin treatment is due to ion exchange. Yu et al. (2009a) in their study considered a pKa value of 2.2 for PFOA and observed a higher adsorption of PFOA onto the anion exchange resins at pH 3 compared to pH 7. Thus, they indicated that the increased adsorption at the lower pH may have been due to the hydrophobic interaction of the uncharged species of PFOA and the resin. However, the pKa of PFOA have been reported to be less than 1 (Ahrens et al. 2012) and thus, PFOA is expected to be in its anionic form at pH 3. Hence, the increased adsorption of PFOA at pH 3 observed by Yu et al. (2009a) may not necessarily have been due to hydrophobic interaction between the neutral species of PFOA and the anion exchange resin surface.

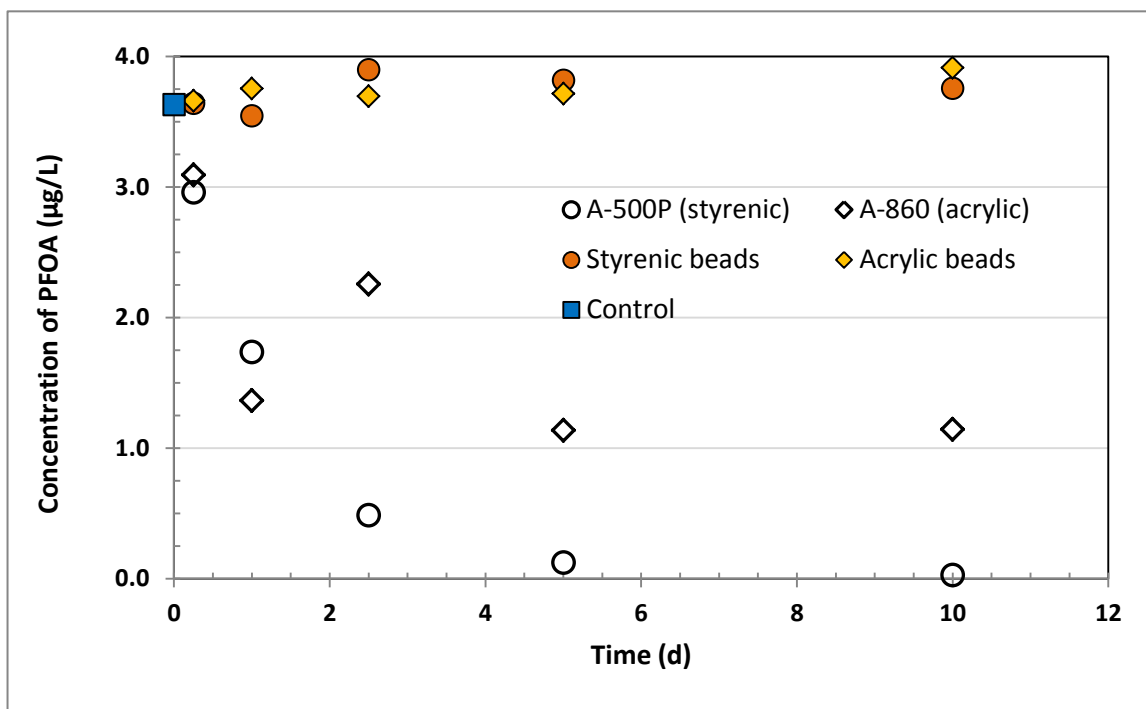


Figure 4.15: Removal kinetics of PFOA in ultrapure water by anion exchange resins and uncharged resin beads; Open symbols are anion exchange resins and colored symbols indicate uncharged resin beads; adsorbent dose- 10 mg/L.

4.3.7 Data Reproducibility

The GC/MS analytical method developed for analyzing PFCAs is time and labour intensive which limited the use of replicates during the current study. However, to address the issue of data reproducibility, single solute PFOA removal kinetic experiments in ultrapure water using ion exchange resins were repeated three times to confirm the trends observed with ion exchange resins in removing PFCAs from ultrapure water. Results of the three sets of experiments examining the removal kinetics of PFOA in ultrapure water by ion exchange are presented in Figure 4.16. It can be seen that the percentage removals of PFOA in each of the three different sets are similar confirming reproducibility of the PFCA removal trends by ion exchange. For example, percent removals of PFOA for all three sets of experiments were greater than 99% with A-500P and 66-69% for A-860 resins. The removal data over time matched nicely for A-500P.

However, for the A-860 resin Set 3 data there may be a problem with two data points (1 d and 2.5 d). However, without those two data points in Set 3, all the data sets 1, 2 and 3 for A-860 follow the same trends over time closely. The difference in percentage removal of PFOA after 1 day with A-860 resin in Set 3 could not be explained. However, it is possible that the Set 3 A-860 resin samples for the 1 d and 2.5 d contact time may have been mistakenly switched during sample analysis which may explain the anomaly observed with the Set 3 results for A-860 resin. Nonetheless, the overall percent removals of PFOA after 10 days were similar for all the three sets of experiments. Also the data presented in Figure 4.16 was fitted to the pseudo-second-order model and the calculated model parameters are graphically presented in Figure 4.17. High correlation ($R^2 = 0.95-0.99$) was observed for all the three sets of experiments for both resins. While still high the correlation with Set 3 for A-860 ($R^2 = 0.95$) was relatively lower than the other two data sets ($R^2 > 0.99$). If the 1 d and 3 d data points for the Set 3 experiments for A-860 resin are either switched or not considered then the fitting correlation becomes similar to the other two sets ($R^2 > 0.99$). As can be seen from Figure 4.17 the estimated q_e values for PFOA for both A-500P and A-860 resin are similar for all three data sets. The initial adsorption rates for A-500P resin were similar for all three data sets (Figure 4.17A). However, for the A-860 resin, there are some differences in initial adsorption rate. As discussed earlier in Set 3, the two data points 1 d and 2.5 d do not follow the same trend as the other two sets and if these two points are either neglected or switched the initial sorption rate does increase for Set 3 data for A-860. The quite high value for Set 1 experiments compared to the other two sets (Figure 4.17B) may have been due to the first data point (0.25 d). Overall, the results of the three sets demonstrate good replication of the PFOA removal trends with the two resins.

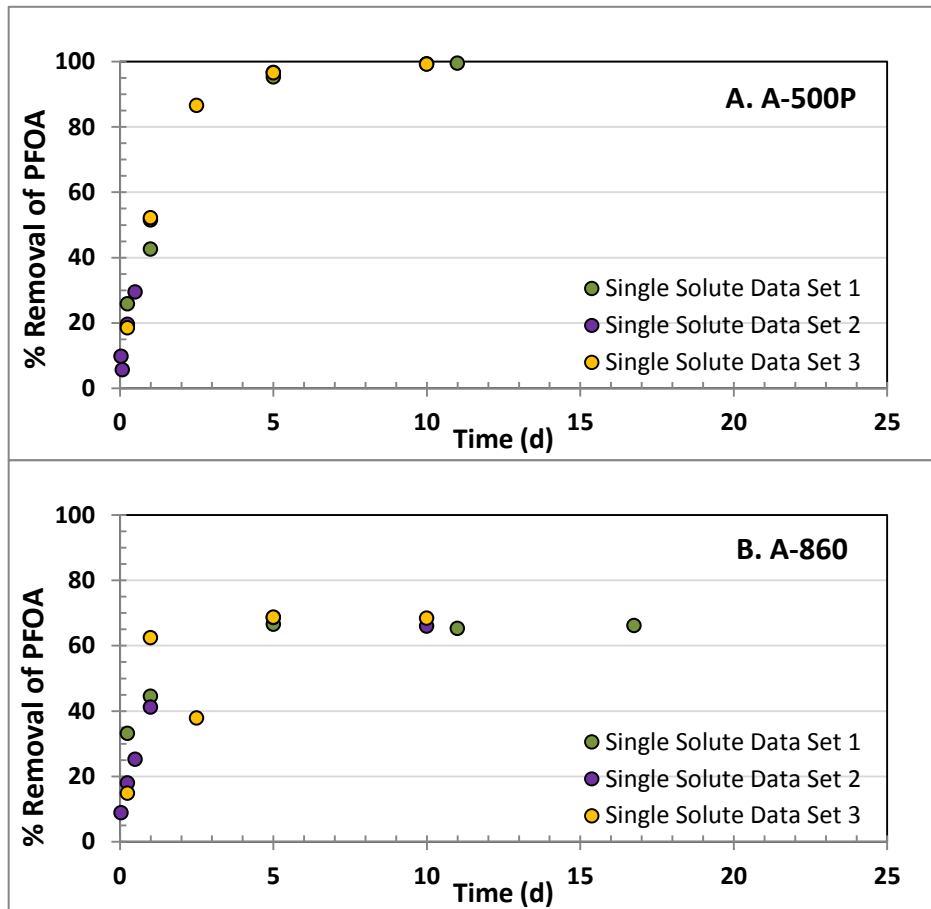


Figure 4.16: Removal of PFOA by anion exchange illustrating the reproducibility of removal trends by A) A-500P, B) A-860.

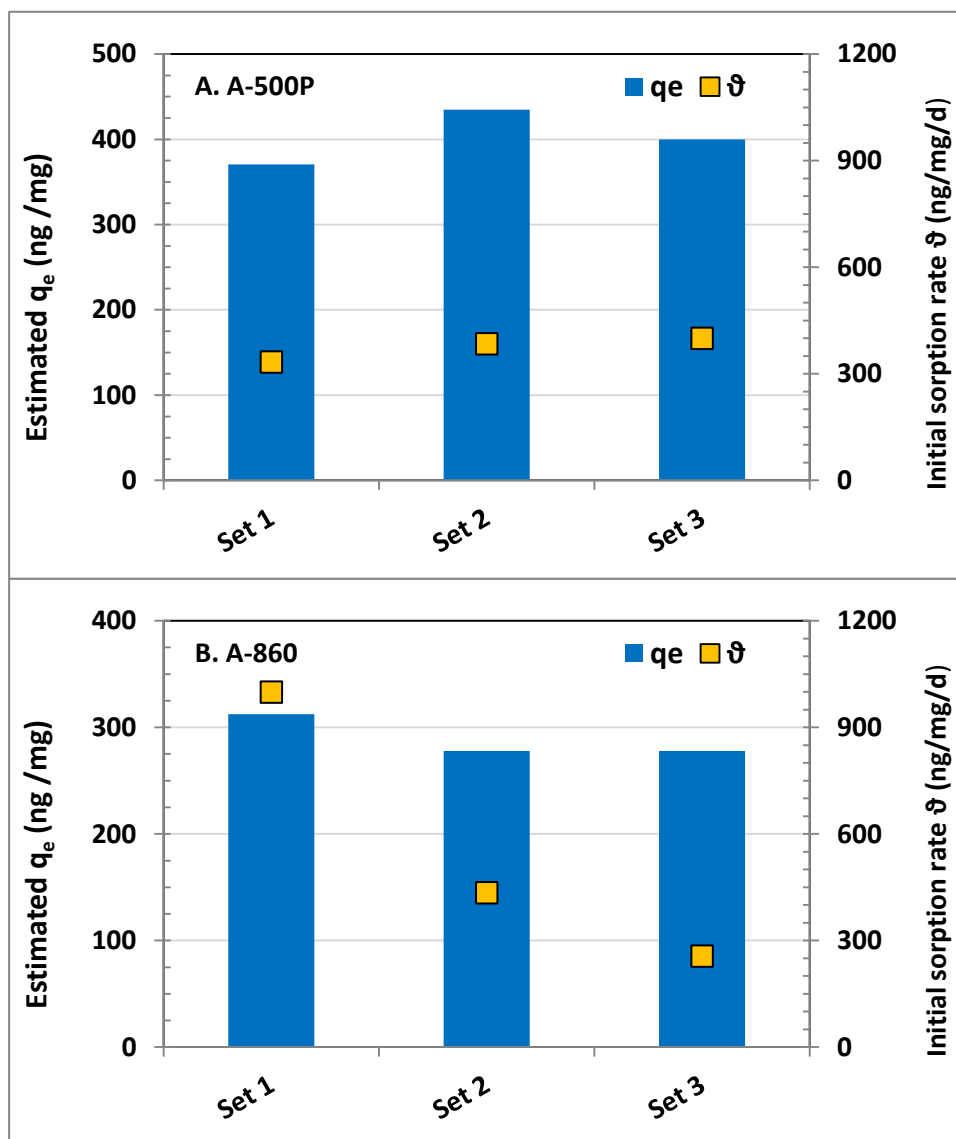


Figure 4.17: Graphical representation of the pseudo-second-order model parameters for PFOA adsorption onto (A) A-500P and (B) A-860 during three different sets of experiments; data used for the model fitting is presented in Figure 4.16.

4.4 Conclusions

The removal potential of three representative PFCAs by several adsorption and ion exchange adsorbents were assessed in ultrapure water. The PFCAs included PFHpA, PFOA, and PFNA.

Under the conditions tested it was observed that:

- Based on Freundlich isotherm and adsorption kinetics investigations, the anion exchange resin A500-P had the highest adsorptive capacity and it displayed the fastest kinetics for the target PFCAs among the investigated adsorbents.
- Among the four GACs, the coal-based F-400 performed best for the three target PFCAs achieving about 92% removal of all target PFCAs following 23 days of equilibration. The coconut shell-based CX carbon showed similar equilibrium adsorption amounts (derived using the pseudo-second-order adsorption kinetics model) for the target PFCAs. However, the more microporous structure of CX carbon may have contributed to slower kinetics compared to F-400 carbon. Wood-based carbons C-Gran and WV-B30 removed less than 60% of all three target compounds except for PFNA with C-Gran following 21 days of equilibration. The negative surface charge may have been responsible for lower removal of anionic PFCAs with the wood-based GACs tested.
- The two alternative adsorbents were relatively ineffective for the removal of the selected PFCAs. Bone char did not remove any of the PFCAs. In bottle point kinetic tests, Biochar removed less than 15% of the PFHpA and about 20% and 40% removal of the PFOA and PFNA, respectively, after 23 days of equilibration. Low secondary micropore volume may have been responsible for their poor PFCA removal performance.
- The bottle point adsorption kinetic experiments indicated that adsorption kinetics were considerably faster for the anion exchange resins compared to the GACs and the alternative adsorbents. Equilibrium was reached for both resins after 10 days with about 90% of the overall removal being achieved within 5 days. The GACs reached equilibrium after 15 days of contact time.

- Results of the isotherm experiments were also consistent with the PFCA removal trends observed in kinetics tests. Of the three adsorbents tested in isotherm studies, A-500P exhibited highest PFCA adsorption capacity for the target PFCAs. F-400 carbon had higher adsorption capacities for PFOA and PFHpA than did the A-860 resin.
- The uncharged styrenic and acrylic beads (base materials) of the two tested resins were unable to remove PFOA. This indicates that hydrophobic interactions did not contribute to removal of PFCAs by anion exchange and it implies that the dominant removal mechanism involves charge interactions between the negatively charged PFCAs and the positively charged anion exchange functional groups.
- In the presence of sulfate, the macroporous styrenic A-500P resin exhibited both faster and better removal of PFOA compared to macroporous acrylic A-860 resin. In presence of a 1 mg/L of sulfate, A-860 lost about 40% of its PFOA equilibrium capacity while at 30 mg/L of sulfate it completely lost the ability to remove PFOA.
- Removals of the individual target PFCAs were not substantially different when present as single solutes or in mixtures with other target PFCAs indicating that direct competition among the PFCAs was minimal.
- For the target PFCAs, chain length dependent removal was only observed for A-860 resin and for the alternative adsorbent Biochar (e.g. PFNA [C9] was more effectively removed than PFHpA [C7]). This trend was, however, not apparent for the A-500P resin and the F-400 and CX GACs.

Chapter 5

PFCA Removal during Drinking Water Treatment by GAC and Ion Exchange from Surface Water: Effect of NOM and Inorganic Anions

Summary

Removals of three PFCAs- perfluoroheptanoic acid (PFHpA), perfluorooctanoic acid (PFOA), and perfluorononanoic acid (PFNA) in Grand River water (GRW) were investigated using two GACs (Calgon F-400 and AquaCarb CX 1230), two anion exchange resins (Purolite A-500P and A-860), and the dairy-manure based alternative adsorbent Biochar. Of the tested adsorbents, PFCA adsorption amount at equilibrium, was similar for the A-500P resin, and F-400 and CX carbons. However, removal kinetics of the target PFCAs were considerably faster with the polystyrenic anionic resin A-500P. Among the GACs, coal-based F-400 exhibited faster removal kinetics of the target PFCAs than coconut-based AquaCarb CX 1230 (CX). The more microporous structure of the CX carbon may have contributed to its relatively slower PFCA removal performance compared to the F-400. The alternative adsorbent Biochar achieved less than 40% removal (at equilibrium) of the target PFCAs from spiked GRW which may have been due to its lower content of secondary micropores. The polyacrylic resin Purolite A-860 failed to achieve appreciable removal of the target PFCAs in GRW. The GRW water matrix (e.g. NOM and inorganic anions) adversely affected adsorption of the target PFCAs onto the tested adsorbents. For the GACs and the Biochar, NOM (especially humic constituents) was the dominant competitor and in the case of anion exchange resins, inorganic anions (especially sulfate) were the dominant competitors. Removals of DOC and humics, and reduction of specific UV absorbance (SUVA), in GRW were greater by the anion exchange resins compared to the

GACs and Biochar. Of the two resins, A-860, due to its hydrophilic structure, exhibited faster removal/reductions for DOC, humics, and SUVA compared to the A-500P. The selected GACs and Biochar failed to reduce the SUVA of GRW indicating that the NOM composition of GRW was not altered following exposure to the F-400 and CX carbons, and the alternative adsorbent Biochar.

5.1 Introduction

PFCs have unique chemical attributes such as extremely high thermal and chemical stability, high polarity, and strong carbon fluorine bonds which make them very stable in the environment and as such they have been detected in various environments including groundwater and surface water used as drinking water sources and even in treated tap water (Rahman et al. 2014; Post et al. 2013; Eschauzier et al. 2010). Of the various classes of PFCs detected in drinking water and tap water, two classes- perfluorinated carboxylic acids (PFCAs) and perfluorinated sulfonic acids (PFSAs) have been found to be more prevalent. Due to their frequent detection in drinking water and potential human health implications, three PFCAs- perfluoroheptanoic acid (PFHpA), perfluorooctanoic acid (PFOA) and perfluorononanoic acid (PFNA) have been included in the final list of USEPA's 3rd unregulated contaminant monitoring rule (USEPA 2011a). PFOA has also been included in the final list of USEPA's 3rd contaminant candidate list and is also being considered for regulatory directives in other jurisdictions (MDH 2011; DWI 2009; USEPA 2011b; Trinkwasserkommission 2006).

PFCAs have a carboxylic acid functional group and an aliphatic carbon backbone in which hydrogen atoms have been replaced by fluorine (Rahman et al. 2014). PFCAs typically have high water solubility and low vapour pressure both of which decrease as carbon chain length increases (Bhatarai and Gramatica 2011; Lei et al. 2004). PFCAs have been suggested to be strongly

acidic (predicted $pK_a < 1$) (Ahrens et al. 2012; Wang et al. 2011b) and as such are expected to remain in anionic form in the aquatic environment and in drinking water. Wastewater treatment plants, industrial discharges, and degradation of consumer products are some important pathways of PFCAs in the aquatic environment (Boulangier et al. 2005; Paustenbach et al. 2007). In addition, studies have also indicated that degradation of precursors compounds such as fluorotelomer alcohols and fluorinated sulfonamides may also lead to formation of PFCAs (Wallington et al. 2006).

Their high environmental stability, low vapour pressure, high water solubility, strongly acidic nature, and presence at ng/L to $\mu\text{g/L}$ concentrations make PFCAs recalcitrant to various drinking water treatment processes including conventional coagulation/flocculation/sedimentation and filtration, biodegradation, chlorination, ozonation, and even advanced oxidation (Xiao et al. 2012b; Thompson et al. 2011b; Shivakoti et al. 2010; Appleman et al. 2014; Quinones and Snyder 2009; Flores et al. 2013; Eschauzier et al. 2012). However, studies (Eschauzier et al. 2012; Yu et al. 2009a; Appleman et al. 2013; Hansen et al. 2010) have indicated that granular activated carbon adsorption (GAC) and ion exchange can be effective in controlling PFCAs in drinking water. In surface water, the presence of natural organic matter (NOM) is expected to adversely impact GAC adsorption of PFCAs due to preloading and direct competition effects (Zhao et al. 2011; Hansen et al. 2010). In support of this, full-scale plant data (Takagi et al. 2011; LHWA 2010; MDH 2008; Hölzer et al. 2009) indicate that frequent reactivation or replacement of GAC is needed to maintain continuous removal of PFCAs from water and breakthrough of PFOA has been observed to occur following as little as 2-3 months into operation (LHWA 2010; Hölzer et al. 2009). Limited bench-scale data (Hansen et al. 2010; Appleman et al. 2013; Zhao et al. 2011) are available regarding the impact of surface water matrices on GAC adsorption of

PFCAs and data is mostly available for PFOA. Even less data are available for PFHpA and PFNA (Hansen et al. 2010; Appleman et al. 2013). Except for the Appleman et al. (2013) study, published studies have for the most part investigated coal-based GACs and Zhao et al. (2011) conducted their study at higher than environmental initial PFCA concentrations. Although coal-based GACs are often found in drinking water treatment plants, there are other base materials for GAC treatment that are available on the market and are also used by water treatment utilities. In addition to conventional GACs, cheaper alternative carbonaceous adsorbents such as dairy manure-based Biochar have been studied and found to be effective for the removal of trace organic contaminants such as atrazine (Cao et al. 2011). Thus, there is an incentive to understand the adsorption behaviour of PFCAs onto adsorbents other than coal-based GACs.

The presence of PFCAs in anionic form in the aquatic environment suggests that anion exchange resin treatment may be effective in removing PFCA from water. Limited full-scale survey and bench-scale studies (mostly in ultrapure water) also confirm anion exchange as a promising technique (Appleman et al. 2014; Dudley 2012; Arevalo Perez 2014; Chularueangaksorn et al. 2013; Yu et al. 2009a; Lampert et al. 2007). Similar to GACs, some studies have shown that uptake of PFCAs with ion exchange resins also increases as carbon chain length increases (Dudley 2012; Arevalo Perez 2014). Yu et al. (2009a) observed during their ultrapure water study that macroporous polystyrenic Amberlite IRA400[®] resin had higher PFOA adsorption capacity than a coal-based GAC. Dudley (2012) noted that removals of shorter chain PFCAs were higher for anionic resins compared to powdered activated carbon used in the study. However, head-to-head comparisons of GAC and anion exchange resin performance for PFCA removal in surface water are unavailable. In addition, the effect of resin base matrix on PFCA removal in surface water is also poorly understood. Dudley (2012) found polystyrenic resins to

be more efficient in removing PFCAs compared to polyacrylic resins, while Deng et al. (2010) found higher removals of PFOS with polyacrylic resin. An understanding of resin matrix effects will assist in selecting appropriate resins for the removal of PFCAs. The presence of anions and potentially even NOM is also expected to affect ion exchange resins by competing for or otherwise blocking access ion exchange sites. As such, there is a need to better understand the effect of other anions present in water on removal of PFCAs. Arevalo Perez (2014), using a magnetic anion exchange resin, found that the impact of pH and NOM was negligible on removal of PFCs while the removal decreased with increasing ionic concentration. Appleman et al. (2014), however, observed that magnetic ion exchange resin targeted to remove NOM was virtually ineffective in removing PFCs at a full-scale plant which the authors noted may have been due to “continual regeneration, as opposed to a complete resin replacement, or insufficient capacity due to improper operation and/or kinetics.” More data are therefore needed to understand the effect of water matrix on PFCA removal by anion exchange.

The purpose of this phase of study was to assess the effect of direct competition from surface water constituents on PFCA removal during adsorption and ion exchange treatment. The objectives were to investigate:

- PFCA adsorption kinetics and equilibrium concentrations for various media including two different GAC base materials, two resin matrices, and the alternative adsorbent, Biochar, on the removal of PFCAs at environmentally relevant concentrations.
- competition between the target PFCAs (mixed solute vs. single solute) and PFCA chain length in surface water
- the impact of NOM competition on adsorption kinetics and equilibrium capacities of PFCAs in surface water

- the impact of competition from the inorganic ions sulfate, nitrate, and chloride in surface water on adsorption kinetics and equilibrium capacities of PFCAs on selected media
- NOM constituent differentiation to attribute the extent of direct competition exerted by various NOM fractions using liquid chromatography with organic carbon detection (LC-OCD) and the organics surrogates UV_{254} and SUVA.
- physico-chemical properties of the tested adsorbents and models to better mechanistically understand PFCA adsorption
- anion exchange resins and Biochar as potential pretreatments to reduce NOM competition in GAC adsorbers or resins being used to remove PFCAs

5.2 Materials and methods

5.2.1 Target compounds

PFHpA (99%), PFOA (96%), and PFNA (97%) were purchased from Sigma-Aldrich (St. Louis, MO, USA). Molecular structures and the physicochemical properties for each of the selected target compounds are provided in Chapter 2 Table 2.1. No pH adjustments were done during this study. Stock solutions of the target PFCAs were prepared in ultrapure water at a concentration of 10 mg/L without any organic solvent and stored for a maximum of 9 months at 4°C. Throughout this phase of study, surface water was spiked as required using the stock prepared in ultrapure water. The individual nominal compound target spike concentration was 3.0 µg/L in all tests. The actual spiked PFCA concentrations were measured at the beginning of each experiment.

5.2.2 Waters

Ultrapure water (UPW) (18.2 Ω) used during the study was generated from a Millipore system (Milli-Q UV Plus[®], Mississauga, ON). Grand River water (GRW) was collected from the Mannheim Water Treatment Plant (Region of Waterloo, ON, Canada). Two batches of GRW

were collected for the study and none of the target PFCAs were detected in the batches. The 1st batch was collected on 03 February, 2014, spiked, and then used to conduct the first set (Set 1) of experiments with the selected adsorbents. The 2nd batch was collected on 09 May, 2014 and a second set of experiments (Set 2) were conducted to confirm the trends observed in Set 1. The raw water was stored at 4°C until spiking for further use. Following spiking with the target PFCAs, raw water was allowed to settle overnight prior to starting kinetic experiments. No pH adjustments were done during this study. Properties of the two batches of GRW are listed in Table 5.1.

Table 5.1: Properties of Grand River Water (GRW)

Parameter	Collection Date	
	03 February, 2014 (Set 1)	09 May, 2014 (Set 2)
pH	8.20	8.50
Conductivity (µS/cm)	762	549
DOC (mg/L)	5.0	4.7
Humics (mg/L)	3.63	3.20
Biopolymers (mg/L)	0.25	0.32
Building Blocks (mg/L)	0.63	0.58
UV ₂₅₄ (1/cm)	0.146	0.146
SUVA (L/mg-m)	2.9	3.1
Alkalinity (mg/L as CaCO ₃)	236	182
Turbidity (NTU)	1.3	5.4
Sulfate (mg/L)	29.3	16.6
Nitrate as nitrogen (mg/L)	3.7	3.0
Chloride (mg/L)	67.4	47.2

5.2.3 Adsorbents

Two GACs - coal-based Filtrasorb 400[®] (F400) (Calgon Carbon, Pittsburgh, PA, USA) and coconut shell-based AquaCarb CX 1230[®] (CX 1230) (Siemens, Warrendale, PA, USA), and an alternative adsorbent- digested dairy manure-based Biochar[®] (Char Technologies, Toronto, ON, Canada) were selected for the current study. The GACs and the Biochar were sieved through a

12 × 30 US standard mesh, washed in ultrapure water (18.2 Ω) to remove fine particles, and then dried at 110°C for at least 24 h to remove any moisture. Adsorbents were not crushed prior to use. Following drying, the adsorbents were sealed with aluminum foil and stored in a desiccator until required. Properties of the selected carbonaceous adsorbents are presented in Chapter 4 Table 4.1.

Two organic scavenging strong base anion resins from Purolite- macroporous polystyrenic A-500P and macroporous polyacrylic A-860 (Purolite, Bala Cynwyd, PA) were selected for this study. Apart from their different resin base matrix, both resins have similar physico-chemical properties including total capacity (Chapter 4 Table 4.2). The resins were not rinsed and were used as received. The adsorbents were also analyzed at a commercial lab for determining pore size distribution and Brunauer-Emmet-Teller (BET) surface area (Quantachrome Instruments, Boynton Beach, FL).

5.2.4 Kinetic tests

Bottle point adsorption kinetic experiments with the selected adsorbents were conducted in 1 L polypropylene opaque bottles (VWR, West Chester, PA) at 150 rpm on an orbital shaker (Barnstead/Thermolyne, Dubuque, IA) at room temperature without pH adjustment. For surface water kinetics experiments, 1 L of spiked surface water was poured into each sample bottle and 100 mg (dry weight) of adsorbent material were added. Spiked raw water blanks were also added to the sampling queue to monitor sample degradation. Sample bottles were then taken off at different time intervals to monitor the time dependent removal of spiked PFCAs, NOM constituents, and anions. As indicated earlier the Set 1 experiments were conducted with river water collected in February 2014 with all the selected adsorbents. Kinetic experiments were conducted by spiking GRW with a mixture of PFCAs (termed here as mixed solute) and also by

spiking GRW with only PFOA (termed as PFOA only). Comparison of the removal results between the two types of experiments should illustrate the effect of target contaminant mixtures on adsorption of individual PFCAs. Both PFOA only and mixed solute kinetic experiments with anion exchange resins A500P and A860 were repeated in the Set 2 experiments to confirm the removal trends observed during the Set 1 experiments. The Set 2 experiments were conducted in duplicate. All experiments were conducted at room temperature (~ 20°C) to minimize the effect of temperature change on adsorption.

5.2.5 Analysis

Analyses of the target compounds in water samples were performed using gas chromatography with mass spectrometry (GC/MS) preceded by solid phase extraction and derivatization. Details of the analytical method can be found in Chapter 3. The method detection limit (MDL) for the established method were established to be 11-30 ng/L in ultrapure water and 16-49 ng/L in surface water depending on the target compounds (Chapter 3 Table 3.1). DOC concentration and the NOM fractions (humic substances, biopolymers, and building blocks) were measured by liquid chromatography with organic carbon detection (LC-OCD) (DOC Labor Dr. Huber, Karlsruhe, Germany). UV₂₅₄ absorbance was measured with UV-Vis spectrometer (Cary 100, Agilent Technologies, Mississauga, ON), and SUVA was calculated as follows: $SUVA = UV_{254}/DOC$. Other water quality parameters including turbidity, pH, hardness, alkalinity, conductivity were also measured. For inorganic anions analyses the Set 1 samples were sent to ALS Environmental Laboratories (Waterloo, ON). The Set 2 inorganic anions samples were analyzed at the University of Waterloo using a Dionex AS-DV ion chromatography system (Thermo Scientific) using standard ASTM test methods for anions in water (ASTM Designation D4327-11). The MDLs for the selected anions reported by the ALS Lab are as follows: sulfate-

2.0 mg/L, nitrate as nitrogen- 0.1 mg/L and chloride- 2.0 mg/L which are similar to the MDLs for the selected anions determined at the Environmental Engineering Lab at the University of Waterloo.

5.3 Results and discussion

5.3.1 Adsorbent properties

Properties of the selected adsorbents and the results of the surface area and pore size distribution analysis of the selected adsorbents are presented in Tables 4.1 and 4.2 in Chapter 4. Details of pore size distribution data for the selected adsorbents are provided in Appendix C. The selected Biochar has a much lower BET surface area and DFT pore volume compared to the conventional GACs- F-400 and CX. Both GACs are microporous as opposed to the Biochar which is mesoporous. However, CX carbon has a higher percentage of primary (<0.8 nm) and secondary micropores (0.8-<2 nm) and a greater BET surface area than the F-400 carbon.

The anion exchange resins: A-500P and A-860 have very low BET surface area and DFT pore volume compared to the carbonaceous adsorbents. The resins, except for their respective resin matrix have similar properties (Table 4.2) including quaternary ammonium as their anion exchange functional group. The exact compositions of the surface functional group of the resins are proprietary but it likely that the compositions are similar. Also, A-860 resin has a more hydrophilic structure and can achieve a higher reversible removal of organics on regeneration and is capable of handling higher levels of dissolved organics. The polystyrenic resin A-500P has higher porosity compared to A-860 and when new may reduce dissolved organics to lower levels compared to the acrylic resin. A-500P due to its more hydrophobic structure is less easy to regenerate and thus is more susceptible to irreversible fouling (Purolite 2006).

5.3.2 PFCA Adsorption Kinetics

The subsequent sections discuss the results obtained during adsorption kinetic experiments conducted in using raw (untreated) Grand River Water. As mentioned earlier, due to the challenges associated with the analytical method used for PFCA detection, the current study was constrained in terms of the number of replicates that could be analyzed. However, to ensure data quality and also to confirm reproducibility of the PFCA removal trends selected kinetic experiments were repeated. Reproducibility of the PFCA removal data is discussed in greater detail in Section 5.3.7.

Results of the Set 1 mix solute adsorption kinetic experiments in GRW are presented in Figure 5.1. Of the selected adsorbents, polystyrenic A-500P resin achieved the highest (> 93%) removal of the target PFCAs at equilibrium while polyacrylic A-860 resin displayed the lowest removal (< 15%). Of the two commercial GACs, coal-based F-400 exhibited higher removal of the target PFCAs compared to the coconut shell-based CX carbon. F-400 achieved more than 85% removal of the target PFCAs within 15 days while CX removed about 74% of the target PFCAs over the same contact time. The CX carbon achieved greater than 93% removal after 22 d. The 22 d sample for F-400 carbon was lost during the experiment and hence, removal of PFCAs with F-400 carbon during mixed solute experiments could not be reported here. However, kinetics experiments with single solute PFOA only experiments show that F-400 carbon achieved about 95% removal of PFOA after 22 days of contact time as opposed to about 91% with CX carbon (Figure 5.1D). Biochar achieved substantially lower removal of PFCAs during the mixed solute experiments with a maximum of 38% removal for PFNA after 22 days of contact time.

For a more quantitative comparison of the adsorption performance of the adsorbents in GRW, a pseudo-second-order model (Ho and McKay 1999; Ho and McKay 1998) was applied to fit the

obtained kinetics data. The pseudo-second-order adsorption kinetics model is expressed in Chapter 4 (Equation 4.4). The model parameters are the pseudo-second order rate constant for adsorption k_2 ($\text{mg}\cdot\text{ng}^{-1}\cdot\text{d}^{-1}$), the total amount adsorbed at equilibrium q_e (ng/mg), and q_t (ng/mg) the amount adsorbed at time t (d). The initial sorption rate ϑ ($\text{ng}\cdot\text{mg}^{-1}\text{d}^{-1}$) reflects kinetic performance and is expressed in Equation 4.5.

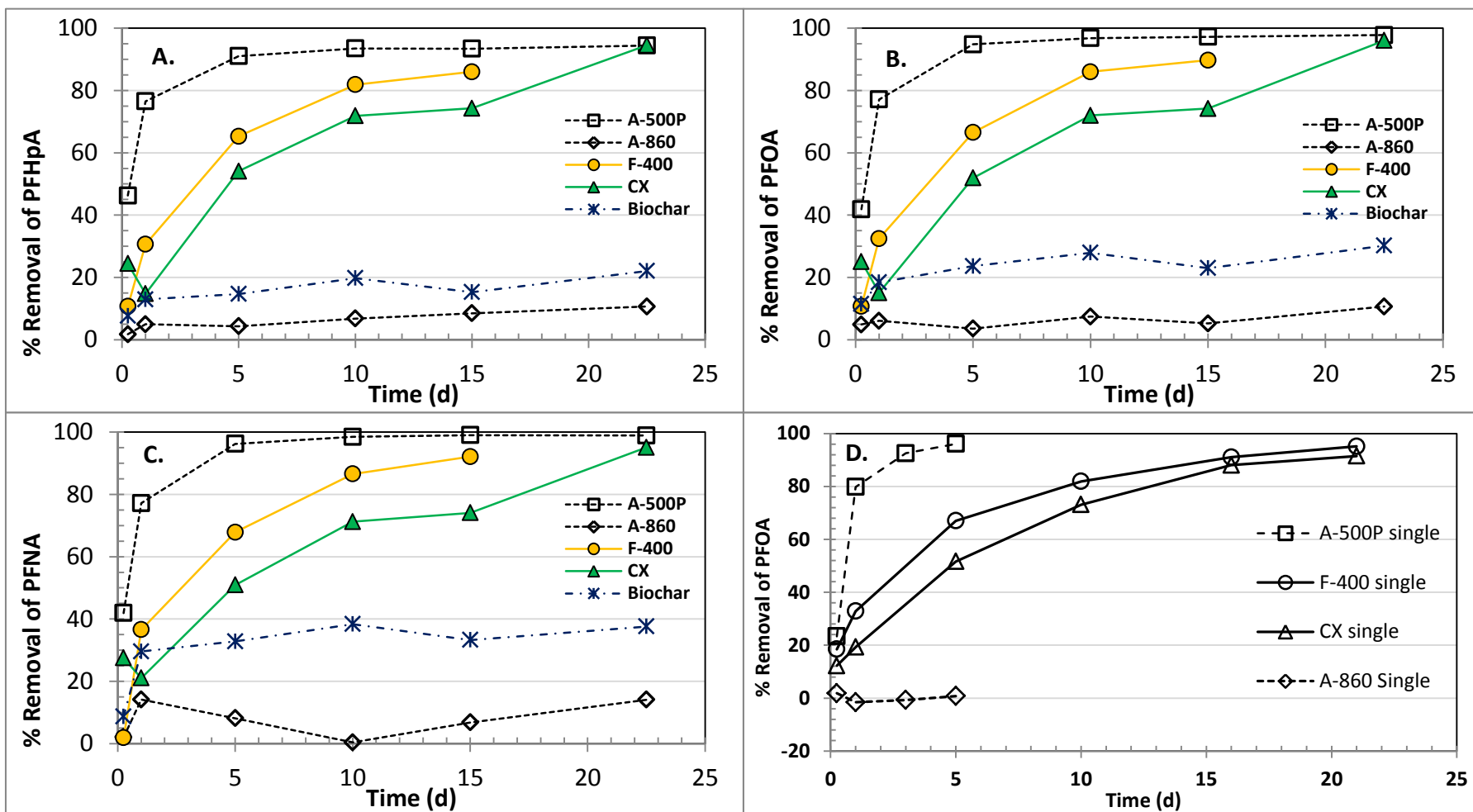


Figure 5.1: PFCA removal over time for the selected adsorbents in Grand River water (GRW); plots A- C show results of mixed solute adsorption experiments (all three target PFCA were spiked into single flasks of ultrapure water); plot D shows results of single solute experiments (only PFOA was spiked); no pH adjustments were done; PFCA initial concentrations for mixed solute experiments: PFHpA- 4.05 $\mu\text{g/L}$, PFOA- 3.58 $\mu\text{g/L}$; and PFNA- 3.56 $\mu\text{g/L}$; PFOA concentrations for single solute only experiments: 3.41-3.81 $\mu\text{g/L}$; adsorbent dose was 100 mg/L.

Figure 5.2 shows the pseudo-second-order model plots fitted to the PFCA removal kinetics data obtained during the mixed solute Set 1 experiments (as shown in Figure 5.1). The model parameters including the corresponding correlation coefficients along with the experimentally derived equilibrium adsorption amounts are presented in Table 5.2. In general, high correlation coefficients ($R^2 > 0.93$) were observed for all adsorbents except for the A-860 ($R^2 = 0.02-0.89$). A-860 resin was the least well performing adsorbent and was impacted most by the GRW matrix compared to the results in ultrapure water which probably explains the poor fitting of the model to the A-860 data. Therefore, the pseudo-second order model should not be used to describe the A-860 data. Uncertainties involved with the linear fitting of the model to the adsorption data sets are expressed by 95% confidence intervals of the slope and intercept, and are listed in Table E5 in Appendix E. Non-linear least squares regression derived values of the adsorption kinetic parameters are listed in Table E6 in Appendix -E.

Model derived equilibrium adsorption amounts (q_e) are similar for the adsorbents A-500P, F-400, and CX (Table 5.2). The experimental q_e values were calculated as per Equation 4.3 in Chapter 4. There is good agreement between the experimental q_e and the model-derived q_e as evident from Table 5.2. Figure 5.3 graphically represents the model derived q_e and θ values. The model derived equilibrium adsorption amounts for A-500P resin and the GACs were similar and are higher than those of the Biochar and the A-860 resin. Indeed the model derived PFCA q_e values for the A-860 resin ranged from 2-5 ng/mg as opposed to 35-39 ng/mg for the A-500P resin. The q_e values are indicative of the PFCA adsorption capacity of the adsorbents. Previously, Newcombe and Cook (2002), investigating removal of geosmin and MIB removal by PAC, noted that removal at contact times of 2 h or less is more important than the equilibrium removal

capacity of the PAC. Thus in terms of application, PFCA removal at earlier contact times may be more important than the equilibrium PFCA removal capacity of the selected adsorbents.

With regard to PFCA removal kinetics, initial adsorption rates were significantly faster for A-500P compared to the other adsorbents. Of the tested commercial GACs, F-400 had a faster adsorption rate compared to CX which may be related to the more microporous structure of the latter (discussed later). Biochar exhibited similar initial adsorption rates as those for the GACs, but exhibited a chain length dependent trend with higher initial adsorption rates for PFNA compared to PFOA and PFHpA. Initial adsorption rates for the A-860 resin were found to be below $1.5 \text{ ng}\cdot\text{mg}^{-1}\cdot\text{d}^{-1}$ in GRW for mixed solute experiments.

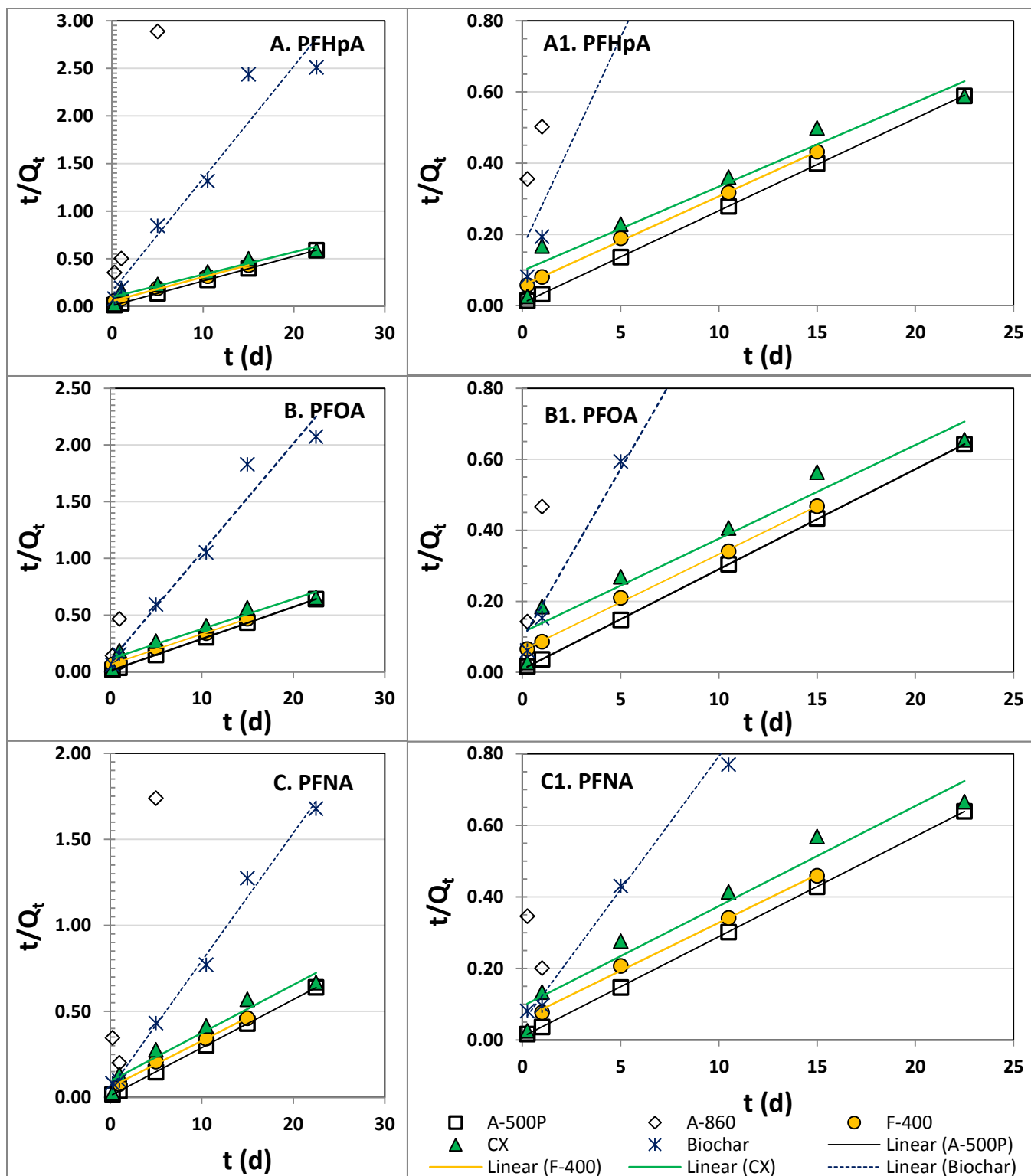


Figure 5.2: Application of the pseudo-second-order model to the PFCA adsorption in GRW onto the selected adsorbents; Plots: A) PFHpA, B) PFOA and C) PFNA; Plots A1, B1 and C1 provide close look at the plots A, B and C, respectively. The lines show linear fitting of the PFCA removals presented in Figure 5.1.

Table 5.2: Pseudo-second-order kinetics model parameters in GRW for the target PFCAs for mixed-solute experiments (calculated using linear least squares regression method)

Adsorbent	q_e (ng/mg)	Exp. q_e (ng/mg)	q_e (ng/mg)	Exp. q_e (ng/mg)	q_e (ng/mg)	Exp. q_e (ng/mg)	k_2 (mg.ng ⁻¹ .d ⁻¹)			β (ng.mg ⁻¹ .d ⁻¹)			R^2		
	PFHpA		PFOA		PFNA		PFHpA	PFOA	PFNA	PFHpA	PFOA	PFNA	PFHpA	PFOA	PFNA
Biochar	8	9	10	11	13	13	0.086	0.099	0.114	6.2	11	21	0.93	0.96	0.99
CX	42	38	38	34	36	34	0.006	0.006	0.008	10	8.9	10.6	0.94	0.94	0.95
F-400	40	35	37	32	37	33	0.011	0.012	0.012	18	16	17	0.99	0.99	0.99
A-500P	39	38	35	35	36	35	0.096	0.093	0.095	143	116	120	0.99	1.00	1.00
A-860	5	4	3	4	2	5	0.057	0.085	0.027	1.2	1.0	0.1	0.89	0.71	0.02

Exp. q_e -experimental q_e ; PFOA removal data presented in Figure 5.1.

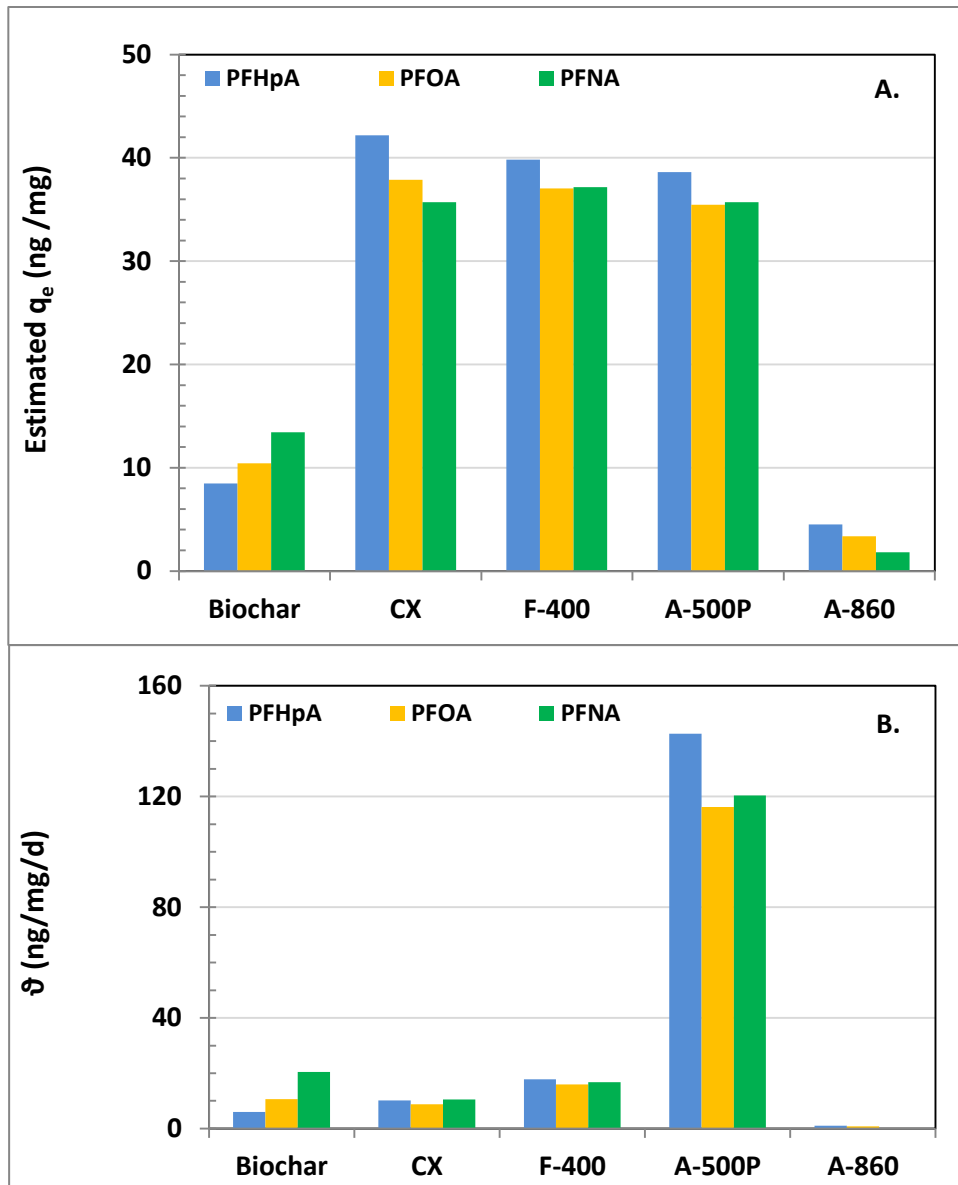


Figure 5.3: Graphical representation of pseudo-second-order kinetics parameters; the model was fitted to time dependent PFCA removal data presented in Figure 5.1. Plot A: Estimated equilibrium sorption amount (q_e); Plot B: Initial sorption rate (ϑ).

It appears that adsorbent properties may have been affecting adsorption of the PFCAs in surface water. The calculated molecular diameters of PFHpA, PFOA, and PFNA are 0.8 nm, 0.9 nm and 1.0 nm, respectively (Wang et al. 2011a). Thus, the primary micropores (< 0.8 nm) in the carbonaceous adsorbents may not be accessible to the target PFCAs. Poor adsorption performance of the Biochar can be attributed to low BET surface area and low micropore content (< 2 nm). CX carbon has a higher percentage of micropores compared to F-400 which has a relatively wider pore size distribution. Thus CX carbon has a relatively compact structure compared to F-400 which may explain the slower kinetics observed with CX carbon (Table 5.2, Figure 5.1). Appleman et al. (2013) also opined that the more microporous structure of coconut shell-based 1240C carbon compared to coal-based F-300 and F-600 may have been responsible for its poor performance compared to the latter two GACs. Thus it is possible that in the current study the more microporous CX was more susceptible to pore blockage compared to F-400. This may have also contributed to the poor kinetic performance of CX in GRW by restricting access of the target PFCA molecules to potential adsorption sites in the secondary micropores (0.8- <2 nm). However, it should also be noted that a broader pore size distribution does not necessarily guarantee a higher micropollutant adsorption capacity in the presence of NOM (Quinlivan et al. 2005). Polyacrylic resin A-860 in GRW lost its PFCA adsorption capacity nearly completely. Direct competition for ion exchange sites with inorganic anions, especially sulfate, and NOM can be responsible for such a reduction. Effect of surface water matrices on PFCA adsorption is discussed in section 5.3.2.

5.3.3 Effect of Surface water Matrix on PFCA Adsorption

Surface water matrices are expected to have adverse impacts on adsorption of micropollutants. With regard to GACs, it was well known that the presence of DOC is expected to adversely

affect both adsorption kinetics and adsorption capacity of micropollutants, and one or two orders of magnitude capacity reduction and substantial reductions in rate of adsorption are not unusual (Pelekani and Snoeyink 1999; Yu et al. 2009b). PFCA removal capacity of anion exchange resins in surface water is also expected to be adversely affected by the presence of NOM and the ionic strength of water (Arevalo Perez 2014, Deng et al. 2010). Adverse impacts of surface water matrices on PFCA removal kinetics were observed in GRW in the current study. Kinetics experiments in GRW were conducted using nearly 10 times more adsorbents compared to UPW experiments (10 mg/L in UPW vs 100 mg/L in GRW) adsorbent had to be used in GRW. Indeed A-860 resin capacity was so severely affected that even following the application of the higher dosage the removal of the PFCAs were less than 15% in GRW. A quantitative illustration of the adverse impact of GRW matrix was made by comparing the pseudo-second-order reaction parameters for the target PFCAs in UPW and GRW. As presented in Figure 5.4 the equilibrium adsorption amount (q_e) for the GACs and the ion exchange resins were 88% to 99% lower in GRW compared to UPW. Reductions in initial adsorption rates (θ) in GRW compared to ultrapure water were also observed (Figure 5.4). The reduction of the initial adsorption rate in GRW for A-860 resin was more than 99% while reduction for the GACs and the A-500P was between 60% and 87% compared to ultrapure water.

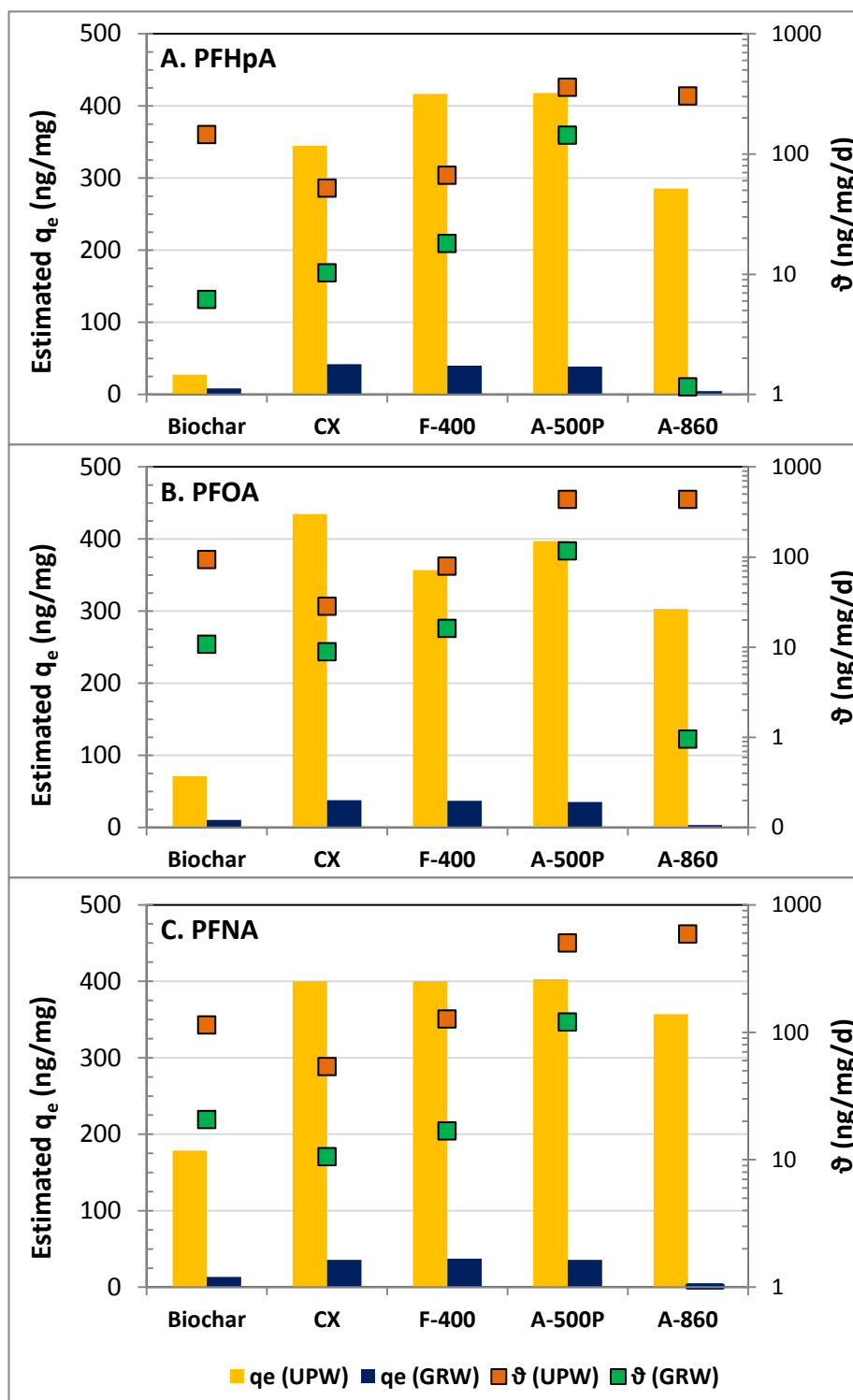


Figure 5.4: Comparison of pseudo-second-order kinetics model parameters (q_e -equilibrium adsorption amount, ϑ - initial adsorption rate) for the target PFCA in ultrapure water (UPW) and GRW (mixed solute) illustrating the impact of GRW matrix on PFCA sorption kinetics; PFCA removal data presented in Figure 4.1 and Figure 5.1.

Arevalo Perez (2014) noted that DOC has relatively less adverse impact on PFCA removal by ion exchange compared to the ionic strength of water. It would therefore not be unexpected that inorganic anions may have been the dominant competition for PFCAs in GRW. Results of the removal kinetics for selected anions (chloride, nitrate, and sulfate) in GRW are shown in Figure 5.5. In GRW, A-860 resin removed more sulfate (9.9 mg/L) compared to A-500P (7.6 mg/L) over the 15 day equilibrium period, while A-500P removed more nitrate. Sulfate selectivity of A-860 was also observed in UPW experiments presented in Chapter 4. Both resins however, removed more sulfate than nitrate. The tested resins also removed similar quantities of DOC in GRW (nearly 75% removal of DOC after 22 days). Analysis of chloride in the resin treated water indicated that when GRW was treated with A-860 more chloride ion sites were exchanged compared to when treated with A-500P. Hence, it can be inferred that the loss of PFCA adsorption capacity of A-860 resulted primarily from the competition exerted by sulfate present in GRW. Adverse impacts of sulfate on PFCA removal capacity of the two selected resins at different sulfate levels in UPW were presented in Chapter 4. It was observed that in UPW at an adsorbent dose of 10 mg/L in presence of 30 mg/L of sulfate (similar to the sulfate level in GRW), A-860 nearly completely lost its PFOA removal capacity. Previously, in non-potable water experiments the adverse impact of sulfate on PFOS removal capacity of anion exchange resins was reported (Deng et al. 2010). However, in contrast to the findings of Deng et al. (2010), higher removals of PFCAs were achieved using a polystyrenic resin in GRW. It appears that the ionic strength of water may be more important than resin base matrix in determining the overall removal of PFCAs in surface water. As expected, anions present in GRW were not removed by the GACs and Biochar (Figure 5.5).

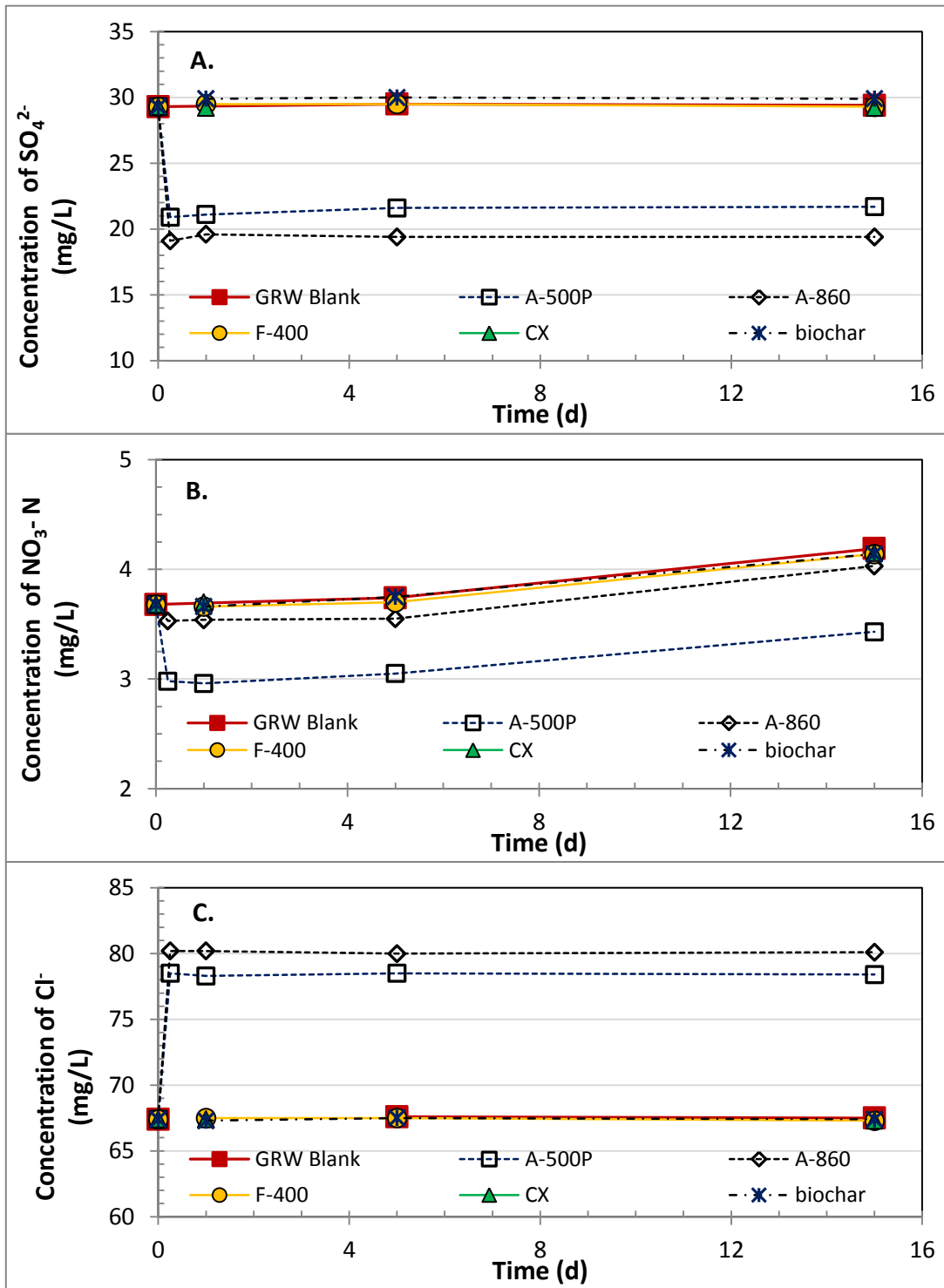


Figure 5.5: Removal of selected anions present in GRW over time (Set 1).

In the case of the carbonaceous adsorbents DOC was an important competitor in GRW for the target PFCAs. It is likely that DOC, which is present at orders of magnitude higher concentration in GRW than the PFCAs, either occupied or blocked access for PFCAs to adsorption sites and thereby reduced the PFCA adsorption capacity of the carbonaceous adsorbents. Appleman et al. (2013) observed rapid breakthrough of GAC filters in presence of DOC and opined that presence of DOC may substantially lower the PFCA removal performance of GACs. The adverse impact of effluent organic matter (EfOM) on PFC adsorption by activated carbon in non-potable water has been reported previously (Yu et al. 2012). The study revealed that the low molecular weight fractions (<1 kDa) of EfOM more adversely impacted on PFC adsorption onto activated carbon than did larger molecular weight fractions (>30 kDa). The negative impact of smaller size fractions of EfOM on activated carbon adsorption of other micropollutants was also noted by (Zietzschmann et al. 2014).

LC-OCD analysis of the DOC present in the GRW (for Set 1 experiments) indicates that humics (0.8-1 kDa), building blocks (0.35-0.6 kDa), and biopolymers (> 20 kDa) constituted 72%, 12%, and 5% of the total DOC. Thus, based on the observations made by Yu et al. (2012) it is unlikely that biopolymer will compete with the PFCA adsorption sites on the GACs. In fact, biopolymers have been reported to be non adsorbable by GAC (Velten et al. 2011). Velten et al. (2011) also demonstrated that humics removal capacity of GAC adsorbents diminishes faster than the lower molecular weight NOM fractions such as building blocks and low molecular weight organics. Thus, in GAC adsorbents, as humics adsorption capacity diminishes, building blocks and low molecular weight organics will likely be the dominant competitors for PFCA molecules. During the current bottle point study, humics being present at significantly higher concentrations compared to other DOC fractions measured (i.e. biopolymer and building blocks), were likely to

have reduced adsorption of the target PFCA onto GAC in GRW. LC-OCD analysis of the raw and treated GRW during the current study indicated that humics removal with the GACs plateaued around 15 d of contact time (discussed in section 5.3.6) which is similar to the time to reach equilibrium for the PFCA as well. On the other hand, high molecular weight biopolymers were poorly removed by both the GACs and the Biochar, and thus probably did not compete for adsorption sites with the target PFCA. Since, surface water matrices will vary depending on their location and source, the PFCA removal trends observed during the current study may vary in other surface water matrices.

5.3.4 Effect of PFCA Chain Length on PFCA adsorption

The effect of PFCA chain length on adsorption of the target PFCA in GRW is illustrated in Figures 5.3 and 5.6. Of the tested adsorbents, the effect of C-F chain length on adsorption of target PFCA in GRW was not prominent for any of the tested adsorbents. Table 5.2 and Figure 5.6 show that none of the tested adsorbent showed any chain length dependent trend for equilibrium adsorption amount and initial adsorption rate except for Biochar which exhibited increased equilibrium adsorption amount and increased initial adsorption rate as the carbon chain length increased. The effects of PFCA chain length observed in GRW are similar to trends observed in ultrapure water (UPW) as discussed in Chapter 4. Previously, however, Dudley (2012) and Arevalo Perez (2014) using adsorbents different than the ones used in the current study noted chain length dependent removal of PFCA. Du et al. (2014) reviewed the adsorption behaviour of PFCs and noted that it is possible that smaller PFCs may exhibit faster adsorption kinetics or even higher adsorption amounts compared to larger PFCs resulting from weaker steric effect and faster diffusion in porous GACs and anion-exchange resins. A previous study that recorded breakthrough times for different PFCA in rapid small scale GAC column tests

observed that while in general chain length dependent pattern was observed the trend was not consistent for all of the PFCAs (Appleman et al. 2013). It is likely that the PFCAs selected for the current study did not have a substantially large difference in chain length (C7-C9) to allow for this trend to be observed.

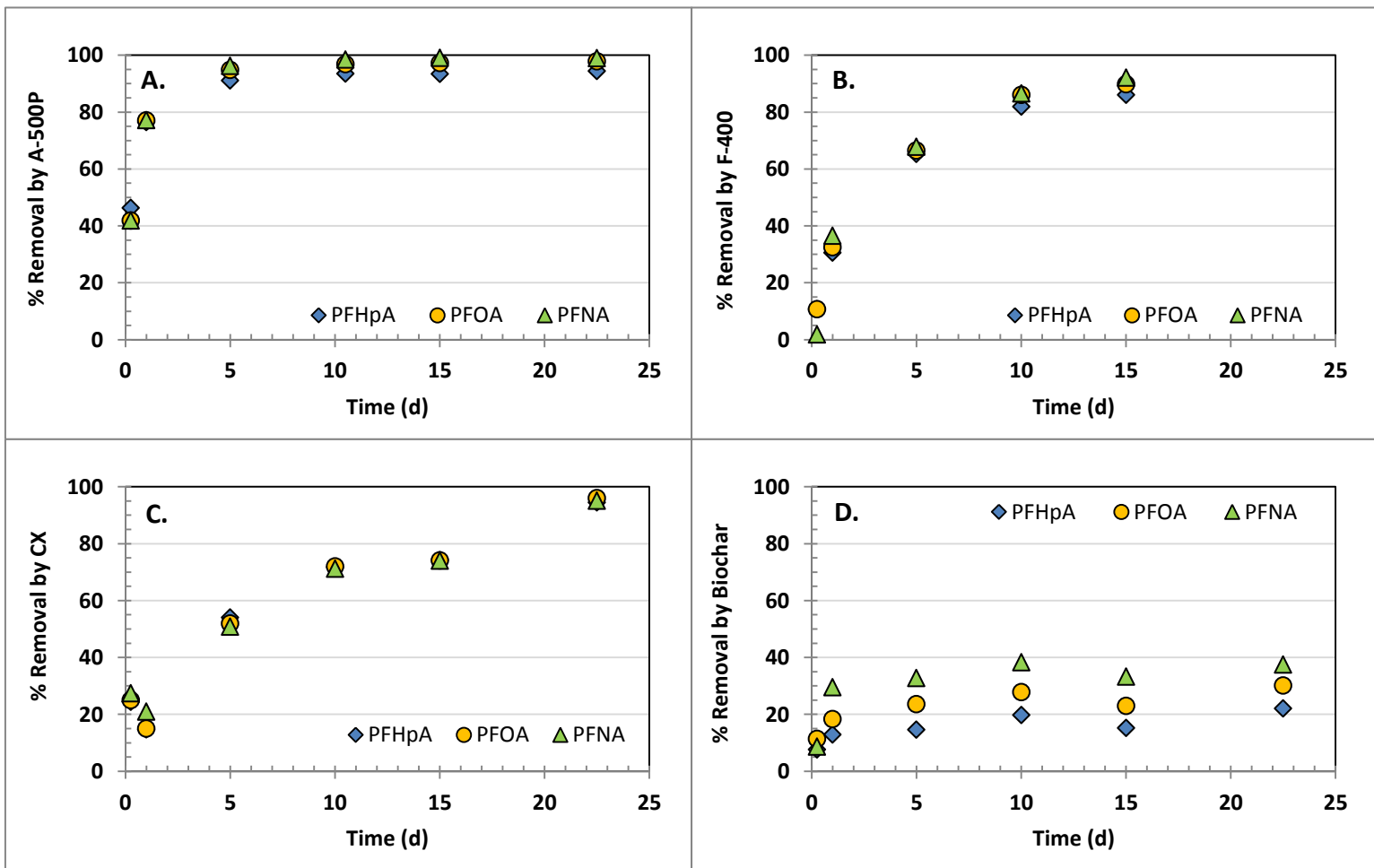


Figure 5.6: Effect of carbon chain length on adsorption of target PFCAs in GRW for selected adsorbents. Plots show results of time dependent PFCAs removal for mixed solute experiments for different adsorbents; no pH adjustments were done; PFCAs initial concentrations for mixed solute experiments: PFHpA- 4.05 $\mu\text{g/L}$, PFOA- 3.58 $\mu\text{g/L}$; and PFNA- 3.56 $\mu\text{g/L}$; adsorbent dose: 100 mg/L.

5.3.5 Effect of Solute Mixture on PFCA Removal

To understand the effect of solute mixtures on the adsorption of individual PFCAs, kinetics experiments were conducted by spiking the same batch of GRW with PFOA (termed as single solute) only as opposed to spiking all three target PFCAs simultaneously (termed as mixed solute). Solute mixture effect experiments for F-400 and CX carbon were conducted in the raw water used in mixed solute Set 1 experiments while those of A-500P and A-860 resins were conducted in the same raw water used for mixed solute Set 2 experiments. Figure 5.7A presents the PFOA removal kinetics in GRW when present in mixture with other PFCAs and when present as a single solute. As can be seen, A-860 was not able to remove PFOA in either mixed solute or single solute experiments. More importantly, it can be seen that in GRW the overall percentage removal of PFOA, whether present in mixtures or individually, did not substantially differ for any of the three adsorbents. This is similar to the UPW experiments in Chapter 4. When these data were fit to the pseudo-second order model, it was observed that the model could describe the CX, F-400, and A-500P data very well ($R^2 = 0.93-0.99$). However, perhaps not surprisingly as A-860 removed little or no PFOA the model fitting for A-860 was poor ($R^2 < 0.6$). Graphical representation of the model derived q_e and θ values are presented in Figure 5.7B. Unlike the percent removal data, it was observed the q_e values for the adsorbents were slightly higher when PFOA was the only PFCA present as opposed to when present in mixture with other PFCAs which indicates that in GRW direct competition among the PFCAs may have been taking place. For example, for CX carbon the q_e value when PFOA was present as the sole PFCA was 41 ng/mg, as opposed to 38 ng/mg, when present in mixture with the other PFCAs. Regardless of small decrease observed with q_e , overall these results indicate that similar to UPW, the effect of direct competition for adsorption sites among the target PFCAs is also minimal in GRW. The

initial PFOA adsorption rate also decreased for the CX and F-400 carbons, however, it slightly increased for the A-500P resin.

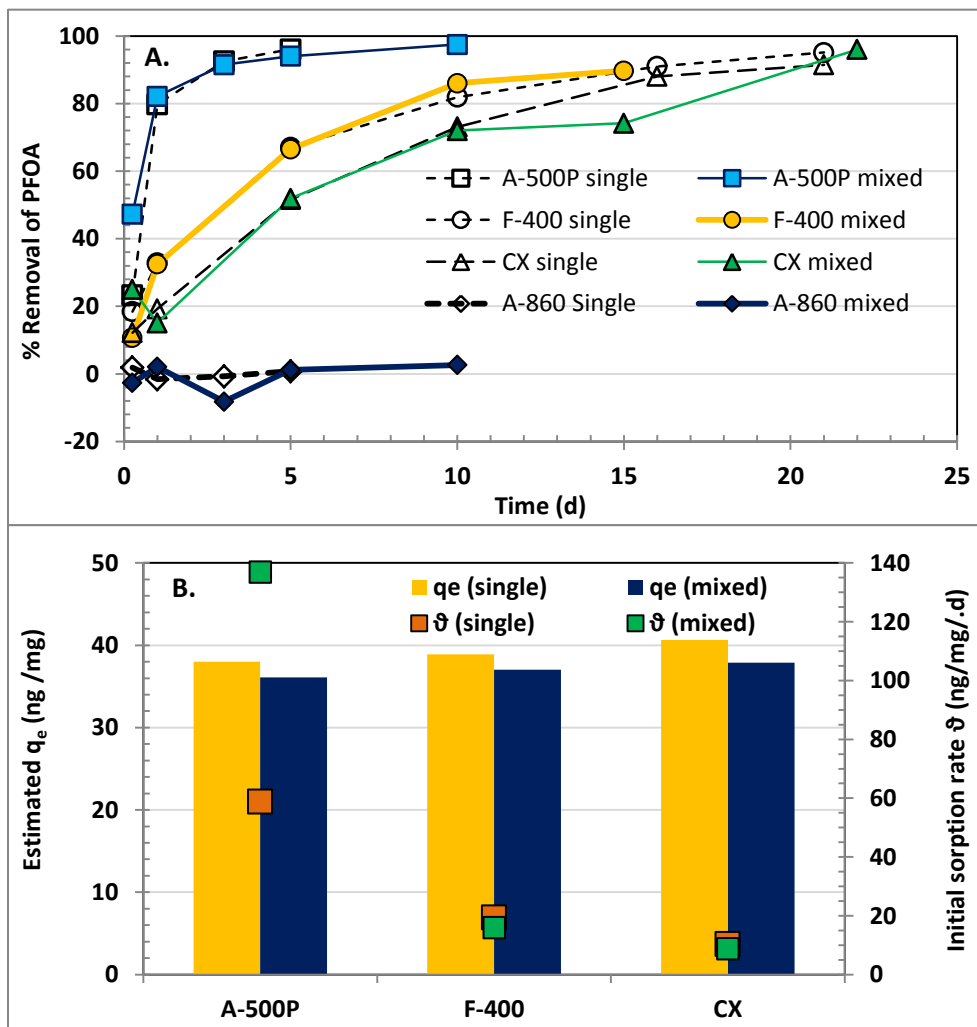


Figure 5.7: Comparison of mixed solute addition vs. individual solute addition on PFOA removal in untreated Grand River water (GRW); adsorbent dose: 100 mg/L; initial target nominal PFOA spiking concentration - 3 $\mu\text{g/L}$; Plot A: Open symbols are for single solute spiking (PFOA only) and solid symbols indicate all 3 PFCAs were spiked simultaneously; data for the A-500P and A-860 resins are average to two replicates. Plot B: pseudo-second order model parameters fitted to data presented in plot A. CX and F-400 single solute experiments were conducted along with Set 1 mixed solute experiments. A-500P and A-860 single solute experiments were conducted along Set 2 mixed solute experiments.

5.3.6 NOM Removal in GRW during Adsorption

NOM removal with the tested adsorbents was studied to determine their NOM removal potential and if the anion exchange resins or the Biochar can be used as a potential pretreatment for GAC adsorbents. The premise was that anion exchange or Biochar pretreatment could remove NOM and thereby reduce competition for adsorption sites and improve PFCA removal performance of downstream GAC adsorbents in surface water.

LC-OCD analysis of the PFCA spiked raw and treated GRW revealed that the anion exchange resins achieved substantially higher and faster adsorption of DOC present in GRW (Figure 5.8). Both resins achieved nearly 75% removal of DOC within 10 days of contact time and the removals did not improve substantially even after an additional 12 days of contact. Among the carbonaceous adsorbents, F-400 removed the most DOC (~ 40%) compared to CX (~25%) and Biochar (<20%). Removal/reduction trends of DOC and DOC fractions with anion exchange resins observed in Set 1 experiments were similar in Set 2 experiments (discussed in detailed in section 5.3.7). Humbert et al. (2008) also reported large differences in NOM removal between anion exchange resins and powdered activated carbon. A more quantitative assessment of the DOC removal kinetics data was achieved by fitting the pseudo-second-order kinetics model to the DOC and humics removal data ($R^2 = 0.91-0.99$). Initial adsorption kinetics values for humics removal with Biochar and A-860 could not be calculated since the fitting generated a negative intercept. Model parameters are presented in Figure 5.9 and it is evident that both anion exchange resins have similar yet substantially higher equilibrium adsorption amounts compared to the other adsorbents. Pore size can exert a negative impact on the adsorption of DOC molecules due to size exclusion (Karanfil 2006). It has been reported that pores larger than 1 nm play important role in the adsorption of DOC by activated carbon (Moore et al. 2001; Owen et al.

1995) while smaller pores may be too small. F-400 has a relatively broader pore size distribution compared to CX carbon (Chapter 4 Table 4.1) which facilitated access of DOC molecules to adsorption sites or may have reduced pore blockage effects in F-400 and hence, may explain higher and faster DOC removal by F-400 (Figure 5.9). Poor removal of DOC by Biochar can be attributed to its low micropore volume.

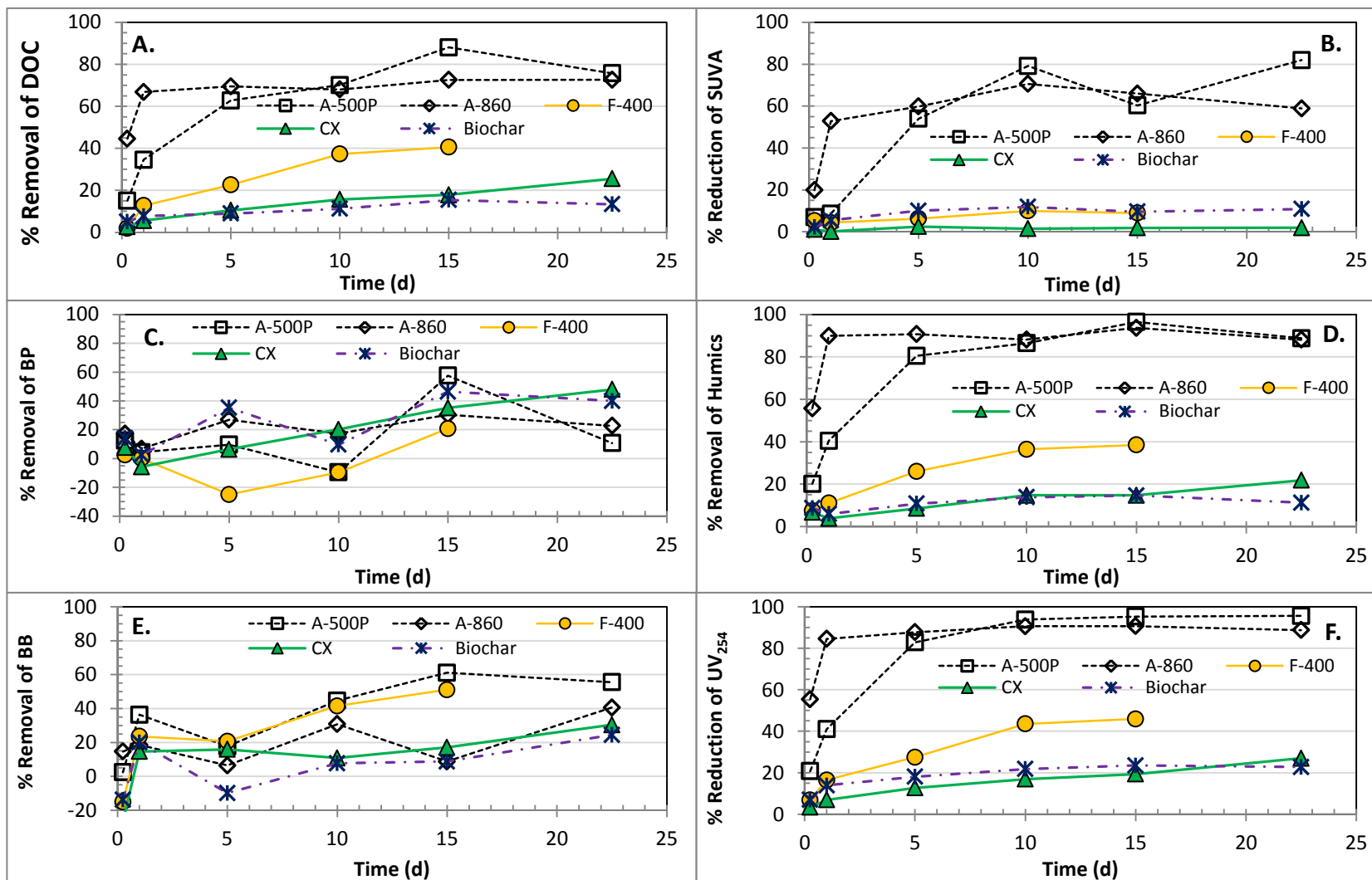


Figure 5.8: Removal of DOC and different DOC fractions in GRW water over time; A) DOC, B) SUVA, C) biopolymers (BP), D) humics, E) building blocks (BB), F) UV_{254} ; Data presented here is for Set 1 experiments; initial DOC- 5.0 mg C/L, humics- 3.6 mg C/L, BP- 0.25 mg C/L, BB- 0.65 mg C/L; adsorbent dose- 100 mg/L.

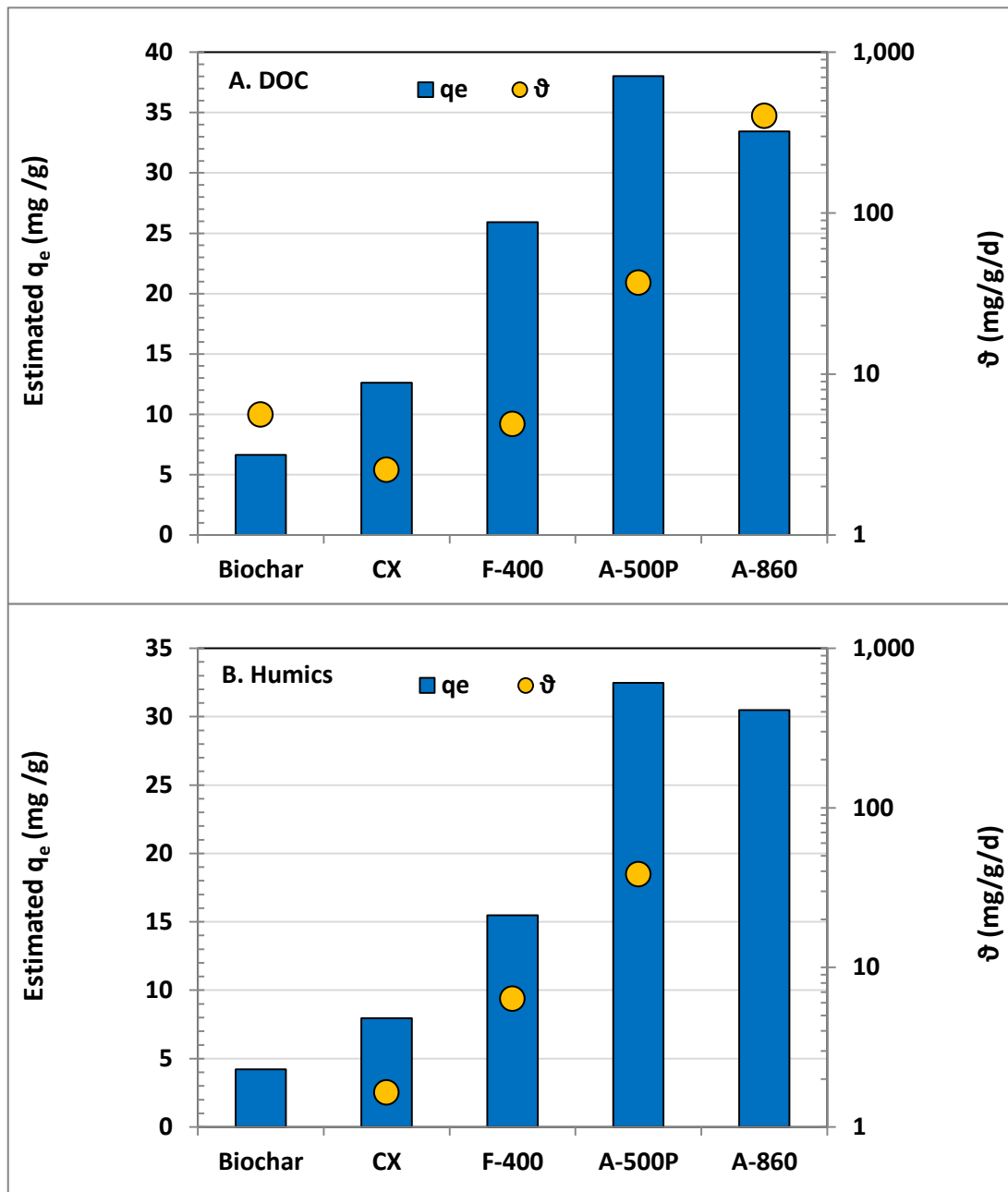


Figure 5.9: Graphical representation of pseudo-second-order model parameters for removal data presented in Figure 5.8. Plot A: Estimated parameters for DOC Plot B: Estimated parameters for humics.

The selected anion exchange resins are marketed as organic scavengers and are capable of achieving high DOC removals (Purolite 2006). As can be seen in Figures 5.8 and 5.9, polyacrylic A-860 being hydrophilic may adsorb DOC faster than polystyrenic A-500P, however, both resins are expected to have similar overall capacities for DOC. NOM removal during ion exchange is caused by the exchange of NOM acids and chloride ions rather than physical adsorption (Cornelissen et al. 2008; Tan et al. 2005). Indeed Bolto et al. (2002) observed that 98-100% of NOM was removed when DOC acid extract without the neutral component was treated with ion exchange resin which substantiates the importance of the ion exchange mechanism. Cornelissen et al. (2008) commented that during ion exchange treatment, physical adsorption may incidentally occur but is “neither an effective nor controllable mechanism compared to the primary mechanism.” It has been reported that sulfate content may be a more important determinant of DOC removal in water compared to other inorganic anions such as bicarbonate, nitrate, and bromide (Ates and Incetan 2013).

The adsorbability of various DOC fractions of GRW with the selected adsorbents can be found in Figure 5.8. The anion exchange resins and F-400 preferentially removed humics compared to other measured LC-OCD fractions. Both anion exchange resins achieved nearly 90% removal of humics as opposed to about 40% by F-400. High removals of humics with anion exchange resins have been observed by others as well (Cornelissen et al. 2008; Grefte et al. 2013a; Grefte et al. 2013b). CX and Biochar did not achieve substantial removal of humics (<20%). Of the two resins, polyacrylic A-860 resin, owing to its hydrophilic structure, more rapidly removed humics compared to the polystyrenic A-500P resin which has a relatively hydrophobic structure. Indeed, humics removal rates appeared to be faster than even overall DOC removal rates. Humics removal rates with carbonaceous adsorbents appear to be similar to overall DOC removal

kinetics. Cornelisson et al. (2008) noted “removal of humic substances and building blocks was caused by ionic interactions between NOM acids/acidic components and the anionic resins.” Of the two resins, A-500P appeared to remove higher concentrations of building blocks (BB) compared to A-860 while F-400 performed better compared to CX and Biochar. Removal of BB with F-400 and A-500P were similar with A-500P showing slightly higher removal. Biopolymer concentrations in the raw and treated water indicated that minimal biopolymer removal was possible with these resins. The scatter in biopolymer percentage reduction observed in Figure 5.8 is likely due to these generally low concentrations of biopolymers. Other studies have also reported the ineffectiveness of anion exchange and GAC treatment in removing biopolymers from water (Cornelissen et al. 2008; Velten et al. 2011).

It can also be seen from Figure 5.8F that the reduction in UV_{254} absorbance in GRW is more substantial and also faster when treated with the anion exchange resins vs. the carbonaceous adsorbents. The rapid reduction of UV_{254} absorbance with anion exchange resins is in line with previous studies (Bolto et al. 2002; Humbert et al. 2008). Specific UV absorbance at 254 nm (SUVA), which is used as a surrogate parameter for the aromatic content of NOM, was also substantially (~60%) decreased following anion exchange resin treatment (Figure 5.8B). Such decreases in SUVA in GRW indicate that DOC composition of GRW is considerably altered following treatment with the two selected anion exchange resins. Humics, the dominant DOC fraction in GRW, were substantially removed by the anion exchange resins compared to the adsorbents (Figures 5.8 and 5.9). This is also reflected in the SUVA reductions and may correspond to the preferential removal of aromatic and hydrophobic high molecular weight humic substances (Grefte et al. 2013b; Humbert et al. 2008). On the other hand, small reductions (<10%) of SUVA values following the GACs and Biochar treatment of GRW indicate that the

carbonaceous adsorbents did not alter the DOC composition in GRW to a large extent. This is consistent with lower humics removal by the carbonaceous adsorbents.

A-500P has a high equilibrium PFCA removal capacity (Figure 5.3) while the DOC removal kinetics with A-860 is substantially faster compared to A-500P (Figure 5.9). Such trends indicate that A-860 could potentially be used as a pre-treatment step for A-500P or can be used as a mixture with A-500P in surface water and thereby reduce direct competition from inorganic anions and NOM for anion exchange sites on A-500P leading to improved adsorption efficiency for the PFCAs. Previously combinations of anion exchange resins and PAC have been shown to improve the removal atrazine in surface water (Humbert et al. 2008) while Hu et al. (2014) observed that anion exchange pre-treatment during bottle point experiments did not affect site competition between NOM and pesticides atrazine. Future studies could thus investigate if combining the anion exchange resins with GAC treatment or even combining the two types of resins can enhance overall PFCA removal in surface water.

5.3.7 Data Reproducibility

The GC/MS analytical method developed for analyzing PFCAs is time and labour intensive which limited the use of replicates possible during this study. Therefore to address the issue of data reproducibility and also to confirm the removal trends observed in GRW in Set 1 experiments, a second set (Set 2) of kinetic experiments were conducted with the two ion exchange resins with two duplicates in Set 2 experiments of GRW for PFCA analysis. Also, since with ion exchange resins equilibrium was achieved relatively quickly, the Set 2 kinetic experiments were conducted up to 10 days as opposed to 22.5 days in Set 1. Table 5.1 provided water quality data of the two batchers of GRW. Both have similar DOC, pH, and SUVA. While turbidity was higher in Set 2 than Set 1, conductivity and concentrations of selected inorganic

anions were slightly lower. Results of the two sets of experiments examining the removal rates of the target PFCAs in GRW by ion exchange are presented in Table 5.3 and Figure 5.10. It can be seen that the percentage removals of the target PFCAs in both Set 1 and Set 2 experiments confirm the reproducibility of the PFCA removal trends by ion exchange. Also, variation between sample replicates is minimal which is represented by the small error bars shown in Set 2 data points in Figure 5.10. The kinetics data presented in Table 5.3 are fitted to the pseudo-second order model for further quantitative analysis. Due to poor removal with A-860 the model poorly described the experimental data. However, the model described A-500P data very well ($R^2 > 0.99$). Graphical representation of the model parameters in Figure 5.11 show that both q_e and θ values for A-500P were similar for all the target PFCAs indicating good reproducibility.

Only one set of samples from Set 2 experiments were analyzed by LC-OCD to confirm if the removal trends for DOC and different fractions of DOC are similar. Removal/reduction data for DOC and its fractions with ion exchange resins for Set 1 and Set 2 experiments are presented in Figure 5.12 and the observed removal trends for DOC, humics and building blocks, and reduction of SUVA and UV_{254} organics are similar. The trends observed with biopolymers although not similar but did indicate that biopolymers are not well removed during ion exchange treatment of GRW.

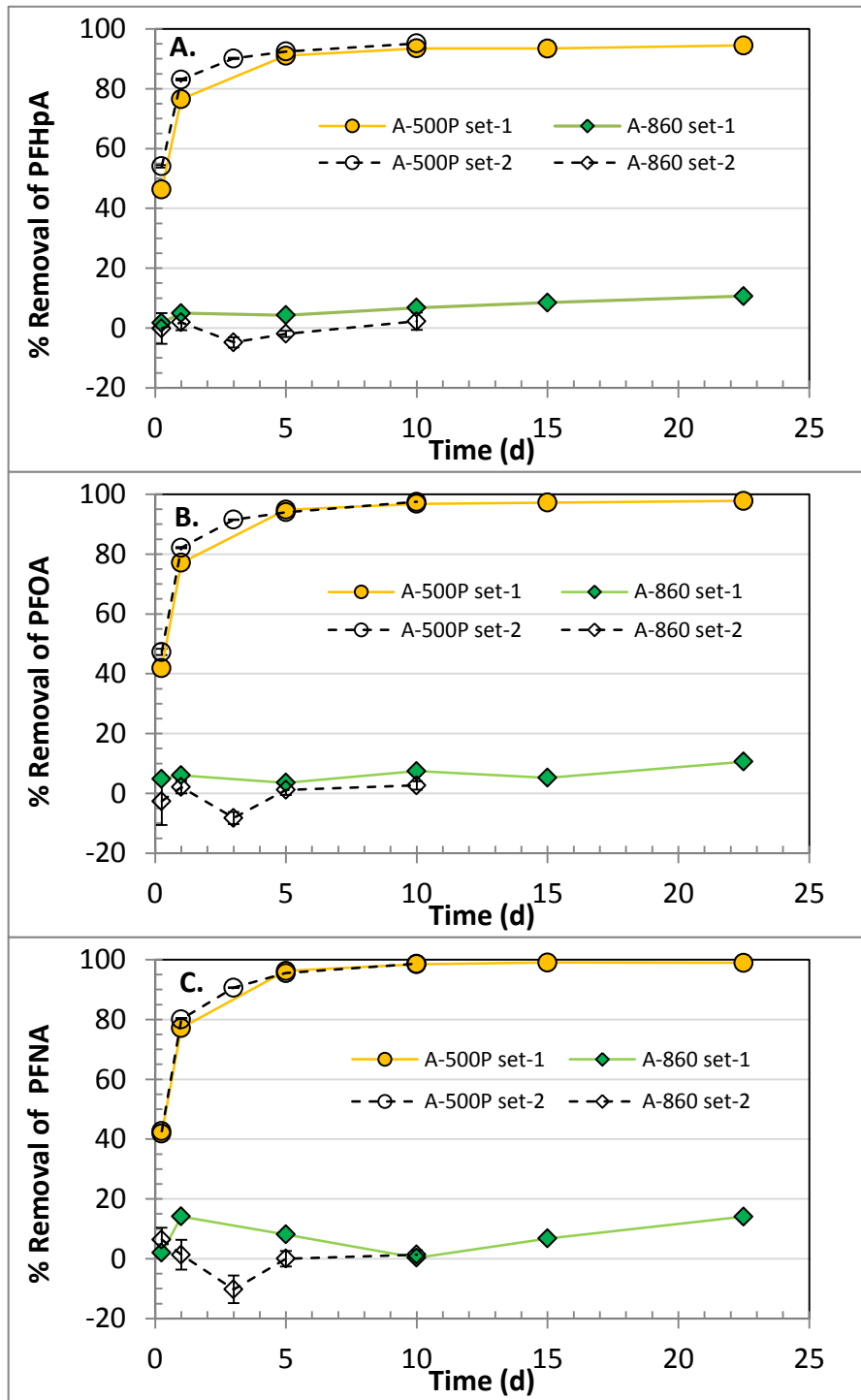


Figure 5.10: Removal of PFCAs by anion exchange resin in GRW illustrating the reproducibility of removal trends. Set 1 experiments were conducted on GRW collected in February 2012 and Set 2 experiments were conducted in GRW collected in May 2012. Error bars in Set-2 experiments indicate the maximum and minimum removals of two replicates.

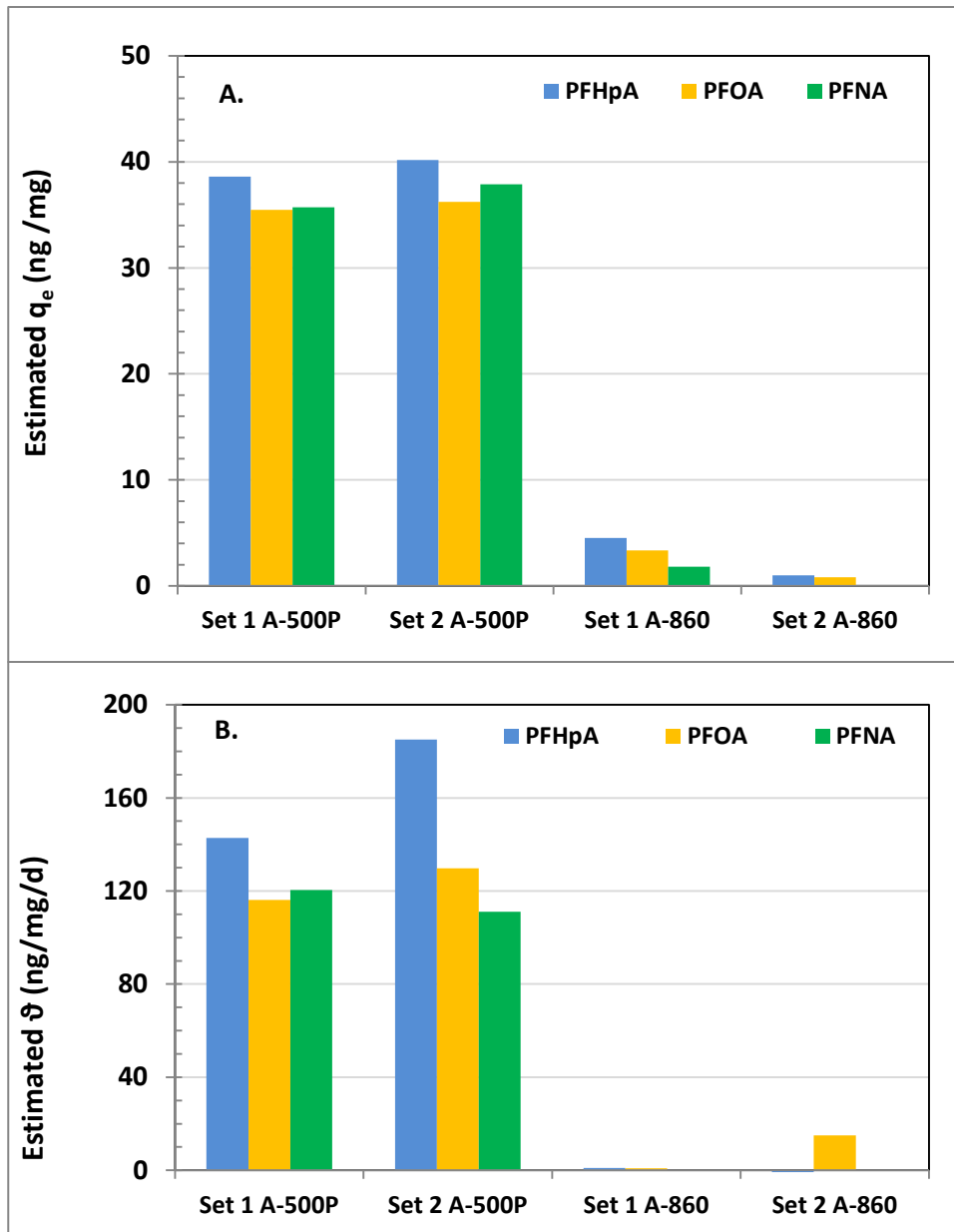


Figure 5.11: Graphical representation of pseudo-second-order model parameters for kinetics data presented in Figure 5.10. Plot A: Estimated equilibrium sorption amount (q_e); Plot B: Initial sorption rate (ϑ).

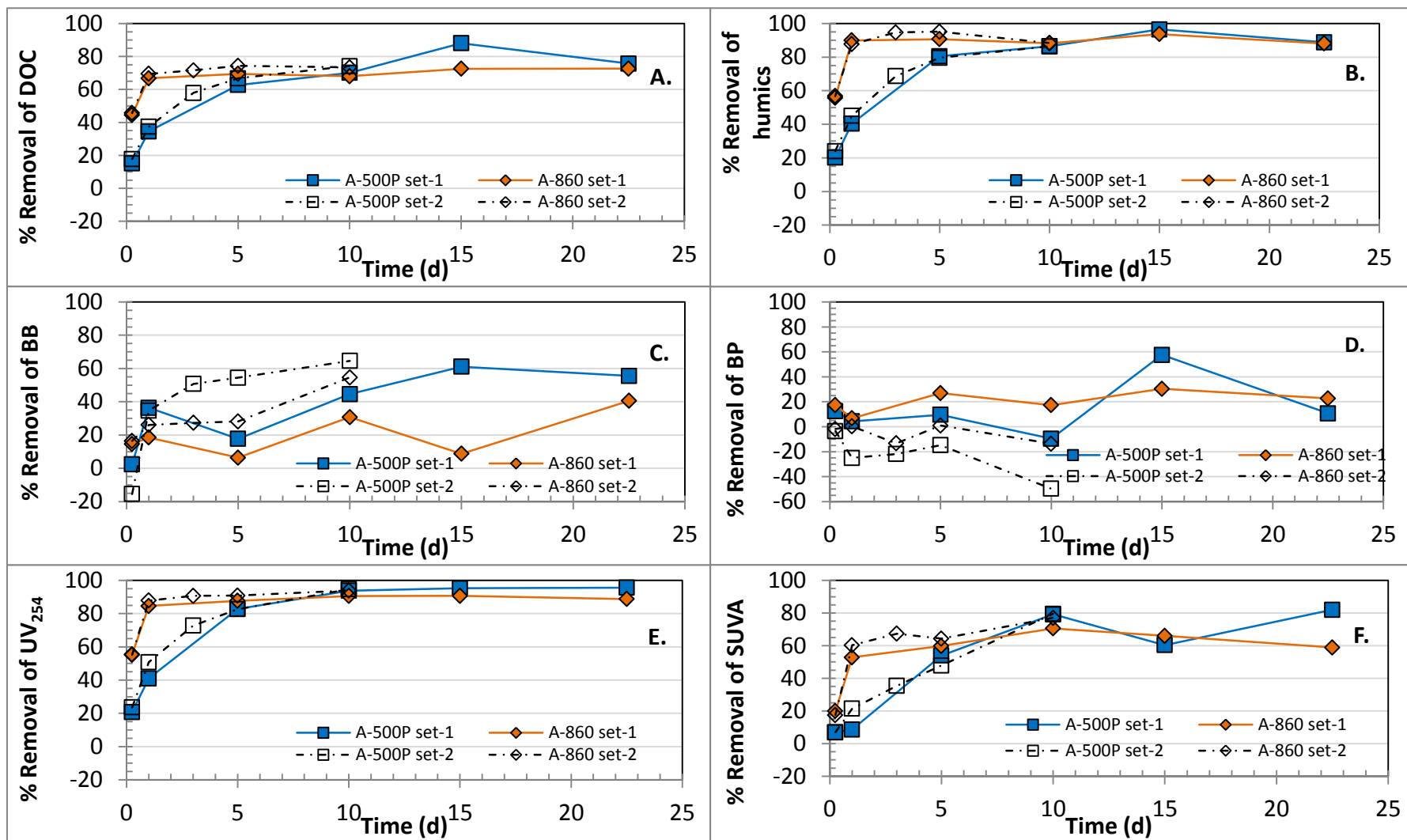


Figure 5.12: Removal of DOC and various DOC fractions by anion exchange resins in GRW illustrating the reproducibility of NOM removal trends. Set 1 experiments were conducted on GRW collected in February 2012 and Set 2 experiments were conducted in GRW collected in May 2012. DOC: 5.0 mg/L for Set 1 and DOC: 4.7 mg/L for Set 2.

5.4 Conclusions

The removal potentials of three selected PFCA in Grand River water (GRW) were assessed using adsorption and ion exchange processes. Under the conditions tested, the following conclusions can be drawn:

- The adsorption capacities of the target PFCA onto the selected adsorbents expressed as the equilibrium sorption amount calculated using a pseudo-second-order kinetics model indicate that the adsorption capacities of the three sorbents A-500P, F-400, and CX carbons were similar in GRW. Adsorption capacity was low for the Biochar and the A-860 ion exchange nearly completely lost its PFCA adsorption capacity in GRW (not seen in ultrapure water).
- PFCA adsorption kinetics for the resin A-500P were considerably faster compared to the GACs and the Biochar. Among the GACs, coal-based F-400 exhibited faster kinetics compared to coconut shell-based CX carbon. The more microporous structure of CX may have contributed to the slower kinetics observed with CX.
- As expected, direct competition from other water constituents adversely affected PFCA removal. Somewhat unexpectedly though, the polyacrylic anion exchange resin, A-860, was unable to achieve substantial removals of the target PFCA in GRW. The pseudo-second-order derived equilibrium PFCA sorption amount for the tested GACs and A-500P resin were 88% to 99% lower in surface water compared to ultrapure water.
- In GRW inorganic anions (sulfate in particular) were the dominant competitors for the anion exchange resin A-860 while for the GACs and Biochar, NOM (especially humics) appears to be the dominant competitor for adsorption sites. Sulfate more severely affected

PFCAs removal capacities of A-860 than for A-500P. Thus, if sulfate is present, particularly at elevated concentrations, utilities considering treatment of perfluorinated compounds should not be using A-860 type ion exchange resins.

- Removal of PFOA was similar when present in solution as a single solute or in mixtures with the other target PFCAs. Similar trends are also expected for the other target PFCAs. PFCAs chain length did not affect removal by individual adsorbents except in the case of Biochar.

NOM removal from GRW was studied to assess the NOM pretreatment potential of various adsorbents.

- The overall removals of DOC and humics, and reductions of SUVA were substantially higher with the anion exchange resins compared to the GACs and the Biochar. Removal of biopolymers and building blocks were low with the tested adsorbents.
- Both resins, achieved similar and high overall reductions in DOC (~ 75%), UV_{254} (~90%), SUVA (60-80%), and humics substances (~90%). Removal/reduction rates of DOC, SUVA, UV_{254} , and humic substances were faster for hydrophilic A-860 compared to A-500P. High SUVA reductions indicate that the GRW NOM composition was altered following resin interactions.
- Analysis of NOM and its fractions revealed that DOC, humic substances, and building blocks were better adsorbed on coal-based F-400 compared to coconut - based CX and Biochar. However, small decreases (< 10%) in SUVA values indicate that the tested carbonaceous adsorbent did not substantially affect the NOM

composition in GRW. Wider pore size distribution of F-400 resulted in higher and faster DOC removal compared to CX and Biochar. Lower micropore volume and lack of BET surface area of the Biochar and relatively lower mesopore content of CX carbon may have been linked to their lower DOC removal performance.

- The tested Biochar will not be efficient as a pretreatment while the tested anion exchange resins may be effective as NOM pretreatment for GACs or for other ion exchange media.

Chapter 6

Conclusions and Recommendations

6.1 Conclusions

The overarching goal of the research presented in this thesis was to investigate the behaviour and fate of perfluorinated compounds (PFCs) during adsorption and ion exchange treatment of drinking water. Initially several classes of PFCs were chosen to select target compounds for the study which were identified as being relevant for drinking water utilities. Following some preliminary work at the NSERC Chair in Water Treatment at the University of Waterloo, perfluorinated carboxylic acids (PFCAs) were selected as the target PFC class for this study. The next goal was to develop a GC/MS method suitable for the simultaneous analysis of trace PFC levels in water. Once the GC/MS method was successfully established, three PFCAs—perfluoroheptanoic acid (PFHpA), perfluorooctanoic acid (PFOA) and perfluorononanoic acid (PFNA) were ultimately selected as target compounds for subsequent drinking water treatment studies. These three compounds were chosen primarily due to the fact that they were identified in the final list of the USEPA's 3rd unregulated contaminants monitoring rule (UCMR3). Removals of the selected PFCs were then evaluated to determine their adsorptive behaviour onto the selected adsorbents in ultrapure water and narrowing down the number of adsorbents for further evaluation in surface water using Grand River water (GRW). For ultrapure water experiments, four commercially available GACs, two anion exchange resins, and two alternative adsorbents were chosen. Based on the results obtained in the ultrapure water study, two GACs, two anion exchange resins, and one alternative adsorbent (Biochar) were selected to determine the impact of GRW characteristics on the adsorption of the target PFCAs. A secondary goal was to assess the potential of the selected anion exchange resins and the Biochar to be used as NOM

pretreatments to minimize competition for PFCA adsorption sites in downstream GAC adsorbers.

The major conclusions drawn from the study are listed below:

6.1.1 Development of a GC/MS Analytical Method and Target Compound Selection

- A GC/MS method for PFCAs containing four to nine carbons (C5-C9) was successfully developed. The established method, with some modifications can also be used to analyze PFBA (C4).
- Using the developed GC/MS method all of the selected PFCAs could be analyzed in ultrapure water at trace concentrations (ng/L- μ g/L). Surface water samples spiked with C5-C9 PFCAs were also successfully analyzed using the developed GC/MS method.
- Using HLB cartridges the method detection limits for PFCAs with six or more carbons ranged from 16 ng/L-30 ng/L in ultrapure water and from 16 ng/L-49 ng/L in Grand River water (GRW). This analytical method is therefore suitable for conducting treatment experiments at trace concentrations including the three selected perfluorinated compounds - PFHpA (C7), PFOA (C8), and PFNA (C9).
- Five individual PFOA isomers were detected in a PFOA technical mixture containing linear and branched PFOA isomers. Only qualitative work with isomers was conducted due to lack of appropriate standards. Once these standards become available, the developed GC/MS-based method can be used for quantitative analysis of PFOA isomers in aqueous samples.

6.1.2 PFCA Adsorption Performance of the Selected Adsorbents

The adsorptive behaviour of the target PFCAs onto different adsorbents at trace concentrations was studied in both ultrapure water and in surface water using GRW. The target initial nominal concentration of the spiked PFCAs was 3 µg/L each.

For ultrapure water experiments, four commercially available GACs including Calgon F-400®, AquaCarb CX 1230® (CX), Norit C-Gran®, Nuchar WV B-30®, and two commercially available ion exchange resins, Purolite A-500P®, and Purolite A-860® were selected. In addition, cattle bone-based Fija Fluor® (bone char) and dairy manure-based (Biochar) were also studied as alternative adsorbents. It was found that:

- Among tested adsorbents the anion exchange resin Purolite A-500P performed the best while the Fija Fluor bone char did not remove the target PFCAs. Single solute adsorption isotherms experiments with the target PFCAs showed that the Freundlich isotherm capacity factor (K_F) values were higher for the A-500 (90-168 [(ng/mg)(L/ng)^{1/n}]) compared to those for F-400 carbon (27-59 [(ng/mg)(L/ng)^{1/n}]) and the A-860 resin (0.0004-3.3 [(ng/mg)(L/ng)^{1/n}]).
- Adsorption kinetics were faster with the two ion exchange resins compared to the GACs and the alternative adsorbents. PFCA adsorption kinetics for the two resins were similar up to 24 h with the A-860 tailing off a bit at that point. Equilibrium was reached for both resins in about 10 days with nearly 90% of the overall removal being achieved within the initial 5 days. The GACs reached equilibrium capacity after 15 days of contact time.
- Among the carbon-based adsorbents, the GACs were more effective than the alternative adsorbent Biochar for removal of the target PFCAs (with the exception of the wood-

based WV-B30 GAC). Among the GACs, performances of the wood-based C-Gran and WV B-30 could not match the performance of F-400 and CX for PFCA removal.

Comparison of F-400 isotherms for PFCAs with those for other micropollutants indicated adsorbability of PFCAs onto F-400 carbon is lower compared to the pesticide atrazine at all equilibrium liquid phase concentrations (10-1000 ng/L) and similar to the taste and odor compounds-geosmin and MIB at concentrations lower than 50 ng/L.

Due to their relatively poor PFCA removal performance in ultrapure water, C-Gran, WV B-30, and Fija Fluor were not further studied in surface water. Accordingly five adsorbents, F-400, CX, A-500P, A-860, and Biochar were chosen for further adsorption performance evaluation in a surface water matrix using GRW.

- The pseudo-second-order kinetics model derived equilibrium adsorption amounts (q_e) for PFCA adsorption in GRW were similar for CX, F-400, and A-500P (35 to 42 ng/mg carbon). A-500P achieved the highest percent removal among the tested adsorbents. Biochar exhibited limited adsorption potential for the target PFCAs and A-860 resin completely lost its PFCA adsorption capacity in GRW.
- Similar to ultrapure water findings, A-500P resin exhibited faster adsorption of the target PFCAs compared to the studied GACs and the Biochar in GRW. For example, the initial adsorption rate (ϑ) calculated from the application of a pseudo-second-order model showed that the rate for A-500P was 6 to 23 times higher compared to the GACs and the Biochar. Adsorption kinetics for F-400 ($\vartheta = 17$ to 18 ng/mg/d) were faster compared to CX carbon ($\vartheta = 9$ to 11 ng/mg/d).

6.1.3 Effect of Adsorbent Properties on PFCA Adsorption

- The wood-based GACs (C-Gran and WV-B30) were less effective compared to the coal-based F-400 and the coconut-based CX in ultrapure water. Although the equilibrium sorption amount appeared to be similar, F-400 exhibited faster adsorptive removal compared to the coconut shell-based CX in both ultrapure water and GRW water. F-400 at a 100 mg/L adsorbent dose achieved a maximum of 92% removal of PFNA after 15 days while CX removed 74% removal of PFNA over the same exposure period in GRW.
- BET surface area did not necessarily indicate superior performance of the GACs. But pore size distribution and surface charge seemed to be related to PFCA adsorption performance. Negative surface charge of wood-based GACs may have been responsible for their relatively poor performance, maybe due to repulsion of the negatively charged PFCAs. The highly microporous structure of the coconut shell-based CX compared to coal-based F-400's may have been responsible for its relatively slower PFCA removal kinetics in both ultrapure water and GRW. Very low total pore volume and BET surface area of the ion exchange resins indicated that the potential for adsorption via hydrophobic adsorption onto the resin surface was either negligible or absent and that PFCAs were primarily removed by charge interactions and not hydrophobic interactions.
- In both ultrapure water and GRW polystyrenic A-500P resin achieved higher adsorption of the target PFCAs compared to the polyacrylic A-860.

6.1.4 Effect of PFCA Carbon Chain Length

- In both ultrapure water and GRW, PFCA carbon chain length did not affect removals for the A-500P resin, and F-400 and CX carbons. A-860 exhibited chain length dependent

removal of the target PFCAs in ultrapure water but this trend could not be confirmed in GRW due to low removals of the PFCAs in surface water.

6.1.5 PFCA Mixtures vs. Adsorption of Individual PFCAs

- Removals of the individual target PFCAs in ultrapure water were similar when present in solution as a single solute or in mixtures with other target PFCAs. A similar trend was also observed in GRW for PFOA indicating that the effect of solute mixture on individual PFCA adsorption is likely to be minimal in surface water. These results indicate the potential for direct competition among the target PFCAs during adsorption with the tested adsorbents is low.

6.1.6 Effect of Surface Water Matrix on PFCA Adsorption

- Surface water constituents in GRW adversely affected PFCA removal by directly competing for adsorption or ion exchange sites. Estimated q_e values were 88 to 99% lower in GRW for the GACs and the resins compared to ultrapure water.
- For carbon-based adsorbents, NOM components were the dominant competitors for the PFCAs. Humic substances were the dominant NOM fraction present in GRW and were preferentially removed by the selected adsorbents competing for adsorption sites with PFCAs in GRW. Neither building blocks nor biopolymers appeared to exert any significant competition in bottle point experiments.
- Inorganic anions, especially sulfate, present in GRW substantially affected the PFCA removal capacity of the ion exchange resins. While both NOM and anions posed competition for adsorption sites, anions, especially sulfate, were more dominant than NOM in the case of ion exchange treatment.

- The presence of sulfate affected the PFCA removal capacity of A-860 resin more substantially than that of A-500P in both ultrapure water and in GRW. Ultrapure water experiments demonstrated that a sulfate concentration of 30 mg/L led to complete loss of PFOA removal capacity for the A-860 resin as opposed to about a 15% capacity reduction for the A-500P resin. Substantial reduction (to about 40%) in PFOA removal capacity of A-860 was observed even at the low sulfate concentration of 1 mg/L.

6.1.7 NOM pretreatment potential of the selected adsorbents

- In GRW the anion exchange resins exhibited higher capacity and faster removal/reduction of DOC, humics, SUVA, and UV₂₅₄ compared to the carbonaceous adsorbents. Both resins, achieved similar and high overall removal/reduction of DOC (~75%), UV₂₅₄ (~90%), SUVA (60-80%), and humic substances (~90%). High SUVA reductions indicate that the NOM composition in GRW was altered following resin treatment.
- Of the two resins, polyacrylic A-860 resin (vs. polystyrenic A-500P) showed faster kinetics in removing DOC and the various DOC fractions. The relatively hydrophilic structure of the A-860 resin may have facilitated the transport of the NOM molecules to the adsorption sites resulting in faster kinetics compared to A-500P.
- Coal-based F-400 achieved higher removals of DOC, humic substances, and building blocks than the coconut shell-based CX and Biochar. However, small reductions (< 10%) in SUVA values indicated that following treatment with the selected carbonaceous adsorbents, NOM composition in GRW was not substantially altered.
- The tested adsorbents were not able to remove biopolymers present in GRW. The removal of building blocks was moderate to low (60% to <20%).

- Biochar cannot be used as an NOM pretreatment step. Fast and high removal/reduction of NOM, humics, and SUVA by anion exchange resins confirm their potential to be used as pretreatments for GAC adsorbers.

6.2 Recommendations

Over the course of this study, some potential research areas which will be of interest to the water treatment industry were identified. Future studies should consider the following suggestions:

- The developed GC/MS method only considered electron impact ionization (EI); however, by using chemical ionization (CI) or negative chemical ionization (NCI) sensitivity of the method can be improved substantially and therefore be made more comparable to LC-MS/MS methods analyzing PFCAs.
- The behaviour and fate of PFCA isomers during adsorption needs to be elucidated. However, appropriate standards for PFCA isomers are at present not readily available. When these isomer standards become available, GC/MS analysis can be used to conduct quantitative analysis of PFCA isomers in environmental samples and in treatment studies.
- Bottle point experiments were employed to study the adsorptive behaviour of the target PFCAs onto the selected adsorbents. Future studies should investigate and validate the trends observed at bench- and pilot-scale using column studies and attempt to determine scale-up factors for full-scale plants.
- For rigorous real world assessments, future studies should also investigate the effect of NOM preloading on GACs and regeneration of ion exchange resin on PFCA removal in surface water (as it pertains to economic viability in particular).

- To further understand direct competition effects of NOM fractions on PFCA adsorption, future studies should isolate various size fractions of NOM and investigate impacts of the isolated fractions on PFCA adsorption separately.
- The potential of ion exchange as a pretreatment to minimize GAC fouling thereby improving GAC bed life for removal of PFCAs and other pollutants needs to be studied. While it is unlikely ion exchange would be used as an NOM pretreatment for GAC at the present time, there is value in at least exploring this potential.
- Studies should consider mixtures of ion exchange resins for the simultaneous removal of PFCAs and NOM (in a single treatment unit).
- The effect of sulfate on PFCA adsorption on the two ion exchange resins was studied here. Future studies should consider investigating the impacts of other inorganic anions such as nitrate, phosphate, and potentially bicarbonate, on anion exchange resins.
- The PFCA removal trends observed in surface water in this study are most likely site-specific and will be different for other sources. Therefore, future studies will need to investigate the effect of different surface waters (and potentially groundwaters) on PFCA adsorption.
- Finally, the adsorption behaviour of shorter chain PFCs should be studied as these these will eventually displace the longer chains studied here.

References

- Ahrens, L., Harner, T., Shoeib, M., Lane, D. A., Murphy, J. G. 2012. Improved characterization of gas-particle partitioning for per- and polyfluoroalkyl substances in the atmosphere using annular diffusion denuder samplers. *Environ. Sci. Technol.* 46(13), 7199-7206.
- Ahrens, L., Shoeib, M., Harner, T., Lee, S. C., Guo, R., Reiner, E. J. 2011. Wastewater treatment plant and landfills as sources of polyfluoroalkyl compounds to the atmosphere. *Environ. Sci. Technol.* 45(19), 8098-8105.
- Ahrens, L. 2011. Polyfluoroalkyl compounds in the aquatic environment: A review of their occurrence and fate. *J. Environ. Monit.* 13(1), 20-31.
- Ahrens, L., Taniyasu, S., Yeung, L. W. Y., Yamashita, N., Lam, P. K. S., Ebinghaus, R. 2010. Distribution of polyfluoroalkyl compounds in water, suspended particulate matter and sediment from Tokyo Bay, Japan. *Chemosphere* 79(3), 266-272.
- Alzaga, R., Salgado-Petinal, C., Jover, E., Bayona, J. M. 2005. Development of a procedure for the determination of perfluorocarboxylic acids in sediments by pressurised fluid extraction, headspace solid-phase microextraction followed by gas chromatographic-mass spectrometric determination. *J. Chromatography A* 1083(1-2), 1-6.
- Alzaga, R. and Bayona, J. M. 2004. Determination of perfluorocarboxylic acids in aqueous matrices by ion-pair solid-phase microextraction-in-port derivatization-gas chromatography-negative ion chemical ionization mass spectrometry. *J. Chromatography A* 1042(1-2), 155-162.
- American Public Health Association (APHA), 2005. *Standard Methods for the Examination of Water and Wastewater American Public Health Association, American Water Works Association, and Water Pollution Control Federation.* 21st edition, Washington, D.C.
- Appleman, T. D., Higgins, C. P., Quinones, O., Vanderford, B. J., Kolstad, C., Zeigler-Holady, J. C., Dickenson, E. R. V. 2014. Treatment of poly- and perfluoroalkyl substances in US full-scale water treatment systems. *Water Res.* 51, 246-255.
- Appleman, T. D., Dickenson, E. R. V., Bellona, C., Higgins, C. P. 2013. Nanofiltration and granular activated carbon treatment of perfluoroalkyl acids. *J. Hazard. Mater.* 260, 740-746.
- Arevalo Perez, E. C. 2014. Removal of perfluorinated compounds by anion exchange: Factors affecting resin performance and regeneration. Master's thesis, Department of Civil, Construction and Environmental Engineering, North Carolina State University.
- Ates, N. and Incetan, F. B. 2013. Competition impact of sulfate on NOM removal by anion-exchange resins in high-sulfate and low-SUVA waters. *Ind. Eng. Chem. Res.* 52(39), 14261-14269.

Atkinson, C., Blake, S., Hall, T., Kanda, R., Rumsby, P. 2008. *Survey of the Prevalence of Perfluorooctane Sulphonate (PFOS), Perfluorooctanoic Acid (PFOA) and Related Compounds in Drinking Water and their Sources*. Report DEFRA 7585, Drinking Water Inspectorate, Department for Environment, Food & Rural Affairs, London, UK [online] Accessed 09/15 2013. http://dwi.defra.gov.uk/research/completed-research/reports/DWI70_2_212PFOS.pdf.

Awad, E., Zhang, X., Bhavsar, S. P., Petro, S., Crozier, P. W., Reiner, E. J., Fletcher, R., Tittiemier, S. A., Braekevelt, E. 2011. Long-term environmental fate of perfluorinated compounds after accidental release at Toronto Airport. *Environ. Sci. Technol.* 45(19), 8081-8089.

Azizian, S. 2004. Kinetic models of sorption: a theoretical analysis. *J. Colloid Interf. Sci.* 276, 47-52.

Barry, V., Winquist, A., Steenland, K. 2013. Perfluorooctanoic acid (PFOA) exposures and incident cancers among adults living near a chemical plant. *Environ. Health Perspect.* DOI:10.1289/ehp.1306615.

Bartell, S. M., Calafat, A. M., Lyu, C., Kato, K., Ryan, P. B., Steenland, K. 2010. Rate of decline in serum PFOA concentrations after granular activated carbon filtration at two public water systems in Ohio and West Virginia. *Environ. Health Perspect.* 118(2), 222-228.

Beltrán, F. J. 2004. *Ozone Reaction Kinetics for Water and Wastewater Systems*. Lewis Publishers, Boca Raton, Florida.

Benskin, J. P., De Silva, A. O., Martin, J. W. 2010. Isomer profiling of perfluorinated substances as a tool for source tracking: A review of early findings and future applications. *Rev. Environ. Contam. Toxicol.*, Vol 208: Perfluorinated Alkylated Substances 208, 111-160.

Betts, K. S. 2007. Perfluoroalkyl acids - What is the evidence telling us? *Environ. Health Perspect.* 115(5), A250-A256.

Bhatarai, B. and Gramatica, P. 2011. Prediction of aqueous solubility, vapor pressure and critical micelle concentration for aquatic partitioning of perfluorinated chemicals. *Environ. Sci. Technol.* 45(19), 8120-8128.

Boiteux, V., Dauchy, X., Rosin, C., Munoz, J. 2012. National screening study on 10 perfluorinated compounds in raw and treated tap water in France. *Arch. Environ. Contam. Toxicol.* 1-12.

Bolto, B., Dixon, D., Eldridge, R., King, S., Linge, K. 2002. Removal of natural organic matter by ion exchange. *Water Res.* 36(20), 5057-5065.

Boulanger, B., Vargo, J. D., Schnoor, J. L., Hornbuckle, K. C. 2005. Evaluation of perfluorooctane surfactants in a wastewater treatment system and in a commercial surface protection product. *Environ. Sci. Technol.* 39(15), 5524-5530.

Brooke, D., Fotitt, A., Nwaogu, T.A. 2004. *Environmental Risk Evaluation Report: Perfluorooctane Sulfonate (PFOS)*. Report produced by Environment Agency's science group, Environment Agency, UK. Accessed 09/27 2013. http://chm.pops.int/Portals/0/docs/from_old_website/documents/meetings/poprc/submissions/Comments_2006/sia/pfos.uk.risk.eval.report.2004.pdf.

Buck, R. C., Franklin, J., Berger, U., Conder, J. M., Cousins, I. T., de Voogt, P., Jensen, A. A., Kannan, K., Mabury, S. A., van Leeuwen, S. P. J. 2011. Perfluoroalkyl and polyfluoroalkyl substances in the environment: Terminology, classification, and origins. *Integr. Environ. Assess. Manage.* 7(4), 513-41.

Cao, X., Ma, L., Liang, Y., Gao, B., Harris, W. 2011. Simultaneous immobilization of lead and atrazine in contaminated soils using dairy-manure biochar. *Environ. Sci. Technol.* 45(11), 4884-4889.

Cao, X. and Harris, W. 2010. Properties of dairy-manure-derived biochar pertinent to its potential use in remediation. *Bioresour. Technol.* 101(14), 5222-5228.

Carter, K. E. and Farrell, J. 2010. Removal of perfluorooctane and perfluorobutane sulfonate from water via carbon adsorption and ion exchange. *Sep. Sci. Technol.* 45(6), 762-767.

Choi, K.-J., Son, H.-J., Kim, S.-H. 2007. Ionic treatment for removal of sulfonamide and tetracycline classes of antibiotic. *Sci. Total Environ.* 387(1-3), 247-256.

Chularueangaksorn, P., Tanaka, S., Fujii, S., Kunacheva, C. 2013. Adsorption of perfluorooctanoic acid (PFOA) onto anion exchange resin, non-ion exchange resin, and granular-activated carbon by batch and column. *Desalin. Water Treat.* DOI:10.1080/19443994.2013.815589.

Comerton, A. M., Andrews, R. C., Bagely, D. M. 2009. The influence of natural organic matter and cations on the rejection of endocrine disrupting and pharmaceutically active compounds by nanofiltration. *Water Res.* 43(3), 613-622.

Conder, J. M., Hoke, R. A., De Wolf, W., Russell, M. H., Buck, R. C. 2008. Are PFCAs bioaccumulative? A critical review and comparison with regulatory criteria and persistent lipophilic compounds. *Environ. Sci. Technol.* 42(4), 995-1003.

Crini, G., Peindy, H.N., Gimbert, F., Robert, C. 2007 Removal of C. I. Basic green 4 (Malachite Green) from aqueous solutions by adsorption using cyclodextrin-based adsorbent: kinetic and equilibrium studies. *Sep. Purif. Technol.* 53, 97-110.

Cornelissen, E. R., Moreau, N., Siegers, W. G., Abrahamse, A. J., Rietveld, L. C., Grefte, A., Dignum, M., Amy, G., Wessels, L. P. 2008. Selection of anionic exchange resins for removal of natural organic matter (NOM) fractions. *Water Res.* 42(1-2), 413-423.

- D'Eon, J. C., Crozier, P. W., Furdui, V. I., Reiner, E. J., Libelo, E. L., Mabury, S. A. 2009. Perfluorinated phosphonic acids in Canadian surface waters and wastewater treatment plant effluent: Discovery of a new class of perfluorinated acids. *Environ. Toxicol. Chem.* 28(10), 2101-2107.
- De Silva, A. O. and Mabury, S. A. 2004. Isolating isomers of perfluorocarboxylates in polar bears (*Ursus maritimus*) from two geographical locations. *Environ. Sci. Technol.* 38(24), 6538-6545.
- Deng, S., Yu, Q., Huang, J., Yu, G. 2010. Removal of perfluorooctane sulfonate from wastewater by anion exchange resins: Effects of resin properties and solution chemistry. *Water Res.* 44(18), 5188-5195.
- Dickenson, E., Appleman, T., Higgins, C. 2012. Treatment of perfluoroalkyl and polyfluoroalkyl substances by North American treatment practices. Poster presented at the *Water Quality and Technology Conference, AWWA*, Toronto, 02-06 November.
- Ding, H., Peng, H., Yang, M., Hu, J. 2012. Simultaneous determination of mono- and disubstituted polyfluoroalkyl phosphates in drinking water by liquid chromatography - electrospray tandem mass spectrometry. *J. Chromatography A* 1227, 245-252.
- Dinglasan, M., Ye, Y., Edwards, E., Mabury, S. 2004. Fluorotelomer alcohol biodegradation yields poly- and perfluorinated acids. *Environ. Sci. Technol.* 38(10), 2857-2864.
- Du, Z., Deng, S., Bei, Y., Huang, Q., Wang, B., Huang, J., Yu, G. 2014. Adsorption behavior and mechanism of perfluorinated compounds on various adsorbents—A review. *J. Hazardous Materials*, 274, 443-454.
- Dudley, L.-A. M. B. 2012. Removal of perfluorinated compounds by powdered activated carbon, superfine powdered activated carbon, and anion exchange resins. Thesis submitted to the Graduate Faculty of the North Carolina State University, (US).
- Dufková, V., Cabala, R., Ševčík, V. 2012. Determination of C 5-C 12 perfluoroalkyl carboxylic acids in river water samples in the Czech Republic by GC-MS after SPE preconcentration. *Chemosphere* 87(5), 463-469.
- Dufková, V., Cabala, R., Maradová, D., Štícha, M. 2009. A fast derivatization procedure for gas chromatographic analysis of perfluorinated organic acids. *J. Chromatography A* 1216(49), 8659-8664.
- DWI 2009. *Guidance on the Water Supply (Water Quality) Regulations 2000 Specific to PFOS (Perfluorooctane Sulphonate) and PFOA (Perfluorooctanoic Acid) Concentrations in Drinking Water.* Accessed 09/24 2013. http://www.dwi.gov.uk/stakeholders/information-letters/2009/10_2009annex.pdf.

Ellis, D., Martin, J., Mabury, S., Hurley, M., Andersen, M., Wallington, T. 2003. Atmospheric lifetime of fluorotelomer alcohols. *Environ. Sci. Technol.* 37(17), 3816-3820.

Emmett, E. A., Shofer, F. S., Zhang, H., Freeman, D., Desai, C., Shaw, L. M. 2006. Community exposure to perfluorooctanoate: Relationships between serum concentrations and exposure sources. *Int. J. Occup. Environ. Med.* 48(8), 759-770.

Engineering Statistics, NIST SEMATECH. *Process Improvement*, Chapter 5. Available: <http://www.itl.nist.gov/div898/handbook/pri/section3/pri3361.htm>; Accessed 10/03 2014.

Eschauzier, C., Hoppe, M., Schlummer, M., De Voogt, P. 2013. Presence and sources of anthropogenic perfluoroalkyl acids in high-consumption tap-water based beverages. *Chemosphere* 90, 36-41.

Eschauzier, C., Beerendonk, E., Scholte-Veenendaal, P., De Voogt, P. 2012. Impact of treatment processes on the removal of perfluoroalkyl acids from the drinking water production chain. *Environ. Sci. Technol.* 46(3), 1708-15.

Eschauzier, C., de Voogt, P., Brauch, H. J., Lange, F. T. 2011. *Fluorinated Surfactants in European Surface Waters, Ground- and Drinking Waters*. In: Knepper, T.P., Lange, F.T. (Eds.), In: *The Handbook of Environmental Chemistry: Fluorinated Surfactants and Transformation Products*; Springer-Verlag, Berlin Heidelberg, 73-102.

Eschauzier, C., Haftka, J., Stuyfzand, P. J., de Voogt, P. 2010. Perfluorinated compounds in infiltrated river Rhine water and infiltrated rainwater in coastal dunes. *Environ. Sci. Technol.* 44(19), 7450-7455.

EU Directive 2006. *2006/122/ECOF the European Parliament and of the Council of 12 December 2006*. Official J. the European Union Accessed 09/27 2013. <http://eur-lex.europa.eu/LexUriServ/LexUriServ.do?uri=OJ:L:2006:372:0032:0034:en:PDF>.

Fei, C., McLaughlin, J. K., Lipworth, L., Olsen, J. 2009. Maternal levels of perfluorinated chemicals and subfecundity. *Hum. Reprod.* 24(5), 1200-1205.

Fei, C., McLaughlin, J. K., Tarone, R. E., Olsen, J. 2007. Perfluorinated chemicals and fetal growth: A study within the Danish National Birth Cohort. *Environ. Health Perspect.* 115(11), 1677-1682.

Flores, C., Ventura, F., Martin-Alonso, J., Caixach, J. 2013. Occurrence of perfluorooctane sulfonate (PFOS) and perfluorooctanoate (PFOA) in N.E. Spanish surface water and their removal in a drinking water treatment plant that combines conventional and advanced treatment in parallel lines. *Sci. Total Environ.* 461-462, 618-626.

Fujii, Y., Harada, K. H., Koizumi, A. 2012. Analysis of perfluoroalkyl carboxylic acids in composite dietary samples by gas chromatography/mass spectrometry with electron capture negative ionization. *Environ. Sci. Technol.* 46(20), 11235-11242.

Giesy, J. and Kannan, K. 2001. Global distribution of perfluorooctane sulfonate in wildlife. *Environ. Sci. Technol.* 35(7), 1339-1342.

Goss, K.-U. 2008. The pKa values of PFOA and other highly fluorinated carboxylic acids. *Environ. Sci. Technol.* 42(2), 456-458.

Government of Canada 2008. *Perfluorooctane Sulfonate and its Salts and Certain Other Compounds Regulations*. Canada Gazette Part II , 142(12), 1322-1347. Accessed 09/28 2013 <http://canadagazette.gc.ca/rp-pr/p2/2008/2008-06-11/pdf/g2-14212.pdf>.

Grefte, A., Dignum, M., Cornelissen, E. R., Rietveld, L. C. 2013a. Natural organic matter removal by ion exchange at different positions in the drinking water treatment lane. *Drink. Water Eng. Sci.* 6(1), 1-10.

Grefte, A., Ross, P. S., Dignum, M., Cornelissen, E. R., Rietveld, L. C. 2013b. The Influence of the removal of specific NOM compounds by anion exchange on ozone demand, disinfection capacity, and bromate formation. *Ozone Sci. Eng.* 35(4), 283-294.

Gump, B. B., Wu, Q., Dumas, A. K., Kannan, K. 2011. Perfluorochemical (PFC) exposure in children: Associations with impaired response inhibition. *Environ. Sci. Technol.* 45(19), 8151-8159.

Hameed, B. H., Salman, J. M., Ahmad, A. L. 2009. Adsorption isotherm and kinetic modeling of 2,4-D pesticide on activated carbon derived from date stones. *J. Hazard. Mater.* 163(1), 121-126.

Hansen, M. C., Borresen, M. H., Schlabach, M., Cornelissen, G. 2010. Sorption of perfluorinated compounds from contaminated water to activated carbon. *J. Soils Sediments* 10(2), 179-185.

Hansen, K., Johnson, H., Eldridge, J., Butenhoff, J., Dick, L. 2002. Quantitative characterization of trace levels of PFOS and PFOA in the Tennessee River. *Environ. Sci. Technol.* 36(8), 1681-1685.

Harris, D. C. 2007. *Quantitative Chemical Analysis*. New York W.H. Freeman & Company, New York.

Haug, L. S., Huber, S., Becher, G., Thomsen, C. 2011. Characterisation of human exposure pathways to perfluorinated compounds - Comparing exposure estimates with biomarkers of exposure. *Environ. Int.* 37(4), 687-693.

Hekster, F. M., Laane, R. W. P. M., De Voogt, P. 2003. Environmental and toxicity effects of perfluoroalkylated substances. *Rev. Environ. Contam. Toxicol.* 179, 99-121.

Higgins, C. P. and Luthy, R. G. 2006. Sorption of perfluorinated surfactants on sediments. *Environ. Sci. Technol.* 40(23), 7251-7256.

Ho, Y. S. 1995. Adsorption of heavy metals from waste streams by peat. PhD thesis, School of Chemical Engineering, University of Birmingham.

Ho, Y.S. 2006. Second-order kinetic model for the sorption of cadmium onto tree fern: A comparison of linear and non-linear methods. *Water Res.*40, 119-125.

Ho, Y. S. and McKay, G. 1999. The sorption of lead(II) ions on peat. *Water Res.* 33(2), 578-584.

Ho, Y. S. and McKay, G. 1998. Sorption of dye from aqueous solution by peat. *Chem. Eng. J.* 70(2), 115-124.

Hoehn, E., Plumlee, M. H., Reinhard, M. 2007. Natural attenuation potential of downwelling streams for perfluorochemicals and other emerging contaminants. *Water Sci. Technol.* 56(11), 59-64.

Hoffman, K., Webster, T. F., Bartell, S. M., Weisskopf, M. G., Fletcher, T., Vieira, V. M. 2011. Private drinking water wells as a source of exposure to perfluorooctanoic acid (PFOA) in communities surrounding a fluoropolymer production facility. *Environ. Health Perspect.* 119(1), 92-97.

Holtcamp, W. 2012. Obesogens: An environmental link to obesity. *Environ. Health Perspect.* 120(2), A62-A68.

Hölzer, J., Göen, T., Rauchfuss, K., Kraft, M., Angerer, J., Kleeschulte, P., Wilhelm, M. 2009. One-year follow-up of perfluorinated compounds in plasma of German residents from Arnsberg formerly exposed to PFOA-contaminated drinking water. *Int. J. Hyg. Environ. Health* 212(5), 499-504.

Hölzer, J., Midasch, O., Rauchfuss, K., Kraft, M., Reupert, R., Angerer, J., Kleeschulte, P., Marschall, N., Wilhelm, M. 2008. Biomonitoring of perfluorinated compounds in children and adults exposed to perfluorooctanoate-contaminated drinking water. *Environ. Health Perspect.* 116(5), 651-657.

Houde, M., Czub, G., Small, J. M., Backus, S., Wang, X., Alaei, M., Muir, D. C. G. 2008. Fractionation and bioaccumulation of perfluorooctane sulfonate (PFOS) isomers in a Lake Ontario food web. *Environ. Sci. Technol.* 42(24), 9397-9403.

Hu, J., Martin, A., Shang, R., Siegers, W., Cornelissen, E., Heijman, B., Rietveld, L. 2014. Anionic exchange for NOM removal and the effects on micropollutant adsorption competition on activated carbon. *Sep. Purif. Technol.* 129, 25-31.

Huber, M., Canonica, S., Park, G., Von Gunten, U. 2003. Oxidation of pharmaceuticals during ozonation and advanced oxidation processes. *Environ. Sci. Technol.* 37(5), 1016-1024.

Huck, P.M. and Sozański, M.M. 2011. *Chemical Basis for Water Technology*. In: Peter Wilderer (Ed.) Treatise on Water Science, Vol. 1, 429-469. Oxford: Academic Press.

Humbert, H., Gallard, H., Suty, H., Croue, J. 2008. Natural organic matter (NOM) and pesticides removal using a combination of ion exchange resin and powdered activated carbon (PAC). *Water Res.* 42(6-7), 1635-1643.

Ingelido, A. M., Marra, V., Abballe, A., Valentini, S., Iacovella, N., Barbieri, P., Porpora, M. G., Di Domenico, A., De Felip, E. 2010. Perfluorooctanesulfonate and perfluorooctanoic acid exposures of the Italian general population. *Chemosphere* 80(10), 1125-1130.

Jahnke, A. and Berger, U. 2009. Trace analysis of per- and polyfluorinated alkyl substances in various matrices-How do current methods perform? *J. Chromatography A* 1216(3), 410-421.

Janesick, A. and Blumberg, B. 2011. Endocrine disrupting chemicals and the developmental programming of adipogenesis and obesity. *Birth Defects Res. C Embryo Today: Rev.* 93(1), 34-50.

Jensen, A. A., Poulsen, P. B., Bossi, R. 2008. *Survey and Environmental/Health Assessment of Fluorinated Substances in Impregnated Consumer Products and Impregnating Agents, No. 99*, Danish Environmental Protection Agency: Copenhagen. Accessed 09/27 2013. <http://www2.mst.dk/udgiv/publications/2008/978-87-7052-845-0/pdf/978-87-7052-846-7.pdf>.

Joensen, U. N., Bossi, R., Leffers, H., Jensen, A. A., Skakkebaek, N. E., Jørgensen, N. 2009. Do perfluoroalkyl compounds impair human semen quality? *Environ. Health Perspect.* 117(6), A256.

Kaiser, M. A., Barton, C. A., Botelho, M., Buck, R. C., Buxton, L. W., Gannon, J., Kao, C. C., Larsen, B. S., Russel, M. H., Wang, N., Waterland, R. L. 2006. Understanding the transport of anthropogenic fluorinated compounds in the environment. *Organohalogen Compd.* 68, 675-678.

Kannan, K., Corsolini, S., Falandysz, J., Fillmann, G., Kumar, K., Loganathan, B., Mohd, M., Olivero, J., Van Wouwe, N., Yang, J., Aldous, K. 2004. Perfluorooctanesulfonate and related fluorochemicals in human blood from several countries. *Environ. Sci. Technol.* 38(17), 4489-4495.

Karanfil, T. 2006. *Activated Carbon Adsorption in Drinking Water Treatment*, Chapter 7, 345-373.

Karanfil, T. and Dastgheib, S. A. 2004. Trichloroethylene adsorption by fibrous and granular activated carbons: Aqueous phase, gas phase, and water vapor adsorption studies. *Environ. Sci. Technol.* 38(22), 5834-5841.

Karrman, A., Ericson, I., van Bavel, B., Darnerud, P. O., Aune, M., Glynn, A., Lignell, S., Lindstrom, G. 2007. Exposure of perfluorinated chemicals through lactation: Levels of matched human milk and serum and a temporal trend, 1996-2004, in Sweden. *Environ. Health Perspect.* 115(2), 226-230.

Kissa, E. 2001. *Fluorinated Surfactants and Repellents*. Marcel Dekker, New York.

- Knox, S. S., Jackson, T., Javins, B., Frisbee, S. J., Shankar, A., Ducatman, A. M. 2011. Implications of early menopause in women exposed to perfluorocarbons. *J. Clin. Endocrinol. Metab.* 96(6), 1747-1753.
- Kolstad, C. 2010. GAC treatment for PFCs in Oakdale. *Breeze*, 143, 14-15. <http://www.mnawwa.org/news/breeze/BreezeFall2010.pdf>; Accessed 09/31 2013.
- Kunacheva, C., Fujii, S., Tanaka, S., Boontanon, S. K., Poothong, S., Wongwatthana, T., Shivakoti, B. R. 2010. Perfluorinated compounds contamination in tap water and bottled water in Bangkok, Thailand. *J. Water Supply Res. Technol-Aqua* 59(5), 345-354.
- Kwon, Y.-N., Shih, K., Tang, C., Leckie, J. O. 2012. Adsorption of perfluorinated compounds on thin-film composite polyamide membranes. *J. Appl. Polym. Sci.* 124(2), 1042-1049.
- Lampert, D. J., Frisch, M. A., Speitel Jr., G. E. 2007. Removal of perfluorooctanoic acid and perfluorooctane sulfonate from wastewater by ion exchange. *Pract. Period. Hazard., Toxic, Radioact. Waste Manag.* 11(1), 60-68.
- Langlois, I., Berger, U., Zencak, Z., Oehme, M. 2007. Mass spectral studies of perfluorooctane sulfonate derivatives separated by high-resolution gas chromatography. *Rapid Commun. Mass Spectrom.* 21(22), 3547-3553.
- Larsen, B. S. and Kaiser, M. A. 2007. Challenges in perfluorocarboxylic acid measurements. *Anal. Chem.* 79(11), 3966-3973.
- Lau, C., Anitole, K., Hodes, C., Lai, D., Pfahles-Hutchens, A., Seed, J. 2007. Perfluoroalkyl acids: A review of monitoring and toxicological findings. *Toxicol. Sci.* 99(2), 366-394.
- Lei, Y., Wania, F., Mathers, D., Mabury, S. 2004. Determination of vapor pressures, octanol-air, and water-air partition coefficients for polyfluorinated sulfonamide, sulfonamidoethanols, and telomer alcohols. *J. Chem. Eng. Data* 49(4), 1013-1022.
- Lindstrom, A. B., Strynar, M. J., Libelo, E. L. 2011. Polyfluorinated compounds: Past, present, and future. *Environ. Sci. Technol.* 45(19), 7954-7961.
- Lipp, P., Sacher, F., Baldauf, G. 2010. Removal of organic micro-pollutants during drinking water treatment by nanofiltration and reverse osmosis. *Desalin. Water Treat.* 13(1-3), 226-237.
- Little Hocking Water Association (LHWA) 2010. *GAC Filter C-8 Sampling Result Summary*; Accessed 09/24 2013. <http://littlehockingwater.org/newsite/?cat=8>.
- Liu, W., Xu, L., Li, X., Jin, Y. H., Sasaki, K., Saito, N., Sato, I., Tsuda, S. 2011a. Human nails analysis as biomarker of exposure to perfluoroalkyl compounds. *Environ. Sci. Technol.* 45(19), 8144-8150.

- Liu, W., Hwang, B., Li, Z., Jen, J., Lee, M. 2011b. Headspace solid phase microextraction in-situ supercritical fluid extraction coupled to gas chromatography-tandem mass spectrometry for simultaneous determination of perfluorocarboxylic acids in sediments. *J. Chromatography A* 1218(43), 7857-7863.
- Liu, J. and Lee, L. S. 2007. Effect of fluorotelomer alcohol chain length on aqueous solubility and sorption by soils. *Environmental Sci. Technol.* 41(15), 5357-5362.
- Liu, J. and Lee, L. 2005. Solubility and sorption by soils of 8 : 2 fluorotelomer alcohol in water and cosolvent systems. *Environ. Sci. Technol.* 39(19), 7535-7540.
- Llorca, M., Farre, M., Pico, Y., Lopez Teijon, M., Alvarez, J. G., Barcelo, D. 2010. Infant exposure of perfluorinated compounds: Levels in breast milk and commercial baby food. *Environ. Int.* 36(6), 584-592.
- Loi-Brügger, A., Panglisch, S., Hoffmann, G., Buchta, P., Gimbel, R., Nacke, C. 2008. Removal of trace organic substances from river bank filtrate - Performance study of RO and NF membranes. *Water Sci. Technol.-Water Supply* 8(1), 85-92.
- Lopez-Espinosa, M., Fletcher, T., Armstrong, B., Genser, B., Dhatariya, K., Mondal, D., Ducatman, A., Leonardi, G. 2011. Association of perfluorooctanoic acid (PFOA) and perfluorooctane sulfonate (PFOS) with age of puberty among children living near a chemical plant. *Environ. Sci. Technol.* 45(19), 8160-8166.
- Lutze, H., Panglisch, S., Axel Bergmann, A., Schmidt, T. C. 2011. *Treatment Options for the Removal and Degradation of Polyfluorinated Chemicals*. In: Knepper, T.P., Lange, F.T. (Eds.), In: The Handbook of Environmental Chemistry: Fluorinated Surfactants and Transformation Products, Springer-Verlag, Berlin Heidelberg, 103-126.
- Mak, Y. L., Taniyasu, S., Yeung, L. W. Y., Lu, G., Jin, L., Yang, Y., Lam, P. K. S., Kannan, K., Yamashita, N. 2009. Perfluorinated compounds in tap water from China and several other countries. *Environ. Sci. Technol.* 43(13), 4824-4829.
- Martin, J. W., Asher, B. J., Beesoon, S., Benskin, J. P., Ross, M. S. 2010. PFOS or PreFOS? Are perfluorooctane sulfonate precursors (PreFOS) important determinants of human and environmental perfluorooctane sulfonate (PFOS) exposure? *J. Environ. Monit.* 12(11), 1979-2004.
- Martin, J. W., Kannan, K., Berger, U., Voogt, P. D., Field, J., Franklin, J., Giesy, J. P., Harner, T., Muir, D. C. G., Scott, B., Kaiser, M., Järnberg, U., Jones, K. C., Mabury, S. A., Schroeder, H., Simcik, M., Sottani, C., Van Bavel, B., Kärman, A., Lindström, G., Van Leeuwen, S. 2004. Analytical challenges hamper perfluoroalkyl research. *Environ. Sci. Technol.* 38(13), 248A-255A.

- Martin, J., Mabury, S., Solomon, K., Muir, D. 2003. Bioconcentration and tissue distribution of perfluorinated acids in rainbow trout (*Oncorhynchus mykiss*). *Environ. Toxicol. Chem.* 22(1), 196-204.
- McDowell, D. C., Huber, M. M., Wagner, M., Von Gunten, U., Ternes, T. A. 2005. Ozonation of carbamazepine in drinking water: Identification and kinetic study of major oxidation products. *Environ. Sci. Technol.* 39(20), 8014-8022.
- McKay, G. 1983. The adsorption of dyestuffs from aqueous solutions using activated carbon. III. Intraparticle diffusion processes. *J. Chem. Tech. Biotechnol.* 33A, 196-204.
- Medellin-Castillo, N. A., Leyva-Ramos, R., Ocampo-Perez, R., de la Cruz, R. F. G., Aragon-Pina, A., Martinez-Rosales, J. M., Guerrero-Coronado, R. M., Fuentes-Rubio, L. 2007. Adsorption of fluoride from water solution on bone char. *Ind. Eng. Chem. Res.* 46(26), 9205-9212.
- Meesters, R. J. W. and Schroder, H. F. 2004. Perfluorooctane sulfonate - A quite mobile anionic anthropogenic surfactant, ubiquitously found in the environment. *Water Sci. Technol.* 50(5), 235-242.
- Melzer, D., Rice, N., Depledge, M. H., Henley, W. E., Galloway, T. S. 2010. Association between serum perfluorooctanoic acid (PFOA) and thyroid disease in the US National Health and Nutrition Examination Survey. *Environ. Health Perspect.* 118(5), 686-692.
- Menéndez-Díaza, J.A. and Martín-Gullón, I. 2006. *Types of Carbon Adsorbents and their Production*. Chapter 1, Activated Carbon Surfaces in Environmental Remediation. T.J. Bandosz (Ed.), Elsevier, New York, NY.
- Minnesota Department of Health (MDH) 2011. *Health Guidelines for Perfluorinated Chemicals (PFCs) in Drinking Water*. Accessed 09/24 2013. <http://www.health.state.mn.us/divs/eh/hazardous/topics/pfcs/drinkingwater.html>.
- Minnesota Department of Health (MDH) 2008. *Public Health Assessment: Perfluorochemical Contamination in Lake Elmo and Oakdale, Washington County, Minnesota*. Accessed 09/24 2013. <http://www.health.state.mn.us/divs/eh/hazardous/topics/pfcs/pha/lakeelmoakdale/>.
- Moeller, A., Ahrens, L., Surm, R., Westerveld, J., van der Wielen, F., Ebinghaus, R., de Voogt, P. 2010. Distribution and sources of polyfluoroalkyl substances (PFAS) in the River Rhine watershed. *Environ. Pollut.* 158(10), 3243-3250.
- Monroy, R., Morrison, K., Teo, K., Atkinson, S., Kubwabo, C., Stewart, B., Foster, W. G. 2008. Serum levels of perfluoroalkyl compounds in human maternal and umbilical cord blood samples. *Environ. Res.* 108(1), 56-62.

- Monteleone, M., Naccarato, A., Sindona, G., Tagarelli, A. 2012. A rapid and sensitive assay of perfluorocarboxylic acids in aqueous matrices by headspace solid phase microextraction-gas chromatography-triple quadrupole mass spectrometry. *J. Chromatography A* 1251, 160-168.
- Moody, C. A., Hebert, G. N., Strauss, S. H., Field, J. A. 2003. Occurrence and persistence of perfluorooctanesulfonate and other perfluorinated surfactants in groundwater at a fire-training area at Wurtsmith Air Force Base, Michigan, USA. *J. Environ. Monit.* 5(2), 341-345.
- Moody, C. A., Martin, J. W., Kwan, W. C., Muir, D. C. G., Mabury, S. C. 2002. Monitoring perfluorinated surfactants in biota and surface water samples following an accidental release of fire-fighting foam into Etobicoke Creek. *Environ. Sci. Technol.* 36(4), 545-551.
- Moody, C. A. and Field, J. A. 1999. Determination of perfluorocarboxylates in groundwater impacted by fire-fighting activity. *Environ. Sci. Technol.* 33(16), 2800-2806.
- Moore, B. C., Cannon, F. S., Westrick, J. A., Metz, D. H., Shrive, C. A., DeMarco, J., Hartman, D. J. 2001. Changes in GAC pore structure during full-scale water treatment at Cincinnati: A comparison between virgin and thermally reactivated GAC. *Carbon* 39(6), 789-807.
- MWH 2005. Water Treatment: Principles and Design. Jon Wiley, Hoboken, New Jersey.
- Newcombe, G. and Cook, D. 2002. Influences on the removal of tastes and odours by PAC. *J. Water Supply Res. T.-AQUA*51(8): 463-474.
- Ochoa-Herrera, V. and Sierra-Alvarez, R. 2008. Removal of perfluorinated surfactants by sorption onto granular activated carbon, zeolite and sludge. *Chemosphere* 72(10), 1588-1593.
- O'Hagan, D. 2008. Understanding organofluorine chemistry. An introduction to the C-F bond. *Chem. Soc. Rev.* 37(2), 308-319.
- Owen, D. M., Amy, G. L., Chowdhury, Z. K., Paode, R., McCoy, G., Viscosil, K. 1995. NOM characterization and treatability. *J. Am. Water Works Assoc.* 87(1), 46-63.
- Pan, Y., Shi, Y., Wang, J., Cai, Y., Wu, Y. 2010. Concentrations of perfluorinated compounds in human blood from twelve cities in China. *Environ. Toxicol. Chem.* 29(12), 2695-2701.
- Parsons, J. R., Saez, M., Dolfing, J., de Voogt, P. 2008. Biodegradation of perfluorinated compounds. *Rev. Environ. Contam. Toxicol.* 196, 53-71.
- Paul, A. G., Jones, K. C., Sweetman, A. J. 2009. A first global production, emission, and environmental inventory for perfluorooctane sulfonate. *Environ. Sci. Technol.* 43(2), 386-392.
- Paustenbach, D. J., Panko, J. M., Scott, P. K., Unice, K. M. 2007. A methodology for estimating human exposure to perfluorooctanoic acid (PFOA): A retrospective exposure assessment of a community (1951-2003). *J. Toxicol. Environ. Health A-Current Iss.* 70(1), 28-57.

Pelekani, C. and Snoeyink, V. L. 2000. Competitive adsorption between atrazine and methylene blue on activated carbon: The importance of pore size distribution. *Carbon* 38(10), 1423-1436.

Pelekani, C. and Snoeyink, V. L. 1999. Competitive adsorption in natural water: Role of activated carbon pore size. *Water Res.* 33(5), 1209-1219.

Pirbazari, M., Ravindran, V., Badriyha, B., Craig, S., McGuire, M. 1993. GAC adsorber design protocol for the removal of off-flavors. *Water Res.* 27(7), 1153-1166.

POPRC 2009. *Decision POPRC-1/7: Perfluorooctane Sulfonate; UNEP/POPS/POPRC.1/10; Stockholm Convention on Persistent Organic Pollutants*. Accessed 09/27 2013. <http://chm.pops.int/Convention/POPsReviewCommittee/Reports/tabid/2301/Default.aspx>.

Post, G. B., Louis, J. B., Lippincott, R. L., Procopio, N. A. 2013. Occurrence of perfluorinated compounds in raw water from New Jersey public drinking water systems. *Environ. Sci. Technol.* 47(23), 13266-13275.

Post, G. B., Cohn, P. D., Cooper, K. R. 2012. Perfluorooctanoic acid (PFOA), an emerging drinking water contaminant: A critical review of recent literature. *Environ. Res.* 116, 93-117.

Post, G. B., Louis, J. B., Cooper, K. R., Boros-Russo, B. J., Lippincott, R. L. 2009. Occurrence and potential significance of perfluorooctanoic acid (PFOA) detected in New Jersey public drinking water systems. *Environ. Sci. Technol.* 43(12), 4547-4554.

Prevedouros, K., Cousins, I. T., Buck, R. C., Korzeniowski, S. H. 2006. Sources, fate and transport of perfluorocarboxylates. *Environ. Sci. Technol.* 40(1), 32-44.

Purolite 2006. Organic Removal by Ion Exchange. Accessed 10/18 2014. <http://www.purolite.com/Customized/Uploads/Pdfs/Organic%20Scavaging.pdf>.

Qu, Y., Zhang, C., Li, F., Bo, X., Liu, G., Zhou, Q. 2009. Equilibrium and kinetics study on the adsorption of perfluorooctanoic acid from aqueous solution onto powdered activated carbon. *J. Hazard. Mater.* 169(1-3), 146-152.

Quinlivan, P. A., Li, L., Knappe, D. R. U. 2005. Effects of activated carbon characteristics on the simultaneous adsorption of aqueous organic micropollutants and natural organic matter. *Water Res.* 39(8), 1663-1673.

Quinones, O. and Snyder, S. A. 2009. Occurrence of perfluoroalkyl carboxylates and sulfonates in drinking water utilities and related waters from the United States. *Environ. Sci. Technol.* 43(24), 9089-9095.

Rahman, M. F., Peldszus, S., Anderson, W. B. 2014. Behaviour and fate of perfluoroalkyl and polyfluoroalkyl substances (PFASs) in drinking water treatment: A review. *Water Res.* 50, 318-340.

- Rayne, S. and Forest, K. 2009. Perfluoroalkyl sulfonic and carboxylic acids: A critical review of physicochemical properties, levels and patterns in waters and wastewaters, and treatment methods. *J. Environ. Sci. Health A-Toxic/hazard. Subst. Environ. Eng.* 44(12), 1145-1199.
- Renner, R. 2006. The long and the short of perfluorinated replacements. *Environ. Sci. Technol.* 40(1), 12-13.
- Rhoads, K. R., Janssen, E. M., Luthy, R. G., Criddle, C. S. 2008. Aerobic biotransformation and fate of N-ethyl perfluorooctane sulfonamidoethanol (N-EtFOSE) in activated sludge. *Environ. Sci. Technol.* 42(8), 2873-2878.
- Rostkowski, P., Taniyasu, S., Yamashita, N., Falandysz, J. 2008. Perfluorinated compounds in potable water. *Roczniki Państwowego Zakładu Higieny* 59(3), 283-92.
- Rumsby, P. C., McLaughlin, C. L., Hall, T. 2009. Perfluorooctane sulphonate and perfluorooctanoic acid in drinking and environmental waters. *Philos. Trans. A- Math. Phys. Eng. Sci.* 367(1904), 4119-4136.
- Schideman, L. C., Mariñas, B. J., Snoeyink, V. L., Campos, C. 2006. Three-component competitive adsorption model for fixed-bed and moving-bed granular activated carbon adsorbers. Part II. Model parameterization and verification. *Environ. Sci. Technol.* 40(21), 6812-6817.
- Schultz, M. M., Barofsky, D. F., Field, J. A. 2003. Fluorinated alkyl surfactants. *J. Environ. Eng. Sci.* 20(5), 487-501.
- Scott, B. F., Moody, C. A., Spencer, C., Small, J. M., Muir, D. C. G., Mabury, S. A. 2006. Analysis for perfluorocarboxylic acids/anions in surface waters and precipitation using GC-MS and analysis of PFOA from large-volume samples. *Environ. Sci. Technol.* 40(20), 6405-6410.
- Seals, R., Bartell, S.M., Steenland, K. 2011. Accumulation and clearance of perfluorooctanoic acid (PFOA) in current and former residents of an exposed community. *Environ. Health Perspect.* 119(1), 119-124.
- Senevirathna, S. T. M. L. D., Tanaka, S., Fujii, S., Kunacheva, C., Harada, H., Shivakoti, B. R., Dinh, H., Ariyadasa, T. 2011. Adsorption of four perfluorinated acids on non ion exchange polymer sorbents. *Water Sci. Technol.* 63(10), 2106-2113.
- Shivakoti, B. R., Fujii, S., Nozoe, M., Tanaka, S., Kunacheva, C. 2010. Perfluorinated chemicals (PFCs) in water purification plants (WPPs) with advanced treatment processes. *Water Sci. Technol.- Water Supply* 10(1), 87-95.
- Sinclair, E. and Kannan, K. 2006. Mass loading and fate of perfluoroalkyl surfactants in wastewater treatment plants. *Environ. Sci. Technol.* 40(5), 1408-1414.
- Skutlarek, D., Exner, M., Faerber, H. 2006. Perfluorinated surfactants in surface and drinking water. *Environ. Sci. Pollut. Res.* 13(5), 299-307.

Sontheimer, H., Crittenden, J. C., Summer, R. S. 1988. Activated carbon for water treatment. DVGW-Forschungsstelle, Engler-Bunte-Institut, Universitat Karlsruhe (TH), Karlsruhe, Germany.

Steenland, K., Fletcher, T., Savitz, D. A. 2010. Epidemiologic evidence on the health effects of perfluorooctanoic acid (PFOA). *Environ. Health Perspect.* 118(8), 1100-1108.

Steinle-Darling, E., Litwiller, E., Reinhard, M. 2010. Effects of sorption on the rejection of trace organic contaminants during nanofiltration. *Environ. Sci. Technol.* 44(7), 2592-2598.

Steinle-Darling, E. and Reinhard, M. 2008. Nanofiltration for trace organic contaminant removal: Structure, solution, and membrane fouling effects on the rejection of perfluorochemicals. *Environ. Sci. Technol.* 42(14), 5292-5297.

Stock, N. L., Muir, D. C. G., Mabury, S. 2009. *Perfluoroalkyl Compounds*. In: Harrad, S. (Ed.), Persistent Organic Pollutants, John Wiley and Sons, Ltd., Chichester, UK, 25-69.

Stock, N. L., Furdui, V. I., Muir, D. C. G., Mabury, S. A. 2007. Perfluoroalkyl contaminants in the Canadian arctic: Evidence of atmospheric transport and local contamination. *Environ. Sci. Technol.* 41(10), 3529-3536.

Stock, N. L., Ellis, D. A., Deleebeeck, L., Muir, D. C. G., Mabury, S. A. 2004. Vapor pressures of the fluorinated telomer alcohols - Limitations of estimation methods. *Environ. Sci. Technol.* 38(6), 1693-1699.

Summers, R.S. 1986. Activated carbon adsorption of humic substances: Effect of molecular size and heterodispersity. PhD thesis, Department of Civil Engineering, Stanford University.

Szajdzinska-Pietek, E. and Gebicki J.L. 2000. Pulse radiolytic investigation of perfluorinated surfactants in aqueous solutions. *Res. Chem. Intermediat.* 26(9), 897-912.

Tabe, S., Yang, P., Zhao, X., Hao, C., Seth, R., Schweitzer, L., Jamal, T. 2010. Occurrence and removal of PPCPs and EDCs in the Detroit River watershed. *Water Sci. Technol.* 5(1), 1-8.

Takagi, S., Adachi, F., Miyano, K., Koizumi, Y., Tanaka, H., Watanabe, I., Tanabe, S., Kannan, K. 2011. Fate of perfluorooctanesulfonate and perfluorooctanoate in drinking water treatment processes. *Water Res.* 45(13), 3925-3932.

Takagi, S., Adachi, F., Miyano, K., Koizumi, Y., Tanaka, H., Mimura, M., Watanabe, I., Tanabe, S., Kannan, K. 2008. Perfluorooctanesulfonate and perfluorooctanoate in raw and treated tap water from Osaka, Japan. *Chemosphere* 72(10), 1409-1412.

Tan, Y. R., Kilduff, J. E., Kitis, M., Karanfil, T. 2005. Dissolved organic matter removal and disinfection byproduct formation control using ion exchange. *Desalination* 176(1-3), 189-200.

Tang, C. Y., Fu, Q. S., Criddle, C. S., Leckie, J. O. 2007. Effect of flux (transmembrane pressure) and membrane properties on fouling and rejection of reverse osmosis and nanofiltration membranes treating perfluorooctane sulfonate containing wastewater. *Environ. Sci. Technol.* 41(6), 2008-2014.

Tang, C. Y., Fu, Q. S., Robertson, A. P., Criddle, C. S., Leckie, J. O. 2006. Use of reverse osmosis membranes to remove perfluorooctane sulfonate (PFOS) from semiconductor wastewater. *Environ. Sci. Technol.* 40(23), 7343-7349.

Tanghe, T. and Verstraete, W. 2001. Adsorption of nonylphenol onto granular activated carbon. *Water Air Soil Pollut.* 131(1-4), 61-72.

Taniyasu, S., Kannan, K., Man, K. S., Gulkowska, A., Sinclair, E., Okazawa, T., Yamashita, N. 2005. Analysis of fluorotelomer alcohols, fluorotelomer acids, and short- and long-chain perfluorinated acids in water and biota. *J. Chromatography A* 1093(1-2), 89-97.

Thompson, J., Eaglesham, G., Mueller, J. 2011a. Concentrations of PFOS, PFOA and other perfluorinated alkyl acids in Australian drinking water. *Chemosphere* 83(10), 1320-1325.

Thompson, J., Eaglesham, G., Reungoat, J., Poussade, Y., Bartkow, M., Lawrence, M., Mueller, J. F. 2011b. Removal of PFOS, PFOA and other perfluoroalkyl acids at water reclamation plants in South East Queensland Australia. *Chemosphere* 82(1), 9-17.

Tolls, J., Sijm, D. T. H. M. 1995. A preliminary evaluation of the relationship between bioconcentration and hydrophobicity for surfactants. *Environ. Toxicol. Chem.* 14(10), 1675-1685.

Tolls, J., Kloepper-Sams, P., Sijm, D. T. H. M. 1994. Surfactant bioconcentration—A critical review. *Chemosphere* 29, 693-717.

Trinkwasserkommission 2006. *Provisional Evaluation of PFT in Drinking Water with the Guide Substances Perfluorooctanoic Acid (PFOA) and Perfluorooctane Sulfonate (PFOS) as Examples*. In: Health GMo, Ed. Bonn: Federal Environment Agency, Germany.

Tsai, Y., Yu-Chen Lin, A., Weng, Y., Li, K. 2010. Treatment of perfluorinated chemicals by electro-microfiltration. *Environ. Sci. Technol.* 44(20), 7914-7920.

Ullah, S., Alsberg, T., Berger, U. 2011. Simultaneous determination of perfluoroalkyl phosphonates, carboxylates, and sulfonates in drinking water. *J. Chromatography A* 1218(37), 6388-6395.

United States National Library of Medicine 2011. ChemID plus database. Accessed 09/27 2013. <http://chem.sis.nlm.nih.gov/chemidplus/>.

USEPA 2012. *New Chemical Review of Alternatives for PFOA and Related Chemicals*. Accessed 09/27 2013. <http://www.epa.gov/oppt/pfoa/pubs/altnewchems.html>.

USEPA 2011a. *Regulatory Determinations for the Third Drinking Water Contaminant Candidate List, Stake holders meetings*, June 16, Washington D.C. Accessed 09/27 2013. <http://water.epa.gov/scitech/drinkingwater/dws/ccl/upload/Preliminary-Regulatory-Determinations-3-June-16th-Public-Meeting-Slides.pdf>.

USEPA 2011b. *Revisions to the Unregulated Contaminants Monitoring Regulations (UCMR3) for Public Water Systems*. Federal Register 76(42), 11713-11737.

USEPA 2011c. *Provisional Health Advisories for Perfluorooctanoic Acid (PFOA) and Perfluorooctane Sulfonate (PFOS)*. Accessed 09/27 2013. http://www.epa.gov/waterscience/criteria/drinking/pha-PFOA_PFOS.pdf.

USEPA 2009a. *Long-chain Perfluorinated Chemicals (PFCs)-Action Plan*. Accessed 09/27 2013. http://www.epa.gov/opptintr/existingchemicals/pubs/pfcs_action_plan1230_09.pdf.

USEPA 2009b. *Code of Federal Regulations*, Title 40, Volume 22, Chapter 1, Parts 141-143. Accessed 09/27 2014. <http://drinkingwater.vt.gov/dwrules/pdf/40cfr.pdf>.

Vecitis, C. D., Park, H., Cheng, J., Mader, B. T., Hoffmann, M. R. 2009. Treatment technologies for aqueous perfluorooctanesulfonate (PFOS) and perfluorooctanoate (PFOA). *Front. Environ. Sci. Eng. in China* 3(2), 129-151.

Velten, S., Knappe, D. R. U., Traber, J., Kaiser, H., von Gunten, U., Boller, M., Meylan, S. 2011. Characterization of natural organic matter adsorption in granular activated carbon adsorbers. *Water Res.* 45(13), 3951-3959.

Vestergren, R. and Cousins, I. T. 2009. Tracking the pathways of human exposure to perfluorocarboxylates. *Environ. Sci. Technol.* 43(15), 5565-5575.

von Gunten, U. 2003. Ozonation of drinking water: Part I. Oxidation kinetics and product formation. *Water Res.* 37(7), 1443-1467.

Wallington, T. J., Hurley, M. D., Xia, J., Wuebbles, D. J., Sillman, S., Ito, A., Penner, J. E., Ellis, D. A., Martin, J., Mabury, S. A., Nielsen, O. J., Andersen, M. P. S. 2006. Formation of C7F15COOH (PFOA) and other perfluorocarboxylic acids during the atmospheric oxidation of 8:2 fluorotelomer alcohol. *Environ. Sci. Technol.* 40(3), 924-930.

Wang, N., Szostek, B., Buck, R. C., Folsom, P. W., Sulecki, L. M., Capka, V., Berti, W. R., Gannon, J. T. 2005a. Fluorotelomer alcohol biodegradation - Direct evidence that perfluorinated carbon chains breakdown. *Environ. Sci. Technol.* 39(19), 7516-7528.

- Wang, N., Szostek, B., Folsom, P. W., Sulecki, L. M., Capka, V., Buck, R. C., Berti, W. R., Gannon, J. T. 2005b. Aerobic biotransformation of C-14-labeled 8-2 telomer B alcohol by activated sludge from a domestic sewage treatment plant. *Environ. Sci. Technol.* 39(2), 531-538.
- Wang, T., Wang, Y., Liao, C., Cai, Y., Jiang, G. 2009. Perspectives on the inclusion of perfluorooctane sulfonate into the Stockholm convention on persistent organic pollutants. *Environ. Sci. Technol.* 43(14), 5171-5175.
- Wang, T., Lin, Z., Yin, D., Tian, D., Zhang, Y., Kong, D. 2011a. Hydrophobicity-dependent QSARs to predict the toxicity of perfluorinated carboxylic acids and their mixtures. *Environ. Toxicol. Pharmacol.* 32(2), 259-265.
- Wang, Z., MacLeod, M., Cousins, I. T., Scheringer, M., Hungerbuehler, K. 2011b. Using COSMOtherm to predict physicochemical properties of poly- and perfluorinated alkyl substances (PFASs). *Environ. Chem.* 8(4), 389-398.
- Weber, W.J. and Morris, J.C. 1963. Kinetics of adsorption on carbon from solution. *J. Sanit. Eng. Div. Am. Soc. Eng.* 89(2), 31-60.
- Wilhelm, M., Bergmann, S., Dieter, H. H. 2010. Occurrence of perfluorinated compounds (PFCs) in drinking water of North Rhine-Westphalia, Germany and new approach to assess drinking water contamination by shorter-chained C4-C7 PFCs. *Int. J. Hyg. Environ. Health* 213(3), 224-232.
- Wu, F.-C., Tseng, R.-L., Huang, S.-C., Juang, R.-S. 2009. Characteristics of pseudo-second-order kinetic model for liquid-phase adsorption: A mini-review. *Chem. Eng. J.* 151(1-3), 1-9.
- Xiao, F., Halbach, T., Simcik, M.F., Gulliver, J.S. 2012a. Input characterization of perfluoroalkyl substances in wastewater treatment plants: Source discrimination by exploratory data analysis. *Water Res.* 9(1), 3101-3109.
- Xiao, F., Simcik, M.F., Gulliver, J.S. 2012b. Mechanisms for removal of perfluorooctane sulfonate (PFOS) and perfluorooctanoate (PFOA) from drinking water by conventional and enhanced coagulation. *Water Res.* 47(1), 49-56.
- Xiao, F., Davidsavor, K.J., Park, S., Nakayama, M., Phillips, B.R. 2012c. Batch and column study: Sorption of perfluorinated surfactants from water and cosolvent systems by Amberlite XAD resins. *J. Colloid Interface Sci.* 368, 505-511.
- Yamashita, N., Kannan, K., Taniyasu, S., Horii, Y., Petrick, G., Gamo, T. 2005. A global survey of perfluorinated acids in oceans. *Marine Pollut. Bull.* 51(8-12), 658-668.
- Yu, J., Lv, L., Lan, P., Zhang, S., Pan, B., Zhang, W. 2012. Effect of effluent organic matter on the adsorption of perfluorinated compounds onto activated carbon. *J. Hazard. Mater.* 225, 99-106.

Yu, Q., Zhang, R., Deng, S., Huang, J., Yu, G. 2009a. Sorption of perfluorooctane sulfonate and perfluorooctanoate on activated carbons and resin: Kinetic and isotherm study. *Water Res.* 43(4), 1150-1158.

Yu, Z., Peldszus, S., Huck, P. M. 2009b. Adsorption of selected pharmaceuticals and an endocrine disrupting compound by granular activated carbon. 1. Adsorption capacity and kinetics. *Environ. Sci. Technol.* 43(5), 1467-1473.

Yu, Z., Peldszus, S., Huck, P. M. 2008. Adsorption characteristics of selected pharmaceuticals and an endocrine disrupting compound-naproxen, carbamazepine and nonylphenol-on activated carbon. *Water Res.* 42(12), 2873-2882.

Yu, Z. 2007. Analysis of selected pharmaceuticals and endocrine disrupting compounds and their removal by granular activated carbon in drinking water treatment. PhD thesis, Department of Civil and Environmental Engineering, University of Waterloo.

Zhao, D., Cheng, J., Vecitis, C. D., Hoffmann, M. R. 2011. Sorption of perfluorochemicals to granular activated carbon in the presence of ultrasound. *J. Phys. Chem. A* 115(11), 2250-2257.

Zietzschmann, F., Worch, E., Altmann, J., Ruhl, A. S., Sperlich, A., Meinel, F., Jekel, M. 2014. Impact of EfOM size on competition in activated carbon adsorption of organic micro-pollutants from treated wastewater. *Water Res.* 65, 297-306.

Zushi, Y., Hogarth, J. N., Masunaga, S. 2012. Progress and perspective of perfluorinated compound risk assessment and management in various countries and institutes. *Clean Technol. Environ. Policy* 14(1), 9-20.

APPENDIX-A

Quantification of Physico-Chemical Properties of PFCs Using Molecular Descriptors and Selection of Treatment Processes

PFCs have only recently generated interest in the drinking water community due to potential human exposure through drinking water. As yet, very few studies are available that have dealt with the fate of PFCs during drinking water treatment. Physico-chemical properties of contaminants often govern their fate during water treatment. Unfortunately, reliable experimental data for physico-chemical properties of most PFCs are not available.

Molecular structures have been suggested to determine physico-chemical and biological properties of molecules. Quantitative structure-property relationship (QSPR) methods are developed based on the hypothesis that a compound's structure determines all its properties and similar chemical structures have similar properties and behaviour. QSPR methods which are based on relationships observed for tested chemicals, allow for the prediction behaviours of untested chemicals without experimentation. Structures of chemicals are represented by a wide range of numerical quantities called molecular descriptors. Todeschini and Consonni (2000) defined molecular descriptors as “the final results of a logic and mathematical procedure which transforms chemical information encoded within a symbolic representation of a molecule into a useful number or the result of some standardized experiment.” For example, $\log K_{OW}$ which is the logarithm of octanol/water partition coefficient, is used to predict the hydrophobicity/hydrophilicity of a compound.

While experimentally derived values of descriptors can provide more accurate results, their availability is constrained due to time consuming and expensive measurements. Also such values are only available for a small subset of compounds. With the advancement of computational techniques, chemistry software packages have been developed to compute or predict molecular descriptors. Comparison between physico-chemical and calculated descriptors have shown similarity of information (Andersson *et al.* 2000, Jin 2007). Hence, due to lack of experimental data, PFCs were characterized using molecular descriptors and the descriptors were calculated using various computer-based predictive tools. Calculated descriptor values of PFCs were compared to various other widely studied micropollutants (Table A1). It was presumed that PFC molecular descriptor values and their comparison with other contaminants would assist in predicting their fate during drinking water treatment. This approach also allowed narrowing down the list of treatment processes to be considered during

the preliminary work for the project.

Table A1: List of selected target PFCA candidates and other micropollutants

Class			Compounds	CASRN	Charge at pH 7	
Perfluorinated compounds (PFCs)	PFC As	No. of carbons	4	PFBA	375-22-4	Negative
			6	PFHxA	307-24-4	
			8	PFOA	335-67-1	
			9	PFNA	375-95-1	
	PFAS s		4	PFBS	375-73-5	
			6	PFHxS	355-46-4	
	PFC precursors	8	PFOS	1763-23-1		
				FOSA	754-91-6	
				8:2 FTOH	865-86-1	
	Other micropollutants	Taste & odor compound			MIB	2371-42-8
			Geosmin	19700-21-1		
Pesticide				Atrazine	1912-24-9	
Plasticizer				Bisphenol A	80-05-7	
Hormone				EE2	57-63-6	
Surfactant				Nonylphenol	104-40-5	
Flame retardant				TCEP	115-96-8	
Pharmaceuticals				Carbamazepine	298-46-4	Negative
				Gemfibrozil	25812-30-0	
				Ibuprofen	15687-27-1	
				Clofibric acid	882-09-7	
				Oxytetracycline	79-57-2	
				Sulfamethoxazole	723-46-6	
Linear alkylbenzene sulfonate (LAS)	Surfactant			LAS C11	50854-94-9	
				LAS C13	25496-01-9	

Approach

A number of micropollutants were selected for comparison with PFCs. These contaminants have diverse chemical structures and belong to various chemical classes such as pesticides, plasticizers, surfactants, hormones, pharmaceuticals, flame retardants, and taste and odor compounds. The pool of chemicals selected for comparison and the selected PFCs are listed in Table A1.

Following the selection of the micropollutants, descriptors relevant to the treatment processes to be considered were selected. A total of 26 suitable descriptors that can be easily interpreted and that can provide simple insight into the possible mechanism underlying various responses were considered. Jin and Peldszus (2010) listed a number of descriptors that are presumed to affect removal mechanisms of compounds during different drinking water treatment processes. Using suitable computing methods the selected descriptors were calculated. The list of the descriptors and their calculation methods are provided in Table A2.

Methods

To calculate molecular descriptors, at first the structure of each compound was obtained from the online database ChemID plus Advanced, (<http://chem.sis.nlm.nih.gov/chemidplus/>) as a Molfile (*.mol). ChemAxon's online calculator Marvin (<http://www.chemaxon.com/marvin/sketch/index.php>) was used to calculate pKa values of the selected compounds. Using the same tool, the dominant species of each compound at pH 7 was determined and the corresponding neutral structure was modified accordingly by ChemDraw software (ChemOffice 2006, ChembridgeSoft). Log K_{OW} and logarithm of octanol/water distribution co-efficient (log D) at pH 7 were also calculated using the Marvin predictive tool. Simplified Molecular Input Line Entry System (SMILES) codes were obtained from the ChemID plus advanced database. The SMILES codes were then used as input for the E-Dragon (<http://www.vcclab.org/lab/edragon/start.html>) computational tool to calculate average molecular weight (AMW), unsaturation index (UI), hydrophilicity factor (Hy) and log of water solubility (log S). Quantum-chemical descriptors such as the highest occupied molecular orbital energy (HOMO) and the lowest unoccupied molecular orbital energy (LUMO) and the HOMO-LUMO energy level difference (GAP) were calculated using HyperChem (HyperChem 7.5, Hypercube, Inc.). Neutral structures of the selected molecules were used as the input for the

HyperChem and the Marvin program. Other structural descriptors such as length, width, van der Waals volume, total surface area, hydrophilic surface area and dipole moment were calculated using Molecular Modeling Pro software (MMP, ChemSW, Inc.). The MMP program allows inputting charged species. In this case, the predominant species of each compound at pH 7 was used as the input. Unlike the traditional approach which typically considers neutral molecules only, the effect of solution pH on the molecular structure was considered here. pKa values of compounds determine the predominant species in solution at a given pH and hence, may also affect behaviour of compounds during water treatment processes. Solution pH also affect polarizability and polar surface area. Distribution co-efficient (logD) values indicate the pH dependent hydrophobic/hydrophilic characteristics of charged compounds. Moreover, molecular characteristics such as molecular dimensions, dipole moment and % hydrophilic surface area are also likely altered when compounds adapt to new structures following the addition or loss of a proton.

Results

PFCs and other selected contaminants were characterized using the selected molecular descriptors. The calculated descriptor values are provided Tables A3 to A6. Figures A1 (a) to A1 (c) show calculated molecular dimensions of the selected compounds. Molecular dimensions of PFCAs and PFSAAs increase with the increasing carbon chain length. FOSA has the highest length to width ratio (Figure A1 (d)). It is evident from the Figure A2 that lengths of PFCs are shorter than other molecules with similar molecular weight. Figure A3 shows that the volume of PFCAs and PFASs increases with increasing carbon chain length. Not surprisingly there is also a positive correlation between total surface area of PFCs with carbon chain length.

Table A2. Selected descriptors and their calculation method

Parameter/descriptors	Unit	Used model/ database	Codes/Species of compounds used as input
Molecular weight (MW)	g/mol	ChemID plus advanced	Neutral
log D (at pH 7)		Marvin	Neutral
log K _{ow}			
pKa			
Polarizability at pH 7 (P)	Å ³		
Average molecular weight (AMW)	g/mol	E-Dragon	Smiles code
Unsaturation index (UI)			
Hydrophilic index (Hy)			
No. double bonds (nDB)			
No. aromatic bonds (nAB)			
No. primary and secondary amines (nN)			
No. of aromatic hydroxyls (nArOH)			
log water solubility (log S)	mol/L		
Dipole moment at pH 7	debye	Molecular Modeling Pro®	Dominant species at pH
Molecular length (L)	Å		
Molecular width (W)	Å		
Ratio of length to width (RLW)			
Molecular depth (D)	Å		
van der Waals volume (Vol.)	cm ³ /mol		
Total Surface area (TSA)	cm ² /mol*10 ⁹		
Hydrophilic surface area (HSA)	cm ² /mol*10 ⁹		
% Hydrophilic surface area (% HSA)	%		
Polar surface area (PSA)	cm ² /mol		
HOMO	eV	HyperChem	Neutral
LUMO			
GAP			

Table A3. Compound ID, formula and molecular descriptors for PFCs and other trace contaminants

Compound	Compound ID	Chemical formula	MW	AMW	log K _{ow}	log D at pH 7	pKa
PFBA	1	C ₄ HF ₇ O ₂	214.04	15.29	2.31	-1.22	1.07
PFHxA	2	C ₆ HF ₁₁ O ₂	314.05	15.7	3.71	0.18	-0.78
PFOA	3	C ₈ HF ₁₅ O ₂	414.06	15.93	5.11	1.58	-4.2
PFNA	4	C ₉ HF ₁₇ O ₂	464.07	16	5.81	2.28	-6.51
PFBS	5	C ₄ HF ₉ O ₃ S	300.09	16.67	2.63	0.25	-3.31
PFHxS	6	C ₆ HF ₁₃ O ₃ S	400.11	16.67	4.03	1.65	-3.32
PFOS	7	C ₈ HF ₁₇ O ₃ S	500.13	16.67	5.43	3.05	-3.32
FOSA	8	C ₈ H ₂ F ₁₇ NO ₂ S	499.141	16.1	4.85	3.91	3.37
8:2 FTOH	9	C ₁₂ H ₅ F ₂₁ O	564.17	14.47	7.01	7.01	15.76
N-EtFOSE	10	C ₁₂ H ₁₀ F ₁₇ NO ₃ S	571.25	12.98	4.97	4.97	15.54
MIB	11	C ₁₁ H ₂₀ O	168.28	5.26	2.27	2.27	
Geosmin	12	C ₁₂ H ₂₂ O	182.31	5.21	3.17	3.17	
Atrazine	13	C ₈ H ₁₄ ClN ₅	215.69	7.7	2.2	2.2	14.48
Bisphenol A	14	C ₁₅ H ₁₆ O ₂	228.29	6.92	4.04	4.04	9.78
EE2	15	C ₂₀ H ₂₄ O ₂	296.41	6.44	3.81	3.67	10.33
4-Nonylphenol	16	C ₁₅ H ₂₄ O	220.36	5.51	5.74	5.74	10.31
TCEP	17	C ₆ H ₁₂ Cl ₃ O ₄ P	285.5	10.98	1.44	1.44	
Carbamazepine	18	C ₁₅ H ₁₂ N ₂ O	236.28	7.88	2.77	2.77	15.96
Gemfibrozil	19	C ₁₅ H ₂₂ O ₃	250.34	6.26	4.39	1.85	4.42
Ibuprofen	20	C ₁₃ H ₁₈ O ₂	206.28	6.25	3.84	1.71	4.85
Clofibric acid	21	C ₁₀ H ₁₁ ClO ₃	214.65	8.59	2.9	-0.38	3.37
Oxytetracycline	22	C ₂₂ H ₂₄ N ₂ O ₉	460.44	8.08	-1.86	-4.54	3.24
Sulfamethoxazole	23	C ₁₀ H ₁₁ N ₃ O ₃ S	253.28	9.05	0.79	0.14	6.16
LAS C11	24	C ₁₇ H ₂₈ O ₃ S	312.47	6.38	6.11	3.74	-1.84
LAS C13	25	C ₁₉ H ₃₂ O ₃ S	340.52	6.19	7	4.63	-1.84

MW- molecular weight; AMW- average molecular weight; AMW calculated with E-Dragon, log K_{ow}, log D at pH7 and pKa with Marvin online tool.

Table A4. Molecular descriptor values for PFCs and other trace contaminants

Compound ID	L	W	D	RLW	Vol.	TSA	HSA	% HSA	PSA	DM
1	8.52	6.39	6.32	1.33	72.33	10.35	7.06	68.20	43.29	13.70
2	9.91	7.27	6.22	1.36	104.40	14.68	11.36	77.34	43.29	16.30
3	11.26	8.05	6.59	1.40	136.93	19.13	15.61	81.63	43.29	9.11
4	12.82	8.35	6.90	1.54	152.44	21.17	17.80	84.06	43.29	15.60
5	9.42	7.16	6.33	1.31	96.67	13.60	10.30	75.76	63.52	16.50
6	11.79	7.16	6.84	1.65	128.75	17.93	14.60	81.41	63.52	22.00
7	13.50	8.60	7.33	1.57	160.82	22.27	18.89	84.84	63.52	23.60
8	15.82	7.27	6.42	2.18	166.78	23.23	19.88	85.57	68.10	25.70
9	14.59	9.43	8.31	1.55	194.37	26.93	22.14	82.22	20.23	3.35
10	14.26	10.71	8.91	1.33	210.82	29.19	21.28	72.90	63.93	6.57
11	8.74	7.70	7.06	1.14	108.41	14.57	1.39	9.55	20.23	1.99
12	9.67	8.70	6.88	1.11	118.38	15.71	1.39	8.85	20.23	1.98
13	13.70	8.38	6.03	1.64	113.55	15.17	6.31	41.62	62.73	2.47
14	12.65	8.33	7.38	1.52	131.89	16.42	2.60	15.81	40.46	3.75
15	14.39	8.60	7.98	1.67	174.92	21.38	2.69	12.57	40.46	2.53
16	18.83	6.91	4.15	2.72	144.14	18.97	1.30	6.84	20.23	2.33
17	13.82	10.61	6.73	1.30	124.22	17.34	6.30	36.33	47.92	2.70
18	11.99	9.19	5.84	1.30	124.93	14.54	6.09	41.93	51.18	3.67
19	14.31	9.20	7.06	1.56	149.64	19.87	3.21	16.17	52.52	26.00
20	12.98	7.41	6.22	1.75	124.20	16.18	2.75	16.98	43.29	25.30
21	11.98	7.57	7.03	1.58	108.32	14.08	2.72	19.29	52.52	14.40
22	14.28	12.55	8.14	1.14	229.04	28.94	22.42	77.48	215.36	20.60
23	15.24	6.74	6.21	2.26	124.18	15.46	10.22	66.12	109.12	9.42
24	18.10	9.62	7.46	1.88	182.70	24.05	4.07	16.94	63.52	43.60
25	23.69	8.44	7.26	2.81	202.66	26.76	4.07	15.23	63.52	55.00

L- length; W- width; D- depth; RLW- ratio of length to width; Vol.- van der Waals volume; TSA- total surface area; HSA- hydrophilic surface area; PSA- polar surface area; DM- dipole moment; L,W,D, RLW, vol., TSA, HSA, % HSA, PSA, DM calculated using Molecular Modeling Pro.

Table A5. Molecular descriptor values for PFCs and other trace contaminants

Compound ID	nDB	nAB	nN	nArOH
1	1	0	0	0
2	1	0	0	0
3	1	0	0	0
4	1	0	0	0
5	2	0	0	0
6	2	0	0	0
7	2	0	0	0
8	2	0	1	0
9	0	0	0	0
10	2	0	1	0
11				
12	0	0	0	0
13	0	6	5	0
14	0	12	0	2
15	0	6	0	1
16	0	6	0	1
17	1	0	0	0
18	2	12	2	0
19	1	6	0	0
20	1	6	0	0
21	1	6	0	0
22	5	6	2	1
23	2	11	3	0
24	2	6	0	0
25	2	6	0	0

nDB- no. of double bonds; nAB- no. of aromatic bonds; nN- no. of primary and secondary amines; nArOH- no. of phenolic group (aromatic hydroxyls); calculated using E-dragon.

Table A2. Molecular descriptor values for PFCs and other trace contaminants

Compound ID	HOMO	LUMO	GAP	Polarizability at 7	Ui	logS	Hy
1	-12.30	-0.73	11.57	9.45	1.00	-3.48	0.25
2	-12.11	-1.20	10.91	13.62	1.00	-4.17	0.17
3	-11.10	-1.55	9.55	17.99	1.00	-4.29	0.12
4	-12.09	-1.45	10.64	19.98	1.00	-4.33	0.10
5	-12.09	-2.36	9.74	13.70	1.59	-3.20	0.26
6	-12.09	-2.34	9.75	18.11	1.59	-3.60	0.19
7	-10.44	-1.86	8.58	22.58	1.59	-3.84	0.14
8	-11.43	-2.08	9.35	23.00	1.59	-3.93	0.71
9	-11.53	-1.26	10.27	26.92	0.00	-4.04	0.05
10	-11.18	-2.10	9.07	32.16	1.59	-4.07	0.05
11	-10.44	3.19	13.63	20.25			
12	-10.22	3.34	13.56	22.19	0.00	-3.55	-0.35
13	-9.44	0.03	9.47	22.59	2.81	-3.90	0.69
14	-8.89	0.37	9.27	25.42	3.70	-3.42	0.30
15	-8.80	0.42	9.23	34.51	3.00	-4.64	0.17
16	-8.86	0.43	9.30	28.53	2.81	-5.30	-0.41
17	-11.52	-0.11	11.40	24.18	1.00	-1.64	-0.42
18	-8.61	-0.46	8.15	25.00	3.91	-3.19	0.32
19	-8.72	0.47	9.19	28.48	3.00	-3.95	-0.33
20	-9.38	0.20	9.58	23.34	3.00	-3.48	-0.33
21	-9.47	-0.17	9.29	20.37	3.00	-2.95	-0.17
22	-9.48	-0.81	8.67	43.09	3.59	-2.52	4.96
23	-9.11	-0.45	8.65	24.80	3.81	-2.74	1.37
24	-10.35	-0.86	9.49	37.15	3.17	-5.77	-0.34
25	-10.36	-0.87	9.49	41.42	3.17	-6.22	-0.37

HOMO- highest occupied molecular orbital; LUMO- lowest unoccupied molecular orbital; GAP- difference between LUMO and HOMO; U_i - unsaturation index; logS- log water solubility; H_y - hydrophilic index; HOMO, LUMO, GAP and polarizability at pH 7 calculated with HyperChem; U_i , log S and H_y calculated using E-dragon.

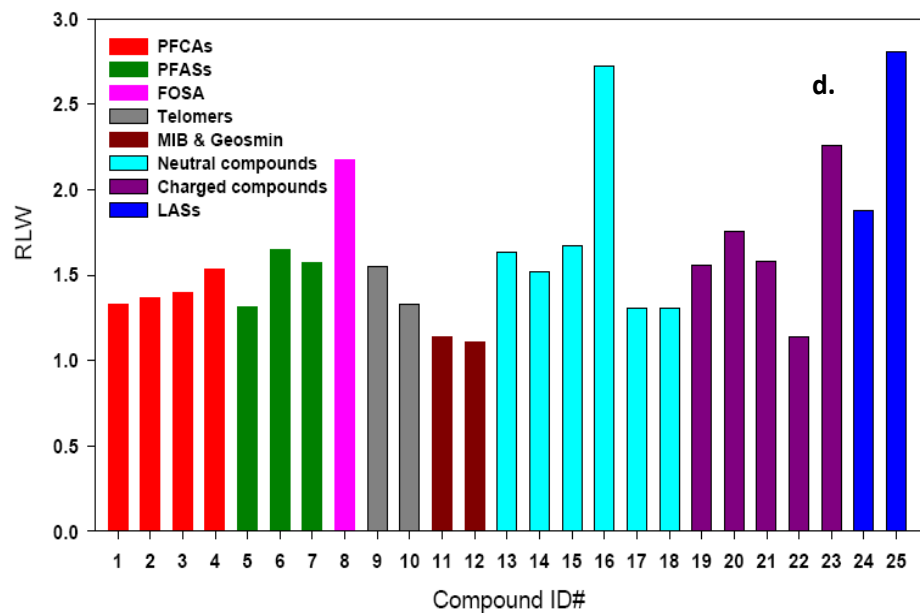
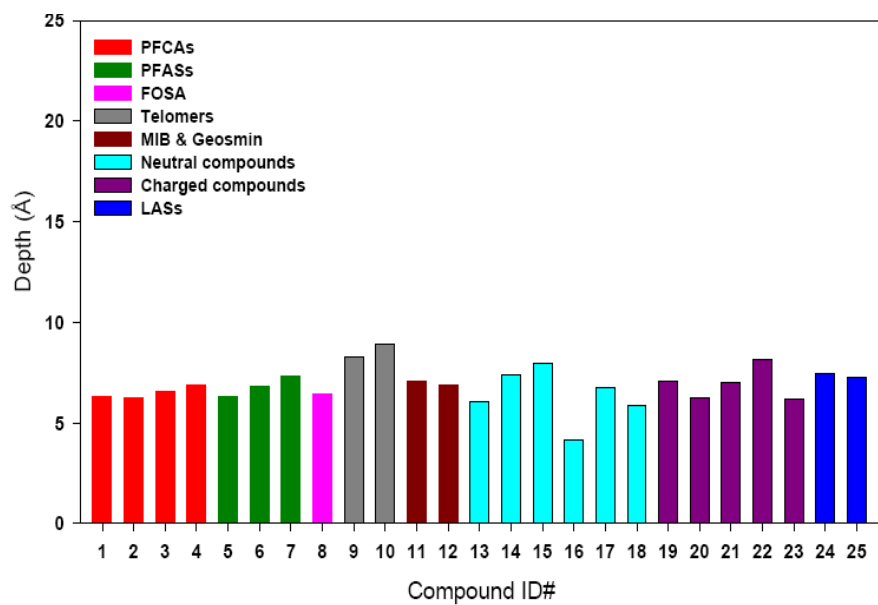
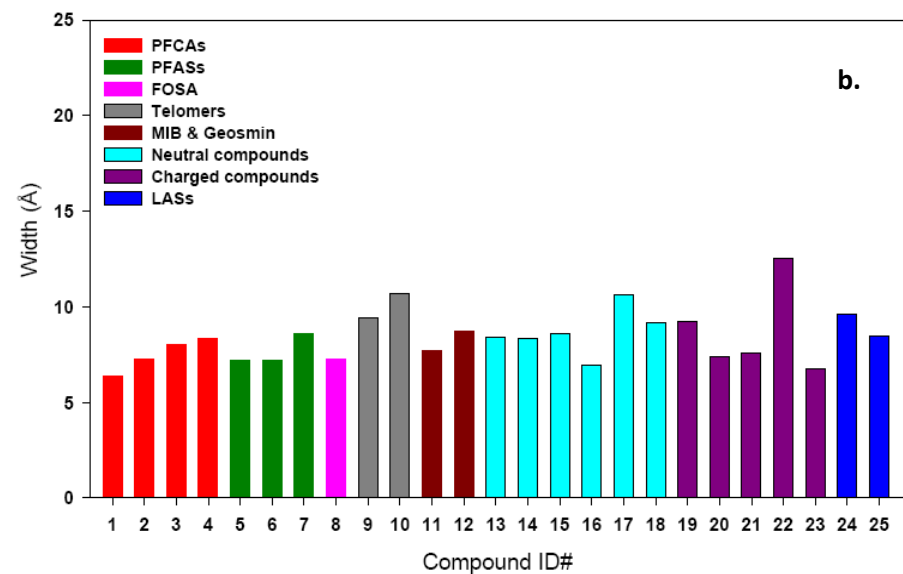
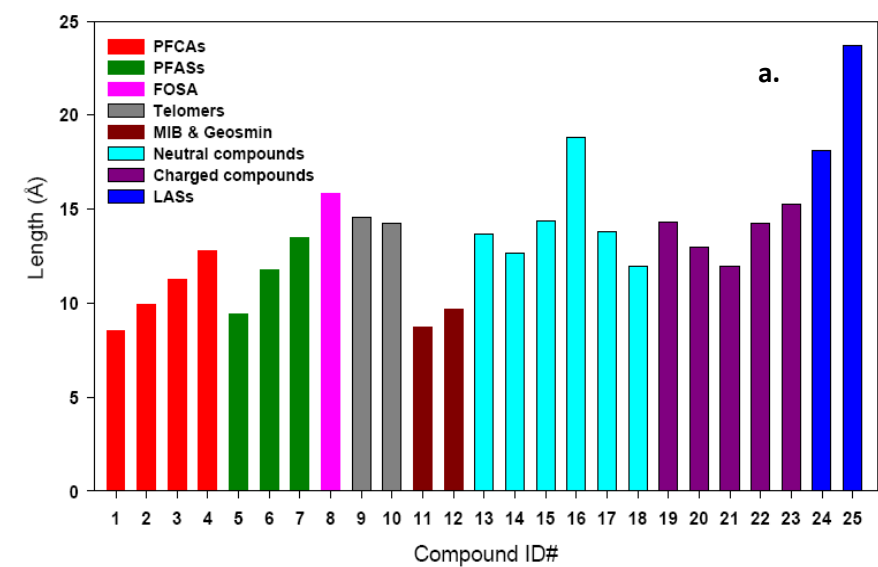


Figure A.1: Molecular dimensions of selected compounds; a. Length b. Width c. Depth d. Ratio of length to width (RLW); compound ID# can be found in Table A1.

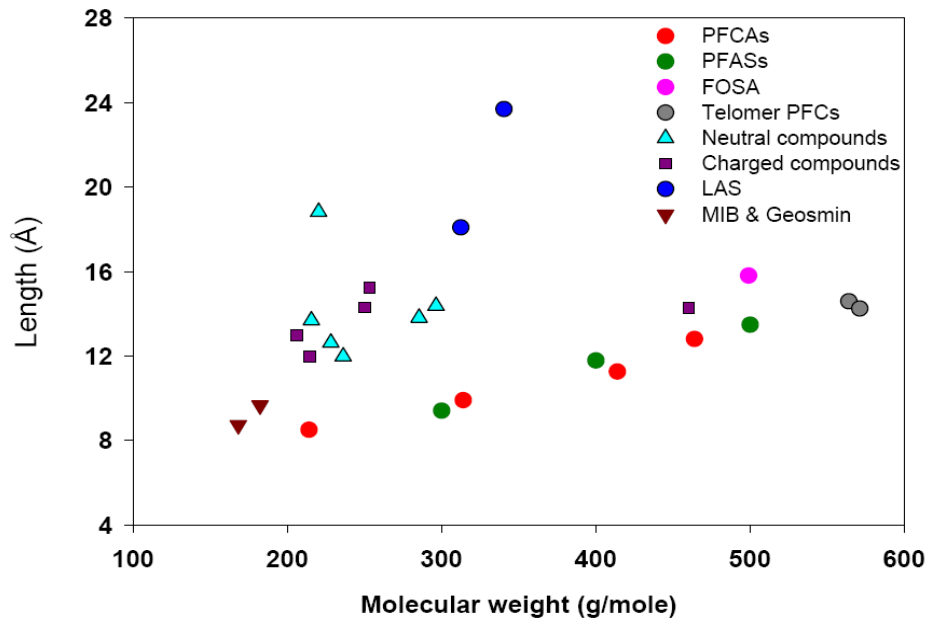


Figure A.2: Length vs molecular weight of selected compounds

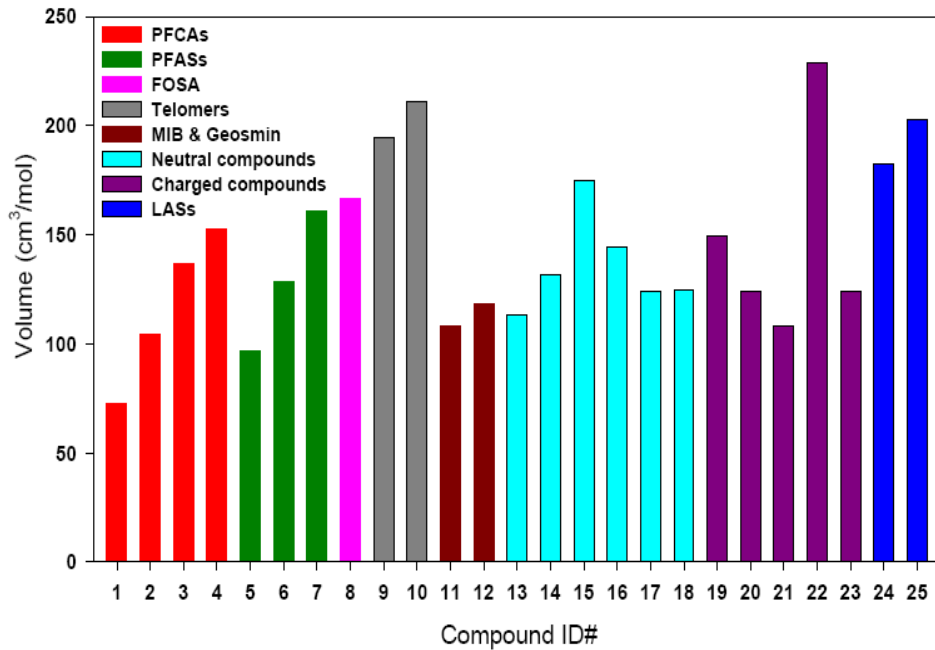


Figure A.3: van der Waals volume of selected compounds

The octanol/water partition co-efficient (K_{OW}) is the ratio of concentration of un-ionized compound between octanol and water. Its logarithm is known as $\log K_{OW}$ and is used as a measure of lipophilicity/hydrophobicity. However, for ionisable compounds $\log K_{OW}$ does not

consider the often-significant solubility of ionized species in the octanol phase. Thus, $\log D$ or the logarithm of distribution co-efficient of octanol/water is preferred for ionic compounds (Cunningham 2004). $\log D$ is pH dependent and the pH at which $\log D$ was calculated for must be specified. Thus for, non-ionisable compounds or neutral compounds $\log K_{OW} = \log D$. Figure A4 shows that the $\log K_{OW}$ of PFCs increases with increasing MW (i.e. carbon chain length). This trend is similar to that reported by Ahrens et al. (2010) who indicated that shorter chain PFCs are more soluble in water compared to the longer chain compounds. Telomer alcohols have high hydrophobicity as shown by their high $\log Kow$ values. However, as indicated above $\log D$ may be more appropriate representation of hydrophilicity of charged compounds. Typically, hydrophilicities of the charged compounds are much higher compared to their neutral species. As seen from Figure A5, $\log D$ values at pH 7 of charged PFCs are relatively lower than compounds with similar molecular weight, which indicates that PFCs in their charged state are more hydrophilic compared to the other selected compounds

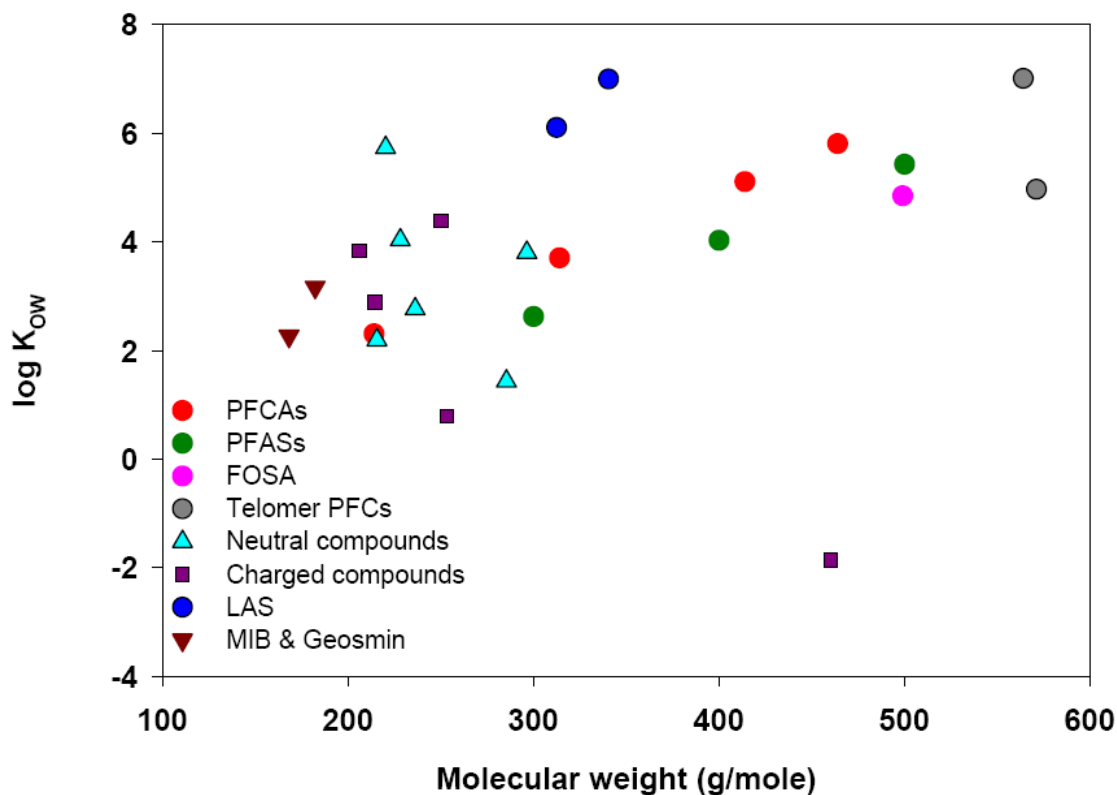


Figure A.4: $\log K_{OW}$ vs molecular weight

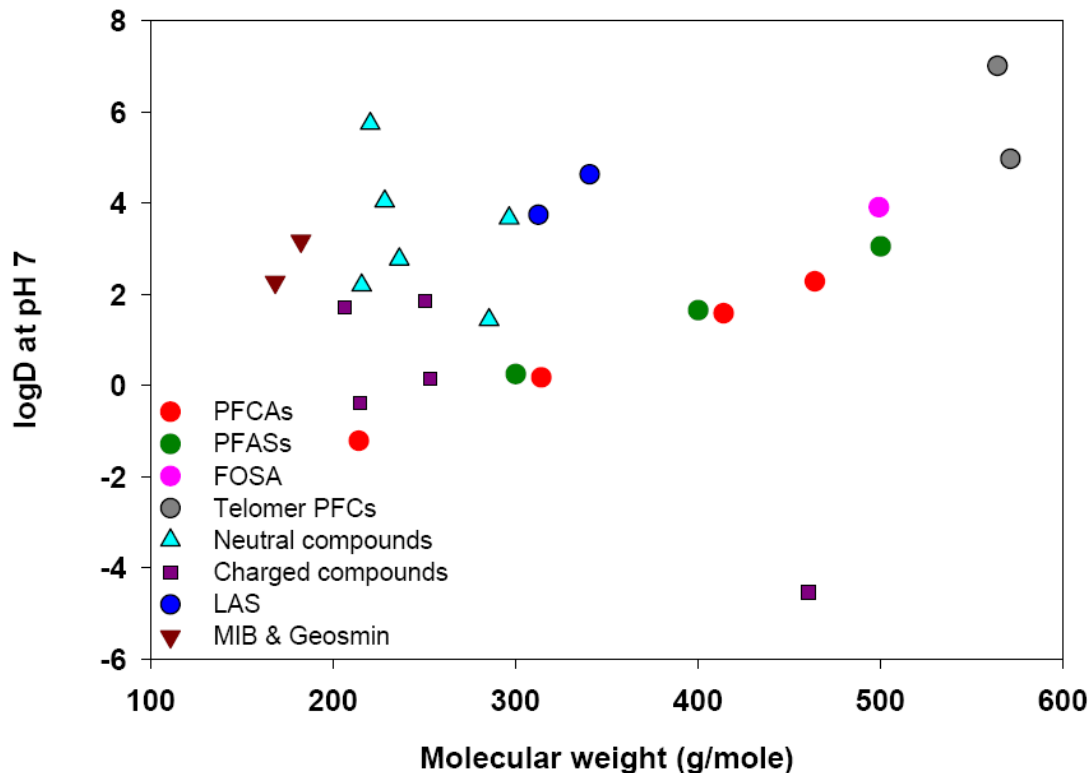


Figure A5: log D at pH 7 vs molecular weight

Removal efficiency of micropollutants is greatly affected by their properties even though individual removal mechanisms may vary considerably. Jin and Peldszus (2010) listed various descriptors relevant for chemical precipitation, oxidation, adsorption, and membrane filtration processes. The current project considered a primary list of treatment processes that included those that were studied by Jin and Peldszus (2010). The following discussion attempts to relate the observed PFCs descriptor values to their response to various forms of treatment by comparing them to descriptor values of other contaminants, where treatment behaviour is known.

As seen from Figure A6 and Figure A7 the hydrophilic surface area of PFCs is much higher compared to the other contaminants considered here. These values are also complemented by the logD values. Interestingly, neutral PFCs have higher logD values and a high hydrophilic surface area than charged PFCs. Previously Westerhoff et al. (2005) and Snyder et al. (2007) showed that a high hydrophobicity of micropollutants positively impacts their removal by coagulation/flocculation/sedimentation. Highly hydrophilic compounds are thus not expected to be removed via chemical precipitation. Thus PFCs due to their high hydrophilicity are probably

not amenable to conventional coagulation/flocculation/sedimentation. Hence chemical precipitation will not be considered for the current project.

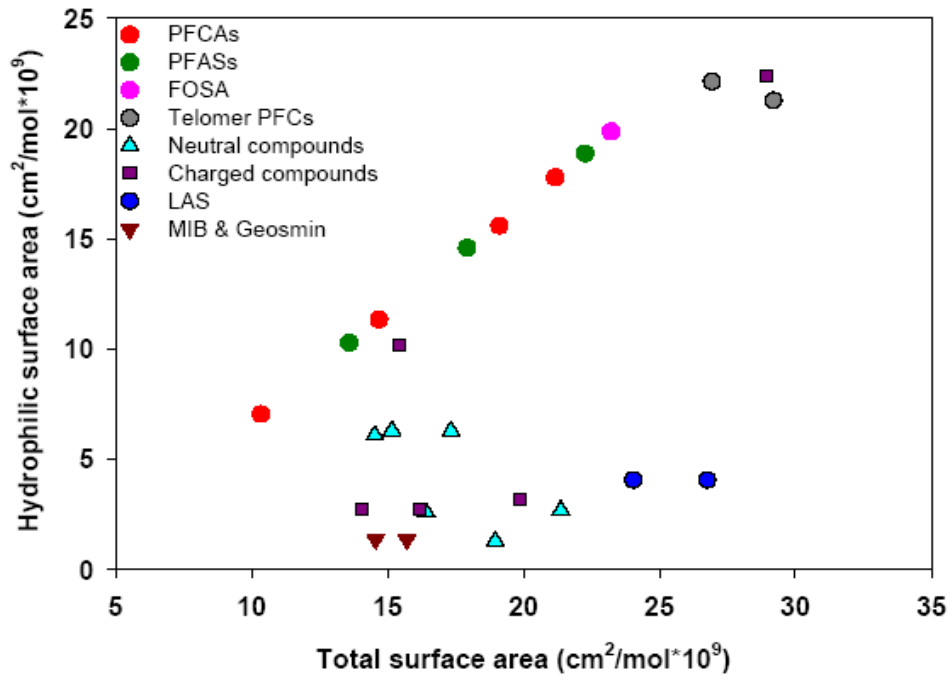


Figure A.6: Hydrophilic surface area vs total surface area

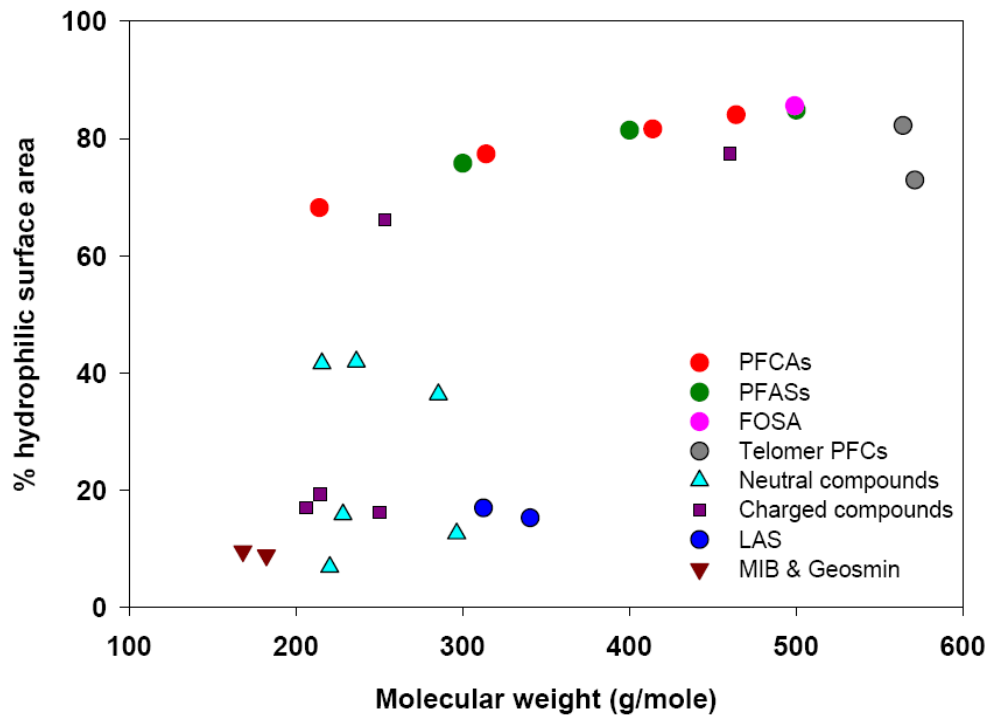


Figure A.7: % Hydrophilic surface area vs molecular weight

As mentioned earlier, O_3 in water leads to the presence of molecular ozone and hydroxyl radicals ($\cdot OH$) (von Gunten 2003). Molecular O_3 reaction is selective. The kinetics of O_3 reaction in water may vary greatly depending on the structure of micropollutants, system pH and the solution matrix. Second-order reaction rate constants can provide an indication of the reactivity of organic compounds with ozone and $\cdot OH$. O_3 rate constants depend on speciation and typically deprotonated species react faster with electrophilic O_3 as they are stronger nucleophils (Huber *et al.* 2003). Presence of functional groups with high electron density such as double bonds, activated aromatic systems, amino groups offer higher reactivity with O_3 . Aromatic systems that are activated by electron donor groups (e.g. $-OH$) may lead to increased reaction rate constants while presence of electron withdrawing groups (e.g. $-Cl$, $-NO_2$, $-COOH$) may lower reactivity. Reactivity of protonated and neutral forms of amines is significantly lower compared to deprotonated amines. Carbamazepine and EE2 displayed high reactivity towards ozone due to the presence of a double bond and an activated aromatic system in their structures, respectively (Mcdowell *et al.* 2005, Huber *et al.* 2003). Sulfamethoxazol has higher reaction rate constants at $pH > 5$ since at those pH values the amino group present in its structure becomes deprotonated. Saturated ring structures of MIB and gesomin are thought to be responsible for poor reaction potential of these two compounds with O_3 (von Gunten 2003). Lack of reactive groups and presence of slightly activated aromatic ring have been attributed for the low second order reaction rate constant of ibuprofen (Huber *et al.* 2003). PFCs are aliphatic molecules with strong saturated C—F bonds. Hence, the number of aromatic bonds (n_{AB}) for the target PFCs is zero as well as the number of phenolic group (n_{ArOH}) is zero (Table A3 in). Presence of electron withdrawing functional groups $-COOH$ and $-SO_3H$ in the structures of PFCAs and PFASs, respectively indicate that those compounds will probably be recalcitrant to O_3 . Also except for FOSA ($n_N=1$), none of the considered PFCs contains amino groups ($n_N=0$) (Table A3 in). At the typical drinking water treatment pH range, FOSA (estimated pK_a 3.32) will be charged and will contain a deprotonated amino group, and hence FOSA may exhibit some reactivity towards O_3 . Presence of electron withdrawing groups, strong C—F bonds together with a lack of activated aromatic systems thus indicate that the second order reaction rate constants of PFCs with O_3 will likely be low.

Quantum-chemical descriptors HOMO, LUMO and GAP are thought to be directly linked to reaction energy. While HOMO is associated with the negative ionization potential, LUMO indicates negative electron affinity. The greater their energy difference or the higher the GAP, the greater the kinetic stability and the lower the reactivity of a compound. Figure A8 compares the HOMO and GAP values of the selected compounds. Clearly PFCs have lower HOMO and higher GAP values compared to most of the other conventional contaminants. This can be related to the ozone reactivity of PFCs. For example: Carbamazepine, sulfamethoxazole and gemfibrozil have low GAP and high HOMO values. Previously Westerhoff *et al.* (2005) showed that these compounds are very easily oxidized with ozone. Ibuprofen and atrazine have higher GAP and lower HOMO values compared to those three compounds and exhibit low to moderate removal with ozone. TCEP has similar quantum descriptor values as those of the PFCs. TCEP like PFCs is aliphatic and Westerhoff *et al.* (2005) observed very low (<5%) removal of TCEP during oxidative treatments. Based on the quantum-descriptor values and the previously outlined reasons it is thus hypothesized that oxidation potential of PFCs are likely to be very low. This is consistent with Schroder and Meesters (2004) who did not observe any appreciable removal of PFCs during their oxidation study with various AOPs. They found that often oxidants transform precursor compounds such as telomer alcohols to terminal PFCs namely PFOA and PFOS. Hence the current project will also exclude ozonation and advanced oxidation processes from the preliminary treatment studies.

carbamazepine than sulfamethoxazole which has a higher dipole moment than carbamazepine. Figure A.9 compares the dipole moment values of PFCs to those of contaminants. The plot shows that PFCs have higher dipole moment than contaminants within a similar MW range. FOSA has a slightly higher dipole moment value than PFOS. Stainle-Darling and Reinhard (2008) reported lower rejection of FOSA compared to PFOS. Telomer alcohols have low dipole moment values, high MW and high log K_{OW} values, and hence may exhibit higher rejection during membrane filtration.

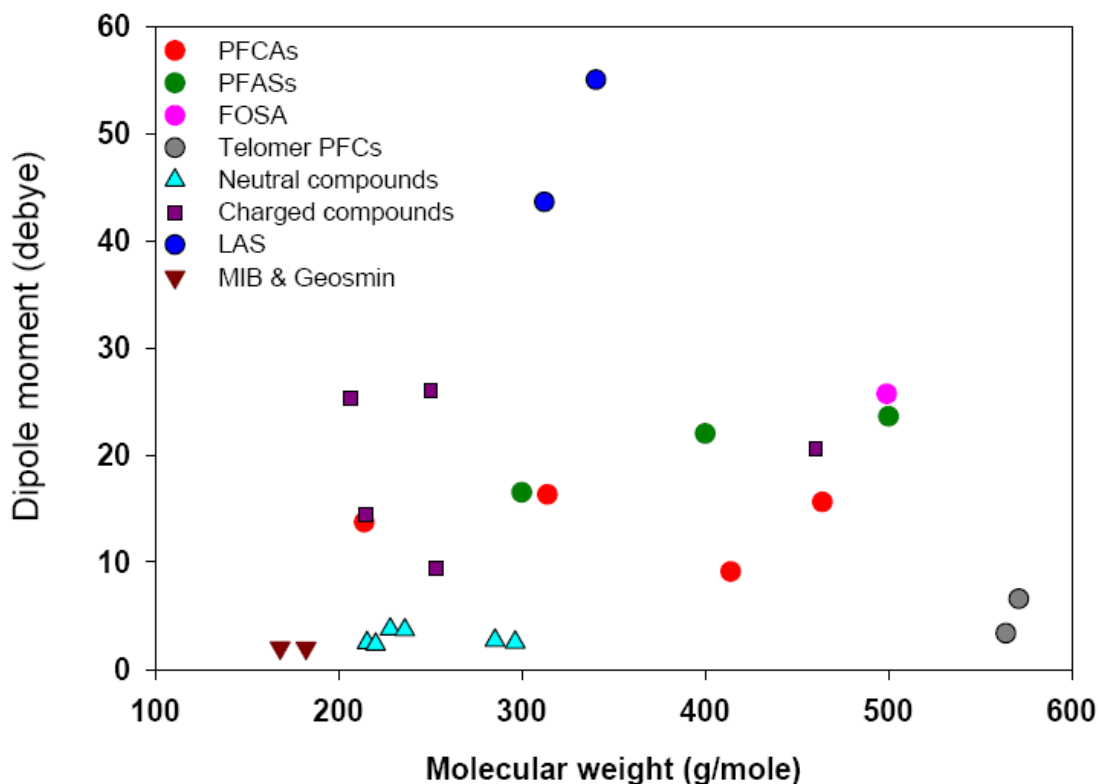


Figure A.9: Dipole moment vs molecular weight

Based on the above discussion it can be presumed that the calculated PFC descriptor values could be used to explain different removal mechanisms.

APPENDIX-B

Blood Serum Half-life of Selected PFCs and Reported Drinking Water Occurrence of PFOA and PFOS

Table B1 : Comparative serum half-life of selected PFAAs

Species	PFSAs			PFCAs		
	PFBS (C4)	PFHxS (C6)	PFOS (C8)	PFBA (C4)	PFOA (C8)	PFNA (C9)
Rainbow Trout		10 d ^a	12 d ^a		4.5 d ^a	
Rats			7 d ^c	1.8 h ^e (♀)	2-4 h ^c (♀)	2 d ^c (♀)
				9.2 h ^e (♂)	6-7 d ^c (♂)	31 d ^c (♂)
Mouse				3.1 h ^e (♀)	17 d ^b (♀)	
				16.3 h ^e (♂)	19 d ^b (♂)	
Rabbit					7 h ^b (♀)	
					5.5 h ^b (♂)	
Dog					8-13 d ^f (♀)	
					20-23 d ^f (♂)*	
Monkeys	3.5-4 d ^b	87 d ^c (♀)	150 d ^c	41 h ^e (♀)	21 d ^f (♀)	
		141 d ^c (♂)		40.3 h ^e (♂)	33 d ^f (♂)	
Humans	1 month ^b	8.5 yr ^d	5.4 yr ^d	3.63 d ^e (♀)	2.9-8.5 yr ^g	
				3.0 d ^e (♂)		

^aMartin et al. (2003); ^bLau et al. (2007); ^cUSEPA (2009a) ^dOlsen et al. (2007); ^eChang et al. 2008;

^fButenhoff et al. (2004); Seals et al. (2011).

♀-female, ♂-male; * values were reported in hours by Butenhoff et al. (2004)

Table B2. Reported concentrations of PFOS/PFOA in drinking water

Region	Country	PFOS (ng/L)	PFOA (ng/L)	Remarks/site of maximum concentration	Reference
Asia	China	1.5-13.2	1.1-109	PFOS-Kunming, Yennan; PFOA- Hangzhou, Zhejiang	Lien et al. 2006
		0.04-11	0.44-78	PFOS- Shenzhen PFOA-Shanghai	Mak et al. 2009
		<0.1-14.8	<0.1-45.9	Shenzhen	Jin et al. 2009
	India	<0.3-8.4	<0.005-2.0	Chennai	Mak et al. 2009
	Malaysia	0.1	0.1	Kota Kinablu; detected at one site	
	Thailand	0.1-1.9	0.2-4.6	Bangkok	Kunacheva et al. 2010
		0.18	3.6	Mean value of tap water samples from Bangkok	
		0.22	10.55	Mean value of bottled water samples from Bangkok	
	Korea	<0.33-3.6	<0.33-33	Other detected PFASs include PFBS, PFHxS, PFHpA, PFNA etc.; Total PFASs ranged from <0.33-61 ng/L; maximum at Busan	Kim et al. 2011
	Japan	<0.1-22	2.3-84	Osaka	Takagi et al. 2008
		1.3-3.7	6.5-48	Osaka	Takagi et al. 2011
		<0.3- 50.9	Not measured	10 of 14 samples had concentrations <4 ng/L; Kinuta waterworks, Setagaya	Harada et al. 2003
		0.03- 12.0	0.7-40.0	Osaka	Saito et al. 2004
		0.1-6.8	0.3-37.5	PFOS- Kotohira; PFOA- Takatsuki, Osaka	Lien et al. 2006
		0.07-1.6	0.18-18	Osaka	Mak et al. 2009
3.9-9.4		12.0-47.5	Water utilities downstream of Yodo river basin	Shivakoti et al. 2010	
Americas	Canada	3.3	2.1	Niagara on the Lake; mean of 5 samples	Mak et al. 2009
			0.2	Calgary and Vancouver	Lien et al. 2006
		2-12	3-32	Detroit River watershed; Water treatment plants located at Windsor, ON and Detroit, MI	Taber et al. 2010
	USA	Not measured	1500-7200	Little Hocking, West Virginia; DuPont plant was considered as the point source of contamination	Emmett et al. 2006
		42-63	25-29	Columbus, Georgia; several users of 3M fluoro chemicals within the immediate vicinity	3M 2001

Region	Country	PFOS (ng/L)	PFOA (ng/L)	Remarks/site of maximum concentration	Reference
		<1.0-57	<5.0-30	PFOA- Clayton County, Georgia PFOS-Los Angeles County, California	Quinones and Snyder 2009
		1.4	1.2	Albany, New York; mean of 5 samples	Mak et al. 2009
	Brazil	0.58-6.70	0.35-2.82	Tijuca	Quinete et al. 2009
Europe	Spain	<0.12-58.12	<0.85-57.43	Barcelona	Ericson et al. 2009
		0.39-0.87	0.32-6.28	PFOS- Tarragona; PFOA-Valls	Ericson et al. 2008
		1.81	2.40	Mean; PFBA: 1.09 ng/L; Catalonia	Domingo et al. 2012
		6.9-71	<4.2-30	Llobregat river water (2008-09)	Flores et al. 2013
		3.0-21*	<4.2-5.5*	Llobregat river water (2010-12)	
	Poland	0.10-0.11	<0.005-0.013	Cdausk	Mak et al. 2009
	Norway	0.57	2.20	Linear PFOS and PFOA constituted 70% and 100%, respectively of the total PFOS and PFOA detected.	Ullah et al. 2011
	UK	16-130	27-263	PFOS- Cambridge; PFOA- Norwich	Atkinson et al. 2008
	Italy	6.20-9.7	1.0-2.9	Raw water from Lake Maggiore	Loos et al. 2007
		6.92	4.92	Linear PFOS and PFOA constituted 74% and 90%, respectively of the total PFOS and PFOA.	Ullah et al. 2011
	Germany	2-22	5-519	PFOS-Hagen, Ruhr area PFOA-Neheim, Ruhr area	Skutlarek et al. 2006
		0.85	0.30	Linear PFOS and PFOA constituted 71% and 100% respectively of the total PFOS and PFOA.	Ullah et al. 2011
		15	23	Reported concentrations are median concentrations. PFBA concentration 19 ng/L; This study is one of the most extensive drinking water PFAS occurrence studies to date	Wilhelm et al. 2010
Belgium	2.71	2.70	PFBS detected at 2.91 ng/L and PFHxA at 3 ng/L. Linear PFOS	Ullah et al. 2011	

Region	Country	PFOS (ng/L)	PFOA (ng/L)	Remarks/site of maximum concentration	Reference
				and PFOA constituted 100% and 64%, respectively of the total PFOS and PFOA.	
	Netherlands	0.40-0.86	5.66-8.56	PFBS and PFHxA detected at concentrations 18.8 ng/L and 5.15 ng/L. Branched isomers constituted over 20% of the total PFOA and PFOS detected.	Ullah et al. 2011
		<0.23	3.6-6.7	PFBA and PFBS detected at mean concentrations 30 ng/L and 20 ng/L, respectively. Branched isomers detected in finished water.	Eschauzier et al. 2012
	France	3 [6]	2 [3]	Mean value when source was surface water; values in parenthesis indicate mean when source was ground water; mean PFBA concentration was 6 ng/L for surface water sources.	Boiteux et al. 2012
	Sweden	8.81	6.18	Linear PFOS and PFOA constituted 68% and 92%, respectively of the total PFOS and PFOA detected.	Ullah et al. 2011
		0.3-0.8	1.3	Orebro; PFOA detected only at site 1	Lien et al. 2006
Oceania	Australia	0-16	0-9.7	PFOA : North Richmond, NSW PFOS: Glununga, SA	Thompson et al. 2011

* Final treated water was a blend of 50% conventional and 50% advanced treatment containing RO system

References

3M 2001. Environmental monitoring – multi-city study; water, sludge, sediment, POTW effluent and landfill leachate samples. Accessed August/11 2011. http://www.ewg.org/files/multicity_full.pdf

Atkinson, C., Blake, S., Hall, T., Kanda, R., Rumsby, P. 2008. Survey of the prevalence of perfluorooctane sulphonate (PFOS), perfluorooctanoic acid (PFOA) and related compounds in drinking water and their sources. Report DEFRA 7585, Drinking Water Inspectorate, Department for Environment, Food & Rural Affairs, London, UK [online] Accessed August/15 2011. http://dwi.defra.gov.uk/research/completed-research/reports/DWI70_2_212PFOS.pdf

Boiteux, V., Dauchy, X., Rosin, C., Munoz, J. -. 2012. National Screening Study on 10 Perfluorinated Compounds in Raw and Treated Tap Water in France. *Archives of Environmental Contamination and Toxicol.* 63, 1-12.

Butenhoff, J.L, Kennedy,G.L, Hinderliter, P.M., Lieder, P.H. Jung, R, Hansen, K.J., G. S. Gorman, G.S., Noker, P. E., Thomford, P. J. 2004. Pharmacokinetics of Perfluorooctanoate in Cynomolgus Monkeys. *Toxicol. Sci.* 82, 394-406.

Chang, S.-C., Das, K., Ehresman, D.J., Ellefson, M.E., Gorman, G.S., Hart, J.A., Noker, P.E., Tan, Y.-M., Lieder, P.H., Lau, C., Olsen, G.W., Butenhoff, J.L. 2008. Comparative pharmacokinetics of perfluorobutyrate in rats, mice,monkeys, and humans and relevance to human exposure via drinking water. *Toxicol. Sci.* 104(1), 40-53.

Domingo, J. L., Ericson-Jogsten, I., Perello, G., Nadal, M., Van Bavel, B., Karrman, A. 2012 Human Exposure to Perfluorinated Compounds in Catalonia, Spain: Contribution of Drinking Water and Fish and Shellfish. *J. Agriculture and Food Chemistry* 60(17), 4408-4415.

Emmett, E. A., Shofer, F. S., Zhang, H., Freeman, D., Desai, C., Shaw, L. M. 2006. Community exposure to perfluorooctanoate: Relationships between serum concentrations and exposure sources. *J. Occupational and Environmental Medicine* 48(8), 759-770.

Ericson, I., Domingo, J. L., Nadal, M., Bigas, E., Llebaria, X., van Bavel, B., Lindstrom, G. 2009. Levels of Perfluorinated Chemicals in Municipal Drinking Water from Catalonia, Spain: Public Health Implications. *Archives of Environmental Contamination and Toxicol.* 57(4), 631-638.

Ericson, I., Nadal, M., van Bavel, B., Lindstrom, G., Domingo, J. L. 2008. Levels of perfluorochemicals in water samples from Catalonia, Spain: is drinking water a significant contribution to human exposure? *Environmental Science and Pollution Res.* 15(7), 614-619.

Eschauzier, C., Beerendonk, E., Scholte-Veenendaal, P., De Voogt, P. 2012. Impact of treatment processes on the removal of perfluoroalkyl acids from the drinking water production chain. *Environ. Sci. Technol.* 46(3), 1708-15.

Flores, C., Ventura, F., Martin-Alonso, J., Caixach, J. 2013. Occurrence of perfluorooctane sulfonate (PFOS) and perfluorooctanoate (PFOA) in N.E. Spanish surface water and their removal in a drinking water treatment plant that combines conventional and advanced treatment in parallel lines. *Sci. Total Environ.* 461-462, 618-626.

Harada, K., Saito, N., Sasaki, K., Inoue, K., Koizumi, A. 2003. Perfluorooctane sulfonate contamination of drinking water in the Tama River, Japan: Estimated effects on resident serum levels. *Bulletin of Environmental Contamination and Toxicol.* 71(1), 31-36.

Jin, Y. H., Liu, W., Sato, I., Nakayama, S. F., Sasaki, K., Saito, N., Tsuda, S. 2009. PFOS and PFOA in environmental and tap water in China. *Chemosphere* 77(5), 605-611.

Kim, S. -, Kho, Y. L., Shoeib, M., Kim, K. -, Kim, K. -, Park, J. -, Shin, Y. 2011. Occurrence of perfluorooctanoate and perfluorooctanesulfonate in the Korean water system: Implication to water intake exposure. *Environmental Pollution* 159(5), 1167-1173.

Kunacheva, C., Fujii, S., Tanaka, S., Boontanon, S. K., Poothong, S., Wongwatthana, T., Shivakoti, B. R. 2010. Perfluorinated compounds contamination in tap water and bottled water in Bangkok, Thailand. *J. Water Supply Research and Technology-Aqua* 59(5), 345-354.

Lau, C., Anitole, K., Hodes, C., Lai, D., Pfahles-Hutchens, A., Seed, J. 2007. Perfluoroalkyl acids: A review of monitoring and toxicological findings. *Toxicol. Sci.* 99(2), 366-394.

Lien, N. P. H., Fujii, S., Takana, S., Nozoe, M., Wirojanagud, W., Anton, A., Lindstrom, G. 2006. Perfluorinated substances in tap water of Japan and several countries and their relationship to surface water contamination. *Environmental Engineering Research* 43, 611–618.

Loos, R., Wollgast, J., Huber, T., Hanke, G. 2007. Polar herbicides, pharmaceutical products, perfluorooctanesulfonate (PFOS), perfluorooctanoate (PFOA), and nonylphenol and its carboxylates and ethoxylates in surface and tap waters around Lake Maggiore in Northern Italy. *Analytical and Bioanalytical Chemistry* 387(4), 1469-1478.

Mak, Y. L., Taniyasu, S., Yeung, L. W. Y., Lu, G., Jin, L., Yang, Y., Lam, P. K. S., Kannan, K., Yamashita, N. 2009. Perfluorinated Compounds in Tap Water from China and Several Other Countries. *Environ. Sci. Technol.* 43(13), 4824-4829.

Martin, J., Mabury, S., Solomon, K., Muir, D. 2003. Bioconcentration and tissue distribution of perfluorinated acids in rainbow trout (*Oncorhynchus mykiss*). *Environ. Toxicol. Chem.* 22(1), 196-204.

Olsen, G. W., Burris, J. M., Ehresman, D. J., Froehlich, J. W., Seacat, A. M., Butenhoff, J. L., Zobel, L. R. 2007. Half-life of serum elimination of perfluorooctanesulfonate, perfluorohexanesulfonate, and perfluorooctanoate in retired fluorochemical production workers. *Environ. Health Perspect.* 115(9), 1298-1305.

Quinete, N., Wu, Q., Zhang, T., Yun, S. H., Moreira, I., Kannan, K. 2009. Specific profiles of perfluorinated compounds in surface and drinking waters and accumulation in mussels, fish, and dolphins from southeastern Brazil. *Chemosphere* 77(6), 863-869.

Quinones, O. and Snyder, S. A. 2009. Occurrence of Perfluoroalkyl Carboxylates and Sulfonates in Drinking Water Utilities and Related Waters from the United States. *Environ. Sci. Technol.* 43(24), 9089-9095.

Saito, N., Harada, K., Inoue, K., Sasaki, K., Yoshinaga, T., Koizumi, A. 2004. Perfluorooctanoate and perfluorooctane sulfonate concentrations in surface water in Japan. *J. Occupational Health* 46(1), 49-59.

Seals, R., Bartell, S.M., Steenland, K. 2011. Accumulation and clearance of perfluorooctanoic acid (PFOA) in current and former residents of an exposed community. *Environ. Health Perspect.* 119(1), 119-124.

Shivakoti, B. R., Fujii, S., Nozoe, M., Tanaka, S., Kunacheva, C. 2010. Perfluorinated chemicals (PFCs) in water purification plants (WPPs) with advanced treatment processes. *Water Sci. Technol. Water Supply* 10(1), 87-95.

Skutlarek, D., Exner, M., Faerber, H. 2006. Perfluorinated surfactants in surface and drinking water. *Environmental Science and Pollution Research* 13(5), 299-307.

Tabe, S., Yang, P., Zhao, X., Hao, C., Seth, R., Schweitzer, L., Jamal, T. 2010. Occurrence and Removal of PPCPs and EDCs in the Detroit River Watershed. *Water Sci. Technol.* 5(1), 1-8.

Takagi, S., Adachi, F., Miyano, K., Koizumi, Y., Tanaka, H., Watanabe, I., Tanabe, S., Kannan, K. 2011. Fate of Perfluorooctanesulfonate and perfluorooctanoate in drinking water treatment processes. *Water Res.*45(13), 3925-3932.

Takagi, S., Adachi, F., Miyano, K., Koizumi, Y., Tanaka, H., Mimura, M., Watanabe, I., Tanabe, S., Kannan, K. 2008. Perfluorooctanesulfonate and perfluorooctanoate in raw and treated tap water from Osaka, Japan. *Chemosphere* 72(10), 1409-1412.

Thompson, J., Eaglesham, G., Mueller, J. 2011. Concentrations of PFOS, PFOA and other perfluorinated alkyl acids in Australian drinking water RID C-6241-2008. *Chemosphere* 83(10), 1320-1325.

Ullah, S., Alsberg, T., Berger, U. 2011. Simultaneous determination of perfluoroalkyl phosphonates, carboxylates, and sulfonates in drinking water. *J. Chromatography A* 1218(37), 6388-6395.

USEPA 2009a. *Long-chain Perfluorinated Chemicals (PFCs)-Action Plan*. Accessed 09/27 2013. http://www.epa.gov/opptintr/existingchemicals/pubs/pfcs_action_plan1230_09.pdf.

Wilhelm, M., Bergmann, S., Dieter, H. H. 2010. Occurrence of perfluorinated compounds (PFCs) in drinking water of North Rhine-Westphalia, Germany and new approach to assess drinking water contamination by shorter-chained C4-C7 PFCs RID D-9552-2011. *International J. Hygiene and Environmental Health* 213(3), 224-232.

APPENDIX- C

Properties of the Selected Adsorbents

Web Links to Product Data Sheet for the Studied Adsorbents

Norit C Gran

Source: http://www.norit.com/files/documents/CGRAN_rev8.pdf; accessed: 25 October, 2014

Filtrisorb 400 (F-400)

Source:

http://www.calgoncarbon.com/media/images/site_library/25_Filtrisorb_400_1019web.pdf;
accessed: 25 October, 2014

Nuchar WV-B30

Source: http://mwv.com/en-us/carbon-technologies/products/asset_upload_file264_9088.pdf;
accessed: 25 October, 2014

Product data sheet for Aquacarb CX 1230

Source:

http://www.evoqua.com/SiteCollectionDocuments/Product_Lines/Westates_Carbon/WS-AC1230CX-DS.pdf; accessed: 25 October, 2014

Purolite A-860

Source:

<http://www.purolite.com/Customized/CustomizedControls/PuroliteProductsManagement/PopupPage.aspx?RelID=619325&Action=ProductDataSheetPDF&LanguageID=®istered=1>;
accessed: 25 October, 2014

Purolite A-500P

Source:

<http://www.purolite.com/Customized/CustomizedControls/PuroliteProductsManagement/PopupPage.aspx?RelID=619325&Action=ProductDataSheetPDF&LanguageID=®istered=1>;
accessed: 25 October, 2014

Fija Fluor

Source:

<http://www.carbonapelsa.com.mx/pages/english/tfijafluore.html>; accessed: 25 October, 2014

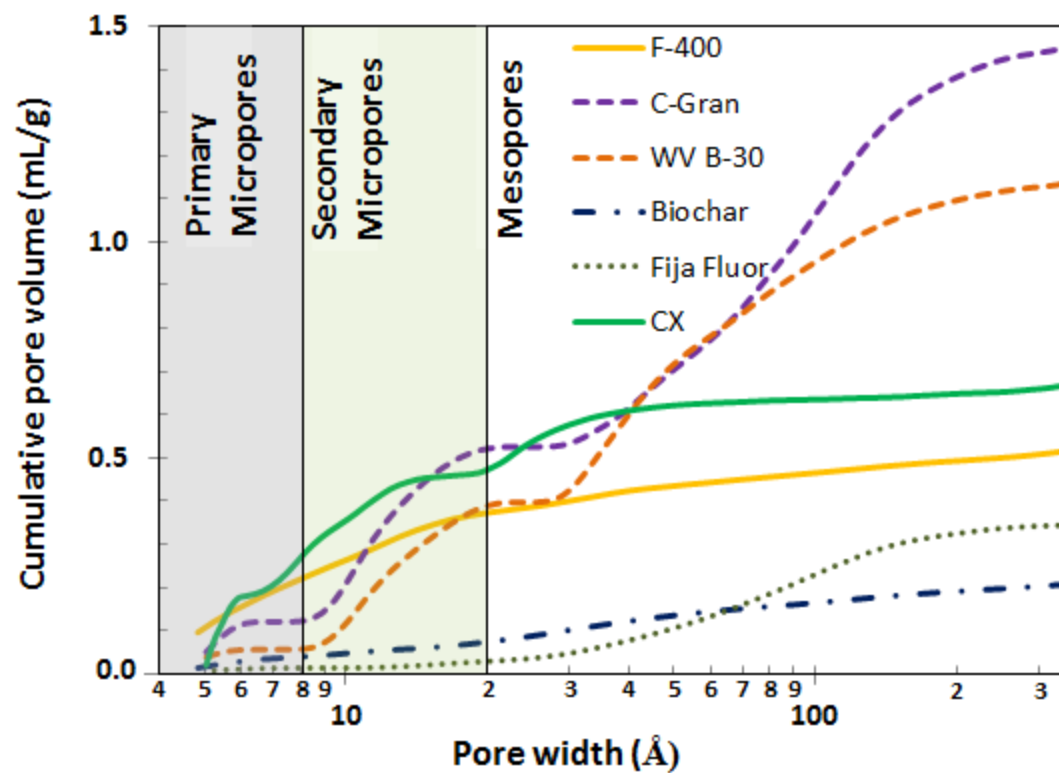


Figure C1: Cumulative pore volume distribution of the GACs and alternative adsorbents used in the current study

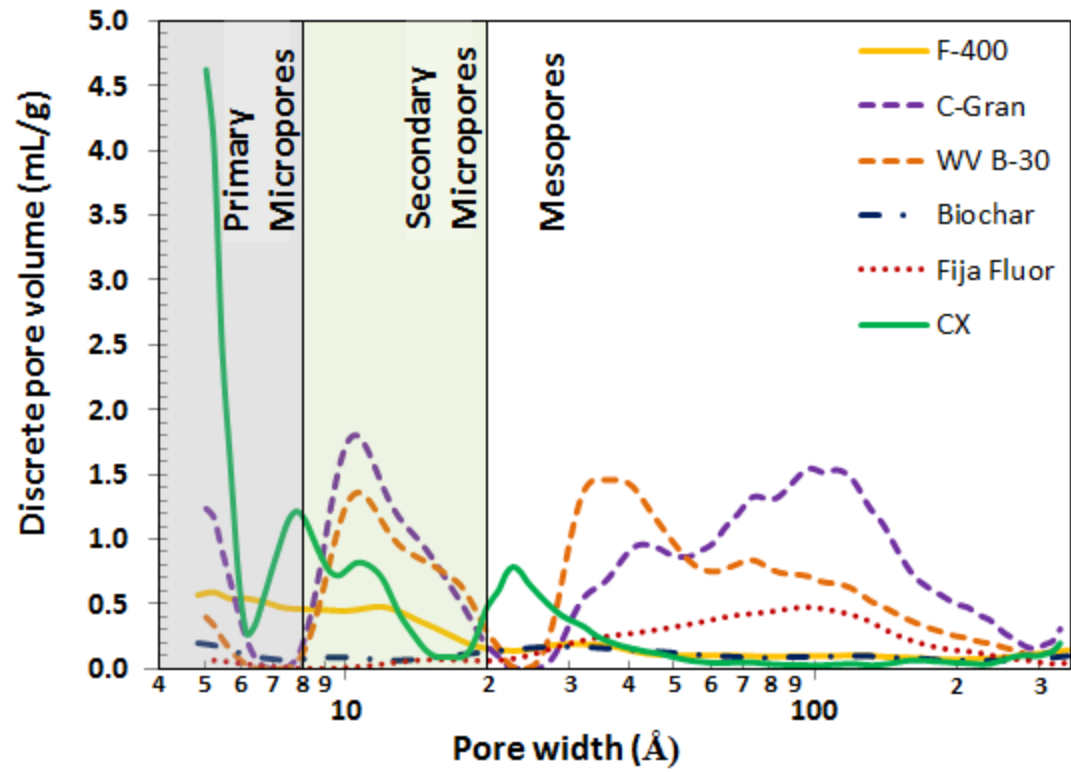


Figure C2: Discrete pore volume distribution of the GACs and alternative adsorbents used in the current study

Details of surface area and pore volume distribution analysis

1. Filtrasorb 400 (F-400)

Quantachrome® ASiQwin™ - Automated Gas Sorption Data
Acquisition and Reduction
© 1994-2013, Quantachrome Instruments
version 3.01



Analysis		Report					
Operator:	lab	Date:	2014/07/03	Operator:	ra	Date:	2014/08/11
Sample ID:	F-400	Filename:	University of Waterloo_F400_070314.qps				
Sample Desc:	Activated carbon	Comment:	University of Waterloo, Lab #4549				
Sample Weight:	0.0315 g	Instrument:	Autosorb iQ Station 1				
Outgas Time:	16.0 hrs	Outgas Temp.:	300 °C	CellType:	6mm w/o rod		
Analysis gas:	Nitrogen	Non-ideality:	6.58e-05 1/Torr	VoidVol Remeasure:	off		
Analysis Time:	30:50 hr:min	Bath temp.:	77.35 K	Warm Zone V:	8.25039 cc		
Analysis Mode:	Standard						
VoidVol. Mode:	He Measure	Cold Zone V:	6.11376 cc				

Multi-Point BET

Data Reduction Parameters Data

Adsorbate	Thermal Transpiration: on	Eff. mol. diameter (D): 3.54 Å	Eff. cell stem diam. (d): 4.0000 mm
	Nitrogen	Temperature 298.150K	
	Molec. Wt.: 28.013	Cross Section: 16.200 Å ²	Liquid Density: 0.806 g/cc

Multi-Point BET Data

Relative Pressure [P/Po]	Volume @ STP [cc/g]	1 / [W((Po/P) - 1)]	Relative Pressure [P/Po]	Volume @ STP [cc/g]	1 / [W((Po/P) - 1)]
9.02336e-03	195.4236	3.7280e-02	3.92911e-02	221.8808	1.4748e-01
1.00012e-02	197.0736	4.1015e-02	4.99157e-02	226.6923	1.8543e-01
2.13276e-02	210.1910	8.2955e-02	7.51901e-02	235.1808	2.7660e-01
2.92224e-02	216.1068	1.1145e-01			

BET summary

Slope = 3.612
Intercept = 5.286e-03
Correlation coefficient, r = 0.999983
C constant = 684.370
Surface Area = 962.621 m²/g



Analysis		Report			
Operator:	lab	Date:	2014/07/03	Date:	2014/08/11
Sample ID:	F-400	Filename:	University of Waterloo_F400_070314.qps		
Sample Desc:	Activated carbon	Comment:	University of Waterloo, Lab #4549		
Sample Weight:	0.0315 g	Instrument:	Autosorb iQ Station 1		
Outgas Time:	16.0 hrs	Outgas Temp.:	300 °C	CellType:	6mm w/o rod
Analysis gas:	Nitrogen	Non-ideality:	6.58e-05 1/Torr	VoidVol Remeasure:	off
Analysis Time:	30:50 hr:min	Bath temp.:	77.35 K	Warm Zone V:	8.25039 cc
Analysis Mode:	Standard				
VoidVol. Mode:	He Measure	Cold Zone V:	6.11376 cc		

DFT method Pore Size Distribution (log)

Data Reduction Parameters Data

DFT method	Thermal Transpiration: on	Eff. mol. diameter (D): 3.54 Å	Eff. cell stem diam. (d): 4.0000 mm
	Calc. Model: N2 at 77 K on carbon (slit pore, QSDFT equilibrium model)		
	Rel. press. range: 0.0000 - 1.0000		Moving pt. avg: 5
Adsorbate	Nitrogen	Temperature: 77.350K	Liquid Density: 0.806 g/cc
	Molec. Wt.: 28.013	Cross Section: 16.200 Å²	

DFT method Pore Size Distribution (log) Data

Pore width [Å]	Cumulative Pore Volume [cc/g]	Cumulative Surface Area [m²/g]	dV(log d) [cc/g]	dS(log d) [m²/g]
4.8400	9.5703e-02	4.2687e+02	5.6906e-01	2.1720e+03
5.2400	1.2054e-01	5.2316e+02	5.9059e-01	2.1428e+03
5.6700	1.4211e-01	6.0276e+02	5.4106e-01	1.8459e+03
6.1400	1.6105e-01	6.6610e+02	5.4267e-01	1.7177e+03
6.6600	1.8048e-01	7.2585e+02	5.2003e-01	1.5143e+03
7.2300	1.9822e-01	7.7583e+02	4.7763e-01	1.2840e+03
7.8500	2.1494e-01	8.1960e+02	4.6078e-01	1.1513e+03
8.5200	2.3176e-01	8.6067e+02	4.5906e-01	1.0548e+03
9.2600	2.4851e-01	8.9785e+02	4.5262e-01	9.3935e+02
10.0700	2.6462e-01	9.2995e+02	4.4720e-01	8.4503e+02
10.9600	2.8097e-01	9.6003e+02	4.6583e-01	8.1306e+02
11.9300	2.9886e-01	9.9051e+02	4.7976e-01	7.8038e+02
12.9900	3.1678e-01	1.0191e+03	4.4374e-01	6.7498e+02
14.1600	3.3278e-01	1.0428e+03	3.7804e-01	5.3373e+02
15.4300	3.4613e-01	1.0610e+03	3.1826e-01	4.1679e+02
16.8200	3.5778e-01	1.0759e+03	2.5326e-01	3.0710e+02
18.3400	3.6620e-01	1.0857e+03	1.8974e-01	2.0851e+02
20.0000	3.7270e-01	1.0925e+03	1.5665e-01	1.5568e+02
21.8300	3.7845e-01	1.0980e+03	1.4118e-01	1.2668e+02
23.8200	3.8363e-01	1.1025e+03	1.4066e-01	1.1273e+02
26.0000	3.8911e-01	1.1067e+03	1.6496e-01	1.1774e+02
28.3800	3.9583e-01	1.1114e+03	1.8860e-01	1.2384e+02
30.9900	4.0312e-01	1.1160e+03	1.9154e-01	1.1836e+02
33.8500	4.1049e-01	1.1205e+03	1.8662e-01	1.0874e+02
36.9800	4.1786e-01	1.1247e+03	1.7313e-01	9.4639e+01
40.3900	4.2447e-01	1.1283e+03	1.4087e-01	7.0506e+01
44.1300	4.2919e-01	1.1305e+03	1.1426e-01	5.0718e+01
48.2300	4.3346e-01	1.1323e+03	1.0701e-01	4.3027e+01
52.7000	4.3754e-01	1.1339e+03	1.0304e-01	3.7914e+01
57.6000	4.4150e-01	1.1353e+03	1.0214e-01	3.4261e+01
62.9600	4.4550e-01	1.1366e+03	1.0342e-01	3.1686e+01
68.8300	4.4956e-01	1.1378e+03	1.0088e-01	2.8352e+01
75.2400	4.5338e-01	1.1389e+03	9.5670e-02	2.4736e+01
82.2700	4.5708e-01	1.1398e+03	9.4646e-02	2.2437e+01
89.9500	4.6085e-01	1.1407e+03	9.7718e-02	2.0908e+01
98.3500	4.6470e-01	1.1415e+03	9.8502e-02	1.9076e+01
107.5500	4.6846e-01	1.1422e+03	9.7705e-02	1.7360e+01
117.6100	4.7228e-01	1.1428e+03	1.0324e-01	1.6883e+01
128.6100	4.7653e-01	1.1435e+03	1.0380e-01	1.5760e+01
140.6600	4.8050e-01	1.1441e+03	9.3441e-02	1.3067e+01
153.8300	4.8397e-01	1.1446e+03	8.7275e-02	1.1075e+01
168.2500	4.8742e-01	1.1450e+03	8.2566e-02	9.6743e+00
184.0200	4.9058e-01	1.1454e+03	7.1246e-02	7.6700e+00
201.2800	4.9313e-01	1.1456e+03	6.9704e-02	6.6600e+00
220.1600	4.9605e-01	1.1459e+03	7.8018e-02	6.7226e+00
240.8200	4.9916e-01	1.1461e+03	8.2465e-02	6.4144e+00
263.4300	5.0234e-01	1.1464e+03	9.4033e-02	6.6293e+00

Continued on next page



Analysis
 Operator: lab Date:2014/07/03
 Sample ID: F-400 Filename: University of Waterloo_F400_070314.qps Date:2014/08/11

Report
 Operator: ra
 University of Waterloo_F400_070314.qps


DFT method Pore Size Distribution (log) Data continued

Pore width [Å]	Cumulative Pore Volume [cc/g]	Cumulative Surface Area [m ² /g]	dV(log d) [cc/g]	dS(log d) [m ² /g]
288.1600	5.0631e-01	1.1467e+03	1.1305e-01	7.4529e+00
315.2200	5.1083e-01	1.1469e+03	1.2395e-01	7.5743e+00
344.8200	5.1645e-01	1.1473e+03	1.4408e-01	8.3586e+00

DFT method summary

Pore volume = 0.503 cc/g
 Surface area = 1095.182 m²/g
 Lower confidence limit = 4.840 Å
 Fitting error = 0.241 %
 Pore width (Mode(dLog)) = 5.240 Å
 Moving point average : 5

2. Aquacarb CX 1230

Quantachrome® ASiQwin™ - Automated Gas Sorption Data Acquisition and Reduction © 1994-2013, Quantachrome Instruments version 3.01					
Analysis		Report			
Operator:	lab	Date:	2014/07/24	Operator:	ra
Sample ID:	CX-1230	Filename:	University of Waterloo_CX-1230_Lab 4549_072414.qps		
Sample Desc:	Carbon	Comment:	University of Waterloo, Lab #4549		
Sample Weight:	0.0212 g	Instrument:	Autosorb iQ Station 1		
Outgas Time:	16.0 hrs	Outgas Temp.:	300 °C		
Analysis gas:	Nitrogen	Non-ideality:	6.58e-05 1/Torr	CellType:	6mm w/o rod
Analysis Time:	38:06 hr:min	Bath temp.:	77.35 K	VoidVol Remeasure:	off
Analysis Mode:	Standard	Cold Zone V:	5.98762 cc	Warm Zone V:	8.03141 cc
VoidVol. Mode:	He Measure				
Multi-Point BET					
Data Reduction Parameters Data					
Adsorbate	Thermal Transpiration: on		Eff. mol. diameter (D): 3.54 Å	Eff. cell stem diam. (d): 4.0000 mm	
	Nitrogen		Temperature 77.350K	Liquid Density: 0.806 g/cc	
	Molec. Wt.:	28.013	Cross Section: 16.200 Å ²		
Multi-Point BET Data					
Relative Pressure [P/Po]	Volume @ STP [cc/g]	1 / [W((Po/P) - 1)]	Relative Pressure [P/Po]	Volume @ STP [cc/g]	1 / [W((Po/P) - 1)]
9.99997e-03	314.4565	2.5701e-02	4.95887e-02	365.8067	1.1412e-01
2.12483e-02	335.8874	5.1714e-02	7.44584e-02	381.7010	1.6863e-01
3.02151e-02	347.6580	7.1705e-02	1.00234e-01	393.3431	2.2660e-01
4.04748e-02	358.1800	9.4227e-02			
BET summary					
		Slope =	2.216		
		Intercept =	4.244e-03		
		Correlation coefficient, r =	0.999976		
		C constant =	523.263		
		Surface Area =	1568.317 m ² /g		



Analysis			Report	
Operator:	lab	Date: 2014/07/24	Operator:	ra
Sample ID:	CX-1230	Filename:	University of Waterloo_CX-1230_Lab 4549_072414.qps	
Sample Desc:	Carbon	Comment:	University of Waterloo, Lab #4549	
Sample Weight:	0.0212 g	Instrument:	Autosorb iQ Station 1	
Outgas Time:	16.0 hrs	Outgas Temp.:	300 °C	
Analysis gas:	Nitrogen	Non-ideality:	6.58e-05 1/Torr	CellType: 6mm w/o rod
Analysis Time:	38:06 hr:min	Bath temp.:	77.35 K	
Analysis Mode:	Standard			VoidVol Remeasure: off
VoidVol. Mode:	He Measure	Cold Zone V:	5.98762 cc	Warm Zone V: 8.03141 cc

DFT method Pore Size Distribution (log)

Data Reduction Parameters Data

DFT method	Thermal Transpiration: on	Eff. mol. diameter (D): 3.54 Å	Eff. cell stem diam. (d): 4.0000 mm
	Calc. Model: N2 at 77 K on carbon (slit pore, QSDFT equilibrium model)		
	Rel. press. range: 0.0000 - 1.0000		Moving pt. avg: 5
Adsorbate	Nitrogen	Temperature 77.350K	
	Molec. Wt.: 28.013	Cross Section: 16.200 Å ²	Liquid Density: 0.806 g/cc

DFT method Pore Size Distribution (log) Data

Pore width [Å]	Cumulative Pore Volume [cc/g]	Cumulative Surface Area [m ² /g]	dV(log d) [cc/g]	dS(log d) [m ² /g]
5.2400	1.3299e-01	5.2740e+02	1.9731e+00	6.9596e+03
5.6700	1.9118e-01	7.3912e+02	1.2627e+00	4.3639e+03
6.1400	2.3718e-01	9.0019e+02	1.1148e+00	3.5860e+03
6.6600	2.7512e-01	1.0189e+03	9.5342e-01	2.7679e+03
7.2300	3.0493e-01	1.1002e+03	8.5182e-01	2.2264e+03
7.8500	3.3496e-01	1.1770e+03	8.7548e-01	2.1648e+03
8.5200	3.6812e-01	1.2580e+03	9.0478e-01	2.0974e+03
9.2600	4.0175e-01	1.3338e+03	8.6583e-01	1.8280e+03
10.0700	4.3197e-01	1.3951e+03	8.0382e-01	1.5304e+03
10.9600	4.6046e-01	1.4473e+03	8.2557e-01	1.4320e+03
11.9300	4.9231e-01	1.5011e+03	8.9134e-01	1.4333e+03
12.9900	5.2632e-01	1.5547e+03	8.6999e-01	1.3051e+03
14.1600	5.5797e-01	1.6010e+03	7.7943e-01	1.0874e+03
15.4300	5.8619e-01	1.6393e+03	6.8316e-01	8.9015e+02
16.8200	6.1137e-01	1.6713e+03	5.5252e-01	6.7248e+02
18.3400	6.3018e-01	1.6934e+03	3.9982e-01	4.4705e+02
20.0000	6.4330e-01	1.7075e+03	2.8971e-01	2.9607e+02
21.8300	6.5341e-01	1.7175e+03	2.1510e-01	2.0171e+02
23.8200	6.6062e-01	1.7239e+03	1.5955e-01	1.3582e+02
26.0000	6.6616e-01	1.7285e+03	1.3721e-01	1.0375e+02
28.3800	6.7131e-01	1.7322e+03	1.2759e-01	8.6701e+01
30.9900	6.7592e-01	1.7352e+03	1.1165e-01	7.0280e+01
33.8500	6.7999e-01	1.7377e+03	9.7978e-02	5.7795e+01
36.9800	6.8375e-01	1.7399e+03	8.6818e-02	4.8290e+01
40.3900	6.8712e-01	1.7417e+03	6.4855e-02	3.3322e+01
44.1300	6.8908e-01	1.7427e+03	4.4245e-02	1.9917e+01
48.2300	6.9064e-01	1.7433e+03	3.7962e-02	1.5444e+01
52.7000	6.9207e-01	1.7439e+03	3.4082e-02	1.2767e+01
57.6000	6.9334e-01	1.7444e+03	3.0706e-02	1.0539e+01
62.9600	6.9451e-01	1.7447e+03	2.8614e-02	8.9161e+00
68.8300	6.9561e-01	1.7451e+03	2.6841e-02	7.5704e+00
75.2400	6.9661e-01	1.7453e+03	2.5304e-02	6.4923e+00
82.2700	6.9758e-01	1.7456e+03	2.4849e-02	5.8573e+00
89.9500	6.9857e-01	1.7458e+03	2.4892e-02	5.3828e+00
98.3500	6.9954e-01	1.7460e+03	2.3824e-02	4.7150e+00
107.5500	7.0044e-01	1.7462e+03	2.1954e-02	3.9815e+00
117.6100	7.0128e-01	1.7463e+03	2.1550e-02	3.5594e+00
128.6100	7.0214e-01	1.7465e+03	2.1016e-02	3.1871e+00
140.6600	7.0294e-01	1.7466e+03	1.9109e-02	2.6577e+00
153.8300	7.0366e-01	1.7467e+03	1.8298e-02	2.3064e+00
168.2500	7.0438e-01	1.7468e+03	1.7742e-02	2.0677e+00
184.0200	7.0507e-01	1.7469e+03	1.5240e-02	1.6471e+00
201.2800	7.0561e-01	1.7469e+03	1.2880e-02	1.2809e+00
220.1600	7.0611e-01	1.7470e+03	1.0499e-02	9.5082e-01
240.8200	7.0642e-01	1.7470e+03	7.8893e-03	6.5494e-01

Quantachrome® ASiQwin™ - Automated Gas Sorption Data
Acquisition and Reduction
© 1994-2013, Quantachrome Instruments
version 3.01



Analysis

Operator: lab
Sample ID: CX-1230

Date: 2014/07/24
Filename:

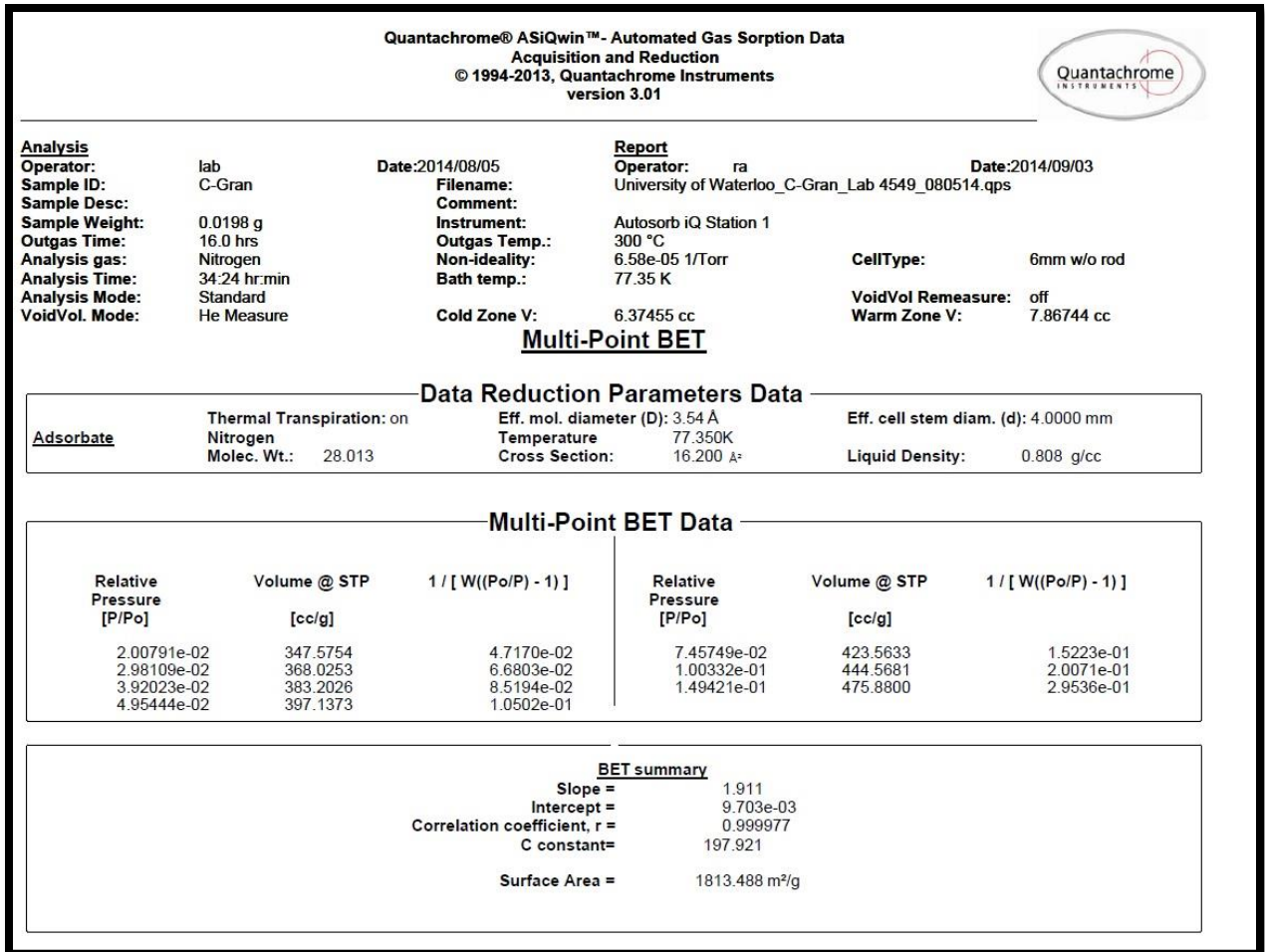
Report

Operator: ra
Date: 2014/08/12
University of Waterloo_CX-1230_Lab 4549_072414.qps

DFT method summary

Pore volume =	0.672 cc/g
Surface area =	1617.270 m ² /g
Lower confidence limit =	5.040 Å
Fitting error =	0.306 %
Pore width (Mode(dLog)) =	5.240 Å
Moving point average :	5

3. Norit C-Gran



Quantachrome® ASiQwin™ - Automated Gas Sorption Data
Acquisition and Reduction
 © 1994-2013, Quantachrome Instruments
 version 3.01



Analysis

Operator: lab
 Sample ID: C-Gran
 Sample Desc:
 Sample Weight: 0.0198 g
 Outgas Time: 16.0 hrs
 Analysis gas: Nitrogen
 Analysis Time: 34:24 hr:min
 Analysis Mode: Standard
 VoidVol. Mode: He Measure

Date: 2014/08/05

Filename:
 Comment:
 Instrument:
 Outgas Temp.: 300 °C
 Non-ideality: 6.58e-05 1/Torr
 Bath temp.: 77.35 K
 Cold Zone V: 6.37455 cc

Report

Operator: ra
 Date: 2014/09/03
 University of Waterloo_C-Gran_Lab 4549_080514.qps
 Autosorb iQ Station 1
 CellType: 6mm w/o rod
 VoidVol Remeasure: off
 Warm Zone V: 7.86744 cc

DFT method Pore Size Distribution (log)

Data Reduction Parameters Data

DFT method	Thermal Transpiration: on	Eff. mol. diameter (D): 3.54 Å	Eff. cell stem diam. (d): 4.0000 mm
	Calc. Model: N2 at 77 K on carbon (slit/cylindr. pores, QSDFT adsorption branch)		
Adsorbate	Rel. press. range: 0.0000 - 1.0000	Temperature: 77.350K	Moving pt. avg: 5
	Nitrogen	Cross Section: 16.200 Å²	Liquid Density: 0.808 g/cc
	Molec. Wt.: 28.013		

DFT method Pore Size Distribution (log) Data

Pore width [Å]	Cumulative Pore Volume [cc/g]	Cumulative Surface Area [m²/g]	dV(log d) [cc/g]	dS(log d) [m²/g]
5.0400	5.0293e-02	2.0960e+02	1.2367e+00	4.7202e+03
5.2400	6.9804e-02	2.8406e+02	1.1635e+00	4.3386e+03
5.4500	8.6754e-02	3.4718e+02	9.1161e-01	3.3373e+03
5.6700	1.0099e-01	3.9894e+02	6.8103e-01	2.4478e+03
5.9000	1.1106e-01	4.3470e+02	4.3952e-01	1.5435e+03
6.1400	1.1698e-01	4.5515e+02	2.3028e-01	7.8867e+02
6.4000	1.1967e-01	4.6419e+02	8.6353e-02	2.8823e+02
6.6600	1.2031e-01	4.6628e+02	1.6759e-02	5.4590e+01
6.9400	1.2031e-01	4.6628e+02	0.0000e+00	0.0000e+00
7.2300	1.2031e-01	4.6628e+02	0.0000e+00	0.0000e+00
7.5300	1.2031e-01	4.6628e+02	1.4418e-02	3.3846e+01
7.8500	1.2080e-01	4.6741e+02	8.1667e-02	1.8652e+02
8.1800	1.2301e-01	4.7243e+02	2.4063e-01	5.3461e+02
8.5200	1.2880e-01	4.8521e+02	5.0334e-01	1.0880e+03
8.8900	1.4033e-01	5.0992e+02	8.4687e-01	1.7834e+03
9.2600	1.5806e-01	5.4694e+02	1.2195e+00	2.5017e+03
9.6600	1.8326e-01	5.9819e+02	1.5427e+00	3.0770e+03
10.0700	2.1340e-01	6.5766e+02	1.7474e+00	3.3793e+03
10.5100	2.4699e-01	7.2180e+02	1.8043e+00	3.3740e+03
10.9600	2.7998e-01	7.8261e+02	1.7351e+00	3.1298e+03
11.4400	3.1143e-01	8.3841e+02	1.5881e+00	2.7557e+03
11.9300	3.3923e-01	8.8578e+02	1.4226e+00	2.3668e+03
12.4500	3.6434e-01	9.2672e+02	1.2773e+00	2.0317e+03
12.9900	3.8693e-01	9.6193e+02	1.1676e+00	1.7739e+03
13.5600	4.0795e-01	9.9323e+02	1.0841e+00	1.5760e+03
14.1600	4.2778e-01	1.0215e+03	1.0100e+00	1.4089e+03
14.7800	4.4605e-01	1.0466e+03	9.2849e-01	1.2444e+03
15.4300	4.6278e-01	1.0686e+03	8.3379e-01	1.0733e+03
16.1100	4.7766e-01	1.0874e+03	7.2721e-01	8.9825e+02
16.8200	4.9043e-01	1.1029e+03	6.1979e-01	7.3435e+02
17.5600	5.0123e-01	1.1154e+03	5.1614e-01	5.8740e+02
18.3400	5.1018e-01	1.1254e+03	3.9787e-01	4.4131e+02
19.1500	5.1674e-01	1.1326e+03	2.7838e-01	3.0497e+02
20.0000	5.2117e-01	1.1374e+03	1.7509e-01	1.8959e+02
21.2063	5.2477e-01	1.1412e+03	9.1643e-02	1.0030e+02
21.9485	5.2570e-01	1.1423e+03	2.9311e-02	3.6317e+01
22.7167	5.2581e-01	1.1425e+03	4.1351e-03	7.7998e+00
23.5118	5.2581e-01	1.1425e+03	0.0000e+00	0.0000e+00
24.3347	5.2581e-01	1.1425e+03	0.0000e+00	0.0000e+00
25.1864	5.2581e-01	1.1425e+03	1.2499e-03	1.7901e+00
26.0679	5.2584e-01	1.1425e+03	1.1673e-02	1.6276e+01
26.9803	5.2613e-01	1.1429e+03	4.5296e-02	6.1667e+01
27.9246	5.2712e-01	1.1443e+03	1.1496e-01	1.5278e+02
28.9020	5.2940e-01	1.1473e+03	2.1948e-01	2.8523e+02
29.9136	5.3341e-01	1.1524e+03	3.4072e-01	4.3366e+02
30.9605	5.3929e-01	1.1599e+03	4.5559e-01	5.6775e+02
32.0442	5.4680e-01	1.1692e+03	5.4381e-01	6.6200e+02

Continued on next page



Analysis
 Operator: lab Date:2014/08/05 **Report**
 Operator: ra Date:2014/09/03
 Sample ID: C-Gran Filename: University of Waterloo_C-Gran_Lab 4549_080514.qps

DFT method Pore Size Distribution (log) Data continued

Pore width [Å]	Cumulative Pore Volume [cc/g]	Cumulative Surface Area [m ² /g]	dV(log d) [cc/g]	dS(log d) [m ² /g]
33.1657	5.5542e-01	1.1796e+03	5.9618e-01	7.0591e+02
34.3265	5.6459e-01	1.1903e+03	6.2787e-01	7.1892e+02
35.5279	5.7418e-01	1.2011e+03	6.6721e-01	7.3564e+02
36.7714	5.8447e-01	1.2122e+03	7.2766e-01	7.7232e+02
38.0584	5.9578e-01	1.2241e+03	8.0188e-01	8.2180e+02
39.3905	6.0825e-01	1.2367e+03	8.7414e-01	8.6788e+02
40.7691	6.2178e-01	1.2499e+03	9.3029e-01	8.9563e+02
42.1960	6.3601e-01	1.2635e+03	9.5798e-01	8.9359e+02
43.6729	6.5043e-01	1.2767e+03	9.5800e-01	8.6449e+02
45.2015	6.6470e-01	1.2894e+03	9.4523e-01	8.2426e+02
46.7835	6.7874e-01	1.3015e+03	9.2386e-01	7.7895e+02
48.4209	6.9238e-01	1.3128e+03	8.9270e-01	7.2799e+02
50.1157	7.0551e-01	1.3234e+03	8.6951e-01	6.8481e+02
51.8700	7.1846e-01	1.3334e+03	8.6197e-01	6.5475e+02
53.6900	7.3135e-01	1.3430e+03	8.6396e-01	6.3252e+02
55.5600	7.4423e-01	1.3523e+03	8.8498e-01	6.2480e+02
57.5100	7.5772e-01	1.3617e+03	9.1862e-01	6.2698e+02
59.5200	7.7166e-01	1.3711e+03	9.4768e-01	6.2570e+02
61.6000	7.8598e-01	1.3804e+03	9.9571e-01	6.3417e+02
63.7600	8.0137e-01	1.3900e+03	1.0738e+00	6.5904e+02
65.9900	8.1795e-01	1.4001e+03	1.1407e+00	6.7617e+02
68.3000	8.3528e-01	1.4102e+03	1.1920e+00	6.8407e+02
70.6900	8.5347e-01	1.4205e+03	1.2610e+00	7.0074e+02
73.1700	8.7298e-01	1.4312e+03	1.3217e+00	7.1009e+02
75.7300	8.9299e-01	1.4418e+03	1.3305e+00	6.9067e+02
78.3790	9.1270e-01	1.4519e+03	1.3110e+00	6.5856e+02
81.1220	9.3220e-01	1.4615e+03	1.3066e+00	6.3557e+02
83.9610	9.5188e-01	1.4710e+03	1.3337e+00	6.2560e+02
86.9000	9.7212e-01	1.4803e+03	1.3855e+00	6.2469e+02
89.9410	9.9314e-01	1.4896e+03	1.4450e+00	6.2811e+02
93.0890	1.0151e+00	1.4990e+03	1.5035e+00	6.3330e+02
96.3470	1.0380e+00	1.5085e+03	1.5444e+00	6.3173e+02
99.7200	1.0613e+00	1.5180e+03	1.5412e+00	6.1064e+02
103.2100	1.0842e+00	1.5269e+03	1.5175e+00	5.7955e+02
106.8200	1.1068e+00	1.5354e+03	1.5211e+00	5.5926e+02
110.5600	1.1296e+00	1.5436e+03	1.5357e+00	5.4548e+02
114.4300	1.1526e+00	1.5517e+03	1.5225e+00	5.2432e+02
118.4360	1.1752e+00	1.5594e+03	1.4842e+00	4.9570e+02
122.5810	1.1972e+00	1.5666e+03	1.4157e+00	4.5762e+02
126.8710	1.2178e+00	1.5732e+03	1.3180e+00	4.1117e+02
131.3120	1.2368e+00	1.5790e+03	1.2305e+00	3.7013e+02
135.9080	1.2547e+00	1.5843e+03	1.1700e+00	3.4005e+02
140.6640	1.2719e+00	1.5892e+03	1.0945e+00	3.0822e+02
145.5880	1.2876e+00	1.5936e+03	9.9250e-01	2.7084e+02
150.6830	1.3018e+00	1.5974e+03	8.9366e-01	2.3588e+02
155.9570	1.3146e+00	1.6007e+03	8.0470e-01	2.0488e+02
161.4160	1.3261e+00	1.6036e+03	7.2710e-01	1.7828e+02
167.0650	1.3365e+00	1.6061e+03	6.7314e-01	1.5915e+02
172.9120	1.3463e+00	1.6084e+03	6.3405e-01	1.4510e+02
178.9640	1.3555e+00	1.6105e+03	5.9674e-01	1.3209e+02
185.2280	1.3643e+00	1.6124e+03	5.6883e-01	1.2141e+02
191.7110	1.3726e+00	1.6141e+03	5.3490e-01	1.1022e+02
198.4210	1.3803e+00	1.6157e+03	4.9930e-01	9.9420e+01
205.3660	1.3876e+00	1.6171e+03	4.8658e-01	9.3561e+01
212.5530	1.3949e+00	1.6185e+03	4.6907e-01	8.7305e+01
219.9930	1.4017e+00	1.6197e+03	4.2775e-01	7.6979e+01
227.6930	1.4078e+00	1.6208e+03	4.0073e-01	6.9612e+01
235.6620	1.4137e+00	1.6218e+03	3.7609e-01	6.3341e+01
243.9100	1.4191e+00	1.6227e+03	3.2425e-01	5.2950e+01
252.4470	1.4235e+00	1.6234e+03	2.7616e-01	4.3624e+01
261.2820	1.4274e+00	1.6241e+03	2.4401e-01	3.7287e+01
270.4270	1.4309e+00	1.6246e+03	2.0775e-01	3.0585e+01
279.8920	1.4337e+00	1.6250e+03	1.7385e-01	2.4633e+01
289.6890	1.4361e+00	1.6253e+03	1.5768e-01	2.1589e+01
299.8280	1.4385e+00	1.6256e+03	1.6676e-01	2.1842e+01

Continued on next page



Analysis

Operator: lab
 Sample ID: C-Gran

Date: 2014/08/05
 Filename:

Report

Operator: ra
 Date: 2014/09/03
 University of Waterloo_C-Gran_Lab 4549_080514.qps

DFT method Pore Size Distribution (log) Data continued


Pore width [Å]	Cumulative Pore Volume [cc/g]	Cumulative Surface Area [m ² /g]	dV(log d) [cc/g]	dS(log d) [m ² /g]
310.3220	1.4411e+00	1.6260e+03	1.9158e-01	2.4090e+01
321.1830	1.4439e+00	1.6263e+03	2.1851e-01	2.6641e+01
332.4240	1.4484e+00	1.6269e+03	3.0715e-01	3.6957e+01

DFT method summary

Pore volume = 1.444 cc/g
 Surface area = 1617.289 m²/g
 Lower confidence limit = 5.040 Å
 Fitting error = 0.229 %
 Pore width (Mode(dLog)) = 10.510 Å
 Moving point average : 5

4. WV- B30

Quantachrome® ASiQwin™ - Automated Gas Sorption Data
Acquisition and Reduction
 © 1994-2013, Quantachrome Instruments
 version 3.01



<p>Analysis Operator: lab Sample ID: WV-B 30 Sample Desc: Carbon Sample Weight: 0.0341 g Outgas Time: 16.0 hrs Analysis gas: Nitrogen Analysis Time: 33:07 hr:min Analysis Mode: Standard VoidVol. Mode: He Measure</p>	<p>Date: 2014/07/14 Filename: University of Waterloo_WV-B 30_071414.qps Comment: University of Waterloo, Lab #4549 Instrument: Autosorb iQ Station 1 Outgas Temp.: 300 °C Non-ideality: 6.58e-05 1/Torr Bath temp.: 77.35 K Cold Zone V: 6.10131 cc</p>	<p>Report Operator: ra Date: 2014/09/03 CellType: 6mm w/o rod VoidVol Remeasure: off Warm Zone V: 8.27629 cc</p>
--	--	---

Multi-Point BET

Data Reduction Parameters Data

Adsorbate	Thermal Transpiration: on	Eff. mol. diameter (D): 3.54 Å
	Nitrogen	Temperature 77.350K
	Molec. Wt.: 28.013	Cross Section: 16.200 Å ²
		Eff. cell stem diam. (d): 4.0000 mm
		Liquid Density: 0.806 g/cc

Multi-Point BET Data

Relative Pressure [P/Po]	Volume @ STP [cc/g]	1 / [W((Po/P) - 1)]	Relative Pressure [P/Po]	Volume @ STP [cc/g]	1 / [W((Po/P) - 1)]
3.01882e-02	293.1375	8.4963e-02	1.01416e-01	367.5144	2.4571e-01
4.05497e-02	307.9722	1.0980e-01	1.49100e-01	402.1852	3.4860e-01
4.96019e-02	319.0014	1.3090e-01	1.99732e-01	433.5316	4.6062e-01
7.64121e-02	346.4072	1.9109e-01			

BET summary

Slope =	2.205
Intercept =	2.071e-02
Correlation coefficient, r =	0.999945
C constant =	107.499
Surface Area =	1564.560 m ² /g



Analysis		Report	
Operator: lab	Date: 2014/07/14	Operator: ra	Date: 2014/09/03
Sample ID: WV-B 30	Filename: University of Waterloo_WV-B 30_071414.qps		
Sample Desc: Carbon	Comment: University of Waterloo, Lab #4549		
Sample Weight: 0.0341 g	Instrument: Autosorb iQ Station 1		
Outgas Time: 16.0 hrs	Outgas Temp.: 300 °C	CellType: 6mm w/o rod	
Analysis gas: Nitrogen	Non-ideality: 6.58e-05 1/Torr	VoidVol Remeasure: off	
Analysis Time: 33:07 hr:min	Bath temp.: 77.35 K	Warm Zone V: 8.27629 cc	
Analysis Mode: Standard			
VoidVol. Mode: He Measure	Cold Zone V: 6.10131 cc		

DFT method Pore Size Distribution (log)

Data Reduction Parameters Data

DFT method	Thermal Transpiration: on	Eff. mol. diameter (D): 3.54 Å	Eff. cell stem diam. (d): 4.0000 mm
	Calc. Model: N2 at 77 K on carbon (slit/cylindr. pores, QSDFT adsorption branch)		
	Rel. press. range: 0.0000 - 1.0000		Moving pt. avg: 5
Adsorbate	Nitrogen	Temperature 77.350K	Liquid Density: 0.806 g/cc
	Molec. Wt.: 28.013	Cross Section: 16.200 Å²	

DFT method Pore Size Distribution (log) Data

Pore width [Å]	Cumulative Pore Volume [cc/g]	Cumulative Surface Area [m²/g]	dV(log d) [cc/g]	dS(log d) [m²/g]
5.0400	3.8109e-02	1.6696e+02	3.9765e-01	1.5178e+03
5.2400	4.4464e-02	1.9134e+02	3.3303e-01	1.2469e+03
5.4500	4.9283e-02	2.0955e+02	2.3141e-01	8.5777e+02
5.6700	5.2725e-02	2.2224e+02	1.5188e-01	5.5422e+02
5.9000	5.4777e-02	2.2962e+02	8.1140e-02	2.8881e+02
6.1400	5.5709e-02	2.3287e+02	3.1588e-02	1.0963e+02
6.4000	5.5964e-02	2.3373e+02	6.5126e-03	2.2077e+01
6.6600	5.5964e-02	2.3373e+02	0.0000e+00	0.0000e+00
6.9400	5.5964e-02	2.3373e+02	0.0000e+00	0.0000e+00
7.2300	5.5964e-02	2.3373e+02	0.0000e+00	0.0000e+00
7.5300	5.5964e-02	2.3373e+02	8.4511e-03	1.9838e+01
7.8500	5.6247e-02	2.3440e+02	4.9633e-02	1.1330e+02
8.1800	5.7598e-02	2.3747e+02	1.5130e-01	3.3582e+02
8.5200	6.1278e-02	2.4557e+02	3.2691e-01	7.0558e+02
8.8900	6.8840e-02	2.6175e+02	5.6708e-01	1.1915e+03
9.2600	8.0824e-02	2.8672e+02	8.4118e-01	1.7205e+03
9.6600	9.8380e-02	3.2230e+02	1.0961e+00	2.1788e+03
10.0700	1.2002e-01	3.6486e+02	1.2784e+00	2.4641e+03
10.5100	1.4487e-01	4.1218e+02	1.3576e+00	2.5314e+03
10.9600	1.6998e-01	4.5835e+02	1.3393e+00	2.4103e+03
11.4400	1.9452e-01	5.0180e+02	1.2519e+00	2.1687e+03
11.9300	2.1661e-01	5.3941e+02	1.1384e+00	1.8921e+03
12.4500	2.3681e-01	5.7234e+02	1.0330e+00	1.6420e+03
12.9900	2.5517e-01	6.0093e+02	9.5484e-01	1.4495e+03
13.5600	2.7246e-01	6.2665e+02	9.0209e-01	1.3089e+03
14.1600	2.8910e-01	6.5035e+02	8.6382e-01	1.2008e+03
14.7800	3.0494e-01	6.7197e+02	8.2834e-01	1.1044e+03
15.4300	3.2019e-01	6.9195e+02	7.9087e-01	1.0110e+03
16.1100	3.3474e-01	7.1020e+02	7.4786e-01	9.1567e+02
16.8200	3.4840e-01	7.2662e+02	7.0079e-01	8.2191e+02
17.5600	3.6115e-01	7.4130e+02	6.4389e-01	7.2525e+02
18.3400	3.7281e-01	7.5421e+02	5.4141e-01	5.9861e+02
19.1500	3.8212e-01	7.6446e+02	4.1185e-01	4.5593e+02
20.0000	3.8900e-01	7.7200e+02	2.8094e-01	3.1189e+02
21.2063	3.9500e-01	7.7860e+02	1.5887e-01	1.8143e+02
21.9485	3.9671e-01	7.8058e+02	5.8926e-02	7.8927e+01
22.7167	3.9704e-01	7.8120e+02	1.4338e-02	2.6730e+01
23.5118	3.9713e-01	7.8137e+02	2.8270e-03	5.1516e+00
24.3347	3.9713e-01	7.8137e+02	4.4224e-03	6.5568e+00
25.1864	3.9726e-01	7.8155e+02	2.8435e-02	4.1176e+01
26.0679	3.9793e-01	7.8252e+02	9.5030e-02	1.3429e+02
26.9803	3.9994e-01	7.8534e+02	2.2458e-01	3.0972e+02
27.9246	4.0432e-01	7.9134e+02	4.2688e-01	5.7483e+02
28.9020	4.1220e-01	8.0186e+02	6.8716e-01	9.0392e+02
29.9136	4.2425e-01	8.1759e+02	9.6131e-01	1.2350e+03
30.9605	4.4034e-01	8.3808e+02	1.1979e+00	1.5014e+03
32.0442	4.5962e-01	8.6202e+02	1.3607e+00	1.6611e+03

Continued on next page



Analysis
 Operator: lab Date:2014/07/14 Report Operator: ra Date:2014/09/03
 Sample ID: WV-B 30 Filename: University of Waterloo_WV-B_30_071414.qps

DFT method Pore Size Distribution (log) Data continued

Pore width [A]	Cumulative Pore Volume [cc/g]	Cumulative Surface Area [m ² /g]	dV(log d) [cc/g]	dS(log d) [m ² /g]
33.1657	4.8082e-01	8.8760e+02	1.4402e+00	1.7079e+03
34.3265	5.0268e-01	9.1319e+02	1.4598e+00	1.6762e+03
35.5279	5.2454e-01	9.3792e+02	1.4586e+00	1.6172e+03
36.7714	5.4634e-01	9.6171e+02	1.4582e+00	1.5600e+03
38.0584	5.6813e-01	9.8467e+02	1.4571e+00	1.5060e+03
39.3905	5.8989e-01	1.0068e+03	1.4445e+00	1.4451e+03
40.7691	6.1138e-01	1.0280e+03	1.4083e+00	1.3647e+03
42.1960	6.3215e-01	1.0479e+03	1.3439e+00	1.2604e+03
43.6729	6.5177e-01	1.0660e+03	1.2633e+00	1.1449e+03
45.2015	6.7012e-01	1.0824e+03	1.1841e+00	1.0361e+03
46.7835	6.8734e-01	1.0972e+03	1.1095e+00	9.3795e+02
48.4209	7.0345e-01	1.1106e+03	1.0351e+00	8.4622e+02
50.1157	7.1845e-01	1.1227e+03	9.6328e-01	7.6155e+02
51.8700	7.3243e-01	1.1336e+03	8.9638e-01	6.8466e+02
53.6900	7.4546e-01	1.1434e+03	8.3731e-01	6.1697e+02
55.5600	7.5756e-01	1.1521e+03	7.9433e-01	5.6431e+02
57.5100	7.6925e-01	1.1603e+03	7.6773e-01	5.2645e+02
59.5200	7.8058e-01	1.1680e+03	7.5172e-01	4.9791e+02
61.6000	7.9173e-01	1.1752e+03	7.5054e-01	4.7974e+02
63.7600	8.0304e-01	1.1824e+03	7.6625e-01	4.7219e+02
65.9900	8.1463e-01	1.1894e+03	7.8720e-01	4.6802e+02
68.3000	8.2651e-01	1.1963e+03	8.0827e-01	4.6448e+02
70.6900	8.3874e-01	1.2033e+03	8.3005e-01	4.6169e+02
73.1700	8.5134e-01	1.2102e+03	8.3950e-01	4.5203e+02
75.7300	8.6389e-01	1.2168e+03	8.2367e-01	4.2913e+02
78.3790	8.7601e-01	1.2231e+03	7.9186e-01	3.9907e+02
81.1220	8.8764e-01	1.2288e+03	7.6211e-01	3.7129e+02
83.9610	8.9889e-01	1.2342e+03	7.4242e-01	3.4897e+02
86.9000	9.0991e-01	1.2393e+03	7.3283e-01	3.3192e+02
89.9410	9.2081e-01	1.2442e+03	7.2890e-01	3.1859e+02
93.0890	9.3168e-01	1.2489e+03	7.2494e-01	3.0662e+02
96.3470	9.4250e-01	1.2534e+03	7.1445e-01	2.9276e+02
99.7200	9.5311e-01	1.2577e+03	6.9343e-01	2.7492e+02
103.2100	9.6332e-01	1.2617e+03	6.7182e-01	2.5693e+02
106.8200	9.7325e-01	1.2654e+03	6.6233e-01	2.4401e+02
110.5600	9.8312e-01	1.2690e+03	6.5830e-01	2.3415e+02
114.4300	9.9292e-01	1.2724e+03	6.4678e-01	2.2277e+02
118.4360	1.0025e+00	1.2757e+03	6.2738e-01	2.0946e+02
122.5810	1.0118e+00	1.2787e+03	5.9807e-01	1.9329e+02
126.8710	1.0205e+00	1.2815e+03	5.5813e-01	1.7417e+02
131.3120	1.0285e+00	1.2840e+03	5.2080e-01	1.5674e+02
135.9080	1.0361e+00	1.2862e+03	4.9559e-01	1.4399e+02
140.6640	1.0434e+00	1.2883e+03	4.7225e-01	1.3270e+02
145.5880	1.0503e+00	1.2902e+03	4.4316e-01	1.2050e+02
150.6830	1.0567e+00	1.2919e+03	4.1427e-01	1.0890e+02
155.9570	1.0628e+00	1.2935e+03	3.8845e-01	9.8601e+01
161.4160	1.0684e+00	1.2949e+03	3.6372e-01	8.9085e+01
167.0650	1.0737e+00	1.2962e+03	3.4122e-01	8.0700e+01
172.9120	1.0787e+00	1.2973e+03	3.2096e-01	7.3452e+01
178.9640	1.0833e+00	1.2984e+03	3.0238e-01	6.6917e+01
185.2280	1.0877e+00	1.2993e+03	2.8705e-01	6.1285e+01
191.7110	1.0919e+00	1.3002e+03	2.6976e-01	5.5591e+01
198.4210	1.0958e+00	1.3010e+03	2.5319e-01	5.0409e+01
205.3660	1.0995e+00	1.3017e+03	2.4498e-01	4.7125e+01
212.5530	1.1032e+00	1.3024e+03	2.3441e-01	4.3633e+01
219.9930	1.1066e+00	1.3030e+03	2.1524e-01	3.8739e+01
227.6930	1.1097e+00	1.3036e+03	2.0319e-01	3.5282e+01
235.6620	1.1127e+00	1.3041e+03	1.9713e-01	3.3059e+01
243.9100	1.1156e+00	1.3046e+03	1.8180e-01	2.9485e+01
252.4470	1.1181e+00	1.3050e+03	1.6389e-01	2.5737e+01
261.2820	1.1205e+00	1.3054e+03	1.5142e-01	2.3054e+01
270.4270	1.1227e+00	1.3057e+03	1.3535e-01	1.9939e+01
279.8920	1.1246e+00	1.3060e+03	1.1415e-01	1.6224e+01
289.6890	1.1262e+00	1.3062e+03	1.0170e-01	1.3909e+01
299.8280	1.1277e+00	1.3064e+03	1.0704e-01	1.4003e+01

Continued on next page



Analysis
 Operator: lab Date:2014/07/14
 Sample ID: WV-B 30 Filename: University of Waterloo_WV-B 30_071414.qps

Report
 Operator: ra Date:2014/09/03

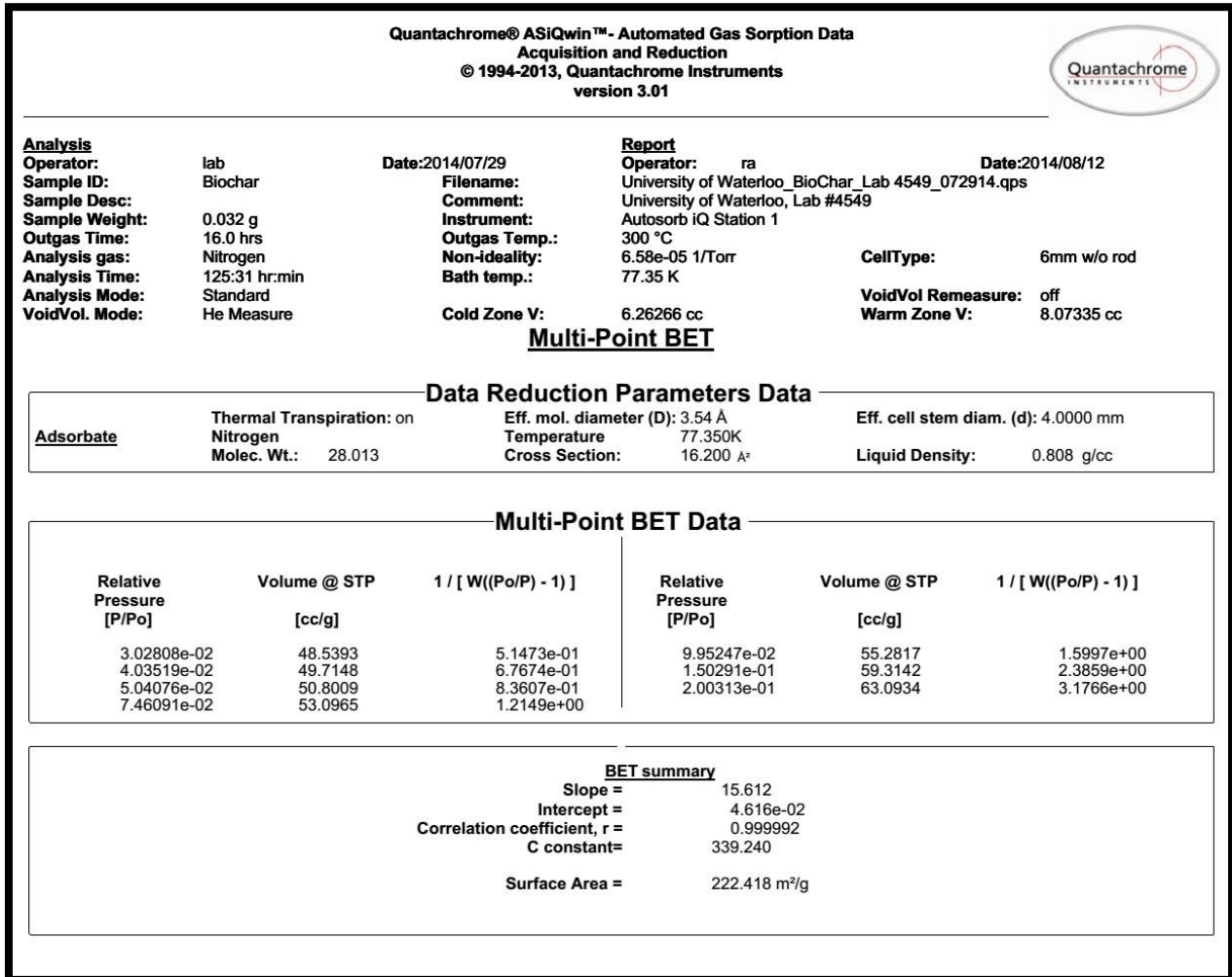
DFT method Pore Size Distribution (log) Data continued

Pore width [Å]	Cumulative Pore Volume [cc/g]	Cumulative Surface Area [m ² /g]	dV(log d) [cc/g]	dS(log d) [m ² /g]
310.3220	1.1294e+00	1.3066e+03	1.2109e-01	1.5237e+01
321.1830	1.1311e+00	1.3068e+03	1.3882e-01	1.6953e+01
332.4240	1.1339e+00	1.3072e+03	1.8356e-01	2.2086e+01

DFT method summary

Pore volume = 1.130 cc/g
 Surface area = 1298.492 m²/g
 Lower confidence limit = 5.040 Å
 Fitting error = 0.291 %
 Pore width (Mode(dLog)) = 34.326 Å
 Moving point average : 5

5. Biochar





Analysis		Report	
Operator:	lab	Operator:	ra
Sample ID:	Biochar	Filename:	University of Waterloo_BioChar_Lab 4549_072914.qps
Sample Desc:		Comment:	University of Waterloo, Lab #4549
Sample Weight:	0.032 g	Instrument:	Autosorb iQ Station 1
Outgas Time:	16.0 hrs	Outgas Temp.:	300 °C
Analysis gas:	Nitrogen	Non-ideality:	6.58e-05 1/Torr
Analysis Time:	125:31 hr:min	Bath temp.:	77.35 K
Analysis Mode:	Standard	CellType:	6mm w/o rod
VoidVol. Mode:	He Measure	VoidVol Remeasure:	off
		Warm Zone V:	8.07335 cc
		Cold Zone V:	6.26266 cc

DFT method Pore Size Distribution (log)

Data Reduction Parameters Data

DFT method	Thermal Transpiration: on	Eff. mol. diameter (D): 3.54 Å	Eff. cell stem diam. (d): 4.0000 mm
Adsorbate	Calc. Model: N2 at 77 K on carbon (slit pore, QSDFT equilibrium model)		Moving pt. avg: 5
	Rel. press. range: 0.0000 - 1.0000		Liquid Density: 0.808 g/cc
	Nitrogen	Temperature 77.350K	
	Molec. Wt.: 28.013	Cross Section: 16.200 Å²	

DFT method Pore Size Distribution (log) Data

Pore width [Å]	Cumulative Pore Volume [cc/g]	Cumulative Surface Area [m²/g]	dV(log d) [cc/g]	dS(log d) [m²/g]
4.8400	1.3394e-02	5.8573e+01	1.9827e-01	7.5674e+02
5.2400	1.9906e-02	8.3609e+01	1.8109e-01	6.6147e+02
5.6700	2.5418e-02	1.0391e+02	1.4227e-01	5.0016e+02
6.1400	3.0055e-02	1.2002e+02	1.1058e-01	3.7003e+02
6.6600	3.3626e-02	1.3162e+02	8.3008e-02	2.5571e+02
7.2300	3.6308e-02	1.3951e+02	6.9048e-02	1.8770e+02
7.8500	3.8659e-02	1.4555e+02	7.0974e-02	1.6838e+02
8.5200	4.1224e-02	1.5137e+02	8.1569e-02	1.7622e+02
9.2600	4.4293e-02	1.5786e+02	8.9709e-02	1.8353e+02
10.0700	4.7662e-02	1.6468e+02	8.8376e-02	1.7328e+02
10.9600	5.0941e-02	1.7102e+02	7.9161e-02	1.4654e+02
11.9300	5.3806e-02	1.7618e+02	6.9187e-02	1.1632e+02
12.9900	5.6262e-02	1.8012e+02	6.5339e-02	9.6050e+01
14.1600	5.8643e-02	1.8343e+02	7.1613e-02	9.2969e+01
15.4300	6.1410e-02	1.8690e+02	8.6369e-02	1.0321e+02
16.8200	6.4884e-02	1.9098e+02	1.0276e-01	1.1483e+02
18.3400	6.8999e-02	1.9549e+02	1.1636e-01	1.2060e+02
20.0000	7.3582e-02	2.0013e+02	1.2966e-01	1.2293e+02
21.8300	7.8730e-02	2.0487e+02	1.4364e-01	1.2426e+02
23.8200	8.4346e-02	2.0959e+02	1.5595e-01	1.2385e+02
26.0000	9.0441e-02	2.1430e+02	1.6627e-01	1.2196e+02
28.3800	9.6954e-02	2.1897e+02	1.7255e-01	1.1724e+02
30.9900	1.0369e-01	2.2344e+02	1.7094e-01	1.0729e+02
33.8500	1.1023e-01	2.2743e+02	1.6338e-01	9.4179e+01
36.9800	1.1645e-01	2.3090e+02	1.5492e-01	8.1831e+01
40.3900	1.2234e-01	2.3392e+02	1.4667e-01	7.0871e+01
44.1300	1.2791e-01	2.3653e+02	1.3826e-01	6.1102e+01
48.2300	1.3317e-01	2.3878e+02	1.2805e-01	5.2014e+01
52.7000	1.3799e-01	2.4068e+02	1.1614e-01	4.3491e+01
57.6000	1.4238e-01	2.4228e+02	1.0583e-01	3.6318e+01
62.9600	1.4641e-01	2.4362e+02	9.7659e-02	3.0450e+01
68.8300	1.5011e-01	2.4473e+02	8.9736e-02	2.5373e+01
75.2400	1.5346e-01	2.4564e+02	8.3698e-02	2.1594e+01
82.2700	1.5668e-01	2.4645e+02	8.4424e-02	1.9843e+01
89.9500	1.6008e-01	2.4722e+02	9.0769e-02	1.9250e+01
98.3500	1.6370e-01	2.4796e+02	9.4325e-02	1.8175e+01
107.5500	1.6732e-01	2.4864e+02	9.4846e-02	1.6834e+01
117.6100	1.7105e-01	2.4929e+02	1.0014e-01	1.6413e+01
128.6100	1.7517e-01	2.4995e+02	9.9994e-02	1.5223e+01
140.6600	1.7898e-01	2.5051e+02	8.9309e-02	1.2509e+01
153.8300	1.8230e-01	2.5096e+02	8.2867e-02	1.0518e+01
168.2500	1.8555e-01	2.5136e+02	7.8268e-02	9.1627e+00
184.0200	1.8855e-01	2.5170e+02	6.7795e-02	7.2944e+00
201.2800	1.9099e-01	2.5195e+02	6.3219e-02	6.1049e+00
220.1600	1.9356e-01	2.5219e+02	6.4739e-02	5.6973e+00
240.8200	1.9609e-01	2.5241e+02	6.3042e-02	5.0091e+00
263.4300	1.9846e-01	2.5259e+02	6.7353e-02	4.8083e+00

Continued on next page



Analysis

Operator: lab
 Sample ID: Biochar

Date: 2014/07/29
 Filename:

Report

Operator: ra
 Date: 2014/08/12
 University of Waterloo_BioChar_Lab 4549_072914.qps

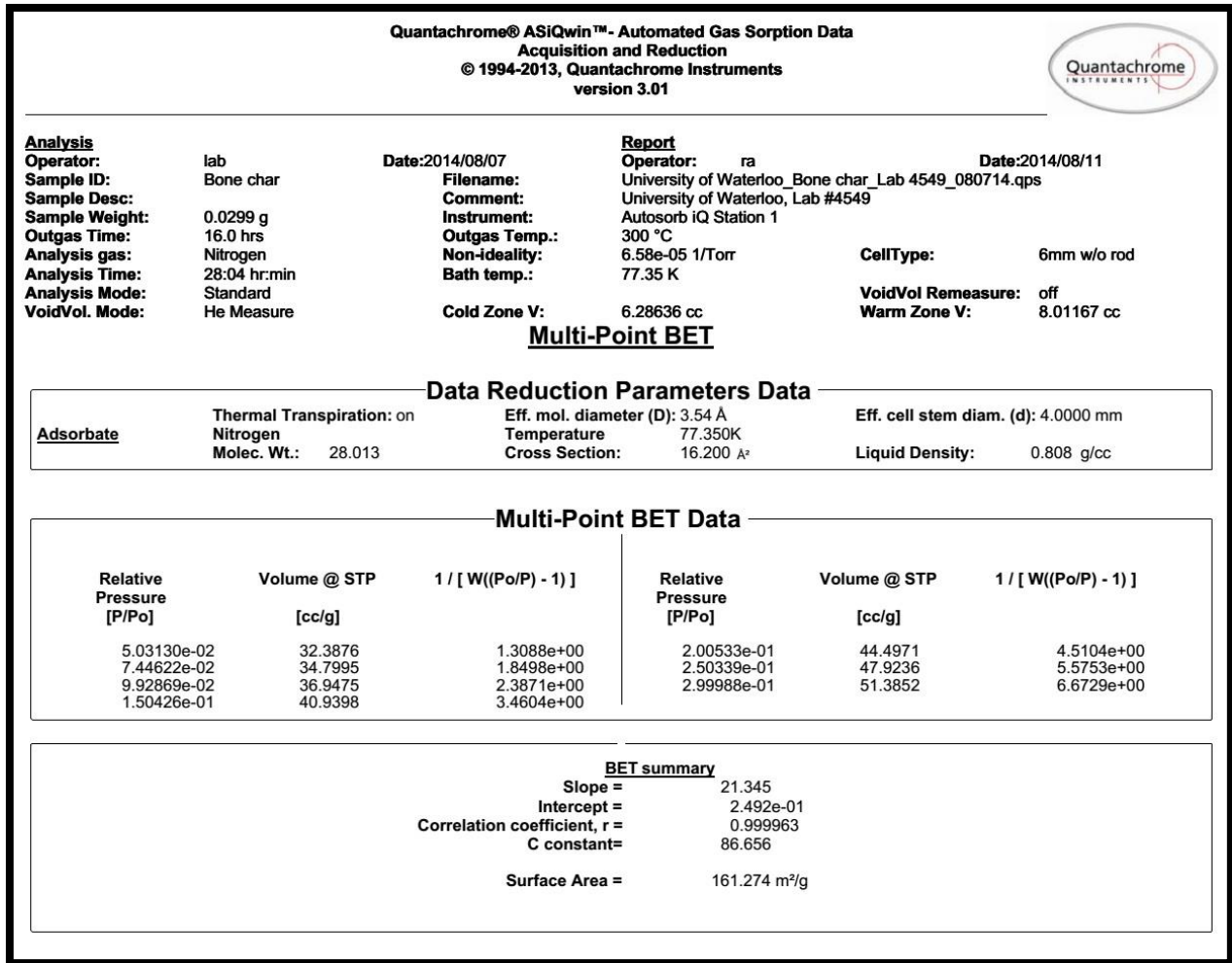
DFT method Pore Size Distribution (log) Data continued

Pore width [Å]	Cumulative Pore Volume [cc/g]	Cumulative Surface Area [m ² /g]	dV(log d) [cc/g]	dS(log d) [m ² /g]
288.1600	2.0127e-01	2.5279e+02	7.7734e-02	5.1433e+00
315.2200	2.0431e-01	2.5298e+02	8.4182e-02	5.1380e+00
344.8200	2.0815e-01	2.5320e+02	9.8663e-02	5.7224e+00

DFT method summary

Pore volume = 0.205 cc/g
 Surface area = 245.038 m²/g
 Lower confidence limit = 4.840 Å
 Fitting error = 0.577 %
 Pore width (Mode(dLog)) = 4.840 Å
 Moving point average : 5

6. Bone Char





Analysis

Operator: lab
 Sample ID: Bone char
 Sample Desc:
 Sample Weight: 0.0299 g
 Outgas Time: 16.0 hrs
 Analysis gas: Nitrogen
 Analysis Time: 28:04 hr:min
 Analysis Mode: Standard
 VoidVol. Mode: He Measure

Date: 2014/08/07

Filename:
 Comment:
 Instrument:
 Outgas Temp.:
 Non-ideality:
 Bath temp.:

Report

Operator: ra
 Date: 2014/08/11
 University of Waterloo_Bone char_Lab 4549_080714.qps
 University of Waterloo, Lab #4549
 Autosorb iQ Station 1
 300 °C
 6.58e-05 1/Torr
 77.35 K
 CellType: 6mm w/o rod
 VoidVol Remeasure: off
 Warm Zone V: 8.01167 cc

Cold Zone V: 6.28636 cc

DFT method Pore Size Distribution (log)

Data Reduction Parameters Data

DFT method	Thermal Transpiration: on	Eff. mol. diameter (D): 3.54 Å	Eff. cell stem diam. (d): 4.0000 mm
	Calc. Model: N2 at 77 K on carbon (slit pore, QSDFT equilibrium model)		
	Rel. press. range: 0.0000 - 1.0000		Moving pt. avg: 5
Adsorbate	Nitrogen	Temperature: 77.350K	Liquid Density: 0.808 g/cc
	Molec. Wt.: 28.013	Cross Section: 16.200 Å²	

DFT method Pore Size Distribution (log) Data

Pore width [Å]	Cumulative Pore Volume [cc/g]	Cumulative Surface Area [m²/g]	dV(log d) [cc/g]	dS(log d) [m²/g]
5.2400	7.5929e-03	3.1822e+01	6.5264e-02	2.3021e+02
5.6700	9.7329e-03	3.9498e+01	5.2346e-02	1.7824e+02
6.1400	1.1340e-02	4.5132e+01	3.5407e-02	1.1859e+02
6.6600	1.2464e-02	4.8872e+01	2.2354e-02	7.2550e+01
7.2300	1.3104e-02	5.0881e+01	1.1151e-02	3.4305e+01
7.8500	1.3373e-02	5.1673e+01	3.9989e-03	1.1648e+01
8.5200	1.3436e-02	5.1849e+01	1.0943e-03	2.7113e+00
9.2600	1.3457e-02	5.1886e+01	2.4978e-03	4.2868e+00
10.0700	1.3592e-02	5.2116e+01	8.6753e-03	1.4047e+01
10.9600	1.4009e-02	5.2783e+01	1.9944e-02	3.0513e+01
11.9300	1.4894e-02	5.4116e+01	3.5384e-02	5.1331e+01
12.9900	1.6392e-02	5.6262e+01	5.2070e-02	7.1870e+01
14.1600	1.8548e-02	5.9207e+01	6.5514e-02	8.6049e+01
15.4300	2.1159e-02	6.2597e+01	7.1761e-02	8.9358e+01
16.8200	2.3930e-02	6.5992e+01	6.9972e-02	8.2019e+01
18.3400	2.6553e-02	6.8998e+01	6.3809e-02	6.9312e+01
20.0000	2.8906e-02	7.1472e+01	6.0531e-02	5.9090e+01
21.8300	3.1215e-02	7.3629e+01	6.8094e-02	5.8121e+01
23.8200	3.3950e-02	7.5861e+01	9.1330e-02	6.8927e+01
26.0000	3.7770e-02	7.8653e+01	1.2861e-01	8.8576e+01
28.3800	4.3161e-02	8.2287e+01	1.7115e-01	1.0977e+02
30.9900	5.0245e-02	8.6755e+01	2.0878e-01	1.2548e+02
33.8500	5.8763e-02	9.1789e+01	2.3665e-01	1.3278e+02
36.9800	6.8296e-02	9.7028e+01	2.5580e-01	1.3263e+02
40.3900	7.8432e-02	1.0215e+02	2.7155e-01	1.2859e+02
44.1300	8.9140e-02	1.0706e+02	2.9064e-01	1.2499e+02
48.2300	1.0066e-01	1.1186e+02	3.1341e-01	1.2301e+02
52.7000	1.1306e-01	1.1660e+02	3.3702e-01	1.2151e+02
57.6000	1.2649e-01	1.2132e+02	3.6360e-01	1.2036e+02
62.9600	1.4108e-01	1.2602e+02	3.9338e-01	1.1904e+02
68.8300	1.5682e-01	1.3064e+02	4.1650e-01	1.1526e+02
75.2400	1.7316e-01	1.3504e+02	4.2946e-01	1.0918e+02
82.2700	1.9008e-01	1.3923e+02	4.4585e-01	1.0414e+02
89.9500	2.0791e-01	1.4328e+02	4.6889e-01	1.0011e+02
98.3500	2.2658e-01	1.4715e+02	4.7406e-01	9.2649e+01
107.5500	2.4483e-01	1.5061e+02	4.5329e-01	8.1708e+01
117.6100	2.6219e-01	1.5366e+02	4.2409e-01	7.1042e+01
128.6100	2.7868e-01	1.5636e+02	3.7552e-01	5.8732e+01
140.6600	2.9275e-01	1.5850e+02	3.0216e-01	4.3727e+01
153.8300	3.0352e-01	1.6000e+02	2.3907e-01	3.1328e+01
168.2500	3.1224e-01	1.6110e+02	1.9579e-01	2.3232e+01
184.0200	3.1934e-01	1.6191e+02	1.6028e-01	1.7273e+01
201.2800	3.2511e-01	1.6250e+02	1.4122e-01	1.3783e+01
220.1600	3.3062e-01	1.6303e+02	1.2648e-01	1.1460e+01
240.8200	3.3534e-01	1.6344e+02	9.8937e-02	8.3589e+00
263.4300	3.3875e-01	1.6372e+02	7.6040e-02	5.8994e+00
288.1600	3.4164e-01	1.6394e+02	6.2586e-02	4.4719e+00

Continued on next page



Analysis

Operator: lab
 Sample ID: Bone char

Date: 2014/08/07
 Filename:

Report

Operator: ra
 Date: 2014/08/11
 University of Waterloo_Bone char_Lab 4549_080714.qps

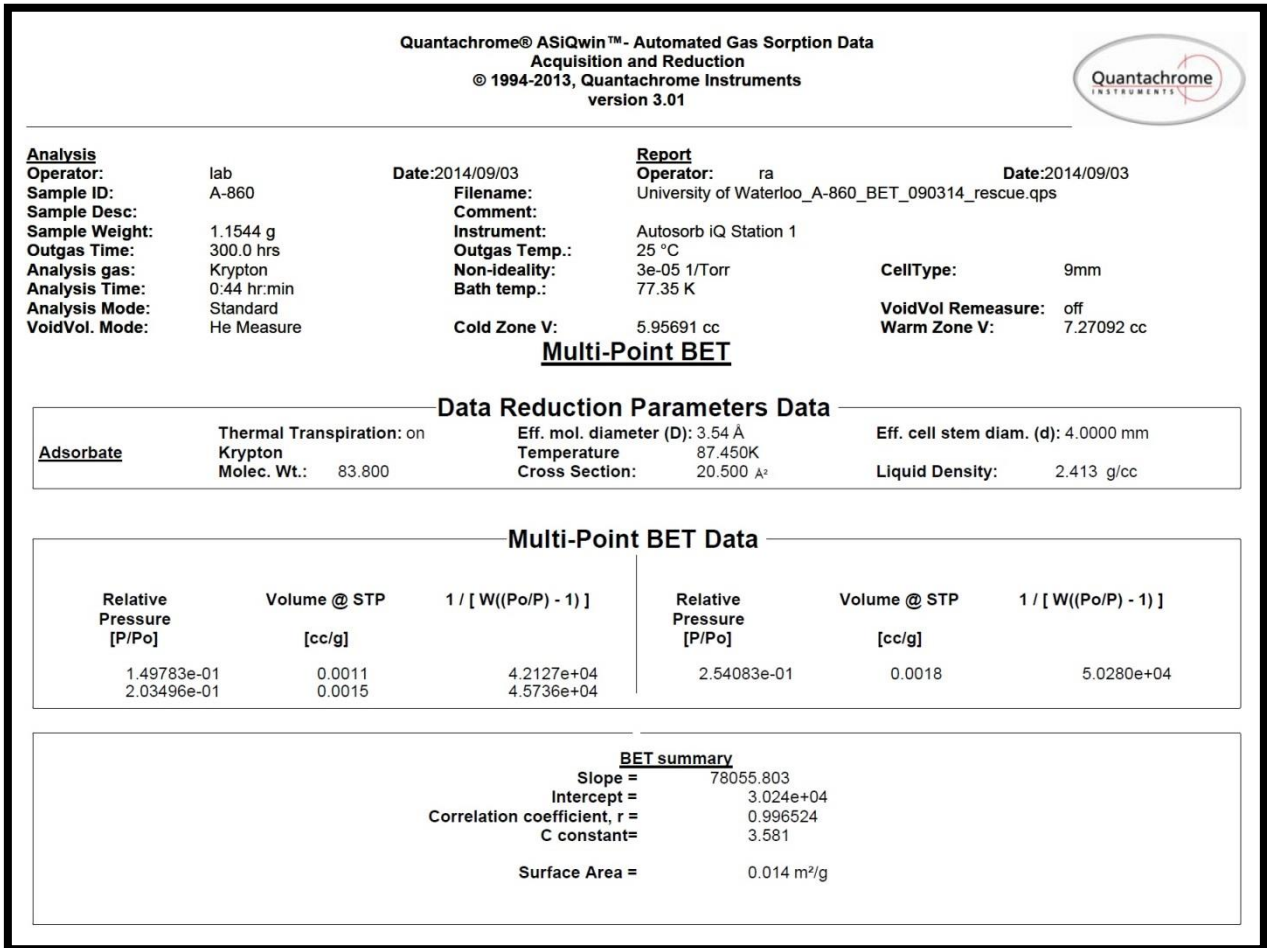
DFT method Pore Size Distribution (log) Data continued

Pore width [Å]	Cumulative Pore Volume [cc/g]	Cumulative Surface Area [m ² /g]	dV(log d) [cc/g]	dS(log d) [m ² /g]
315.2200	3.4311e-01	1.6403e+02	3.8083e-02	2.3365e+00
344.8200	3.4486e-01	1.6413e+02	4.4699e-02	2.5927e+00

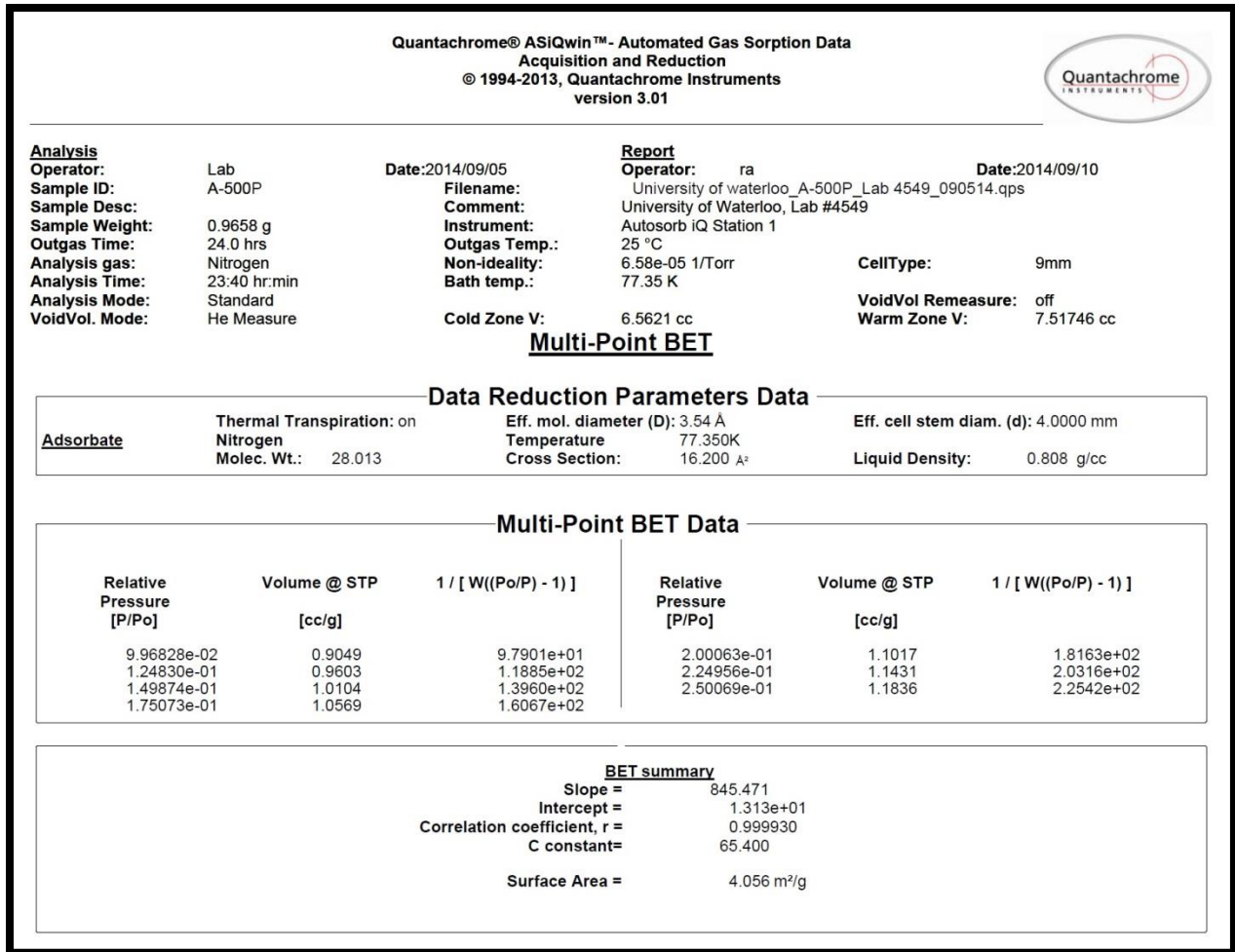
DFT method summary

Pore volume = 0.342 cc/g
 Surface area = 159.829 m²/g
 Lower confidence limit = 5.240 Å
 Fitting error = 1.193 %
 Pore width (Mode(dLog)) = 98.350 Å
 Moving point average : 5

7. Purolite A-860



8. Purolite A-500P





Analysis			Report	
Operator:	Lab	Date: 2014/09/05	Operator: ra	Date: 2014/09/10
Sample ID:	A-500P	Filename:	University of Waterloo_A-500P_Lab 4549_090514.qps	
Sample Desc:		Comment:	University of Waterloo, Lab #4549	
Sample Weight:	0.9658 g	Instrument:	Autosorb iQ Station 1	
Outgas Time:	24.0 hrs	Outgas Temp.:	25 °C	
Analysis gas:	Nitrogen	Non-ideality:	6.58e-05 1/Torr	CellType: 9mm
Analysis Time:	23:40 hr:min	Bath temp.:	77.35 K	
Analysis Mode:	Standard			VoidVol Remeasure: off
VoidVol. Mode:	He Measure	Cold Zone V:	6.5621 cc	Warm Zone V: 7.51746 cc

DFT method Pore Size Distribution (log)

Data Reduction Parameters Data

DFT method	Thermal Transpiration: on	Eff. mol. diameter (D): 3.54 Å	Eff. cell stem diam. (d): 4.0000 mm
	Calc. Model: N2 at 77 K on silica (cylindr. pore, NLDFT equilibrium model)		
	Rel. press. range: 0.0000 - 1.0000		Moving pt. avg: off
Adsorbate	Nitrogen	Temperature 77.350K	
	Molec. Wt.: 28.013	Cross Section: 16.200 Å ²	Liquid Density: 0.808 g/cc

DFT method Pore Size Distribution (log) Data

Pore width [Å]	Cumulative Pore Volume [cc/g]	Cumulative Surface Area [m ² /g]	dV(log d) [cc/g]	dS(log d) [m ² /g]
12.2000	0.0000e+00	0.0000e+00	0.0000e+00	0.0000e+00
12.7300	0.0000e+00	0.0000e+00	0.0000e+00	0.0000e+00
13.2600	0.0000e+00	0.0000e+00	0.0000e+00	0.0000e+00
13.7900	0.0000e+00	0.0000e+00	0.0000e+00	0.0000e+00
14.3200	0.0000e+00	0.0000e+00	0.0000e+00	0.0000e+00
14.9800	0.0000e+00	0.0000e+00	0.0000e+00	0.0000e+00
15.6400	0.0000e+00	0.0000e+00	0.0000e+00	0.0000e+00
16.3100	0.0000e+00	0.0000e+00	0.0000e+00	0.0000e+00
16.9700	0.0000e+00	0.0000e+00	0.0000e+00	0.0000e+00
17.8000	0.0000e+00	0.0000e+00	0.0000e+00	0.0000e+00
18.6800	0.0000e+00	0.0000e+00	0.0000e+00	0.0000e+00
19.4800	0.0000e+00	0.0000e+00	0.0000e+00	0.0000e+00
20.2700	0.0000e+00	0.0000e+00	0.0000e+00	0.0000e+00
21.0700	0.0000e+00	0.0000e+00	0.0000e+00	0.0000e+00
21.8600	0.0000e+00	0.0000e+00	0.0000e+00	0.0000e+00
22.6600	0.0000e+00	0.0000e+00	0.0000e+00	0.0000e+00
23.4500	0.0000e+00	0.0000e+00	0.0000e+00	0.0000e+00
24.2500	0.0000e+00	0.0000e+00	0.0000e+00	0.0000e+00
25.0400	0.0000e+00	0.0000e+00	0.0000e+00	0.0000e+00
25.8300	0.0000e+00	0.0000e+00	0.0000e+00	0.0000e+00
27.0300	0.0000e+00	0.0000e+00	0.0000e+00	0.0000e+00
28.2200	5.1952e-06	7.3638e-03	4.5753e-04	6.3041e-01
29.4100	1.6768e-05	2.3104e-02	8.2867e-04	1.1006e+00
30.6000	3.4335e-05	4.6067e-02	1.2655e-03	1.6178e+00
31.7900	5.9537e-05	7.7778e-02	1.7432e-03	2.1495e+00
32.9800	9.1041e-05	1.1599e-01	2.1859e-03	2.6007e+00
34.1800	1.2835e-04	1.5965e-01	2.6699e-03	3.0677e+00
35.3700	1.7216e-04	2.0920e-01	3.1591e-03	3.5115e+00
36.5600	2.2070e-04	2.6231e-01	3.5873e-03	3.8603e+00
37.7500	2.7362e-04	3.1838e-01	3.5819e-03	3.7132e+00
39.3400	3.3471e-04	3.8049e-01	3.6383e-03	3.6243e+00
40.9300	4.0141e-04	4.4568e-01	4.0389e-03	3.8717e+00
42.5200	4.7106e-04	5.1120e-01	4.3782e-03	4.0429e+00
44.1100	5.4368e-04	5.7705e-01	4.7021e-03	4.1887e+00
45.7000	6.1834e-04	6.4240e-01	4.9802e-03	4.2858e+00
47.2800	6.9379e-04	7.0623e-01	5.2778e-03	4.3912e+00
48.8700	7.7206e-04	7.7030e-01	4.9971e-03	4.0092e+00
50.8600	8.5219e-04	8.3332e-01	4.6235e-03	3.5691e+00
52.8500	9.2927e-04	8.9166e-01	4.7719e-03	3.5458e+00
54.8300	1.0080e-03	9.4906e-01	4.9418e-03	3.5428e+00
56.8200	1.0847e-03	1.0031e+00	4.9498e-03	3.4272e+00
58.8000	1.1582e-03	1.0531e+00	4.9943e-03	3.3420e+00
60.7900	1.2312e-03	1.1011e+00	4.5846e-03	2.9611e+00
63.1700	1.3010e-03	1.1453e+00	4.1089e-03	2.5560e+00
65.5600	1.3660e-03	1.1850e+00	4.0880e-03	2.4508e+00
67.9400	1.4302e-03	1.2228e+00	4.1464e-03	2.4006e+00
70.3200	1.4922e-03	1.2581e+00	3.8800e-03	2.1653e+00

Continued on next page



Analysis
 Operator: Lab Date:2014/09/05 **Report**
 Operator: ra Date:2014/09/10
 Sample ID: A-500P Filename: University of Waterloo_A-500P_Lab 4549_090514.qps

DFT method Pore Size Distribution (log) Data continued

Pore width [Å]	Cumulative Pore Volume [cc/g]	Cumulative Surface Area [m ² /g]	dV(log d) [cc/g]	dS(log d) [m ² /g]
73.1000	1.5536e-03	1.2916e+00	3.6510e-03	1.9618e+00
75.8800	1.6129e-03	1.3229e+00	3.7449e-03	1.9389e+00
78.6700	1.6730e-03	1.3535e+00	3.9521e-03	1.9748e+00
81.4500	1.7345e-03	1.3836e+00	3.9028e-03	1.8806e+00
84.6200	1.7966e-03	1.4130e+00	3.8102e-03	1.7684e+00
87.8000	1.8587e-03	1.4413e+00	3.8985e-03	1.7454e+00
90.9800	1.9193e-03	1.4679e+00	3.9891e-03	1.7242e+00
94.1600	1.9798e-03	1.4937e+00	3.9286e-03	1.6382e+00
97.7300	2.0414e-03	1.5188e+00	3.8582e-03	1.5513e+00
101.3100	2.1025e-03	1.5430e+00	4.0348e-03	1.5656e+00
104.8800	2.1651e-03	1.5669e+00	4.0877e-03	1.5301e+00
108.8500	2.2299e-03	1.5907e+00	4.1527e-03	1.4987e+00
112.8300	2.2969e-03	1.6144e+00	4.5194e-03	1.5741e+00
116.8000	2.3683e-03	1.6389e+00	4.6914e-03	1.5772e+00
121.1700	2.4422e-03	1.6633e+00	4.6663e-03	1.5139e+00
125.5400	2.5145e-03	1.6863e+00	5.0270e-03	1.5735e+00
129.9100	2.5942e-03	1.7109e+00	5.2797e-03	1.5966e+00
134.6700	2.6755e-03	1.7350e+00	5.3876e-03	1.5724e+00
139.4400	2.7599e-03	1.7592e+00	5.6466e-03	1.5899e+00
144.6000	2.8500e-03	1.7841e+00	5.8559e-03	1.5917e+00
149.7700	2.9416e-03	1.8086e+00	5.9019e-03	1.5480e+00
155.3300	3.0334e-03	1.8322e+00	6.0096e-03	1.5204e+00
160.8900	3.1285e-03	1.8559e+00	6.5611e-03	1.6001e+00
166.8500	3.2373e-03	1.8820e+00	7.3153e-03	1.7222e+00
172.8100	3.3556e-03	1.9093e+00	7.3146e-03	1.6645e+00
179.1600	3.4634e-03	1.9334e+00	6.3156e-03	1.3885e+00
185.5200	3.5503e-03	1.9521e+00	5.7816e-03	1.2242e+00
192.2700	3.6407e-03	1.9710e+00	7.2291e-03	1.4739e+00
199.0200	3.7708e-03	1.9971e+00	9.2392e-03	1.8224e+00
206.1700	3.9208e-03	2.0262e+00	9.6046e-03	1.8308e+00
213.7200	4.0680e-03	2.0538e+00	9.9332e-03	1.8263e+00
221.2700	4.2257e-03	2.0823e+00	9.9485e-03	1.7686e+00
229.2100	4.3704e-03	2.1075e+00	9.7957e-03	1.6782e+00
237.5500	4.5278e-03	2.1340e+00	1.0339e-02	1.7093e+00
246.2900	4.6931e-03	2.1609e+00	1.0588e-02	1.6905e+00
255.0300	4.8542e-03	2.1861e+00	1.1150e-02	1.7170e+00
264.1700	5.0324e-03	2.2131e+00	1.2211e-02	1.8152e+00
273.7000	5.2289e-03	2.2418e+00	1.3723e-02	1.9679e+00
283.6300	5.4561e-03	2.2739e+00	1.3657e-02	1.8946e+00
293.9600	5.6525e-03	2.3006e+00	1.2366e-02	1.6538e+00
304.6800	5.8406e-03	2.3253e+00	1.4272e-02	1.8374e+00
315.4100	6.0890e-03	2.3568e+00	1.6984e-02	2.1162e+00
326.5300	6.3514e-03	2.3889e+00	1.6472e-02	1.9854e+00
338.0500	6.5849e-03	2.4166e+00	1.8248e-02	2.1169e+00
349.9700	6.9008e-03	2.4527e+00	2.1688e-02	2.4355e+00
362.2800	7.2369e-03	2.4898e+00	2.0965e-02	2.2783e+00
374.9900	7.5295e-03	2.5210e+00	2.0506e-02	2.1487e+00
388.1000	7.8500e-03	2.5540e+00	2.3313e-02	2.3593e+00
401.6000	8.2237e-03	2.5912e+00	2.7119e-02	2.6527e+00
415.5100	8.6537e-03	2.6326e+00	2.9010e-02	2.7465e+00
429.8100	9.0790e-03	2.6722e+00	2.8824e-02	2.6384e+00
444.5000	9.4980e-03	2.7099e+00	3.0848e-02	2.7273e+00
459.6000	9.9767e-03	2.7516e+00	3.1903e-02	2.7331e+00
475.0900	1.0420e-02	2.7889e+00	2.7328e-02	2.2685e+00
490.9800	1.0761e-02	2.8167e+00	2.9255e-02	2.3381e+00
507.2700	1.1253e-02	2.8555e+00	3.4749e-02	2.6966e+00
523.9500	1.1741e-02	2.8928e+00	3.4122e-02	2.5648e+00
541.0300	1.2208e-02	2.9272e+00	3.7401e-02	2.7175e+00
558.5100	1.2779e-02	2.9682e+00	3.7859e-02	2.6735e+00
576.3800	1.3248e-02	3.0007e+00	3.6797e-02	2.5119e+00
594.6500	1.3781e-02	3.0366e+00	4.2209e-02	2.7933e+00
613.3200	1.4387e-02	3.0761e+00	4.7221e-02	3.0314e+00
632.3900	1.5043e-02	3.1176e+00	5.8964e-02	3.6651e+00
651.8500	1.5947e-02	3.1731e+00	7.6068e-02	4.5924e+00
671.7100	1.7036e-02	3.2379e+00	7.9238e-02	4.6536e+00

Continued on next page



Analysis

Operator: Lab
 Sample ID: A-500P

Date: 2014/09/05
 Filename:

Report

Operator: ra
 Date: 2014/09/10
 University of waterloo_A-500P_Lab 4549_090514.qps

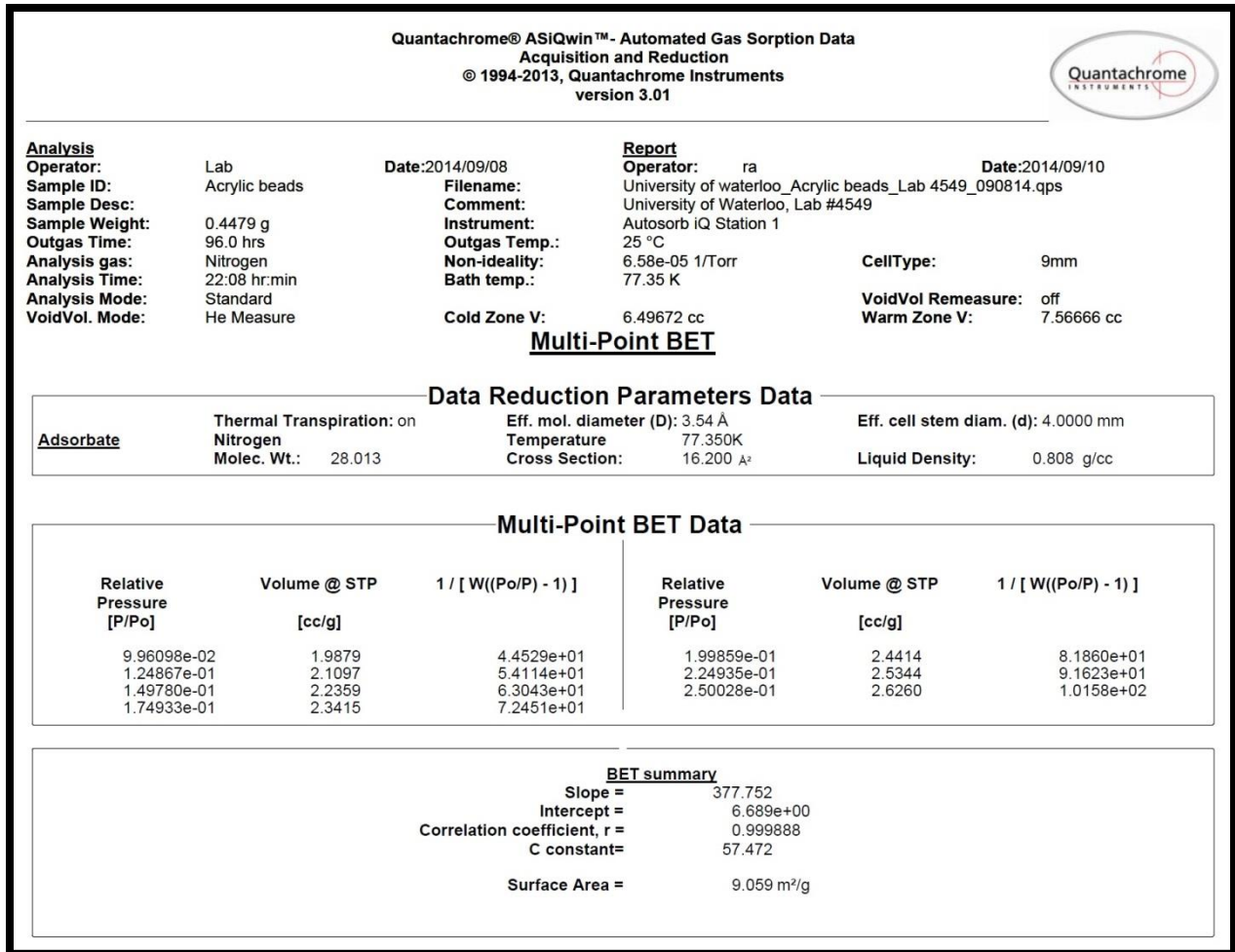
DFT method Pore Size Distribution (log) Data continued

Pore width [Å]	Cumulative Pore Volume [cc/g]	Cumulative Surface Area [m ² /g]	dV(log d) [cc/g]	dS(log d) [m ² /g]
691.9700	1.8003e-02	3.2938e+00	7.5767e-02	4.3159e+00
712.6300	1.8981e-02	3.3487e+00	7.0961e-02	3.9308e+00
733.6800	1.9806e-02	3.3937e+00	7.8501e-02	4.2090e+00
755.1300	2.0956e-02	3.4546e+00	9.1888e-02	4.8674e+00

DFT method summary

Pore volume = 0.021 cc/g
 Surface area = 3.455 m²/g
 Lower confidence limit = 12.200 Å
 Fitting error = 1.470 %
 Pore width (Mode(dLog)) = 755.130 Å
 Moving point average : off

9. Acrylic beads



Quantachrome® ASiQwin™ - Automated Gas Sorption Data
Acquisition and Reduction
 © 1994-2013, Quantachrome Instruments
 version 3.01



Analysis			Report		
Operator:	Lab	Date: 2014/09/08	Operator:	ra	Date: 2014/09/10
Sample ID:	Acrylic beads	Filename:	University of waterloo_Acrylic beads_Lab 4549_090814.qps		
Sample Desc:		Comment:	University of Waterloo, Lab #4549		
Sample Weight:	0.4479 g	Instrument:	Autosorb iQ Station 1		
Outgas Time:	96.0 hrs	Outgas Temp.:	25 °C		
Analysis gas:	Nitrogen	Non-ideality:	6.58e-05 1/Torr	CellType:	9mm
Analysis Time:	22:08 hr:min	Bath temp.:	77.35 K	VoidVol Remeasure:	off
Analysis Mode:	Standard	Cold Zone V:	6.49672 cc	Warm Zone V:	7.56666 cc
VoidVol. Mode:	He Measure				

DFT method Pore Size Distribution (log)

Data Reduction Parameters Data

DFT method	Thermal Transpiration: on	Eff. mol. diameter (D): 3.54 Å	Eff. cell stem diam. (d): 4.0000 mm
	Calc. Model: N2 at 77 K on silica (cylindr. pore, NLDFT equilibrium model)		
Adsorbate	Rel. press. range: 0.0000 - 1.0000	Temperature 77.350K	Moving pt. avg: off
	Nitrogen	Cross Section: 16.200 Å ²	Liquid Density: 0.808 g/cc
	Molec. Wt.: 28.013		

DFT method Pore Size Distribution (log) Data

Pore width [Å]	Cumulative Pore Volume [cc/g]	Cumulative Surface Area [m ² /g]	dV(log d) [cc/g]	dS(log d) [m ² /g]
12.2000	0.0000e+00	0.0000e+00	0.0000e+00	0.0000e+00
12.7300	0.0000e+00	0.0000e+00	0.0000e+00	0.0000e+00
13.2600	0.0000e+00	0.0000e+00	0.0000e+00	0.0000e+00
13.7900	0.0000e+00	0.0000e+00	0.0000e+00	0.0000e+00
14.3200	0.0000e+00	0.0000e+00	0.0000e+00	0.0000e+00
14.8500	0.0000e+00	0.0000e+00	0.0000e+00	0.0000e+00
15.3800	0.0000e+00	0.0000e+00	0.0000e+00	0.0000e+00
15.9100	0.0000e+00	0.0000e+00	0.0000e+00	0.0000e+00
16.4400	0.0000e+00	0.0000e+00	0.0000e+00	0.0000e+00
16.9700	0.0000e+00	0.0000e+00	0.0000e+00	0.0000e+00
17.5000	0.0000e+00	0.0000e+00	0.0000e+00	0.0000e+00
18.0300	0.0000e+00	0.0000e+00	0.0000e+00	0.0000e+00
18.5600	0.0000e+00	0.0000e+00	0.0000e+00	0.0000e+00
19.0900	0.0000e+00	0.0000e+00	0.0000e+00	0.0000e+00
19.6200	0.0000e+00	0.0000e+00	0.0000e+00	0.0000e+00
20.1500	0.0000e+00	0.0000e+00	0.0000e+00	0.0000e+00
20.6800	0.0000e+00	0.0000e+00	0.0000e+00	0.0000e+00
21.2100	0.0000e+00	0.0000e+00	0.0000e+00	0.0000e+00
21.7400	0.0000e+00	0.0000e+00	0.0000e+00	0.0000e+00
22.2700	0.0000e+00	0.0000e+00	0.0000e+00	0.0000e+00
22.8000	0.0000e+00	0.0000e+00	0.0000e+00	0.0000e+00
23.3300	0.0000e+00	0.0000e+00	0.0000e+00	0.0000e+00
23.8600	0.0000e+00	0.0000e+00	0.0000e+00	0.0000e+00
24.3900	0.0000e+00	0.0000e+00	0.0000e+00	0.0000e+00
24.9200	0.0000e+00	0.0000e+00	0.0000e+00	0.0000e+00
25.4500	0.0000e+00	0.0000e+00	0.0000e+00	0.0000e+00
25.9800	0.0000e+00	0.0000e+00	0.0000e+00	0.0000e+00
26.5100	0.0000e+00	0.0000e+00	0.0000e+00	0.0000e+00
27.0400	0.0000e+00	0.0000e+00	0.0000e+00	0.0000e+00
27.5700	0.0000e+00	0.0000e+00	0.0000e+00	0.0000e+00
28.1000	0.0000e+00	0.0000e+00	0.0000e+00	0.0000e+00
28.6300	0.0000e+00	0.0000e+00	0.0000e+00	0.0000e+00
29.1600	0.0000e+00	0.0000e+00	0.0000e+00	0.0000e+00
29.6900	0.0000e+00	0.0000e+00	0.0000e+00	0.0000e+00
30.2200	0.0000e+00	0.0000e+00	0.0000e+00	0.0000e+00
30.7500	0.0000e+00	0.0000e+00	0.0000e+00	0.0000e+00
31.2800	0.0000e+00	0.0000e+00	0.0000e+00	0.0000e+00
31.8100	0.0000e+00	0.0000e+00	0.0000e+00	0.0000e+00
32.3400	0.0000e+00	0.0000e+00	0.0000e+00	0.0000e+00
32.8700	0.0000e+00	0.0000e+00	0.0000e+00	0.0000e+00
33.4000	0.0000e+00	0.0000e+00	0.0000e+00	0.0000e+00
33.9300	0.0000e+00	0.0000e+00	0.0000e+00	0.0000e+00
34.4600	0.0000e+00	0.0000e+00	0.0000e+00	0.0000e+00
34.9900	0.0000e+00	0.0000e+00	0.0000e+00	0.0000e+00
35.5200	0.0000e+00	0.0000e+00	0.0000e+00	0.0000e+00
36.0500	0.0000e+00	0.0000e+00	0.0000e+00	0.0000e+00
36.5800	0.0000e+00	0.0000e+00	0.0000e+00	0.0000e+00
37.1100	0.0000e+00	0.0000e+00	0.0000e+00	0.0000e+00
37.6400	0.0000e+00	0.0000e+00	0.0000e+00	0.0000e+00
38.1700	0.0000e+00	0.0000e+00	0.0000e+00	0.0000e+00
38.7000	0.0000e+00	0.0000e+00	0.0000e+00	0.0000e+00
39.2300	0.0000e+00	0.0000e+00	0.0000e+00	0.0000e+00
39.7600	0.0000e+00	0.0000e+00	0.0000e+00	0.0000e+00
40.2900	0.0000e+00	0.0000e+00	0.0000e+00	0.0000e+00
40.8200	0.0000e+00	0.0000e+00	0.0000e+00	0.0000e+00
41.3500	0.0000e+00	0.0000e+00	0.0000e+00	0.0000e+00
41.8800	0.0000e+00	0.0000e+00	0.0000e+00	0.0000e+00
42.4100	0.0000e+00	0.0000e+00	0.0000e+00	0.0000e+00
42.9400	0.0000e+00	0.0000e+00	0.0000e+00	0.0000e+00
43.4700	0.0000e+00	0.0000e+00	0.0000e+00	0.0000e+00
44.0000	0.0000e+00	0.0000e+00	0.0000e+00	0.0000e+00
44.5300	0.0000e+00	0.0000e+00	0.0000e+00	0.0000e+00
45.0600	0.0000e+00	0.0000e+00	0.0000e+00	0.0000e+00
45.5900	0.0000e+00	0.0000e+00	0.0000e+00	0.0000e+00
46.1200	0.0000e+00	0.0000e+00	0.0000e+00	0.0000e+00
46.6500	0.0000e+00	0.0000e+00	0.0000e+00	0.0000e+00
47.1800	0.0000e+00	0.0000e+00	0.0000e+00	0.0000e+00
47.7100	0.0000e+00	0.0000e+00	0.0000e+00	0.0000e+00
48.2400	0.0000e+00	0.0000e+00	0.0000e+00	0.0000e+00
48.7700	0.0000e+00	0.0000e+00	0.0000e+00	0.0000e+00
49.3000	0.0000e+00	0.0000e+00	0.0000e+00	0.0000e+00
49.8300	0.0000e+00	0.0000e+00	0.0000e+00	0.0000e+00
50.3600	0.0000e+00	0.0000e+00	0.0000e+00	0.0000e+00
50.8900	0.0000e+00	0.0000e+00	0.0000e+00	0.0000e+00
51.4200	0.0000e+00	0.0000e+00	0.0000e+00	0.0000e+00
51.9500	0.0000e+00	0.0000e+00	0.0000e+00	0.0000e+00
52.4800	0.0000e+00	0.0000e+00	0.0000e+00	0.0000e+00
53.0100	0.0000e+00	0.0000e+00	0.0000e+00	0.0000e+00
53.5400	0.0000e+00	0.0000e+00	0.0000e+00	0.0000e+00
54.0700	0.0000e+00	0.0000e+00	0.0000e+00	0.0000e+00
54.6000	0.0000e+00	0.0000e+00	0.0000e+00	0.0000e+00
55.1300	0.0000e+00	0.0000e+00	0.0000e+00	0.0000e+00
55.6600	0.0000e+00	0.0000e+00	0.0000e+00	0.0000e+00
56.1900	0.0000e+00	0.0000e+00	0.0000e+00	0.0000e+00
56.7200	0.0000e+00	0.0000e+00	0.0000e+00	0.0000e+00
57.2500	0.0000e+00	0.0000e+00	0.0000e+00	0.0000e+00
57.7800	0.0000e+00	0.0000e+00	0.0000e+00	0.0000e+00
58.3100	0.0000e+00	0.0000e+00	0.0000e+00	0.0000e+00
58.8400	0.0000e+00	0.0000e+00	0.0000e+00	0.0000e+00
59.3700	0.0000e+00	0.0000e+00	0.0000e+00	0.0000e+00
59.9000	0.0000e+00	0.0000e+00	0.0000e+00	0.0000e+00
60.4300	0.0000e+00	0.0000e+00	0.0000e+00	0.0000e+00
60.9600	0.0000e+00	0.0000e+00	0.0000e+00	0.0000e+00
61.4900	0.0000e+00	0.0000e+00	0.0000e+00	0.0000e+00
62.0200	0.0000e+00	0.0000e+00	0.0000e+00	0.0000e+00
62.5500	0.0000e+00	0.0000e+00	0.0000e+00	0.0000e+00
63.0800	0.0000e+00	0.0000e+00	0.0000e+00	0.0000e+00
63.6100	0.0000e+00	0.0000e+00	0.0000e+00	0.0000e+00
64.1400	0.0000e+00	0.0000e+00	0.0000e+00	0.0000e+00
64.6700	0.0000e+00	0.0000e+00	0.0000e+00	0.0000e+00
65.2000	0.0000e+00	0.0000e+00	0.0000e+00	0.0000e+00
65.7300	0.0000e+00	0.0000e+00	0.0000e+00	0.0000e+00
66.2600	0.0000e+00	0.0000e+00	0.0000e+00	0.0000e+00
66.7900	0.0000e+00	0.0000e+00	0.0000e+00	0.0000e+00
67.3200	0.0000e+00	0.0000e+00	0.0000e+00	0.0000e+00

Continued on next page



Analysis
 Operator: Lab Date: 2014/09/08
 Sample ID: Acrylic beads Filename: University of waterloo_Acrylic beads_Lab 4549_090814.qps

Report
 Operator: ra Date: 2014/09/10

DFT method Pore Size Distribution (log) Data continued

Pore width [Å]	Cumulative Pore Volume [cc/g]	Cumulative Surface Area [m ² /g]	dV(log d) [cc/g]	dS(log d) [m ² /g]
73.1000	4.0606e-03	3.5537e+00	8.6892e-03	4.6710e+00
75.8800	4.1986e-03	3.6265e+00	8.5154e-03	4.4106e+00
78.6700	4.3321e-03	3.6944e+00	8.5248e-03	4.2619e+00
81.4500	4.4608e-03	3.7576e+00	7.8416e-03	3.7815e+00
84.6200	4.5804e-03	3.8141e+00	7.1915e-03	3.3391e+00
87.8000	4.6953e-03	3.8665e+00	7.2458e-03	3.2438e+00
90.9800	4.8085e-03	3.9162e+00	7.5433e-03	3.2598e+00
94.1600	4.9244e-03	3.9655e+00	7.7748e-03	3.2400e+00
97.7300	5.0501e-03	4.0169e+00	8.0157e-03	3.2221e+00
101.3100	5.1792e-03	4.0679e+00	8.6547e-03	3.3574e+00
104.8800	5.3155e-03	4.1199e+00	8.9956e-03	3.3665e+00
108.8500	5.4596e-03	4.1728e+00	9.2216e-03	3.3280e+00
112.8300	5.6081e-03	4.2255e+00	9.9087e-03	3.4518e+00
116.8000	5.7630e-03	4.2785e+00	1.0087e-02	3.3916e+00
121.1700	5.9205e-03	4.3305e+00	9.9132e-03	3.2164e+00
125.5400	6.0736e-03	4.3793e+00	1.0581e-02	3.3121e+00
129.9100	6.2406e-03	4.4307e+00	1.0970e-02	3.3180e+00
134.6700	6.4081e-03	4.4805e+00	1.1127e-02	3.2473e+00
139.4400	6.5827e-03	4.5305e+00	1.1697e-02	3.2934e+00
144.6000	6.7695e-03	4.5822e+00	1.2153e-02	3.3033e+00
149.7700	6.9599e-03	4.6331e+00	1.2266e-02	3.2173e+00
155.3300	7.1508e-03	4.6822e+00	1.2527e-02	3.1690e+00
160.8900	7.3495e-03	4.7316e+00	1.3788e-02	3.3622e+00
166.8500	7.5792e-03	4.7867e+00	1.5644e-02	3.6822e+00
172.8100	7.8351e-03	4.8459e+00	1.5877e-02	3.6126e+00
179.1600	8.0700e-03	4.8984e+00	1.3894e-02	3.0540e+00
185.5200	8.2633e-03	4.9401e+00	1.2897e-02	2.7308e+00
192.2700	8.4656e-03	4.9821e+00	1.7472e-02	3.5584e+00
199.0200	8.7963e-03	5.0486e+00	2.1791e-02	4.3039e+00
206.1700	9.1262e-03	5.1126e+00	2.0665e-02	3.9408e+00
213.7200	9.4359e-03	5.1706e+00	2.0747e-02	3.8150e+00
221.2700	9.7631e-03	5.2297e+00	2.0614e-02	3.6648e+00
229.2100	1.0062e-02	5.2819e+00	2.0252e-02	3.4696e+00
237.5500	1.0387e-02	5.3367e+00	2.1358e-02	3.5310e+00
246.2900	1.0729e-02	5.3922e+00	2.2226e-02	3.5477e+00
255.0300	1.1073e-02	5.4461e+00	2.3949e-02	3.6876e+00
264.1700	1.1458e-02	5.5044e+00	2.6611e-02	3.9553e+00
273.7000	1.1889e-02	5.5675e+00	3.0647e-02	4.3936e+00
283.6300	1.2404e-02	5.6400e+00	3.0873e-02	4.2833e+00
293.9600	1.2847e-02	5.7003e+00	2.7058e-02	3.6205e+00
304.6800	1.3245e-02	5.7526e+00	3.1186e-02	4.0131e+00
315.4100	1.3801e-02	5.8230e+00	3.6748e-02	4.5815e+00
326.5300	1.4351e-02	5.8904e+00	3.3306e-02	4.0172e+00
338.0500	1.4803e-02	5.9440e+00	3.5156e-02	4.0788e+00
349.9700	1.5409e-02	6.0132e+00	4.4760e-02	5.0203e+00
362.2800	1.6149e-02	6.0949e+00	4.6582e-02	5.0612e+00
374.9900	1.6806e-02	6.1650e+00	4.5908e-02	4.8107e+00
388.1000	1.7522e-02	6.2388e+00	4.8993e-02	4.9631e+00
401.6000	1.8265e-02	6.3128e+00	5.2853e-02	5.1716e+00
415.5100	1.9088e-02	6.3920e+00	5.6266e-02	5.3258e+00
429.8100	1.9924e-02	6.4698e+00	5.6720e-02	5.1919e+00
444.5000	2.0749e-02	6.5441e+00	6.0772e-02	5.3730e+00
459.6000	2.1692e-02	6.6261e+00	6.2527e-02	5.3570e+00
475.0900	2.2557e-02	6.6989e+00	4.8494e-02	4.0329e+00
490.9800	2.3083e-02	6.7418e+00	4.9109e-02	3.9208e+00
507.2700	2.3955e-02	6.8105e+00	6.6251e-02	5.1353e+00
523.9500	2.4953e-02	6.8868e+00	6.9847e-02	5.2500e+00
541.0300	2.5909e-02	6.9574e+00	7.6757e-02	5.5770e+00
558.5100	2.7083e-02	7.0415e+00	7.7751e-02	5.4906e+00
576.3800	2.8046e-02	7.1084e+00	7.5545e-02	5.1571e+00
594.6500	2.9140e-02	7.1819e+00	8.6234e-02	5.7071e+00
613.3200	3.0373e-02	7.2623e+00	8.0628e-02	5.1906e+00
632.3900	3.1294e-02	7.3206e+00	1.0280e-01	6.3741e+00
651.8500	3.3093e-02	7.4310e+00	1.5503e-01	9.3564e+00
671.7100	3.5356e-02	7.5657e+00	1.6479e-01	9.6780e+00

Continued on next page



Analysis

Operator: Lab
Sample ID: Acrylic beads

Date: 2014/09/08
Filename:

Report

Operator: ra
Date: 2014/09/10
 University of Waterloo_Acrylic beads_Lab 4549_090814.qps

DFT method Pore Size Distribution (log) Data continued


Pore width [Å]	Cumulative Pore Volume [cc/g]	Cumulative Surface Area [m ² /g]	dV(log d) [cc/g]	dS(log d) [m ² /g]
691.9700	3.7367e-02	7.6820e+00	1.5765e-01	8.9801e+00
712.6300	3.9404e-02	7.7964e+00	1.4766e-01	8.1796e+00
733.6800	4.1121e-02	7.8900e+00	1.6360e-01	8.7719e+00
755.1300	4.3520e-02	8.0170e+00	1.9171e-01	1.0155e+01

DFT method summary

Pore volume = 0.044 cc/g
 Surface area = 8.017 m²/g
 Lower confidence limit = 12.200 Å
 Fitting error = 1.440 %
 Pore width (Mode(dLog)) = 755.130 Å
 Moving point average : off

10. Styrenic beads

Quantachrome® ASiQwin™ - Automated Gas Sorption Data
 Acquisition and Reduction
 © 1994-2013, Quantachrome Instruments
 version 3.01



Analysis		Report	
Operator: lab	Date: 2014/09/03	Operator: ra	Date: 2014/09/03
Sample ID: Styrene beads	Filename:	University of Waterloo_Styrene beads_BET_090314_rescue.qps	
Sample Desc:	Comment:		
Sample Weight: 2.6622 g	Instrument: Autosorb iQ Station 2		
Outgas Time: 300.0 hrs	Outgas Temp.: 25 °C		
Analysis gas: Krypton	Non-ideality: 3e-05 1/Torr	CellType:	9mm
Analysis Time: 0:51 hr:min	Bath temp.: 77.35 K	VoidVol Remeasure:	off
Analysis Mode: Standard		Warm Zone V:	8.94146 cc
VoidVol. Mode: He Measure	Cold Zone V: 5.12284 cc		

Multi-Point BET

Data Reduction Parameters Data

Adsorbate	Thermal Transpiration: on Argon87 Molec. Wt.: 39.948	Eff. mol. diameter (D): 3.54 Å Temperature 87.450K Cross Section: 14.200 Å²	Eff. cell stem diam. (d): 4.0000 mm Liquid Density: 1.400 g/cc
------------------	--	---	---

Multi-Point BET Data

Relative Pressure [P/Po]	Volume @ STP [cc/g]	1 / [W((Po/P) - 1)]	Relative Pressure [P/Po]	Volume @ STP [cc/g]	1 / [W((Po/P) - 1)]
7.66216e-02	0.0018	2.5221e+04	2.02061e-01	0.0031	4.5406e+04
1.01380e-01	0.0021	2.9758e+04	2.49549e-01	0.0035	5.2899e+04
1.51536e-01	0.0027	3.7579e+04	3.05681e-01	0.0040	6.2345e+04

BET summary

Slope =	160136.331
Intercept =	1.319e+04
Correlation coefficient, r =	0.999845
C constant =	13.137
Surface Area =	0.012 m²/g

APPENDIX-D

Time Dependent PFCA Removal in Single Solute Adsorption Kinetic Experiments

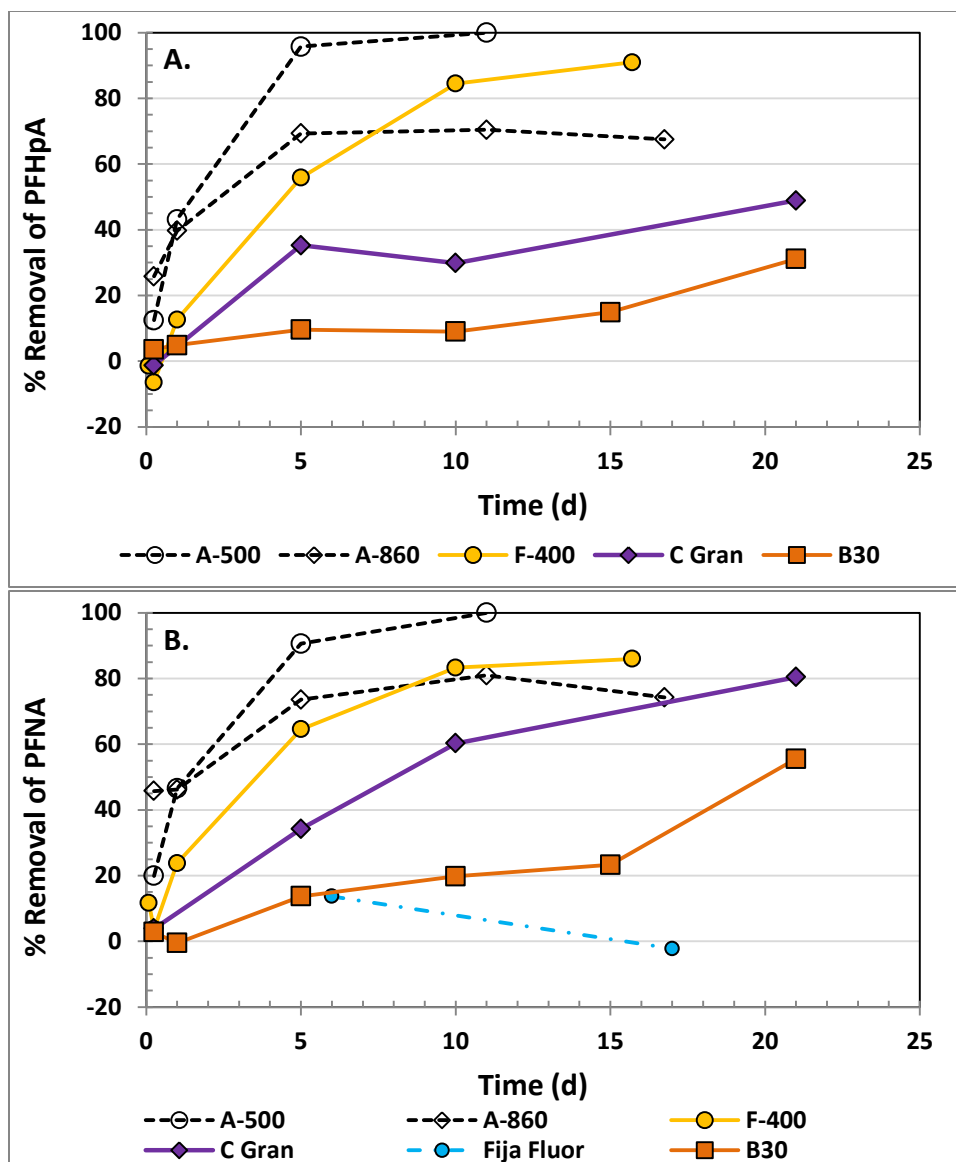


Figure D1. Removal of A) PFHpA and B) PFNA by different adsorbents during single solute adsorption kinetics experiments in ultrapure water. Adsorbent dose: 10 mg/L; no pH adjustments were done

APPENDIX-E

Additional Data on Kinetics and Isotherm Model Derived Adsorption Parameters

Table E1. Confidence intervals for pseudo-second-order kinetics model linear fitting parameters for ultrapure water kinetics experimental data

Adsorbent	$1/q_e$			$1/(k_2 q_e^2)$			R^2		
	PFHpA	PFOA	PFNA	PFHpA	PFOA	PFNA	PFHpA	PFOA	PFNA
Biochar	0.0363 <i>(0.0243-0.0483)</i>	0.0141 <i>(0.0106-0.0175)</i>	0.0056 <i>(0.0043-0.0069)</i>	0.0069 <i>(-0.1399-0.1537)</i>	0.0107 <i>(-0.0315-0.0529)</i>	0.0088 <i>(-0.0074-0.0249)</i>	0.94	0.97	0.97
WV B-30	0.0199 <i>(0.0073-0.0326)</i>	0.0102 <i>(0.0028-0.0176)</i>	0.0124 <i>(0.0059-0.0189)</i>	0.0403 <i>(-0.0657-0.1464)</i>	0.0139 <i>(-0.0481-0.0759)</i>	0.0174 <i>(-0.0373-0.072)</i>	0.89	0.81	0.92
C-Gran	0.0058 <i>(-0.0006-0.0122)</i>	0.0054 <i>(0.0053-0.0055)</i>	0.0025 <i>(0.0010-0.0040)</i>	0.0123 <i>(-0.0636-0.0883)</i>	-0.001 <i>(-0.0025-0.0004)</i>	0.0233 <i>(0.0053-0.0413)</i>	0.88	0.96	0.96
CX	0.0034 <i>(0.0012-0.0055)</i>	0.0033 <i>(-0.0010-0.0075)</i>	0.0025 <i>(0.0007-0.0044)</i>	0.0119 <i>(-0.0141-0.0378)</i>	0.0190 <i>(-0.0371-0.0750)</i>	0.0186 <i>(-0.0039-0.0412)</i>	0.79	0.52	0.78
F-400	0.0024 <i>(0.0012-0.0037)</i>	0.0028 <i>(0.0017-0.0039)</i>	0.0025 <i>(0.0018-0.0032)</i>	0.0151 <i>(-0.0004-0.0306)</i>	0.0127 <i>(-0.0009-0.0264)</i>	0.0079 <i>(-0.0006-0.0166)</i>	0.88	0.92	0.96
A-500P	0.0024 <i>(0.0020-0.0028)</i>	0.0025 <i>(0.0021-0.0029)</i>	0.0025 <i>(0.0022-0.0028)</i>	0.0028 <i>(0.0003-0.0053)</i>	0.0023 <i>(-4E-06-0.0045)</i>	0.0020 <i>(0.0001-0.0039)</i>	0.99	0.99	0.99
A-860	0.0035 <i>(0.0034-0.0036)</i>	0.0033 <i>(0.0032-0.0034)</i>	0.0028 <i>(0.0027-0.0029)</i>	0.0033 <i>(0.0020-0.0046)</i>	0.0023 <i>(0.0008-0.0038)</i>	0.0017 <i>(0.0003-0.0030)</i>	0.99	0.99	0.99

Values in italic in parenthesis indicate 95% confidence intervals for the linear fitting parameters

Table E2. Pseudo-second-order kinetics parameters calculated using non-linear least squares regression (for Ultrapure water)*

Adsorbent	Pseudo-second-order parameter	PFHpA	PFOA	PFNA
A-500	q_e (ng.mg ⁻¹)	432	409	414
	K_2 (mg.ng ⁻¹ .d ⁻¹)	0.0017	0.0023	0.0026
	ϑ (ng.mg ⁻¹ .d ⁻¹)	331	389	447
A-860	q_e (ng.mg ⁻¹)	294	305	365
	K_2 (mg.ng ⁻¹ .d ⁻¹)	0.003	0.004	0.004
	ϑ (ng.mg ⁻¹ .d ⁻¹)	260	363	495
F-400	q_e (ng.mg ⁻¹)	376	350	403
	K_2 (mg.ng ⁻¹ .d ⁻¹)	0.0007	0.0008	0.0008
	ϑ (ng.mg ⁻¹ .d ⁻¹)	103	102	134
CX	q_e (ng.mg ⁻¹)	344	319	368
	K_2 (mg.ng ⁻¹ .d ⁻¹)	0.0006	0.0007	0.0006
	ϑ (ng.mg ⁻¹ .d ⁻¹)	71	71	90
Biochar	q_e (ng.mg ⁻¹)	30	71	167
	K_2 (mg.ng ⁻¹ .d ⁻¹)	0.14	0.024	0.006
	ϑ (ng.mg ⁻¹ .d ⁻¹)	130	119	167

*Fitted to time dependent PFCA removal data presented in Figure 4.1

Table E3. Fitted pseudo-first-order model parameters for adsorption kinetics data in ultrapure water

Adsorbent	q _e (ng/mg)	Experimental q _e (ng/mg)	q _e (ng/mg)	Experimental q _e (ng/mg)	q _e (ng/mg)	Experimental q _e (ng/mg)	K ₁ (1/d)			R ²		
	PFHpA		PFOA		PFNA		PFHpA	PFOA	PFNA	PFHpA	PFOA	PFNA
F-400	373	307	330	290	380	341	0.35	0.33	0.34	0.9	0.9	0.9
A-500P	387	371	346	362	351	371	0.77	0.74	0.80	0.99	0.99	0.99
A-860	164	276	204	290	250	347	0.27	0.37	0.4	0.89	0.99	0.99

Table E4. Freundlich isotherm parameters for selected adsorbents in ultrapure water (calculated using linear least squares regression)

Compound	Freundlich intensity factor $1/n$ (dimensionless)			Freundlich capacity factor K_f [(ng/mg)(L/ng) ^{1/n}]			R^2		
	A-860 resin	F-400 GAC	A-500P resin	A-860 resin	F-400 GAC	A-500P resin	A-860 Resin	F-400 GAC	A-500P resin
PFHpA	0.91 (0.69-1.13)	0.36 (0.23-0.50)	0.30 (0.14-0.45)	0.34 (0.07-1.7)	59 (24.95-138)	168 (67.2-422.3)	0.94	0.88	0.88
PFOA	1.86 (1.64-2.07)	0.34 (0.22-0.46)	0.30 (0.23-0.37)	<0.01 (0.0001- 0.0021)	47 (22.3-100.1)	126 (87-183.3)	0.99	0.89	0.95
PFNA	0.79 (0.29-1.28)	0.41 (0.27-0.56)	0.39 (0.19-0.59)	3.33 (0.15-74.7)	27 (10.2-69.8)	90 (27.4-295.4)	0.72	0.89	0.79

Values in parenthesis are 95% confidence intervals

Table E5. Confidence intervals for pseudo-second-order kinetics model linear fitting parameters for Grand River water kinetics experimental data

Adsorbent	$1/q_e$			$1/(k_2q_e^2)$			R^2		
	PFHpA	PFOA	PFNA	PFHpA	PFOA	PFNA	PFHpA	PFOA	PFNA
Biochar	0.1181 <i>(0.0737 - 0.1625)</i>	0.0959 <i>(0.0704- 0.1214)</i>	0.0744 <i>(0.0647- 0.0841)</i>	0.1626 <i>(-0.3708- 0.6961)</i>	0.0929 <i>(-0.2133- 0.3992)</i>	0.04855 <i>(-0.0678- 0.1649)</i>	0.93	0.96	0.99
CX	0.0237 <i>(0.0157- 0.0217)</i>	0.0264 <i>(0.0170- 0.0357)</i>	0.0279 <i>(0.0193- 0.0366)</i>	0.0974 <i>(0.00143- 0.19339)</i>	0.1126 <i>(0.0002- 0.2249)</i>	0.0945 <i>(-0.0096- 0.1986)</i>	0.94	0.94	0.95
F-400	0.0251 <i>(0.0238- 0.0265)</i>	0.0271 <i>(0.0249- 0.0291)</i>	0.0269 <i>(0.0221- 0.0316)</i>	0.0557 <i>(0.0443- 0.0671)</i>	0.0621 <i>(0.0446- 0.0797)</i>	0.0594 <i>(0.0141- 0.1048)</i>	0.99	0.99	0.99
A-500P	0.0259 <i>(0.0267- 0.0262)</i>	0.0282 <i>(0.028- 0.0284)</i>	0.0280 <i>(0.0278- 0.0282)</i>	0.0071 <i>(0.0039- 0.0102)</i>	0.0086 <i>(0.0062- 0.0109)</i>	0.0082 <i>(0.0059- 0.0106)</i>	0.99	1.00	1.00
A-860	0.2212 <i>(0.1126- 0.3297)</i>	0.2988 <i>(0.0371- 0.5604)</i>	0.5537 <i>(-4.723- 5.831)</i>	0.8661 <i>(-0.4389- 2.171)</i>	1.052 <i>(-2.094- 4.198)</i>	11.18 <i>(-52.28- 74.64)</i>	0.89	0.71	0.02

Values in italic in parenthesis indicate 95% confidence intervals for the linear fitting parameters

Table E6. Pseudo-second-order kinetics parameters calculated using non-linear least squares regression (for Grand River Water)*

Adsorbent	Pseudo-second-order parameter	PFHpA	PFOA	PFNA
A-500	q_e (ng.mg ⁻¹)	39	36	36
	K_2 (mg.ng ⁻¹ .d ⁻¹)	0.10	0.09	0.08
	ϑ (ng.mg ⁻¹ .d ⁻¹)	147	108	106
A-860	q_e (ng.mg ⁻¹)	4	2	1
	K_2 (mg.ng ⁻¹ .d ⁻¹)	0.07	3.4	0.84
	ϑ (ng.mg ⁻¹ .d ⁻¹)	1	20	2
F-400	q_e (ng.mg ⁻¹)	40	37	38
	K_2 (mg.ng ⁻¹ .d ⁻¹)	0.011	0.011	0.011
	ϑ (ng.mg ⁻¹ .d ⁻¹)	17	16	15
CX	q_e (ng.mg ⁻¹)	44	40	37
	K_2 (mg.ng ⁻¹ .d ⁻¹)	0.004	0.004	0.006
	ϑ (ng.mg ⁻¹ .d ⁻¹)	9	7	8
Biochar	q_e (ng.mg ⁻¹)	8	10	13
	K_2 (mg.ng ⁻¹ .d ⁻¹)	0.30	0.25	0.15
	ϑ (ng.mg ⁻¹ .d ⁻¹)	17	24	27

*Fitted to time dependent PFCA removal data presented in Figure 5.1